

**SYNTHESIS, CHARACTERIZATION AND OLEFIN
POLYMERIZATION REACTIVITY OF SOME EARLY
AND LATE TRANSITION METAL COMPLEXES**

A THESIS
SUBMITTED TO THE
UNIVERSITY OF PUNE
FOR THE DEGREE OF
DOCTOR OF PHILOSOPHY
IN
CHEMISTRY

BY
A. RAJESH

**POLYMER SCIENCE AND ENGINEERING DIVISION
NATIONAL CHEMICAL LABORATORY
PUNE 411 008
INDIA**

SEPTEMBER 2007

DECLARATION BY RESEARCH GUIDE

Certified that the work incorporated in the thesis entitled: “**Synthesis, characterization and olefin polymerization reactivity of some early and late transition metal complexes**”, submitted by Mr. A. Rajesh, for the Degree of **Doctor of Philosophy**, was carried out by the candidate, under my supervision at Polymer Science and Engineering Division, National Chemical Laboratory, Pune 411 008, India. Such material as has been obtained from other sources has been duly acknowledged in the thesis.

Dr. S. Sivaram
(Research Guide)

DECLARATION BY RESEARCH SCHOLAR

I hereby declare that the thesis entitled: “**Synthesis, characterization and olefin polymerization reactivity of some early and late transition metal complexes**”, submitted for the Degree of **Doctor of Philosophy** to the University of Pune, has been carried out by me at Polymer Science and Engineering Division, National Chemical Laboratory, Pune 411 008, India, under the supervision of Dr. S. Sivaram. The work is original and has not been submitted in part or fully by me for any other degree or diploma to this or any other University.

A. Rajesh
(Research Scholar)

Dedicated to My Parents

Acknowledgement

I wish to express my deep sense of gratitude to my research supervisor Padma Shri Dr. Swaminathan Sivaram, Director, National Chemical Laboratory, for his invaluable guidance, constant inspiration, encouragement and constructive criticism during all stages of my work. His kind and understanding nature has made this training period a comfortable, inspiring and enlightening experience for me.

I am very much grateful to Dr. T.P.Mohandas and Dr. P.R. Rajamohanan for their valuable suggestions, useful discussions and help during various stage of the work.

I am thankful to all my lab-mates, Drs. Rajesh Kumar, Yanjarappa, Saptarshi, Subramanyam and Mrs. Amrita for their extensive help and cooperation throughout the entire period of my research at NCL. I convey my sincere thanks to Dr. P.K.Saxena, Mr D.H. Gholap, Mrs. Dhoble, Drs. D. Baskaran, P.P.Wadgaonkar, U. Natarajan, (Mr & Mrs) Idage, C. Ramesh, R. A. Kulkarni, C.V. Avadhani and Mr. Menon for their helpful attitude at all times of need. I am also thankful to all members of Polymer Chemistry Division, NCL, for maintaining a warm and friendly atmosphere.

I thank all my friends, Santhosh, Thomas, Joseph, Sony, Radhakrishnan, Tony, Harikrishna, Praveen, Pradeep, Suresh, Shivsankar, Rajagopal, Sureshan, Jayaprakash, Suju, Jinu, Shiju, Biju, Jolly, Shankar, Shijo, Mangalesh, Devraj, Prabal, Bhoje, Shyamroy, Raghu, Mahua, Sulatha, Nirmala, Gnaneshwar, Anuj, and Mallikarjun, for their friendship and cooperation.

I express my sincere thanks to Drs. Subhash Padhye, D.Srinivas, Mohan Bhadbhade, and Rajesh Gonnade for their help and useful discussions in understanding various analytical techniques.

I wish to thank Mr. Shaikh, Mrs. Gracy and Ms. Khare for their help in office matters.

I am thankful to my parents, brother, sister and all other family members for their love, unfailing support, trust and encouragement.

Finally, my thanks are due to Council of Scientific and Industrial Research, Government of India, for awarding the Junior and Senior Research Fellowships, and, Director, National Chemical Laboratory, to carry out my research work and extending all possible infrastructural facilities, and to allow to submit this work in the form of a thesis for the award of Ph.D. degree.

September 2007

A. Rajesh

CONTENTS

Glossary	viii
List of Tables	ix
List of Figures	xi
List of Schemes	xiii

CHAPTER 1. HOMOGENEOUS TRANSITION METAL CATALYSTS FOR OLEFIN POLYMERIZATION

1.1	Introduction	2
1.2	Early transition metal catalysts	2
1.2.1	Group 4 metallocenes	2
1.2.1.1	Brief historical perspective	2
1.2.1.2	Cocatalysts	5
1.2.1.2.1	Methylaluminoxane (MAO)	5
1.2.1.2.2	Modified methylaluminoxane (MMAO)	5
1.2.1.2.3	Other alkyl aluminoxanes	6
1.2.1.2.4	Boron cocatalysts	6
1.2.1.3	Mechanism of polymerization	6
1.2.2	Group 4 non-metallocene catalysts	7
1.2.2.1	Constrained geometry catalysts	7
1.2.2.2	Chelating diamides	10
1.2.2.3	β -Diketiminates	11
1.2.2.4	Chelating alkoxides and aryloxides	12
1.3	Late transition metal catalysts	14
1.3.1	Group 8 metal catalysts	15
1.3.2	Group 9 metal catalysts	20
1.3.3	Group 10 metal catalysts	21
1.3.4	Group 11 metal catalysts	33

1.4	Conclusions	36
1.5	References	37
CHAPTER 2. SCOPE AND OBJECTIVES		
2.1	Introduction	53
2.2	Objectives of the present work	55
2.3	References	56
CHAPTER 3. EXPERIMENTAL METHODS		
3.1	Introduction	59
3.2	Materials	59
3.3	Purification and drying	63
3.4	Polymerization techniques	63
3.4.1	Apparatus used for polymerization of ethylene at one bar pressure	63
3.4.2	Polymerization of ethylene at 1 bar pressure	65
3.4.3	Polymerization of ethylene at higher pressures	65
3.5.	Characterization techniques	66
3.5.1	Gel permeation chromatography	66
3.5.2	Differential scanning calorimetry	66
3.5.3	Intrinsic viscosity	67
3.5.4	Infra red spectra	67
3.6.5	Nuclear magnetic resonance spectra	67
3.5.6	Cyclic voltametry	67
3.5.7	Single crystal X-ray diffraction	67
3.5.8	Electron paramagnetic resonance spectra (EPR)	68
3.6.	References	69

CHAPTER 4. POLYMERIZATION OF ETHYLENE USING (α -DIIMINE) COPPER (II) COMPLEXES

4.1	Introduction	70
4.2	Experimental	73
4.2.1	Materials and their purification	73
4.2.2	Synthesis of (α -diimine) copper complexes	73
4.2.2.1	Synthesis of [(N,N'-diisopropylbenzene)-2,3-naphthyl-(1,4-diazabutadiene)] dichlorocopper(II) (2a)	73
4.2.2.1.1	Synthesis of [(N,N'-diisopropylbenzene)-2,3-naphthyl-(1,4-diazabutadiene)] (1a)	73
4.2.2.1.2	Synthesis of 2a	73
4.2.2.2	Synthesis of [(N,N'-diisopropylbenzene)-2,3-naphthyl-(1,4-diazabutadiene)] dibromocopper(II) (2b)	74
4.2.2.3	Synthesis of [(N,N'-2-tert-butylbenzene)-2,3-naphthyl-(1,4-diazabutadiene)] dichloro copper(II) (2c)	74
4.2.2.3.1	Synthesis of [(N,N'-2-tert-butylbenzene)-2,3-naphthyl-(1,4-diazabutadiene)] (1b)	74
4.2.2.3.2	Synthesis of 2c	74
4.2.2.4	Synthesis of [(N,N'-diisopropylbenzene)-2,3-naphthyl-(1,4-diazabutadiene)] chloro copper(I) (3a)	75
4.2.2.5	Synthesis of [(N,N'-diisopropylbenzene)-2,3-naphthyl-(1,4-diazabutadiene)] bromo copper(I) (3b)	75
4.2.2.6	Synthesis of [(N,N'-diisopropylbenzene)-2,3-naphthyl-(1,4-diazabutadiene)] dibromonickel(II) (4)	75
4.2.2.7	Synthesis of [(N,N'-diisopropylbenzene)(1,4-diazabutadiene)] dichloro copper(II) (6)	76
4.2.2.7.1	Synthesis of [(N,N'-diisopropylbenzene)(1,4-diazabutadiene)] (5)	76
4.2.2.7.2	Synthesis of 6	76
4.2.3	Synthesis of bis(oxazoline) copper(II) complexes	77
4.2.3.1	Synthesis of 2,2'-bis(1,3-oxazoline) dichlorocopper(II) (10a)	77
4.2.3.1.1	Synthesis of 2,2'-bis(1,3-oxazoline) (9a)	77

	4.2.3.1.2	Synthesis of 10a	78
4.2.3.2		Synthesis of 2,2'-bis[(4,4-dimethyl)-1,3-oxazoline]dichloro copper(II) (10b)	78
	4.2.3.2.1	Synthesis of 2,2'-bis[(4,4-dimethyl)-1,3-oxazoline] (9b)	78
	4.2.3.2.2	Synthesis of 10b	79
4.2.3.3		Synthesis of 2,2'-bis[(4-isopropyl)-1,3-oxazoline]dichloro copper(II) (10c)	79
	4.2.3.3.1	Synthesis of 2,2'-bis[(4-isopropyl)-1,3-oxazoline] (9c)	79
	4.2.3.3.2	Synthesis of 10c	80
4.2.3.4		Synthesis of 2,2'-bis[(4-tert-butyl)-1,3-oxazoline]dichloro copper(II) (10d)	81
	4.2.3.4.1	Synthesis of 2,2'-bis[(4-tert-butyl)-1,3-oxazoline] (9d)	81
	4.2.3.4.2	Synthesis of 10d	81
4.2.4		Synthesis of bis(benzimidazole) copper(II) complexes	82
	4.2.4.1	Synthesis of [1,1'-bis(benzimidazolyl) ethane] dichloro copper (II) (13a)	82
	4.2.4.1.1	Synthesis of [1,1'-bis(benzimidazolyl)ethane] (12a)	82
	4.2.4.1.2	Synthesis of 13a	83
	4.2.4.2	Synthesis of [1,1'-bis(benzimidazolyl) ethane] dibromo copper(II) (13c)	83
	4.2.4.3	Synthesis of [1,1'-bis(benzimidazolyl) pentane] dibromo copper(II) (13b)	83
	4.2.4.3.1	Synthesis of [1,1'-bis(benzimidazolyl)pentane] (12b)	83
	4.2.4.3.2	Synthesis of 13b	84
4.3		Results and discussion	84
	4.3.1	Synthesis and characterization of α -diimine copper complexes	84
	4.3.1.1	Crystal structure of copper complexes 2a-2c	85
	4.3.1.2	Spectroscopy	89
	4.3.1.3	Electrochemical studies	93
	4.3.2	Synthesis and characterization of bis(oxazoline)copper(II) complexes	94
	4.3.3	Synthesis and characterization of bis(benzimidazole)copper(II) complexes	95

4.3.4	Polymerization of ethylene using copper complexes	96
4.3.4.1	Polymerization of ethylene using (α -diimine) copper complexes 2a-2c, 3a, 3b, 6	96
4.3.4.1.1	Polymerization of ethylene at 1 bar ethylene pressure	96
4.3.4.1.2	Polymerization of ethylene at 3 and 5 bar ethylene pressures	96
4.3.4.2	Polymerization of ethylene using bis(oxazoline) and bis(benzimidazole) copper(II) complexes	103
4.3.4.3	Nature of active species in the polymerization of ethylene using copper(II) complexes	105
4.4	Conclusions	107
4.5	References	108

CHAPTER 5. POLYMERIZATION OF ETHYLENE USING *ansa*- η 5-MONOFUORENYL COMPLEXES OF GROUP 4 METALS

5.1	Introduction	111
5.2	Experimental	112
5.2.1	Materials	112
5.2.2	Synthesis of the complexes	112
5.2.2.1	Synthesis of <i>ansa</i> -(η 5-fluorenylcyclohexanolato) bis(tetrahydrofuran) titanium(IV)dichloride(3a)	112
5.2.2.1.1	Synthesis of <i>trans</i> -2-[9-(H)-fluorenyl] cyclohexanol (2)	112
5.2.2.1.2	Synthesis of TiCl ₄ (thf) ₂	113
5.2.2.1.3	Synthesis of 3a	113
5.2.2.2	Synthesis of <i>ansa</i> -(η 5-fluorenylcyclohexanolato) bis(tetrahydrofuran) zirconium(IV)dichloride(3b)	114
5.2.2.2.1	Synthesis of ZrCl ₄ (thf) ₂	114
5.2.2.2.2	Synthesis of 3b	114
5.2.2.3	Synthesis of <i>ansa</i> -(η 5-fluorenylcyclohexanolato)	

	bis(tetrahydrofuran) hafnium(IV)dichloride(3c)	115
	5.2.2.3.1 Synthesis of HfCl ₄ (thf) ₂	115
	5.2.2.3.2 Synthesis of 3c	115
5.3	Results and Discussion	115
5.3.1	Synthesis of <i>trans</i> -2-[9-(H)-fluorenyl cyclohexanol and its metal complexes	115
5.3.2	Polymerization of ethylene using complexes 3a-3c	123
5.3.2.1	Polymerization at 1 bar ethylene pressure	123
5.3.2.2	Polymerization at 5 bar ethylene pressure	123
5.3.2.2.1	Effect of nature of metal	123
5.3.2.2.2	Effect of MAO concentration	124
5.3.2.2.3	Effect of cocatalyst on polymerization of ethylene using complex 3b	125
5.3.2.2.4	Effect of added TMA	125
5.3.2.2.5	Effect of temperature	125
5.3.2.3	Characterization of polymer and oligomer fractions	126
5.3.2.3.1	Characterization of Fraction A	126
5.3.2.3.2	Characterization of Fraction A by ¹³ C NMR spectroscopy	128
5.3.2.3.3	Characterization of Fractions B and C by ¹ H and ¹³ C NMR spectroscopy	133
5.3.2.4	Copolymerization of ethylene with higher α-olefins	135
5.4	Conclusions	140
5.5	References	142
CHAPTER 6. POLYMERIZATION OF ETHYLENE USING AMIDO FUNCTIONALIZED HALF-SANDWICH COMPLEXES OF GROUP 4 METALS		
6.1	Introduction	144
6.2	Experimental	145
6.2.1	Materials	145
6.2.2	Synthesis of complexes	145

6.2.2.1	Synthesis of [(2,6-diisopropylphenylamido) (fluorenyl) diphenylsilane] titanium(IV) dichloride (3a)	145
6.2.2.1.1	Synthesis of [(2,6-diisopropylphenylamido) (fluorenyl) diphenylsilane] (2a)	145
6.2.2.1.2	Synthesis of 3a	146
6.2.2.2	Synthesis of [(2,6-diisopropylphenylamido) (fluorenyl) diphenylsilane] zirconium(IV) dichloride (3b)	147
6.2.2.3	Synthesis of [(2,6-dimethylphenylamido) (fluorenyl) diphenylsilane] titanium(IV) dichloride (3c)	147
6.2.2.3.1	Synthesis of [(2,6-dimethylphenylamido) (fluorenyl) diphenylsilane] (2b)	147
6.2.2.3.2	Synthesis of 3c	148
6.2.2.4	Synthesis of [(2,6-dimethylphenylamido) (fluorenyl) diphenylsilane] zirconium(IV) dichloride (3d)	148
6.3	Results and discussion	149
6.3.1	Synthesis and characterization of ligands and complexes	149
6.3.2	Ethylene polymerization using complexes 3a-3d	156
6.4	Conclusions	160
6.5	References	161
	CHAPTER 7. SUMMARY AND CONCLUSIONS	163
	APPENDIX A	I
	APPENDIX B	XXV

GLOSSARY

BuLi	Butyl lithium
CGC	Constrained geometry catalyst
COD	Cycloocatadiene
COSY	Correlation spectroscopy
Cp	Cyclopentadienyl
DEAC	Diethylaluminium chloride
Flu	Fluorenyl
Ind	Indenyl
MAO	Methylaluminoxane
MMAO	Modified methylaluminoxane
MWD	Molecular weight distribution
NOESY	Nuclear overhauser effect spectroscopy
PE	Polyethylene
PP	Polypropylene
PS	Polystyrene
TIBAL	Triisobutyl aluminium
TEAL	Triethylaluminium
THF	Tetrahydrofuran
TMA	Trimethylaluminium

LIST OF TABLES

Table 3.1	List of chemicals used	59
Table 4.1	Selected bond lengths and bond angles for complexes 2a-2c	87
Table 4.2	Polymerization of ethylene using the complexes 2a-2c and 6 /MAO	96
Table 4.3	Effect of temperature on catalyst activity and polymer properties using complex 2a /MAO	98
Table 4.4	Effect of Al/Cu ratio on catalyst activity and polymer properties using 2a /MAO	100
Table 4.5	Effect of diluent on catalyst activity and polymer properties	101
Table 4.6	Comparison of (α -diimine) copper and nickel catalysts	101
Table 4.7	Copolymerization of ethylene and hexene-1 using 2a /MAO	102
Table 5.1	^1H NMR assignment for 2	117
Table 5.2	Coupling constants of protons H_1 and H_2	120
Table 5.3	Effect of metal on catalyst activity and polymer properties using 3a-3c /MAO	123
Table 5.4	Polymerization of ethylene using 3b /MAO: Effect of Al/Zr ratio	124
Table 5.5	Ethylene polymerization using 3b :Effect of TMA	125
Table 5.6	Effect of temperature on polymerization of ethylene using 3b /MAO	126
Table 5.7	Characterization of Fraction A obtained with 3b /MAO	126
Table 5.8	^{13}C Chemical shifts and assignments for branched poly(ethylene)s	131
Table 5.9	Nature of branching and branching distribution of Fraction A obtained using 3b /MAO	133
Table 5.10	^1H NMR chemical shifts and their assignments for Fractions B and C	134
Table 5.11	Characterization of Fractions B and C	135
Table 5.12	Polymerization of ethylene with higher α -olefins using 3b /MAO	136
Table 6.1	Selected bond lengths and bond angles for 2a and 2b	154
Table 6.2	Polymerization of ethylene using complexes 3a-3d : Effect of metal and amido nitrogen substituent	157

Table 6.3	Polymerization of ethylene using complex 3b /MAO : Effect of Al/Zr ratio	157
Table 6.4	Polymerization of ethylene using complex 3b /MAO : Effect of polymerization temperature	158
Table 6.5	Comparison of 3b with N-alkyl substituted complexes	158

LIST OF FIGURES

Figure 3.1	Set up for polymerization of ethylene at one bar pressure	64
Figure 3.2	Buchi miniclave	66
Figure 4.1	Molecular structure and numbering scheme for 2a	88
Figure 4.2	Molecular structure and numbering scheme for 2b	88
Figure 4.3	Molecular structure and numbering scheme for 2c	89
Figure 4.4	IR spectra of 1a , 2a and 2b	90
Figure 4.5	UV –visible spectra of complexes 2a-2c	91
Figure 4.6	EPR spectra of complexes 2a-2c	92
Figure 4.7	Cyclic voltagrams of complexes 2a-2c	93
Figure 4.8	DSC thermogram of poly(ethylene)s obtained with 2a	99
Figure 4.9	¹³ C NMR spectrum of poly(ethylene)s prepared using catalyst 2a /MAO at 40°C	99
Figure 4.10	GPC of poly(ethylene)s obtained using 2a /MAO	100
Figure 4.11	GPC of poly(ethylene)s prepared using (α-diimine) copper and nickel complexes/MAO	102
Figure 4.12	Quantitative ¹³ C NMR spectrum of ethylene/hexene-1 copolymer prepared using 2a /MAO	103
Figure 4.13	Correlation between redox potential of the complexes 2a-2c and polymerization activity	106
Figure 4.14	Probable active species in the polymerization of ethylene with 2a /MAO	107
Figure 5.1.	¹ H NMR spectrum (in CDCl ₃ , 400 MHz) of 2	117
Figure 5.2.	¹³ C NMR spectrum (in CDCl ₃ , 100 MHz) of 2	118
Figure 5.3.	¹³ C-DEPT spectrum (in CDCl ₃ , 100 MHz) of 2	118
Figure 5.4.	COSY spectrum of 2	119
Figure 5.5	NOESY spectrum of 2	121
Figure 5.6	NOESY spectrum of 2 showing strong NOE between aromatic and	

	cyclohexyl ring protons	121
Figure 5.7	^1H NMR spectrum (in C_6D_6 , 500 MHz) of zirconium complex 3b	122
Figure 5.8	DSC thermogram of poly(ethylene)s obtained by 3a and 3b /MAO	124
Figure 5.9	DSC thermograms of Fraction A produced with catalyst 3b /MAO at different temperatures	127
Figure 5.10	GPC of Fraction A produced by 3b /MAO	127
Figure 5.11	Quantitative ^{13}C NMR spectrum (in $\text{C}_2\text{D}_2\text{Cl}_4$) of Fraction A obtained from 3b /MAO at 25°C	128
Figure 5.12	Quantitative ^{13}C NMR spectrum (in $\text{C}_2\text{D}_2\text{Cl}_4$) of Fraction A obtained from 3b /MAO at 40°C	129
Figure 5.13	Quantitative ^{13}C NMR spectrum (in $\text{C}_2\text{D}_2\text{Cl}_4$) of Fraction A obtained from 3b /MAO at 60°C	129
Figure 5.14	Quantitative ^{13}C NMR spectrum ($\text{C}_6\text{H}_4\text{Cl}_2/\text{C}_6\text{D}_6$) of Fraction A obtained from 3b /MAO at 80°C	130
Figure 5.15	Quantitative ^{13}C NMR spectrum (in $\text{C}_2\text{D}_2\text{Cl}_4$) of Fraction A obtained from 3b /MAO at 100°C	130
Figure 5.16	Nomenclature for branched poly(ethylene)s	131
Figure 5.17	^1H NMR spectrum of Fraction B obtained by 3b /MAO at 100°C	133
Figure 5.18	^{13}C NMR spectrum of Fraction B obtained by 3b /MAO at 100°C	134
Figure 5.19	^{13}C NMR spectrum (in $\text{C}_2\text{D}_2\text{Cl}_4$) of ethylene/hexene-1 copolymer	136
Figure 5.20	^{13}C NMR spectrum (in $\text{C}_2\text{D}_2\text{Cl}_4$) of ethylene/octene-1 copolymer	137
Figure 6.1	^1H NMR spectrum (CDCl_3 , 200 MHz) of 2a	151
Figure 6.2	^{13}C NMR spectrum (CDCl_3 , 50 MHz) of 2a	151
Figure 6.3	^1H NMR spectrum (CDCl_3 , 200 MHz) of 2b	152
Figure 6.4	^{13}C NMR spectrum (CDCl_3 , 50 MHz) of 2b	152
Figure 6.5	Molecular structure and numbering scheme for 2a	153
Figure 6.6	Molecular structure and numbering scheme for 2b	154
Figure 6.7	^1H NMR spectrum (C_6D_6 , 500 MHz) of 3b	155
Figure 6.8	^1H NMR spectrum (C_6D_6 , 500 MHz) of 3d	156

LIST OF SCHEMES

Scheme 1.1	Cossee mechanism for olefin polymerization using Ziegler-Natta catalysts	7
Scheme 4.1	Synthesis of (α -diimine) copper (II) and (I) complexes	86
Scheme 4.2	Synthesis of bis(oxazoline) ligands and copper(II) complexes	94
Scheme 4.3	Synthesis of bis(benzimidazole) ligands and copper(II) complexes	95
Scheme 5.1	Synthesis of <i>trans</i> -2-[9-H]-fluorenyl cyclohexanol and the metal complexes	116
Scheme 5.2	Mechanism for the formation of methyl branches	140
Scheme 6.1	Synthesis of the ligands and metal complexes 3a-3d	150

CHAPTER 1

HOMOGENEOUS TRANSITION METAL CATALYSTS FOR OLEFIN POLYMERIZATION

1.1. Introduction

In 1955, Ziegler discovered that poly(ethylene)s can be obtained by the polymerization of ethylene at atmospheric pressure and room temperature by using transition metal catalysts¹. This discovery led to the birth of polyolefin industry worldwide. Today annual production of poly(ethylene)s and poly(propylene)s exceed more than 100 million tons and constitute more than 55% of the global plastics industry. Polyolefins are characterized by several advantages, such as low weight, low energy consumption during polymerization and processing, low emission of volatiles, wide property ranges, versatility in application and ease of recycling. Group IV metallocene complexes have attracted considerable attention during the past two decades as a new class of catalysts capable of producing novel tailored polyolefin structures. More recently, there are many reports on polymerization of olefins by non-metallocene early and late transition metal catalysts. In this chapter, the advances in homogeneous transition metal catalysts for olefin polymerization are reviewed, with special reference to non-metallocene early and late transition metal catalysts.

1.2. Early transition metal catalysts

1.2.1. Group 4 metallocenes

1.2.1.1. Brief historical perspective

As early as 1957, metallocene catalysts for ethylene polymerization were reported by Natta et al² and by Breslow and Newburg³. They found that bis(cyclopentadienyl)titanium dichloride when activated with triethylaluminium or diethylaluminium chloride was effective in polymerizing ethylene. However, these catalysts were of no commercial importance as their catalyst activities were much lower than classical Ziegler-Natta catalysts and they were inactive towards polymerization of other α -olefins. In 1975, Meyer et al⁴ observed that addition of small amounts of water to bis(cyclopentadienyl)titanium dichloride-dimethylaluminium chloride system led to a significant increase in ethylene polymerization rate. Reichert and Meyer also reported a similar increase in activity upon addition of water to titanocene/diethylaluminium chloride system. Soon after, Kaminsky and Sinn⁵ reported that ethylene polymerization

activity increased to about 10^4 g PE $\text{mmol}^{-1}\text{Ti h}^{-1}$ when trimethylaluminium(TMA) pretreated with water (Al:H₂O = 2:1 to 5:1) was added to bis(cyclopentadienyl) titanium dimethyl. They attributed this increase in activity to the formation of an aluminoxane *via* hydrolysis of TMA. This was further evidenced by Kaminsky and Sinn^{6,7} from the observation that bis(cyclopentadienyl) zirconium dimethyl when activated with a preformed methylaluminoxane (MAO) resulted in an ethylene polymerization activity of about 10^4 g PE $\text{mmol}^{-1}\text{Zr h}^{-1}$. However, these early catalyst systems were unsuitable for commercial production of poly(ethylene)s and resulted in non-stereospecific polymerization of propylene to atactic poly(propylene)s due to symmetric nature of the active sites⁸.

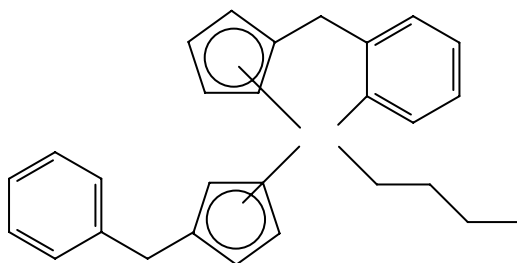
Significant increase in catalyst activity and molecular weights were reported by Ewen⁹ by modification of the structure of Kaminsky catalyst. He also reported the first stereoselective polymerization of propylene using a Cp₂TiPh₂/MAO system. This catalyst was shown to produce isotactic poly(propylene)s with a novel stereoblock structure by a chain-end stereocontrol mechanism, wherein, the chirality of the last inserted monomer unit determines the stereocontrol during polymerization. But the most significant breakthrough in the field of stereospecific propylene polymerization was on account of the discovery of *ansa*-metallocenes by Brintzinger et al¹⁰. They found that racemic isomer of *ansa*-metallocenes, such as, ethylene bis(indenyl)zirconium dichloride and ethylene bis(tetrahydroindenyl)zirconium dichloride in conjunction with MAO produced poly(propylene)s with very high activities and isotacticities of more than 95%. Ewen also reported the analogous hafnium catalysts which produced high molecular weight, highly isotactic poly(propylene)s¹¹. In these cases, stereocontrol is by enantiomorphic or catalytic site control mechanism, where, chirality of catalyst determines the stereochemistry of polymerization. Syndiospecific propylene polymerization was first reported by Ewen et al¹² using a Cs-symmetric catalyst, namely, isopropylidene cyclopentadienyl fluorenyl zirconium and hafnium dichlorides.

Cyclic olefins such as cyclopentene and norbornene were also polymerized by metallocene catalysts¹³⁻³². While classical Ziegler-Natta catalysts produce ring-opened products,

metallocene catalysts promote vinyl polymerization. Further developments led to catalysts which are capable of polymerizing styrene to syndiotactic poly(styrene)s³³⁻³⁶. Monomers containing functional groups such as hydroxyl, amino, carboxyl etc. were also homo-and copolymerized using metallocene catalysts³⁷⁻⁵⁴. In general, metallocene catalysts are capable of polymerizing almost all vinyl monomers with very high activity resulting in polymers with narrow molecular weight and composition distributions.

A number of reviews are available on metallocene catalyzed olefin polymerization⁵⁵⁻⁷⁷.

Recently a new family of metallacyclic metallocene catalysts (**1**) was reported by Alt⁷⁸. These catalysts exhibit higher activity than metallocenes and are self immobilizing in solution. These catalysts do not contain any halides and so the polymers produced do not release any hydrogen halides on thermal decomposition or combustion. This property



1

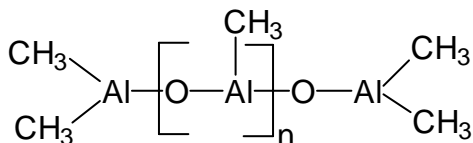
makes them eco-friendly. Higher activities of these catalysts may be attributed to their rigid structure and absence of halides. When the metallacycles are activated with MAO, the ring expands through repeated insertion of ethylene into the M-C σ -bond, finally resulting in an insoluble polymer that is directly attached to one π ligand of the active catalyst. Poly(ethylene)s produced by metallacycles possess lower molecular weights than metallocene dichlorides, presumably, due to more facile chain transfer reaction.

1.2.1.2. Cocatalysts

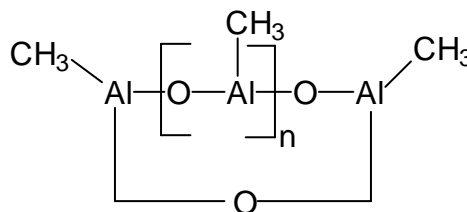
1.2.1.2.1. Methylaluminoxane(MAO)

Metallocene complexes as such are not olefin polymerization catalysts; they need to be activated with another component, usually, an organoaluminium compound in order to

exhibit polymerization activity. The most commonly used cocatalyst is methylaluminoxane (MAO). MAO is obtained by controlled hydrolysis of TMA. The exact structure of MAO still remains obscure. However, several studies have shown that MAO is composed of oligomers of $[-\text{Al}(\text{CH}_3)\text{-O-}]$ units with linear or cage structures and a molecular weight of roughly 800-1200. Generally, TMA (either unreacted or formed by disproportionation reactions between the oligomeric components) is present along with MAO. The role of MAO is to alkylate the metallocene dichloride and then abstract a methide ion to generate an electron deficient species which is responsible for the polymerization activity. TMA present in MAO acts as a scavenger of impurities as well as a chain transfer agent⁷⁹.



Linear structure



Cyclic structure

Recently Kissin and Brandolini reported an alternative route for synthesis of MAO by reaction of TMA with bis(trialkyltin)oxides $\text{R}_3\text{Sn-O-SnR}_3$ or with Me_3SnOH . They found that MAO produced by using AlMe_3 : Sn compound > 1 act as efficient cocatalysts for alkene polymerization as well as syndiospecific polymerization of styrene⁸⁰.

1.2.1.2.2. Modified methylaluminoxane (MMAO)

MMAO is a modified methylaluminoxane in which 25 % of the methyl groups are replaced by isobutyl groups. MMAO has got a longer shelf life than MAO⁸¹.

1.2.1.2.3. Other alkylaluminoxanes

Other than MAO, aluminoxanes such as ethylaluminoxane and isobutylaluminoxane are often employed in polymerization. These are obtained by hydrolysis of triethylaluminium and triisobutylaluminium respectively. They exhibit much lower activities when compared to MAO. Cryoscopic, ^1H , ^{17}O and ^{27}Al NMR studies have

shown that ethylaluminumoxane has a trimeric structure, while a dimeric structure has been proposed for isobutylaluminumoxane⁸².

1.2.1.2.4. Boron cocatalysts

One of the disadvantages of metallocene/MAO systems is the large amount of expensive MAO that is often needed for appreciable polymerization activity. Several organoboron compounds such as B(C₆F₅)₃, [PhNHMe₂][B(C₆F₅)₃], [Ph₃C][B(C₆F₅)₄] were also found to be efficient activators for metallocene-catalyzed polymerization of olefins. Reaction of these compounds with metallocene dialkyls such as Cp₂Zr(CH₃)₂ and Et(Ind)₂Zr(CH₃)₂ results in the formation of a 14 electron species, [Cp₂Zr(CH₃)]⁺ which is the true active species in polymerization^{83,84}. It was observed by Bochmann and Lancaster⁸⁵ that zirconium dibenzyl complexes react with boron activators to give cationic Zr-benzyl complexes which are thermally more stable than analogous cationic methyl complexes. This may be attributed to Zr-phenyl interaction that reduces electron deficiency of the metal center. Several modifications of boron cocatalysts have been reported recently. It is generally observed that more weakly coordinating anions result in higher polymerization activity. Certain carboranes were also found to be effective activators for metallocene-catalyzed olefin polymerizations^{86,87}.

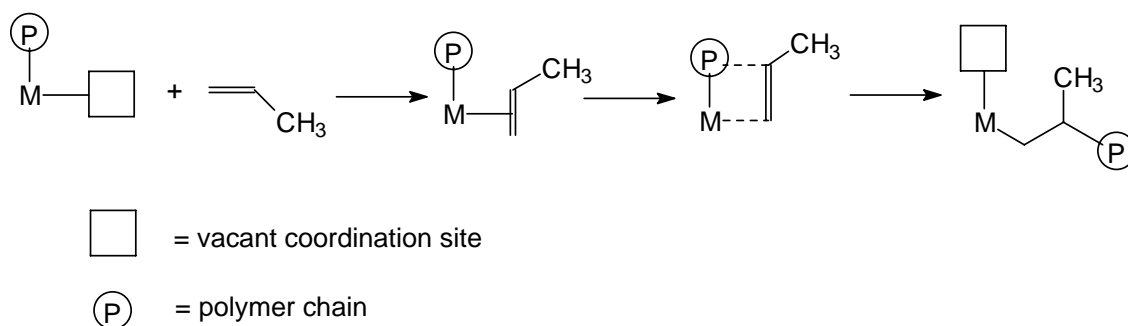
Several types of cocatalysts, their role as activators in olefin polymerization and their activation mechanism were recently reviewed by Chen and Marks⁸⁸.

1.2.1.3. Mechanism of polymerization

It is now well established that reaction of zirconocene dichlorides or dialkyls yield three co-ordinated 14 electron species which is the true active species in polymerization. MAO first alkylates the metallocene dichloride and then abstracts a methide ion resulting in the formation of the active species. MAO also acts as a counterion which hinders recombination of zirconocene cation with chloride or methide ion.

The Cossee mechanism^{89, 90} originally proposed for conventional Ziegler-Natta catalysts is also the most plausible mechanism for metallocene catalysts. It involves coordination

of the monomer at the vacant site of the metal center, followed by migratory insertion into the M-R bond. Polymer chain growth occurs through a four-membered transition state. Molecular orbital calculations have shown that once the olefin coordinates to the metal, insertion takes place rapidly. The driving force for this is the energy gained upon transformation of M-R and C=C bonds to M-C and C-C bonds.

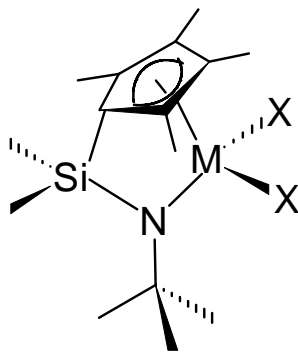


Scheme 1.1 Cossee mechanism for olefin polymerization using Ziegler-Natta catalysts

1.2.2. Group 4 non-metallocene catalysts

1.2.2.1. Constrained geometry catalysts (CGC)

Researchers at Dow^{91,92} and Exxon⁹³⁻⁹⁵ contributed to the development of metallocene analogous, mono-cyclopentadienyl amido complexes (**2**) which are known as “constrained geometry catalysts”. These mono-cyclopentadienyl complexes are characterized by a covalently linked amide donor which stabilizes the metal center electronically, and a short bridging group which opens up one side of the complex. The Cp-M-N angle is less than 115°. As a consequence, these complexes are capable of incorporating long chain α -olefins and sterically hindered monomers such as styrene into polyethylene chains.



2

Constrained geometry catalysts produce polyolefins with narrow molecular weight and comonomer distributions. Generally, narrow molecular weight and comonomer distributions were found to improve physical properties at the expense of processability. Dow has developed a new technology called “INSITE” which produces polymers with good physical properties without sacrificing processability⁹⁶. Improved processability could be due to the presence of small amounts of long chain branching resulting from reincorporation of α -olefins produced as a result of β -H transfer at higher temperatures. Evidence for this mechanism was reported by Soga and coworkers^{97,98} who polymerized ethylene with oligoethylene and polypropylene macromonomer.

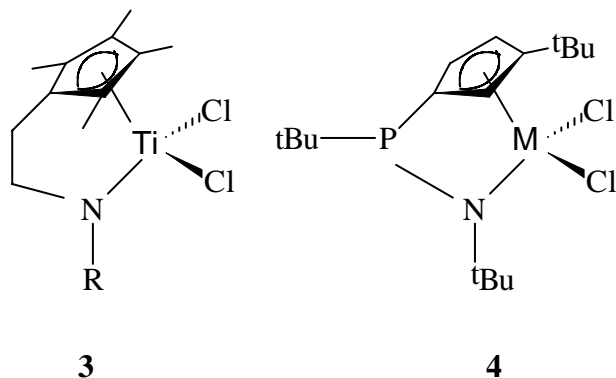
Dow INSITE technology is capable of producing polyolefin elastomers (POE) and polyolefin plastomers (POP) by copolymerization of ethylene with α -olefins such as hexene-1, octene-1 and decene-1. Stevens studied the effect of Cp substituents, bridging group and metal in the copolymerization of ethylene with octene-1 using the constrained geometry catalyst, $[\text{Me}_2\text{Si}(\text{Me}_4\text{Cp})\text{N}^t\text{Bu}]\text{TiCl}_2/\text{MAO}$ ⁹⁹. Ultra-low density elastomers with as high as 56 mol% octene-1 content were obtained under appropriate polymerization conditions.

Conventional Ziegler-Natta catalysts incorporate only very small amounts of styrene (<1 mol %) into polyethylene chains^{100,101}. In most cases, mixtures of homopolymers were produced and polymer molecular weights were also very low^{102,103}. Metallocenes exhibit very low activities and poor regiospecificity in such copolymerizations. Constrained

geometry catalysts are capable of copolymerizing ethylene and styrene with very high activities, high styrene contents and no contamination with polystyrene impurities¹⁰⁴⁻¹⁰⁹. The reactivity ratios calculated by Fineman-Ross method was found to be 23.4 for ethylene and 0.015 for styrene. Sernetz et al studied the effect of ligands on ethylene-styrene copolymerization using constrained geometry catalysts. They observed that sterically hindered catalysts show higher activity due to high electron density at the metal¹¹⁰. Xu obtained a perfectly alternating ethylene-styrene copolymer with well-defined isotactic structure using the catalyst system $[\text{Me}_2\text{Si}(\text{Flu})(\text{N}^t\text{Bu})\text{TiMe}][\text{B}(\text{C}_6\text{F}_5)_4]$ ¹¹¹. In another study, Chung and Lu reported copolymerization of ethylene with a reactive monomer such as p-methylstyrene which can form crosslinking networks to produce stable residues desirable for elastomers¹¹². A broad range of polyolefin elastomers based on terpolymers of ethylene with p-methyl styrene and a third olefin such as propylene and octene-1 was also produced using constrained geometry catalysts.

Copolymerization of ethylene with cyclic olefins such as norbornene using various constrained geometry catalysts has been reported¹¹³. In all cases, unexpectedly low norbornene incorporations (<50 mol %) were observed. Microstructure of the copolymers depends on catalyst structure, yielding copolymers with mainly isolated norbornene units, alternating monomer sequences or short norbornene microblocks.

Several modifications of constrained geometry catalysts have been reported in the literature. Teuben and coworkers¹¹⁴ reported ethylene bridged titanium complexes (**3**) which showed higher activities for homopolymerization of ethylene and its copolymerization with octene-1 than the corresponding SiMe_2 bridged complexes. A phosphorus-bridged cyclopentadienyl amide titanium complex (**4**) was reported by Kotov et al¹¹⁵ which produced linear high molecular weight poly(ethylene)s with an activity of $100 \text{ g PE mmol}^{-1}\text{Ti h}^{-1} \text{ bar}^{-1}$. Park and coworkers reported bridged cyclopentadienyl hydrazido titanium complexes which exhibit lower activities for polymerization of ethylene but produce high molecular weight polymers¹¹⁶.



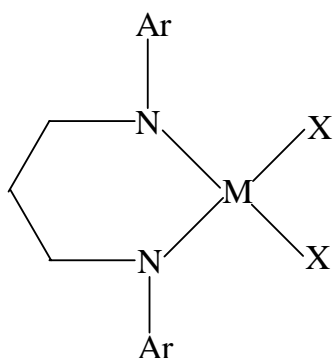
Several indenyl and fluorenyl constrained geometry catalysts that exhibit higher activities for the polymerization of ethylene have also been reported¹¹⁷⁻¹²¹. Klosin et al reported heteroatom substituted constrained geometry complexes which when activated with $B(C_6F_5)_3$ show dramatic increase in activity for ethylene/octene-1 copolymerizations¹²².

Bazan and coworkers reported the use of a combination of a constrained geometry catalyst and a boratabenzene zirconium catalyst for obtaining long chain branched poly(ethylene)s without addition of another olefin¹²³. The boratabenzene complex oligomerizes ethylene to α -olefins which get incorporated into polyethylene chains produced from constrained geometry catalysts. This is termed as “tandem catalysis” wherein two independent catalysts work cooperatively to produce a single product¹²⁴.

1.2.2.2. Chelating diamides

In 1996, McConville and coworkers reported chelating diamide complexes of titanium (**5**) bearing bulky substituents which are capable of polymerizing higher α -olefins with very high activities^{125,126}. For example, hexene-1 is polymerized with an activity of 3.5×10^5 g poly(hexene) $\text{mmol}^{-1} \text{Ti h}^{-1}$. Activities of these catalysts decrease in toluene which may be attributed to the possible coordination of toluene to titanium that decreases the rate of insertion of hexene-1. It was observed that chain transfer to aluminium is the only chain termination mechanism for these catalysts when MAO was used as cocatalyst¹²⁷. However, when boron activators such as $B(C_6F_5)_3$ are used, no chain transfer occurs, resulting in a living polymerization system. Thus the catalyst system

$[\text{ArN}(\text{CH}_2)_3\text{NAr}]\text{TiMe}_2/\text{B}(\text{C}_6\text{F}_5)_3$ polymerizes hexene-1, octene-1 and decene-1 with high molecular weights and narrow polydispersities(1.05-1.11). Catalyst activities and polymer molecular weights increase when polymerizations are run in dichloromethane which may be due to greater charge separation between the ions in presence of polar solvent. Uozumi and coworkers obtained isotactic poly(propylene)s using chelating diamide complexes with various $\text{AlR}_3/\text{Ph}_3\text{CB}(\text{C}_6\text{F}_5)_4$ cocatalysts and found that higher isotacticities were observed when bulky aluminium alkyls such as trihexyl or trioctyl aluminum were used^{128, 129}. Isotacticities were also found to increase in presence of cyclohexene at low propylene concentrations. Several modifications of these catalysts have been reported by research groups of Shiono¹³⁰, Park^{131,132} and Nomura¹³³⁻¹³⁵.

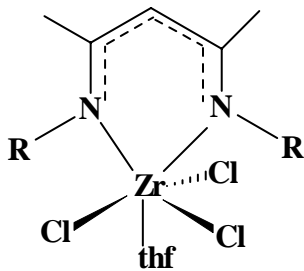


M = Ti, Zr
X = Cl, Me, CH₂Ph

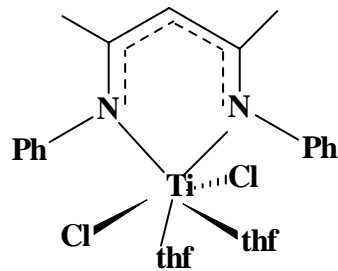
5

1.2.2.3. β -Diketiminates

Recently several early transition metal complexes bearing β -diketimate or “nacnac” ligands have been reported. However, their polymerization activities were very low. Jin and Novak reported a series of mono(β -diketimate) zirconium(IV) complexes (**6**) which exhibit activity of $45\text{g PE mmol}^{-1} \text{Zr h}^{-1} \text{bar}^{-1}$ ¹³⁶. These catalysts were stable for longer



6



7

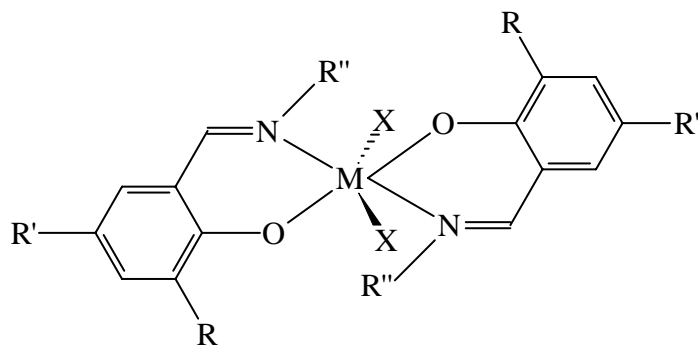
reaction periods (16 h). A β -diketiminato Ti (III) complex (**7**) was reported by Theopold which also exhibit very low activity¹³⁷.

Collins and coworkers reported bis(β -diketiminato) zirconium complexes which are slightly more active than the mono(β -diketiminato) complexes and yield poly(ethylene)s with narrow molecular weight distributions¹³⁸. Zirconium complexes in which the β -diketiminato ligand is in the η^5 coordination mode (6 electron donor) exhibit activities as high as $2200 \text{ g mmol}^{-1}\text{Zr h}^{-1} \text{ bar}^{-1}$ when electron withdrawing $p\text{-CF}_3\text{C}_6\text{H}_3$ substituents are present on the nitrogen¹³⁹.

1.2.2.4. Chelating alkoxides and aryloxides

In 1999, Fujita reported group 4 metal complexes based on chelating bis(phenoxyimine) ligands (**8**) which showed very high activity and afforded poly(ethylene)s with very high molecular weights^{140,141}. A series of complexes with differing substituents on the aromatic as well as on the imino nitrogen and their polymerization activities have been reported¹⁴²⁻¹⁶³. The nature of metal, substituents on imino nitrogen and *ortho*-substituents on phenoxy moiety were found to have a dramatic influence on catalyst activity and molecular weight of the polymer. Catalyst activity decreases in the order $\text{Zr} \gg \text{Hf} > \text{Ti}$ ¹⁴⁵. Polymerization activity decreases and molecular weight increases up on increasing the steric bulk of the imino substituent. Increasing the steric bulk of the *ortho*-phenoxy substituent increases catalyst activity, which is believed to be due to better cation-anion separation in the active species as well as increased protection of the oxygen towards

electrophilic attack by TMA present in MAO^{144,145}. When bulky substituent such as cumyl was present at the *ortho*-position of phenoxide moiety, very high molecular weight poly(ethylene)s were obtained. When the imino nitrogen was substituted with cyclic groups such as cyclopropyl, cyclobutyl, cyclopentyl or cyclohexyl, vinyl-terminated linear, low molecular weight poly(ethylene)s were produced. Phenoxy-imine catalysts possessing hexyl or cyclohexyl group on imino nitrogen and cumyl and methoxy groups at the *ortho*- and *para*- positions of the phenoxide, respectively, are thermally stable at 75°C. Replacing the phenoxy-imine ligands by a phenoxy-pyridine or phenoxy-indolide ligands resulted in complexes which showed lower activities. Polymerization of higher olefins such as propylene and hexene-1 as well as copolymerization of ethylene with propylene using the Group 4 bis(phenoxyimine) complexes are also reported in the literature.



8

Living polymerization of ethylene and propylene at room temperature as well as at 75°C was achieved with phenoxyimine catalysts bearing fluorinated substituents such as C₆F₅, C₆H₂F₃, C₆H₃F₂ or C₆H₄F on imino nitrogen. Density functional theory (DFT) calculations showed that in the active species, fluorine adjacent to the imine nitrogen interacts with β-H of the polymer chain resulting in the prevention of β-H transfer. Living polymerization of propylene was found to be syndiospecific via a chain-end control mechanism. Polyethylene-*b*-(polyethylene-*co*-polypropylene) diblock and polyethylene-*b*-(polyethylene-*co*-polypropylene)-*b*-polypropylene triblock copolymers were synthesized under these conditions.

Several complexes which contain aryloxy or alkoxide ligands in combination with cyclopentadienyl moiety were active for polymerization of olefins. Marks et al reported a phenolic bifunctional mono-Cp titanium complex which in combination with boron activators was active for polymerization of ethylene, propylene and styrene¹⁶⁴. Gielens et al reported a cationic titanium complex with linked Cp-alkoxide ancillary ligand which polymerized propylene to atactic poly(propylene)s in presence of $B(C_6F_5)_3$ ¹⁶⁵. Several non-bridged titanium cyclopentadienyl-aryloxy complexes of the type $CpTi(OAr)X_2$ and their use in polymerization of olefins were reported by Nomura et al¹⁶⁶⁻¹⁷¹. These complexes are capable of producing poly(ethylene)s, poly(ethylene-co-octene-1) and poly(ethylene-co-styrene) with reasonable activity, molecular weight, polydispersity and composition distribution.

Kasi and Coughlin immobilized cyclopentadienyl aryloxy titanium complexes (piano stool complexes) on 4-hydroxystyrene-styrene copolymer and examined such polymer supported complexes for polymerization of olefins¹⁷². These supported catalysts produced branched poly(ethylene)s with exclusively butyl branches in contrast to the unsupported catalyst that produces high density poly(ethylene)s. Presence of macroligated catalyst is vital for formation of butyl branches in poly(ethylene)s. Formation of butyl branches was attributed to the production of hexene-1 by trimerization of ethylene and subsequent copolymerization with ethylene. Copolymerization of ethylene with octene-1 and styrene¹⁷³ was also studied using these catalysts.

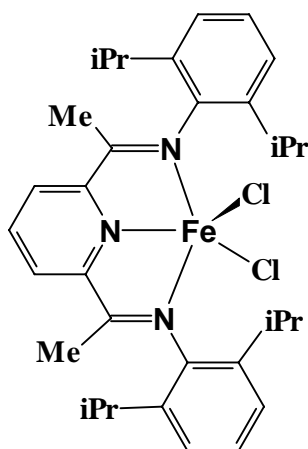
1.3. Late transition metal catalysts

In contrast to the wealth of information on olefin polymerization using early transition metal catalysts, there are only few reports of the use of late transition metal complexes for olefin polymerization. This is because late transition metal catalysts were generally expected to exhibit lower activities for olefin insertion relative to early metal catalysts, since β -hydride elimination competes with chain growth resulting in the formation of low molecular weight materials. However with the discovery by Brookhart and his group of a new family of cationic nickel(II) and palladium(II) catalysts capable of producing high

molecular weight poly(ethylene)s and poly(α -olefin)s, the field of late transition metal catalysts underwent a major transformation¹⁷⁴. Lower oxophilicity and greater functional group tolerance of late transition metals relative to early metals make them attractive as potential catalysts for copolymerization of ethylene with polar comonomers such as (meth)acrylates, vinyl acetate, CO etc. Many catalysts based on group 8-11 metals for polymerization of olefins are reported in the literature.

1.3.1. Group 8 metal catalysts

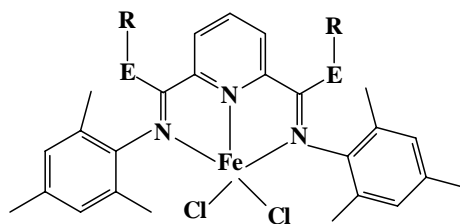
One of the recent additions to growing number of highly active non-metallocene polymerization catalysts are based on bis (imino) pyridine iron systems (**9**) with bulky substituents at *ortho*-positions of the aromatic ring, developed by Gibson and coworkers¹⁷⁵. These complexes have a five-coordinate pseudo-square pyramidal conformation. Steric bulk of *ortho*-substituents above and below the metal center is crucial for the formation of high molecular weight polymers¹⁷⁶. When a less bulky 2-MeC₆H₄ substituent was present, these catalysts showed remarkable selectivity towards oligomerization¹⁷⁷⁻¹⁷⁸. In addition to β -H transfer, chain transfer to aluminium was also a chain termination mechanism for these catalysts resulting in the formation of polymers with broad and sometimes bimodal molecular weight distributions¹⁷⁶. Substitution of the central pyridine donor for a pyrimidine ring resulted in slight reduction of activity and formation of polymers with narrow molecular weight distributions and an increased proportion of unsaturated end groups¹⁷⁹.



9

Nature of the pendant imino donor also influences polymerization activity and resulting polymer properties. Ketimine complexes are about an order of magnitude more active than their aldimine analogues¹⁷⁶. When the imino moiety was replaced by neutral amino donors, only low to moderate ethylene polymerization activities were observed. This observation may be due to the different orientation of the aryl substituents when the amino donor is used which may lead to more hindered access of the monomer¹⁸⁰.

Several groups have studied the effect of aryl substitution pattern on catalytic activity and resulting polymer properties. Gibson and coworkers have recently reported iron catalysts that bear ether and thioether substituents (**10**) that exhibit ethylene polymerization activity¹⁸¹. They found that the methoxy-substituted catalyst system was inactive towards polymerization whereas the bulky ether and thioether substituted systems showed higher activity for polymerization of ethylene resulting in broad molecular weight distributions.

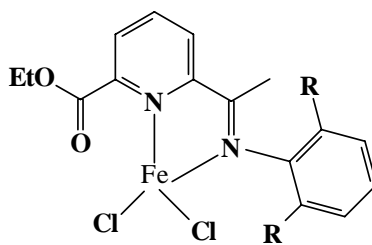


E = O, S

10

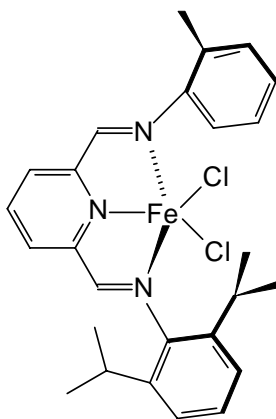
Several 2-(carboxylato)-6-iminopyridine iron catalysts with alkyl or halogen substituents at *ortho*-position (**11**) have been reported which in presence of MAO oligomerize or polymerize ethylene depending on steric bulk at *ortho*-positions¹⁸². All these complexes oligomerize ethylene to produce butenes and hexenes and small amounts of higher oligomers with more than 93% selectivity for linear α -olefins. Catalysts with methyl or ethyl substituents also produce isolable amounts of poly(ethylene)s. Catalyst activity increased four fold when polymerization was performed in dichloromethane rather than in toluene. Presence of an auxiliary ligand such as PPh₃ was found to enhance catalyst activity marginally. Bis(imino)pyridyl iron complexes with *ortho*-CF₃ aryl substituents were reported by Gibson and coworkers. These complexes exhibit higher activities for polymerization of ethylene than their non-fluorinated analogues¹⁸³. The activities as high

as $17000 \text{ g mmol}^{-1} \text{ h}^{-1} \text{ bar}^{-1}$ were obtained. Introduction of *ortho*-CF₃ substituent also increased the polymer molecular weights.



11

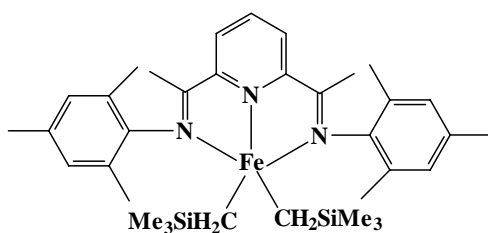
Bianchini et al reported a C₁-symmetric iron complex (**12**) that simultaneously polymerized and oligomerized ethylene to α -olefins with Schulz-Flory distribution¹⁸⁴. Due to the C₁-symmetry of the complex two atropisomeric propagating alkyl species may be formed. An incoming ethylene molecule will have *re* and *si* faces available at the metal for coordination and propagation. Insertion through *re* face leads to polyethylene production while insertion through *si* face results in only α -olefins. Poly(ethylene)s produced by this catalyst are highly crystalline with no branching. Oligomerization was highly selective with 95% even α -olefins with Schulz-Flory distribution parameter of 0.71.



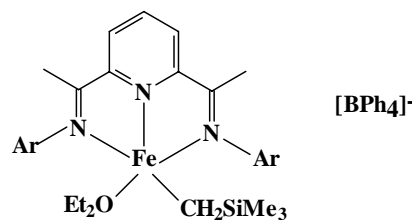
12

Synthesis of single component iron (II) alkyl complexes (**13**) by direct alkylation of the dichloride complexes has been reported recently¹⁸⁵. This complex showed low activity

for polymerization of ethylene and produced polymers with narrower molecular weight distributions than the corresponding chloride complexes. Campora et al synthesized a bis(pyridine) iron dialkyl complex (**14**) by the reaction of bis(pyridine)iron dichloride with alkyl magnesium chloride followed by reaction with 2,6-diiminopyridine ligands¹⁸⁶. This complex showed ethylene polymerization activity in presence of MMAO. The activities increased in presence of TIBAL or TMA. Even $ZnMe_2$ and $MeAl(OAr)_2$ also activated this catalyst.



13



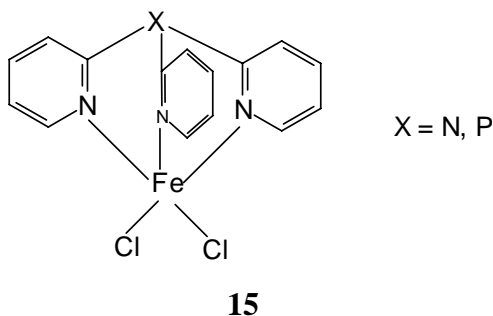
14

A novel macrocyclic trinuclear bis(imino)pyridyl iron catalyst was reported in which the central iron atom is located inside the macrocyclic ligand¹⁸⁷. The catalyst exhibited higher activity and longer lifetime for polymerization of ethylene using MMAO and resulted in poly(ethylene)s with high molecular weights and high melting points. Formation of high molecular weight polymers may be due to the fact that the macrocyclic ligand restrains the active iron centre from deactivation and controls the chain transfer reactions.

Gibson et al reported bis(imino)pyridine iron complexes bearing ferrocenyl substituents that when activated with MAO produce linear poly(ethylene)s with an activity of 6900 g PE $mmol^{-1}Fe h^{-1}bar^{-1}$ and Mw as high as 9×10^5 . These complexes exhibit quasi-reversible oxidation and reduction waves that make them applicable for redox-active polymerization of ethylene¹⁸⁸.

Iron(II) complexes based on tris(pyridyl)amine and tris(pyridyl)phosphine ligands¹⁸⁹ have been employed as catalysts for polymerization of ethylene along with MAO. The catalysts exhibited moderate to high activities ($32-271 g PE mmol^{-1}Fe h^{-1}bar^{-1}$) and no significant increase in activity was observed on changing the bridgehead nitrogen atom

by a phosphorus atom. However five-to-six-fold increase in catalyst activities was observed at higher polymerization temperatures. Molecular weights as high as 304,000 were obtained even at 60°C and monomodal molecular weight distributions were in the range of 4.7-7.1.



Self immobilization of bis(imino)pyridyl iron complexes has been achieved by employing ligands bearing ω -alkenyl substituents¹⁹⁰. Such self immobilized catalysts produced poly(ethylene)s with monomodal molecular weight distributions, in contrast to the unsubstituted catalysts that result in bimodal molecular weight distributions. The monomodal molecular weight distributions can be attributed to incorporation of the active centers in the growing chains that prevents interaction with MAO counterion which in turn disfavours the chain transfer reactions.

Copolymerization of ethylene with higher α -olefins were also studied using the bis(imino)pyridine iron complexes. However in all cases very low α -olefin incorporation was observed¹⁹¹⁻¹⁹⁴.

Other catalysts for polymerization of ethylene based on tridentate ligands such as furan¹⁹⁵ and pyrrole^{196,197} derivatives have also been reported. However catalytic activities of these complexes are generally very low.

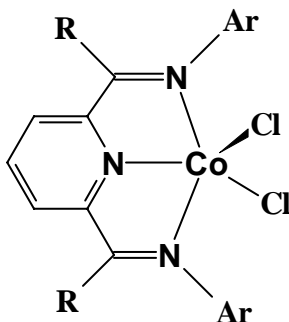
Active species for polymerization in the case of iron based catalysts was initially presumed to be a 14 electron cationic Fe(II) alkyl species¹⁹⁸. Based on EPR and Mossbauer studies Gibson and coworkers reported that the initial Fe(II) complex is

oxidized to an Fe(III) species upon activation with MAO¹⁹⁹. However recent study by Bryliakov et al revealed that in the case of bis(imino)pyridyl Fe(II) complex, [LFe(II)Cl(μ-R)₂ AlR₂] or [LFe(II)R(μ-R)₂ AlR₂] are the active species for AlR₃ activated systems whereas for MAO activated systems ionic species of the type [LFe(II)(μ-Me) (μ-Cl) AlMe₂] [Me-MAO]⁻ or [LFe(II) (μ-Me)₂ AlMe₂] [Me-MAO]⁻ are formed²⁰⁰.

1.3.2. Group 9 metal catalysts

As early as 1985, Brookhart and coworkers reported Co(III) complexes of the general structure [C₅Me₅P(OMe)₃CO(CH₂=CHR)-μ-H]⁺ (R = H, alkyl or aryl) which are active for polymerization of ethylene. This cationic compound shows a β-agostic interaction and inserts ethylene in a living fashion to form high molecular weight polymers (M_n = 20,000) with narrow polydispersity (M_w/M_n = 1.11-1.16). Activities are generally low which can be improved by use of non-coordinating counter ions such as B[3,5-(CF₃)₂C₆H₃]₄⁻. End functionalized poly(ethylene)s can be synthesized using this system when R possesses a functional group such as C₆H₅, C₆H₄CF₃, SiEt₃, SiMe₂Cl etc²⁰¹.

High activity cobalt catalysts for polymerization of ethylene based on bis(imino)pyridine ligands (**16**) exhibit an activity of 460 gPE mmol⁻¹ Co h⁻¹ bar⁻¹ when activated by MAO which is the highest for cobalt based catalysts reported to date¹⁷⁵. Cobalt catalysts based on bis(phosphinimide) pyridine²⁰² or imino pyrrolide¹⁹⁶ ligands exhibit only moderate activities for polymerization of ethylene.



16

Longo et al reported that cobaltocene showed an activity of 30 g PE mmol⁻¹ Co h⁻¹ bar⁻¹ for ethylene and resulted in poly(ethylene)s with narrow polydispersity and melting point of 136°C²⁰³.

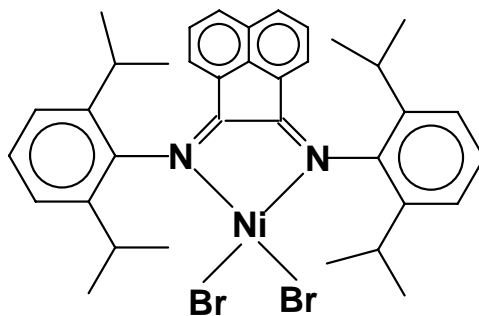
A cobalt diimine complex was also found to exhibit an activity of 340 gPE mmol⁻¹Co h⁻¹ bar⁻¹ upon activation with MAO. The catalyst produced branched oligomeric oils in contrast to the related nickel complexes, which result in high molecular weight poly(ethylene)s with very high activity²⁰⁴⁻²⁰⁵.

A dicationic triazacyclononane based rhodium complex was reported that show very low activity of about one turn over per day at 60 bar ethylene pressure²⁰⁶. This is the first example of a catalyst capable of polymerizing ethylene in water²⁰⁷.

Mechanistic investigations on cobalt bis(imino)pyridyl catalysts revealed that a cationic Co(I) alkyl species that contain no Co-alkyl bond is formed initially upon activation with MAO. Polymerization is initiated from this species by the incorporation of alkyl groups from the cocatalyst involving attack of methide ion on a Co-ethylene species^{208,209}.

1.3.3. Group 10 metal catalysts

An significant advance in the field of late transition metal polymerization is due to Brookhart and coworkers who showed that nickel(II) and palladium(II) complexes bearing bulky α -diimine ligands (**17**) are capable of polymerizing ethylene and higher α -olefins to high molecular weight polymers¹⁷⁴. The steric and electronic factors of the α -diimine ligands can be varied to obtain polymers with specific properties. Hindered aryl groups on the α -diimine nitrogen atoms block the axial coordination sites and retard chain transfer relative to propagation, resulting in high molecular weight polymers.



17

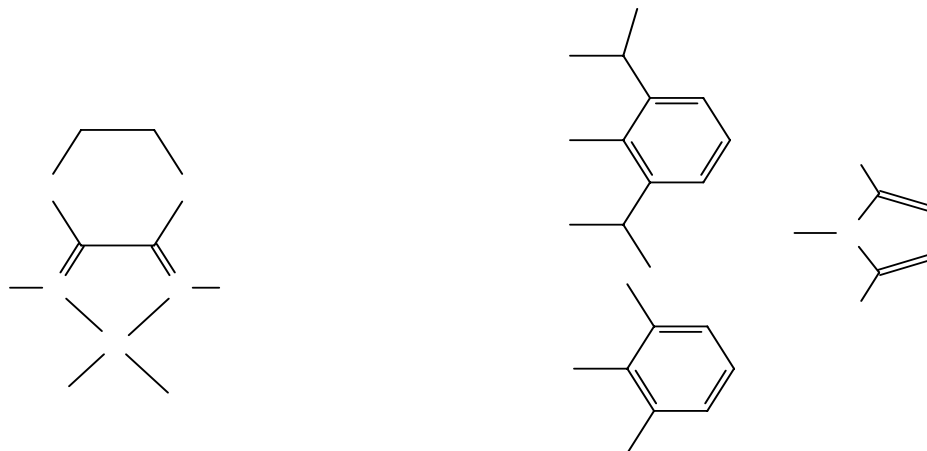
These complexes polymerize ethylene, producing poly(ethylene)s with microstructures ranging from almost linear to hyperbranched depending on the catalyst used and reaction conditions. Nickel(II) and palladium(II) complexes also exhibit good functional group tolerance and, hence, can be used for copolymerization of ethylene with polar comonomers such as acrylates. A variety of complexes is reported in academic and patent literature and is reviewed by Ittel et al²¹⁰ and Gibson and Spitzmesser²¹¹.

Strauch et al²¹² reported that reaction of (α -diimine)Ni(η^4 -butadiene) with B(C₆F₅)₃ produces a zwitterionic complex which polymerizes ethylene without any cocatalyst with an activity of 80 gPE mmol⁻¹ Ni h⁻¹ bar⁻¹.

Several neutral and cationic nickel and palladium complexes with unsymmetrical imino-pyridine ligands are reported which generally show very low activities for polymerization of ethylene and produce low molecular weight polymers²¹³⁻²¹⁷.

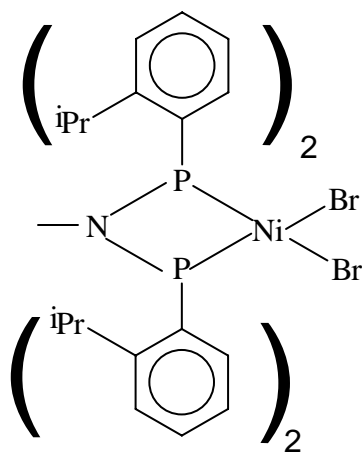
A novel family of nickel and palladium diimine complexes bearing 1,4-dithiane, triazole or imino carboxylate ligands were reported by scientists from Eastman Tennessee and has been introduced under the name GAVILAN catalyst technology²¹⁸⁻²²⁴. This family of catalysts (**18**) exhibit excellent catalyst activity and thermal stability at commercially relevant process temperatures. They produced branched poly(ethylene)s with narrow molecular weight distributions. They were also active for polymerization of α -olefins,

cycloolefins, copolymerization of olefins with polar comonomers like carbon monoxide, vinyl ethylene carbonate etc. Copolymerization of norbornene and functional group containing norbornene has also been achieved using these catalysts. The copolymers exhibit narrow molecular weight and composition distributions.

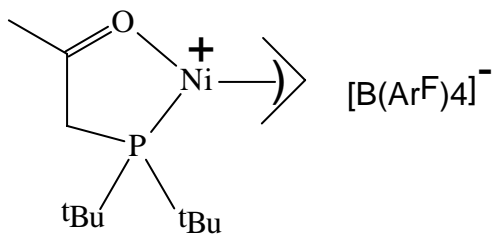


18

In addition to the α -diimine complexes, several phosphorus based nickel and palladium complexes are reported. Pringle, Wass and coworkers²²⁵ reported a phosphine-based nickel complex (**19**) which showed high ethylene polymerization activities of 2200 gPE mmol⁻¹ Ni h⁻¹. Brookhart and coworkers²²⁶ reported a single component nickel catalyst bearing a neutral [PO] ligand (**20**) which exhibit ethylene polymerization activity of 700 gPE mmol⁻¹ Ni h⁻¹ bar⁻¹. This catalyst also copolymerized ethylene with methyl-10-undecenoate with upto 6.6 mol% comonomer incorporation.

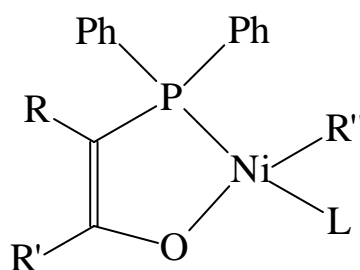


19



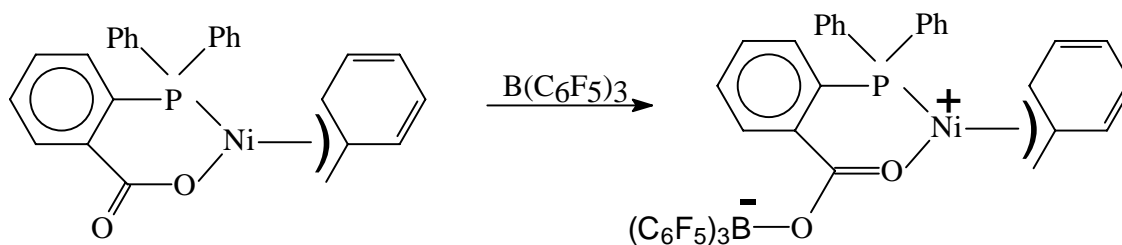
20

Nickel catalysts based on monoanionic [PO] ligands have been extensively studied for ethylene oligomerization in the so-called Shell Higher Olefin Process (SHOP). High molecular solid poly(ethylene)s can also be obtained by using these catalysts by proper choice of reaction conditions^{227,228}. Soula et al reported the nickel catalyst (**21**) which exhibit activities upto 5300 gPE mmol⁻¹ Ni h⁻¹ bar⁻¹ when the R' substituent is CF₃, C₃F₇ or C₆F₅ resulting in linear poly(ethylene)s with narrow molecular weight distributions²²⁹. It was observed by Gibson et al that presence of bulky groups adjacent to the oxygen donor leads to a dramatic increase in activity probably due to steric protection of the relatively exposed O-donor atom²³⁰.



21

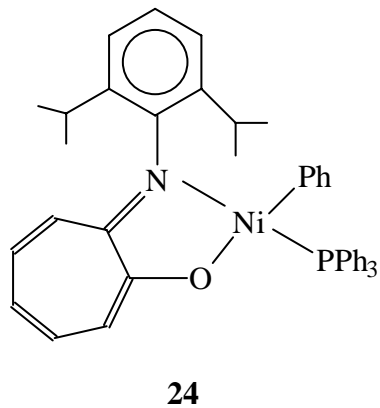
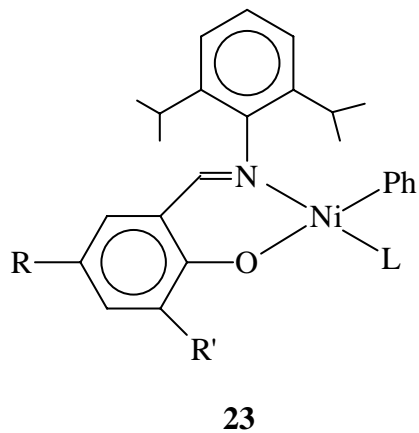
Bazan and coworkers reported that addition of B(C₆F₅)₃ to phosphino-carboxylate nickel complex leads to a cationic species (**22**) which oligomerizes ethylene to predominantly butene-1²³¹.



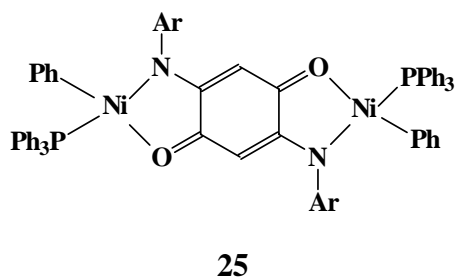
22

Salicylaldiminato nickel complexes (**23**)²³² bearing bulky imino substituents exhibit ethylene polymerization activities of several hundred g mmol⁻¹ Ni h⁻¹ bar⁻¹. These complexes also copolymerize ethylene with polar comonomers. A single component nickel complex bearing an amido-aldehyde [NO] ligand for polymerization of ethylene

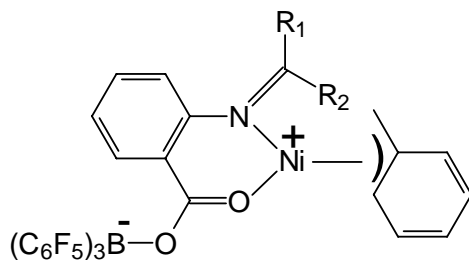
was reported²³³. Brookhart et al reported an anilinetropone based nickel complex (**24**) which produces high molecular weight poly(ethylene)s with moderate activity²³⁴.



Ethylene polymerization using neutral single component binuclear nickel complexes (**25**) of bridging ligands containing 2,5-disubstituted amino p-benzoquinone has been reported²³⁵. Catalyst activities were comparable to those of Grubbs catalyst and moderately branched poly(ethylene)s with broad molecular weight distributions were obtained. Interaction between the two metals creates more than one active species during polymerization which may be the reason for the broad molecular weight distributions.



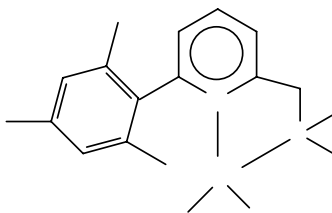
Recently, zwitterionic (2-alkylideneamino)benzoato nickel complexes (**26**) were reported that polymerize ethylene at elevated temperatures and pressures²³⁶. This complex exhibited activity at 80°C which implies that the active species was stable even at higher temperatures. However rapid deactivation of the catalyst was observed at 98°C. Branched poly(ethylene)s with low molecular weights (Mw = 10,000) and narrow molecular weight distributions (2-3) were obtained.



26

A new class of oligomerization catalysts based on nickel complexes having sterically hindered tris(pyrazolyl) borate ligands has been reported²³⁷. This complex selectively produces butene-1 when activated with MAO or TMA. Catalyst activity and selectivity depends on nature of the cocatalyst which indicates that these cocatalysts act as ligands attached to the metal centre.

A pyridine based bulky phosphine nickel complex (**27**) catalyzes the polymerization and oligomerization of ethylene²³⁸. At Al/Ni ratio of 150, the catalyst produced linear poly(ethylene)s in poor yields with bimodal molecular weight distributions. The polymer was found to be orthorhombic by XRD. However, at Al/Ni of 500, ethylene was oligomerized to butenes and hexenes by the catalyst. Another peculiar feature of this catalyst was that considerable amount of polymer was obtained when the reaction was carried out in presence of carbondioxide under high pressures.

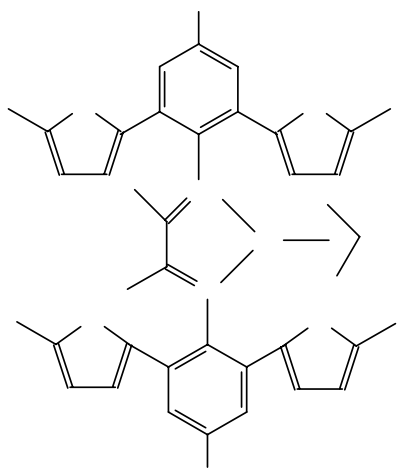


27

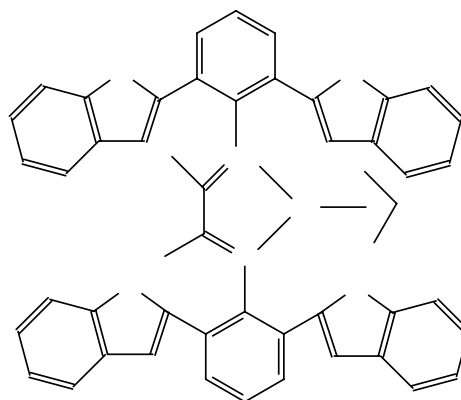
Nickel isocyanide complexes²³⁹ function as active catalysts for polymerization of ethylene when activated with MAO. Catalyst activity and resulting polymer properties

are found to be strongly dependent on the substituents on the aryl group particularly at the 2 and 2,6-positions. 2-aryl and 2,6-diaryl phenylisocyanide complexes showed higher activities than the 2-alkyl and 2,6-dialkyl substituted complexes. 2,6-diphenyl phenyl isocyanide complexes resulted in polymers with higher molecular weights than the 2-phenyl phenyl isocyanide complexes. Poly(ethylene)s produced have narrow molecular weight distributions.

Ionkin et al reported that *ortho*-5-methylfuran and benzofuran substituted η^3 -allyl nickel complexes (**28**, **29**) show superior polymerization stability at elevated temperatures²⁴⁰. The 5-methyl furan substituted complex exhibited activity at 120°C whereas the benzofuran substituted complex was active even at 150°C. The benzofuran substituted complex also resulted in ultrahigh molecular weight poly(ethylene)s ($M_w = 2,486,000$) at 70°C.

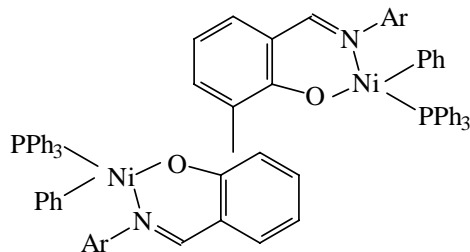


28



29

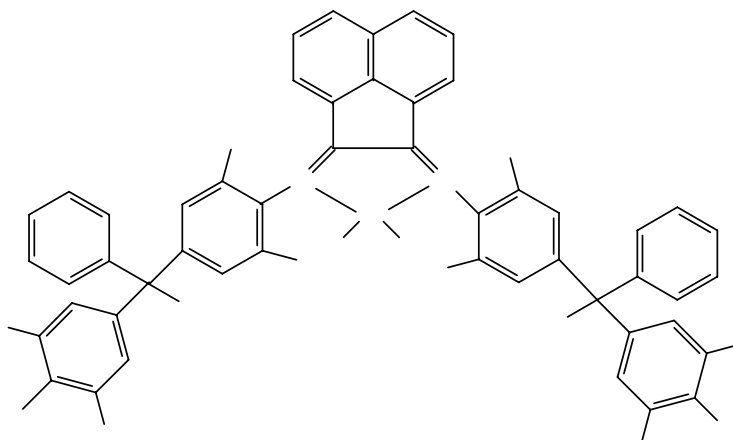
A novel binuclear 3,3'-bisalicylaldimine based neutral nickel complex (**30**) acts as a single component catalyst in the polymerization of ethylene. High activity and high molecular weight poly(ethylene)s with broad molecular weight distributions are produced by this catalyst²⁴¹.



30

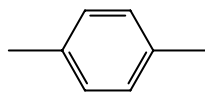
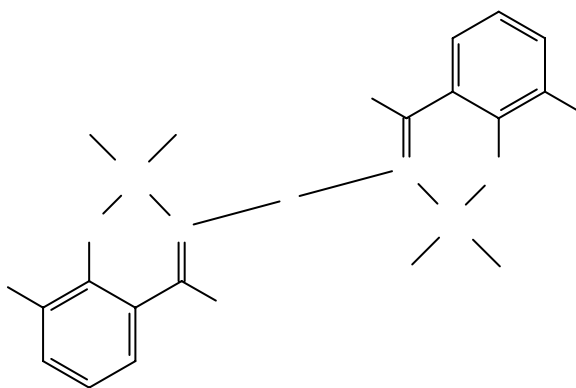
Novel nickel and palladium complexes containing macrocyclic α -diimine ligands have been reported²⁴². They exhibit high activities ($42,000 \text{ gPE mmol}^{-1} \text{ Ni h}^{-1}$) at 90°C and result in methyl branched poly(ethylene)s with high molecular weights and narrow molecular weight distributions. Branching density was higher when compared to acyclic counterparts and indicates enhanced chain walking process. High molecular weight poly(ethylene)s were obtained even at higher temperatures that may be due to blocking of the axial sites by the cyclophane ring even at these temperatures. However catalysts bearing C_6 hydrocarbon bridges²⁴³ exhibited low catalytic activities for polymerization of ethylene which may be due to significant steric constraint imposed by the alkyl bridges on the catalytic centre. Moreover, proximity of alkyl hydrogens to the metal centers may result in catalyst deactivation via intermolecular C-H activation followed by decomposition.

Kim et al²⁴⁴ reported novel nickel complexes (**31**) bearing diimine ligands with different steric bulk that are highly active for polymerization of ethylene. Catalyst activities as high as $10^6 \text{ g PE mmol}^{-1} \text{ Ni h}^{-1} \text{ bar}^{-1}$ were obtained. By proper choice of ligand architecture and temperature a range of polyethylene materials with high molecular weights and varying degrees of branching were obtained.



31

Binuclear neutral nickel complexes (**32**) bearing salicylaldiminato ligands²⁴⁵ polymerize ethylene with an activity of $6.7 \text{ gPE mmol}^{-1} \text{ Ni h}^{-1}$. Molecular weights in the range 4.4×10^5 and molecular weight distribution of 2.2 were obtained. Branched poly(ethylene)s with predominantly methyl branches resulted from the use of this catalyst.

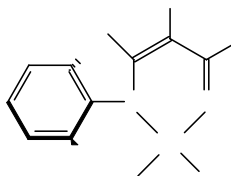


32

Recent studies on similar binuclear nickel complexes by Chen et al²⁴⁶ showed that substituents at *ortho*-position of phenyl rings and arene bridge of the ligand dramatically influence the polymerization behavior. Catalysts with small substituents (H, Me) at *ortho*-position of the phenolic ring were less active at lower temperatures where as those with bulky *ortho*-substituents such as *t*-butyl or phenyl showed optimal activities even at lower temperatures. Presence of an electron withdrawing substituent such as nitro group improved the catalyst activity significantly due to decrease in ethylene insertion barrier and resulted in very high molecular weight poly(ethylene)s. These binuclear catalysts were found to be thermally more stable than analogous mononuclear catalysts.

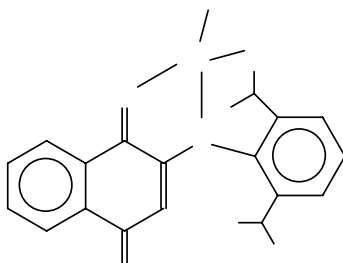
Bimetallic nickel complexes based on macrocyclic tetraaminodiphenols have been reported which when activated with B(C₆F₅)₃ produce methyl branched poly(ethylene)s with lower molecular weights (38,000) and broad molecular weight distributions (Mw/Mn =5-10)²⁴⁷.

Brookhart and coworkers reported polymerization of ethylene using a series of new neutral (N, O) chelated nickel complexes (**33**) based on anilino-substituted enone ligands bearing electron withdrawing trifluoromethyl and trifluoroacetyl groups²⁴⁸. The complexes when activated with Ni(COD)₂ or B(C₆F₅)₃ produced moderately branched poly(ethylene)s (35-55 branches/1000 C). The catalyst that does not have methyl group on the α -carbon to the nitrogen exhibited maximum activity even at 60°C and longer life times at 35°C.



A novel catalytic system for polymerization of ethylene was obtained *in situ* by oxidative addition of 8-hydroxyquinoline based ligands to Ni(COD)₂ and MAO²⁴⁹. When the ligand is 8-hydroxyquinoline, only oligomers were obtained. However 5, 7-dinitro-8-hydroxy quinoline resulted in linear poly(ethylene)s.

A novel nickel(II) complex bearing 2-(2,6-diisopropylanilino)-1,4-naphthoquinone ligand (**34**) was reported by Shiono²⁵⁰. The complex alone polymerized ethylene to linear polymers with a low activity. However, when activated with 4 eqv of B(C₆F₅)₃ the complex resulted in uniquely branched poly(ethylene)s consisting of both short and long chain branches. The short chain branches were mainly composed of methyl, ethyl and propyl and the long chain branches contain more than seven carbon atoms. It was proposed that coordination of B(C₆F₅)₃ to the oxygen at 4-position forms a zwitterionic complex that is more active than the neutral nickel complex for polymerization and β-H elimination. Vinyl-terminated macromonomers are formed as a result of β-H elimination which in turn are copolymerized with ethylene to form long chain branching.

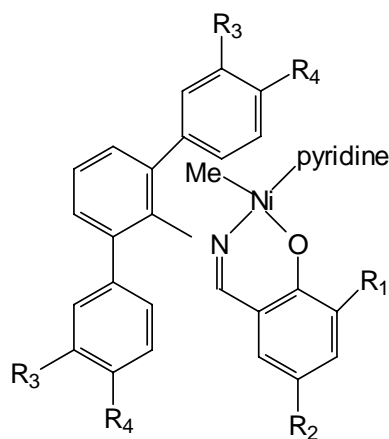


34

Several mono-nuclear and dendritic nickel(II) complexes based on N,N'-iminopyridine chelating ligands have been synthesized and investigated for polymerization of ethylene²⁵¹. These complexes when activated with MAO polymerized ethylene with low to moderate activity resulting in a mixture of toluene soluble oligomers together with solid polymer. Catalytic properties were found to be sensitive to ligand structure and dendrimer generation. For higher dendrimer generation, more oligomers were produced than polymer and higher molecular weight and molecular weight distribution were

observed. Moreover, branching degree of polymers also decreased progressively with dendrimer generation.

Several new κ^2 -(N,O)-salicylaldiminato nickel(II) complexes(**35**) for polymerization of ethylene have been studied by Mecking and coworkers²⁵². These complexes act as single component catalysts above 15°C and highest catalyst activities were observed in the temperature range 40-75°C. 3', 5'-substitution of the terphenyl group was found to have a major influence on the polyethylene microstructure. Electron withdrawing and sterically demanding substituents at the 3',5' positions of the terphenyl ring decreased the degree of branching and resulted in higher molecular weights when compared to electron donating and small substituents.



35

Slurry phase polymerization of ethylene to branched polymer has been studied using α -diimine nickel catalysts covalently linked to silica supports²⁵³. These nickel complexes were prepared by the reaction of α -diimine ligands with pendant amino or hydroxyl functionalities with the linker of the silica support. TMA, tetrachlorosilane and trichloroborane were used as efficient linkers, with TMA being the most preferred. High catalyst loadings have been achieved using this approach and highly active polymerization catalysts have been obtained by the activation of these precatalysts with alkyl aluminum cocatalysts. One of the features of these catalysts is that inexpensive ethyl aluminium sesquichloride is a very efficient cocatalyst even at low Al/Ni ratios. Catalyst activity increased with ethylene pressure and at higher pressures (50 bar) high

productivities were obtained even at 80°C. No reactor fouling was observed. Such supported late transition metal catalysts may be potential candidates for industrial slurry polymerization processes.

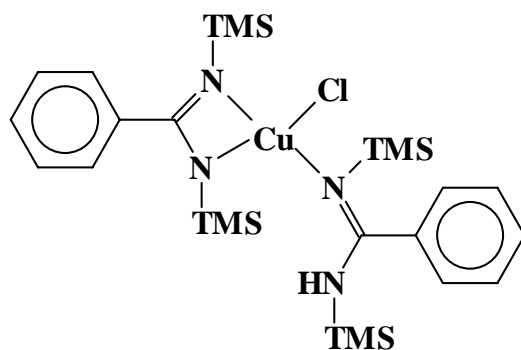
Copolymerization of ethylene with polar comonomers using nickel and palladium catalysts have also been investigated by several groups²⁵⁴⁻²⁶¹.

Polyolefins with novel microstructures and properties can be obtained by reactor blending of nickel and palladium catalysts with early transition metal catalysts²⁶²⁻²⁶⁵.

Mechanism of olefin polymerization by nickel based catalysts has been widely investigated²⁶⁶. A number of spectroscopic²⁶⁷⁻²⁷¹ and computational²⁷²⁻²⁷⁸ studies have been carried out to investigate the mechanistic aspects of nickel and palladium catalyzed olefin polymerizations. All these studies revealed that a cationic alkyl ethylene complex is the resting state of the catalyst system. A series of β -H elimination and reinsertion reactions via β -agostic cationic alkyl intermediate leads to the formation of highly branched polymer.

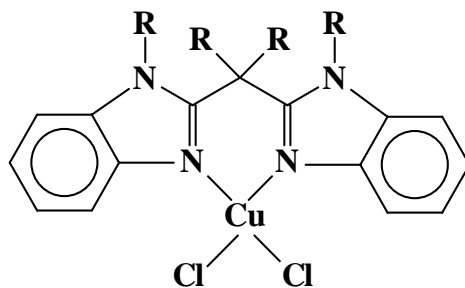
1.3.4. Group 11 metal catalysts

Reports on olefin polymerization using copper complexes are very rare. A benzamidinate-based copper complex (**36**) which polymerizes ethylene was reported by Shibayama et al²⁷⁹⁻²⁸¹. The complex when activated with MAO produced poly(ethylene)s with Mw of 820,000 and a T_m of 138°C.



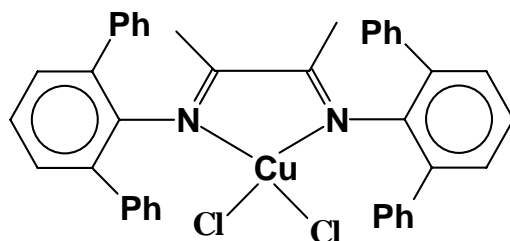
36

Bis(benzimidazole) complexes of copper (**37**) are reported to homopolymerize ethylene and acrylates and also copolymerize these monomers. Linear poly(ethylene)s with narrow molecular weight distributions were obtained using these catalysts. Copolymerization of ethylene with acrylates has also been achieved to produce in-chain copolymers with high acrylate incorporation²⁸²⁻²⁸⁵.



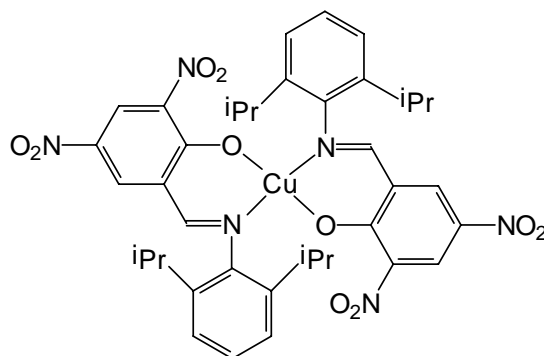
37

Gibson and coworkers reported an α -diimine copper(II) catalyst (**38**) which was active for polymerization of ethylene. They observed that *ortho*-phenyl substituents play a special role in stabilizing the active species²⁸⁶.



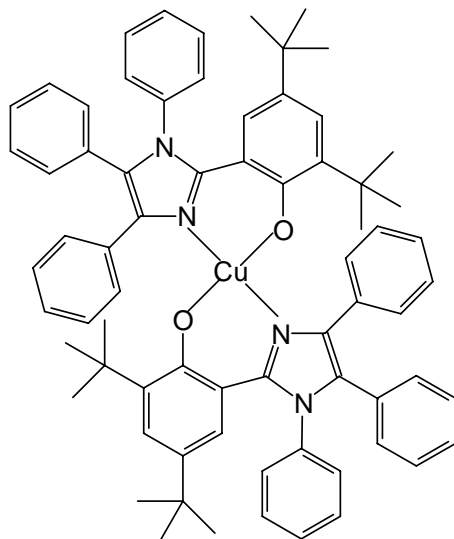
38

Several bis(salicylaldiminato)copper(II) complexes (**39**) along with MAO were found to be efficient catalysts for vinyl polymerization of norbornene²⁸⁷. The resulting poly(norbornene)s possess high molecular weights and non-stereoregular vinyl-type structure indicative of a non-radical mechanism. The N,O-chelate ligand on the metal center appears to be necessary for stabilization of the active species. ESR studies on the polymerization system supports the formation of a Cu (I) active species.



39

Copper (II) complexes based on bis{{2'-(4',6'-di-*t*-butylhydroxy-phenyl)-1,4,5-triphenylimidazole}} (**40**) were reported to be active for the vinyl addition polymerization of norbornene when activated with MAO²⁸⁸. Catalyst activities as high as 3.16×10^5 g PNB mol⁻¹Cu h⁻¹ were observed which are higher than those exhibited by bis(salicylaldiminate) copper (II) complexes. Atactic poly(norbornene)s with high molecular weights (10^6) were obtained using this catalyst. This is one of the catalysts that possess highest activities for vinyl addition polymerization of norbornene.



40

1.4. Conclusions

Past ten years have witnessed significant advances in the area of non-metallocene olefin polymerization catalysts. The search for new generation of non-metallocene catalysts have led to the identification of a variety of new ligands and complexes that are useful for the synthesis of poly(olefin)s with diverse structures and properties. New organometallic complexes have been discovered which show a range of catalytic behavior, from oligomerization to polymerization, from low molecular weights to extremely high molecular weights, from linear to branched and exhibiting propensities to incorporate a range of comonomers into copolymers. A few of these catalytic systems show “living” or “quasi-living” polymerization behavior, which provides the synthetic chemists new opportunities to prepare block copolymers and functional polymers. The ability of certain complexes to act as single component catalysts systems has enabled polymerization of ethylene in aqueous emulsions. In spite of all these developments, early transition metal Ziegler-Natta and metallocene complexes hold their own unique status, in view of their ability to polymerize propylene in a stereospecific manner. This is still difficult to accomplish using late transition metal catalysts.

1.5. References

- 1 Ziegler, K. *Angew. Chem.* **1955**, *67*, 541.
- 2 Natta, G.; Pino, P.; Mazzanti, G.; Giannini, U. *J. Am. Chem. Soc.* **1957**, *79*, 2997.
- 3 Breslow, D. S.; Newburg, N. R. *J. Am. Chem. Soc.* **1957**, *79*, 5072.
- 4 Reichert, K. H.; Meyer, K. R. *Makromol. Chem.* **1973**, *169*, 163.
- 5 Andresen, A.; Cordes, H. G.; Herwig, J.; Kaminsky, W.; Merck, A.; Mottweiler, R.; Pein, J.; Sinn, H.; Vollmer, H. J. *Angew. Chem. Int. Ed. Engl.* **1976**, *15*, 630.
- 6 Sinn, H.; Kaminsky, W.; Vollmer, H. J.; Woldt, R. *Angew. Chem. Int. Ed. Engl.* **1980**, *19*, 390.
- 7 Sinn, H.; Kaminsky, W. *Adv. Organomet. Chem.* **1980**, *18*, 99.
- 8 Kaminsky, W.; Miri, M.; Sinn, H.; Woldt, R. *Macromol. Chem. Rapid Commun.* **1983**, *4*, 417.
- 9 Ewen, J. A. *J. Am. Chem. Soc.* **1984**, *106*, 6355.
- 10 Wild, F. R. W. P.; Zsolnai, L.; Huttner, G.; Brintzinger, H. H. *J. Organomet. Chem.* **1982**, *232*, 233.
- 11 Ewen, J.A.; Haspelslagh, L.; Atwood, J.L.; Zhang, H. *J. Am. Chem. Soc.* **1987**, *109*, 6544.
- 12 Ewen, J. A.; Jones, R. L.; Razavi, A.; Ferrara, J. P. *J. Am. Chem. Soc.* **1988**, *110*, 6255.
- 13 Kaminsky, W.; Spiehl, R. *Makromol. Chem.* **1989**, *190*, 515.
- 14 Kaminsky, W.; Bark, A.; Steiger, R. *J. Mol. Catal.* **1992**, *74*, 109.
- 15 Cherdron, H.; Brekner, M. J.; Osan, F. *Angew. Makromol. Chem.* **1994**, *223*, 121.
- 16 Wendt, R.A.; Mynott, R.; Hauschild, K.; Ruchatz, D.; Fink, G. *Macromol. Chem. Phys.* **1999**, *200*, 1340.
- 17 Arndt-Rosenau, M.; Beulich, I. *Macromolecules* **1999**, *32*, 7335.
- 18 Tritto, I.; Boggioni, L.; Sacchi, M. C.; Locatelli, P.; Ferro, D. R.; Provasoli, A. *Macromol. Rapid Commun.* **1999**, *20*, 279.
- 19 Bergstrom, C. H.; Ruotoistenmaki, J.; Aitola, E. T.; Seppala, J. V. *J. Appl. Polym. Sci.* **2000**, *77*, 1108.
- 20 Lasarov, H.; Pakkanen, T. T. *Macromol. Chem. Phys.* **2000**, *201*, 1780.

- 21 Lee, D. -H.; Jung, H. -K.; Kim, W. -S.; Min, K. -E.; Park, L.- S.; Seo, K. -H.; Kang, I. -K.; Noh, S. -K. *Polymer* **2000**, *24*, 445.
- 22 Lee, D. -H.; Jung, H. -K.; Choi, Y. -Y.; Kim, H. -J.; Kim, W. -S.; Min, K. -E.; Park, L. -S.; Kang, I. -K. *Polymer* **2000**, *24*, 751.
- 23 Kaminsky, W.; Beulich, I.; Arndt-Rosenau, M. *Macromol. Symp.* **2001**, *173*, 211.
- 24 Tritto, I.; Marestin, G.; Boggioni, L.; Sacchi, M. C.; Brintzinger, H. -H.; Ferro, D. R. *Macromolecules* **2001**, *34*, 5770.
- 25 Lee, D. -H.; Lee, J. -H.; Kim, H. -J.; Kim, W. -S.; Min, K. -E.; Park, L. -S.; Seo, K. -H.; Kang, I. -K. *Polymer* **2001**, *25*, 468.
- 26 Tritto, I.; Boggioni, L.; Jansen, J. C.; Thorshaug, K.; Sacchi, M. C.; Ferro, D. *Macromolecules* **2002**, *35*, 616.
- 27 Naga, N.; Imanishi, Y. *Macromol. Chem . Phys.* **2002**, *203*, 159.
- 28 Wendt, R. A.; Mynott, R.; Fink, G. *Macromol. Chem. Phys.* **2002**, *203*, 2531.
- 29 Wendt, R. A.; Fink, G. *J. Mol. Catal. A. Chem.* **2003**, *203*, 101.
- 30 Kaminsky, W.; Tran, P. -D.; Werner, R. *Macromol. Symp.* **2004**, *213*, 101.
- 31 Lee, S. -G.; Hong, S. -D.; park, Y. -W.; Jeong, B. -G.; Nam, D. -W.; Jung, H.Y.; Lee, H.; Song, K. H. *J. Organomet. Chem.* **2004**, *689*, 2586.
- 32 Donner, M.; Fernandez, M.; Kaminsky, W. *Macromol. Symp.* **2006**, *236*, 193.
- 33 Po, R.; Cardi, N. *Prog. Polym. Sci.* **1996**, *21*, 47.
- 34 Tomotsu, N.; Ishihara, N.; Newman, T. H.; Malanga, M. T. *J. Mol. Catal. A. Chem.* **1998**, *128*, 167.
- 35 Kaminsky, W.; Lenk, S. *Macromol. Symp.* **1997**, *118*, 45.
- 36 Schellenberg, J.; Tomotsu, N. *Prog. Polym. Sci. (Oxford)* **2002**, *27*, 1925.
- 37 Bruzaud, S.; Cramail, H.; Duvignac, L.; Deffieux, A. *Macromol. Chem. Phys.* **1997**, *198*, 291.
- 38 Stehling, U. M.; Stein, K. M.; Kesti, M. R.; Waymouth, R. M. *Macromolecules* **1998**, *31*, 2019.
- 39 Mulhaupt, R.; Duschek, T.; Rieger, B. *Macromol. Chem. Macromol. Symp.* **1991**, *48/49*, 317.
- 40 Stehling, U. M.; Stein, K. M.; Fischer, D.; Waymouth, R. M. *Macromolecules* **1999**, *32*, 14.

- 41 Chung, T. C.; Lu, H. L. *J. Mol. Catal. A. Chem.* **1997**, *115*, 115.
- 42 Aaltonen, P.; Lofgren, B. *Macromolecules* **1995**, *28*, 5353.
- 43 Aaltonen, P.; Lofgren, B. *Eur. Polym. J.* **1997**, *33*, 1187.
- 44 Aaltonen, P.; Fink, G.; Lofgren, B.; Seppala, J. *Macromolecules* **1996**, *29*, 5255.
- 45 Goretzki, R.; Fink, G. *Macromol. Rapid. Commun.* **1998**, *19*, 511.
- 46 Goretzki, R.; Fink, G. *Macromol. Chem. Phys.* **1999**, *200*, 881
- 47 Radhakrishnan, K.; Sivaram, S. *Macromol. Chem. Rapid. Commun.* **1998**, *19*, 581.
- 48 Schneider, M. J.; Schafer, R.; Mulhaupt, R. *Polymer* **1997**, *38*, 2455.
- 49 Kesti, M. R.; Coates, G. W.; Waymouth, R. M. *J. Am. Chem. Soc.* **1992**, *114*, 9679.
- 50 Wilen, C. E.; Luttkhedde, H.; Hjertberg, T.; Nasman, J. H. *Macromolecules* **1996**, *29*, 8569.
- 51 Hakala, K.; Lofgren, B.; Helaja, T. *Eur. Polym. J.* **1998**, *34*, 1093.
- 52 Hakala, K.; Helaja, T.; Lofgren, B. *J. Polym. Sci. A. Polym. Chem.* **2000**, *38*, 1966.
- 53 Hakala, K.; Helaja, T.; Lofgren, B. *Polym. Bull.* **2001**, *46*, 123.
- 54 Lipponen, S.; Seppala, J. *J. Polym. Sci. A. Polym. Chem.* **2002**, *40*, 1303.
- 55 Montagna, A. A.; Dekmezian, A. H.; Burkhart, R. M. *Chemtech* **1997**, *27*, 26.
- 56 Hackmann, M.; Rieger, B. *Cattech* **1997**, *1*, 79.
- 57 Brintzinger, H. H.; Fischer, D.; Mulhaupt, R.; Rieger, B.; Waymouth, R. M. *Angew. Chem. Int. Ed. Engl.* **1995**, *34*, 1143.
- 58 Reddy, S. S.; Sivaram, S.; *Prog. Polym. Sci.* **1995**, *20*, 309.
- 59 Horton, A. D. *TRIP* **1994**, *2*, 158.
- 60 Kaminsky, W.; Arndt, M. *Adv. Polym. Sci.* **1997**, *127*, 143.
- 61 Soga, K.; Shiono, T. *Prog. Polym. Sci.* **1997**, *22*, 1503.
- 62 Gupta, V. K.; Satish, S.; Bhardwaj, I. S. *JMS Rev. Macromol. Chem. Phys.* **1994**, *C34*, 439.
- 63 Huang, J.; Reuspel, G. L. *Prog. Polym. Sci.* **1995**, *20*, 459.
- 64 Kaminsky, W. *Macromol. Chem. Phys.* **1996**, *197*, 3907.
- 65 Bochmann, M. *J. Chem. Soc. Dalton Trans.* **1996**, 255.
- 66 Fink, G.; Mulhaupt, R.; Brintzinger, H. H. *"Ziegler Catalysts"*; Springer: Berlin, **1995**.
- 67 Hamielec, A. E.; Soares, J. B. P. *Prog. Polym. Sci.* **1996**, *21*, 651.
- 68 Mashima, K.; Nakayama, Y.; Nakamura, A. *Adv. Polym. Sci.* **1997**, *133*, 1.

- 69 Kaminsky, W. *J. Chem. Soc. Dalton. Trans.* **1998**, 1413.
- 70 Jordan, R. F. *Adv. Organomet. Chem.* **1991**, 32, 325.
- 71 Kaminsky, W.; Scheirs, J. *Metallocene based polyolefins*, Wiley, **2000**, Vol I and II.
- 72 Coates, G.W. *Chem. Rev.* **2000**, 100, 1223.
- 73 Alt, H. G.; Koppl, A. *Chem. Rev.* **2000**, 100, 1205.
- 74 Resconi, L.; Cavallo, L.; Fait, A.; Poimontesi, F. *Chem. Rev.* **2000**, 100, 1253
- 75 Hlatky, G. G. *Chem. Rev.* **2000**, 100, 1347.
- 76 Fink, G.; Steinmetz, B.; Zechlin, J.; Przybyla, C.; Tesche, B. *Chem. Rev.* **2000**, 100, 1377.
- 77 Pedeutour, J.; Radhakrishnan, K.; Cramail, H.; Deffieux, A. *Macromol. Rapid Commun.* **2001**, 22, 1095.
- 78 Alt, H. G.; Licht, E. H.; Licht, A. I.; Schneider, K. J. *Coord. Chem. Rev.* **2006**, 250, 2.
- 79 Giannetti, E.; Nicoletti, G.; Mazzochi, R. *J. Polym. Sci., Polym. Chem. Ed.* **1985**, 23, 2117.
- 80 Kissin, Y. V.; Brandolini, A. *J. Am. Chem. Soc.* **2003**, 36, 18..
- 81 Small, B. L.; Brookhart, M. *J. Am. Chem. Soc.* **1998**, 120, 7143.
- 82 Sugano, T.; Matsubara, T.; Fujita, T.; Takahashi, T. *J. Mol. Catal.* **1993**, 82, 93.
- 83 Taube, R.; Krukowa, L. J. *J. Organomet. Chem.* **1988**, 347, C 9.
- 84 Chien, J. C. W.; Tsai, W. M.; Rausch, M. D. *J. Am. Chem. Soc.* **1991**, 113, 8570.
- 85 Bochmann, M.; Lancaster, S. J. *Organometallics* **1993**, 12, 633.
- 86 Crowther, D. J.; Borkowsky, S. L.; Swenson, D.; Meyer, T. Y.; Jordan, R. F. *Organometallics* **1993**, 12, 2897.
- 87 Hlatky, G. G.; Eckman, R. R.; Turner, H. W. *Organometallics* **1992**, 11, 1413.
- 88 Chen, E.Y.; Marks T.J. *Chem. Rev.* **2000**, 100, 1391.
- 89 Cossee, P. *J. Catal.* **1964**, 3, 80.
- 90 Arlman, E. J.; Cossee, P. *J. Catal.* **1964**, 3, 99.
- 91 Stevens, J. C.; Timmers, F. J.; Wilson, D. R.; Schmidt, G. F.; Nickias, P. N.; Rosen, R. K.; Knight, G. W.; Lai, S. -Y. *EP 0416815*, Dow Chem. Co. **1991**.
- 92 Stevens, J. C.; Neithamer, D. R. *EP 0418044*, Dow, **1991**.
- 93 Canich, J. A. M. *US 5026798*, Exxon, **1991**.
- 94 Canich, J. A. M.; Licciardi, G.F. *US 5057475*, Exxon, **1991**.

- 95 Canich, J. A. M. *EP 0420436*, Exxon, **1991**.
- 96 Chum, P. S.; Kao, C. I.; Knight, G. W. *Plastics Engineering* **1995**, June, 21.
- 97 Shiono, T.; Moriki, Y.; Soga, K. *Macromol. Symp.* **1995**, 97, 161.
- 98 Soga, K.; Uozumi, T.; Nakamura, S.; Toneri, T.; Teranishi, T.; Sano, T.; Arai, T. Shiono, T. *Macromol. Chem. Phys.* **1996**, 197, 4237.
- 99 Stevens, J. C. *Stud. Surf. Sci. Catal.* **1994**, 89, 277.
- 100 Mani, R.; Burns, C. M. *Macromolecules* **1991**, 24, 5476.
- 101 Soga, K.; Lee, D.; Yangihara, H. *Polym. Bull.* **1988**, 20, 237..
- 102 Kakugo, M.; Miyatake, T.; Mizunuma, K. *Stud. Surf. Sci. Catal.* **1990**, 56, 517.
- 103 Miyatake, K.; Mizunuma, M.; Kakugo, M. *Makromol. Chem. Macromol. Symp.* **1993**, 66, 203.
- 104 Sernetz, F. G.; Mulhaupt, R.; Waymouth, R. M. *Macromol. Chem. Phys.* **1996**, 197, 1071.
- 105 Nomura, K.; Okumara, H.; Komatsu, T.; Naga, N.; Imanishi, Y. *J. Mol. Catal. A. Chem.* **2002**, 190, 225.
- 106 Noh, S. -K.; Lee, J.; Lee, D. -H. *J. Organomet. Chem.* **2003**, 667, 53.
- 107 Noh, S. K.; Lee, M.; Kum, D. H.; Kim, K.; Lyoo, W. S.; Lee, D. -H. *J. Polym. Sci. Part A. Polym. Chem.* **2004**, 42, 1712.
- 108 Skeril, R.; Sindelar, P.; Salajka, Z.; Varga, V.; Cisarova, I.; Pinkas, J.; Horacek, M.; Mach, K. *J. Mol. Catal. A. Chem.* **2004**, 224, 97.
- 109 Martinez, S.; Exposito, M. T.; Ramos, J.; Cruz, V.; Martinez, M. C.; Lopez, M.; Munoz-Escalona, A.; Martinez-Salazar, J. *J. Polym. Sci. Part A. Polym. Chem.* **2005**, 43, 711.
- 110 Sernetz, F. G.; Mulhaupt, R.; Amor, F. J. *J. Polym. Sci., Part A. Polym. Chem.* **1997**, 35, 1571.
- 111 Xu, G. *Macromolecules* **1998**, 31, 2395.
- 112 Chung, T. C.; Lu, H. L. *J. Polym. Sci. A. Polym. Chem.* **1997**, 35, 575.
- 113 Ruchatz, D.; Fink, G. *Macromolecules* **1998**, 31, 4674.
- 114 van Leusen, D.; Beetstra, D. J.; Hessen, B.; Teuben, J. H. *Organometallics* **2000**, 19, 4084.
- 115 Kotov, V. V.; Avtomonov, E. V.; Sundermeyer, J.; Harms, K.; Lemenovskii, D. *Eur. J.*

- Inorg. Chem.* **2002**, 678.
- 116 Park, J. T.; Yoon, S. C.; Bae, B. J.; Seo, W. S.; Suh, I. H.; Han, T. K.; Park, J. R. *Organometallics* **2000**, 19, 1269.
- 117 Reb, A.; Alt, H. G. *J. Mol. Catal. A. Chem.* **2001**, 174, 35.
- 118 Alt, H. G.; Föttinger, K.; Milius, W. J. *J. Organomet. Chem.* **1999**, 572, 21..
- 119 Alt, H. G.; Reb, A. *J. Mol. Catal. A. Chem.* **2001**, 175, 43.
- 120 Alt, H. G.; Reb, A.; Milius, W. J. *J. Organomet. Chem.* **2001**, 628, 169.
- 121 Alt, H. G.; Reb, A.; Kundu, K. *J. Organomet. Chem.* **2001**, 628, 211.
- 122 Klosin, J.; Kruper Jr, W. J.; Nickias, P. N.; Roof, G. R.; De Waele, P. *Organometallics* **2001**, 20, 2663.
- 123 Barnhart, R. W.; Bazan, G. C.; Mourey, T. *J. Am. Chem. Soc.* **1998**, 120, 1082.
- 124 Wasilke, J. -C.; Obrey, S. J.; Tom Baker, R.; Bazan, G. C. *Chem. Rev.* **2005**, 105, 1001.
- 125 Scollard, J. D.; McConville, D. H.; Payne, N. C.; Vittal, J. J. *Macromolecules* **1996**, 29, 5241.
- 126 Scollard, J. D.; McConville, D. H. *J. Am. Chem. Soc.* **1996**, 118, 10008.
- 127 Scollard, J. D.; McConville, D. H.; Vittal, J. J.; Payne, N. C. *J. Mol. Catal. A. Chem.* **1998**, 128, 201.
- 128 Uozumi, T.; Tsubaki, S.; Jin, J. Z.; Ahn, C. H.; Sano, T.; Soga, K. *Macromol. Chem. Phys.* **2001**, 202, 3279.
- 129 Tsubaki, S.; Jin, J. Z.; Sano, T.; Uozumi, T.; Soga, K. *Macromol. Chem. Phys.* **2001**, 202, 482.
- 130 Hagimoto, H.; Shiono, T.; Ikeda, T. *Macromol. Rapid Commun.* **2002**, 23, 7 .
- 131 Lee, C. H.; La, Y. H.; Park, S. J.; Park, J. W. *Organometallics* **1998**, 17, 3648.
- 132 Lee, C. H.; La, Y. H.; Park, S. J.; Park, J. W. *Organometallics* **2000**, 19, 344.
- 133 Nomura, K.; Naofumi, N.; Takaoki, K.; Imai, A. *J. Mol. Catal. A. Chem.* **1998**, 130, L 209.
- 134 Nomura, K.; Naga, N.; Takaoki, K. *Macromolecules* **1998**, 31, 8009.
- 135 Nomura, K.; Oya, K.; Imanishi, Y. *Polymer* **2000**, 41, 2755.
- 136 Jin, X.; Novak, B.M. *Macromolecules* **2000**, 22, 6205.
- 137 Kim, W. K.; Fevola, M. J.; Liable-Sands, L. M.; Rheingold, A. L.; Theopold, K. H.

- Organometallics* **1998**, *17*, 4541.
- 138 Vollmerhaus, R.; Rahim, M.; Tomaszewski, R.; Xin, S. K.; Taylor, N. J.; Collins, S. *Organometallics* **2000**, *19*, 2161.
- 139 Rahim, M.; Taylor, N. J.; Xin, S. K.; Collins, S. *Organometallics* **1998**, *17*, 1315.
- 140 Matsui, S.; Mitani, M.; Saito, J.; Tohi, Y.; Makio, H.; Tanaka, H.; Fujita, T. *Chem. Lett.* **1999**, 1263.
- 141 Matsui, S.; Tohi, Y.; Mitani, M.; Saito, J.; Makio, H.; Tanaka, H.; Nitabaru, M.; Nakano, T.; Fujita, T. *Chem. Lett.* **1999**, 1065.
- 142 Matsui, S.; Mitani, M.; Saito, J.; Matsukawa, N.; Tanaka, H.; Nakano, T.; Fujita, T. *Chem. Lett.* **2000**, 554.
- 143 Saito, J.; Mitani, M.; Matsui, S.; Kashiwa, N.; Fujita, T. *Macromol. Rapid Commun.* **2000**, *21*, 1333.
- 144 Matsui, S.; Mitani, M.; Tohi, Y.; Saito, J.; Makio, H.; Matsukawa, N.; Takagi, Y.; Tsuru, K.; Nitabaru, M.; Nakano, T.; Tanaka, H.; Kashiwa, N.; Fujita, T. *J. Am. Chem. Soc.* **2001**, *123*, 6847.
- 145 Matsui, S.; Fujita, T. *Catal. Today* **2001**, *66*, 63.
- 146 Kojoh, S.; Matsugi, T.; Saito, J.; Mitani, M.; Fujita, T. *Chem. Lett.* **2001**, 822.
- 147 Matsukawa, N.; Matsui, S.; Mitani, M.; Saito, J.; Tsuru, K.; Kashiwa, N.; Fujita, T. *J. Mol. Catal. A. Chem.* **2001**, *169*, 99.
- 148 Saito, J.; Mitani, M.; Matsui, S.; Mohri, J.; Kojoh, S.; Kashiwa, N.; Fujita, T. *Angew. Chem. Int. Ed.* **2001**, *40*, 2918.
- 149 Saito, J.; Mitani, M.; Onda, M.; Mohri, J.; Ishii, J.I.; Yoshida, Y.; Nakano, T.; Tanaka, H.; Matsugi, T.; Kojoh, S.; Kashiwa, N.; Fujita, T. *Macromol. Rapid Commun.* **2001**, *22*, 1072.
- 150 Saito, J.; Mitani, M.; Mohri, J.; Ishii, S.; Yoshida, Y.; Matsugi, T.; Kojoh, S.; Kashiwa, N.; Fujita, T. *Chem. Lett.* **2001**, 576.
- 151 Inoue, Y.; Nakano, T.; Yanaka, H.; Kashiwa, N.; Fujita, T. *Chem. Lett.* **2001**, 1060.
- 152 Mitani, M.; Mohri, J.; Yoshida, Y.; Saito, J.; Ishii, S.; Tsuru, K.; Matsui, S.; Furuyama, R.; Nakano, T.; Tanaka, H.; Kojoh, S.; Matsugi, T.; Kashiwa, N.; Fujita, T. *J. Am. Chem. Soc.* **2002**, *124*, 3327.
- 153 Mitani, M.; Furuyama, R.; Mohri, J.-i.; Saito, J.; Ishii, S.; Terao, H.; Kashiwa, N.;

- Fujita, T. *J. Am. Chem. Soc.* **2001**, *124*, 7888.
- 154 Saito, J.; Mitani, M.; Matsui, S.; Tohi, Y.; Makio, H.; Nakano, T.; Tanaka, H.; Kashiwa, N.; Fujita, T. *Macromol. Chem. Phys.* **2002**, *203*, 59.
- 155 Ishii, S. -I.; Saito, J.; Mitani, M.; Mohri, J. -C.; Matsukawa, N.; Tohi, Y.; Matsui, S.; Kashiwa, N.; Fujita, T. *J. Mol. Catal. A. Chem.* **2002**, *179*, 11.
- 156 Ishii, S.; Mitani, M.; Saito, J.; Matura, S.; Kojoh, S.; Kashiwa, N.; Fujita, T. *Chem. Lett.* **2002**, 740.
- 157 Suzuki, Y.; Kashiwa, N.; Fujita, T. *Chem. Lett.* **2002**, 358.
- 158 Saito, J.; Onda, M.; Matsui, S.; Furuyama, R.; Tanaka, H.; Fujita, T. *Macromol. Rapid Commun.* **2002**, *23*, 1118.
- 159 Tohi, Y.; Makio, H.; Matsui, S.; Onda, M.; Fujita, T. *Macromolecules* **2003**, *36*, 523
- 160 Mitani, M.; Furuyama, R.; Mohri, J.; Saito, J.; Ishii, S.; Terao, H.; Nakano, T.; Tanaka, H.; Fujita, T. *J. Am. Chem. Soc.* **2003**, *125*, 4293.
- 161 Ishii, S.; Furuyama, R.; Matsukawa, N.; Saito, J.; Mitani, M.; Tanaka, H.; Fujita, T. *Macromol. Rapid Commun.* **2003**, *24*, 452.
- 162 Furuyama, R.; Saito, J.; Ishii, S.; Mitani, M.; Matsui, S.; Tohi, Y.; Makio, H.; Matsukawa, N.; Tanaka, H.; Fujita, T. *J. Mol. Catal. A. Chem.* **2003**, *200*, 31.
- 163 Bando, H.; Nakayama, T.; Sonobe, Y.; Fujita, T. *Macromol. Rapid Commun.* **2003**, *24*, 732.
- 164 Chen, Y. -X.; Fu, P. -F.; Stern, C. L.; Marks, T. J. *Organometallics* **1997**, *16*, 5958.
- 165 Gielen, E. E. C. G.; Tiesnitsch, J. Y.; Hessen, B.; Teuben, J. H. *Organometallics* **1998**, *17*, 1652.
- 166 Nomura, K.; Naga, N.; Miki, M.; Yanagi, K.; Imai, A. *Organometallics* **1998**, *17*, 2152.
- 167 Nomura, K.; Naga, N.; Miki, M.; Yanagi, K. *Macromolecules* **1998**, *31*, 7588.
- 168 Nomura, K.; Oya, K.; Komatsu, T.; Imanishi, Y. *Macromolecules* **2000**, *33*, 3187.
- 169 Nomura, K.; Komatsu, T.; Imanishi, Y. *Macromolecules* **2000**, *33*, 8122.
- 170 Nomura, K.; Oya, K.; Imanishi, Y. *J. Mol. Catal. A. Chem.* **2001**, *17*, 127.
- 171 Nomura, K.; Okumura, H.; Komatsu, T.; Naga, N. *Macromolecules* **2002**, *35*, 5388.
- 172 Kasi, R.M.; Coughlin, E.B. *Macromolecules* **2003**, *36*, 6300.
- 173 Craymer, J.F.; Kasi, R.M.; Coughlin, E.B. *Polyhedron* **2005**, *24*, 1347.

- 174 Johnson, L. K.; Killian, C. M.; Brookhart, M. *J. Am. Chem. Soc.* **1995**, *117*, 6414.
- 175 Britovsek, G. J. P.; Gibson, V. C.; Kimberley, B. S.; Maddox, P. J.; McTavish, S. J.; Solan, G. A.; White, A. J. P., Williams, D.J. *Chem. Commun.* **1998**, 849.
- 176 Britovsek, G. J. P.; Bruce, M.; Gibson, V. C.; Kimberley, B. S.; Maddox, P. J.; Mastroianni, S.; McTavish, S. J.; Redshaw, C.; Solan, G. A.; Stromberg, S.; White, A. J. P., Williams, D. J. *J. Am. Chem. Soc.* **1999**, *121*, 8728.
- 177 Small, B. L.; Brookhart, M. *J. Am. Chem. Soc.* **1998**, *120*, 7143.
- 178 Britovsek, G. J. P.; Mastroianni, S.; Solan, G. A.; Baugh, S. P. D.; Redshaw, C.; Gibson, V. C.; White, A. J. P.; Williams, D. J.; Elsegood, M. R. J. *Chem. Eur. J.* **2000**, *6*, 2221.
- 179 Gibson, V. C.; Hoarau, O. D.; Kimberley, B. S.; Maddox, P. J. (BP Chemicals Ltd., UK) *PCT Int. Appl. WO 0158966*, **2001**.
- 180 Britovsek, G. J. P.; Gibson, V. C.; Mastroianni, S.; Oakes, D. C. H.; Redshaw, C.; Solan, G. A.; White, A. J. P.; Williams, D.J. *Eur. J. Inorg. Chem.* **2001**, 431.
- 181 Smit, T. M.; Tomov, A. K.; Gibson, V. C.; White, A. J. P.; Williams, D.J. *Inorg. Chem.* **2004**, *43*, 6511.
- 182 Sun, W. -H.; Tang, X.; Gao, T.; Wu, B.; Zhang, W.; Ma, H. *Organometallics* **2004**, *23*, 5037.
- 183 Tellman, K. P.; Gibson, V. C.; White, A. J. P.; Williams, D. J. *Organometallics* **2005**, *24*, 280.
- 184 Bianchianni, C.; Giambastiani, G.; Guerrero, I. R.; Meli, A.; Passaglia, E.; Gragnoli, T. *Organometallics* **2004**, *23*, 6387.
- 185 Bouwkamp, M. W.; Lobkovsky, E.; Chirik, P. J. *J. Am. Chem. Soc.* **2005**, *127*, 9660.
- 186 Campora, J.; Naz, A. M.; Palma, P.; Alvarez, E.; Reyes, M. L. *Organometallics* **2005**, *24*, 4878..
- 187 Liu, J.; Li, Y.; Liu, J.; Li, Z. *Macromolecules* **2005**, *38*, 2559.
- 188 Gibson, V. C.; Long, N. J.; Oxford, P. J.; White, A. J. P.; Williams, D. J. *Organometallics* **2006**, *25*, 1932.
- 189 Karam, A.; Tenia, R.; Martinez, M.; Lopez-Linares, F.; Albano, C.; Diaz-Barrios, A.; Sanchez, Y.; Catari, E.; Casas, E.; Pekarar, S.; Albornoz, A. *J. Mol. Catal. A. Chem.* **2007**, *265*, 127.

- 190 Seitz, M.; Milius, W.; Alt, H. G. *J. Mol. Catal. A. Chem.* **2007**, 261, 246.
- 191 Britovsek, G. J. P.; Dorer, B. A.; Gibson, V. C.; Kimberley, B. S.; Solan, G. A. (BP Chemicals Ltd.; UK) *PCT Int. Appl. WO 991281*, **1999**.
- 192 Bennett, A. M. A.; Feldman, J.; McCord, E. F. (E.I. duPont de Nemours and Co., USA) *PCT Int Appl. WO 9962967*, **1999**.
- 193 Xu, W.; Wang, Q.; Wurz, R. P. (Nova Chemicals, Switzerland) EP1046647, **2000**.
- 194 Kirsten, M. O.; Gonioukh, A.; Lilge, D.; Lehmann, S.; Bildstein, B.; Amort, C.; Malaun, M. (BASF, A.-G.; Germany) *PCT Int. Appl. WO 0114391*, **2001**.
- 195 Tohi, Y.; Matsui, S.; Fujita, T. (Mitsui Chemicals Inc., Japan) *PCT Int. Appl. WO 9965952*, **1999**.
- 196 Bawson, D.M.; Walker, D. A.; Thornton-Pett, M.; Bochmann, M. *J. Chem.Soc. Dalton Trans.* **2000**, 459.
- 197 Tohi, Y.; Matsui, S.; Fujita, T. (Mitsui Chemicals Inc., Japan) *PCT Int. Appl. WO 9965951* **1999**.
- 198 Luo, H. -K. Yang, Z. -H.; Mao, B. -Q.; Yu, D. -S.; Tang, R. -G. *J. Mol. Catal. A: Chem.* **2002**, 177, 195.
- 199 Britovsek, G. J. P.; Clentsmith, G. K. B.; Gibson, V. C.; Goodgame, D. M. L.; McTavish, S. J.; Pankhurst, Q. *Catal. Commun.* **2002**, 3, 207.
- 200 Bryliakov, K. P.; Semikolenova, N. V.; Zakharov, V. A.; Talsi, E. P. *Organometallics* **2004**, 23, 5375.
- 201 Schmidt, G. F.; Brookhart, M. *J. Am. Chem. Soc.* **1985**, 107, 1443.
- 202 Al-Benna, S.; Sarsfield, M. J.; Thornton-Pett, M.; Ormsby, D. L.; Maddox, P. J.; Bres, P.; Bochmann, M. *J. Chem. Soc. Dalton Trans.* **2000**, 4247.
- 203 Longo, P.; Grisi, F.; Proto, A.; Zambelli, A. *Macromol. Rapid Commun.* **1998**, 19, 31.
- 204 Johnson, L. K.; Killian, C. M.; Arthur, S. D.; Feldman, J.; McCord, E. F.; McLain, S. J.; Kreutzer, K. A.; Bennett, M. A.; Coughlin, E. B (E.I. du Pont de Nemours and Co., USA; University of North Carolina at Chapel Hill) *PCT Int. Appl. WO 9623010*, **1996**.
- 205 Laine, T. V.; Klinga, M.; Maaninen, A.; Aitola, E.; Leskela, M. *Acta Chem. Scand.* **1999**, 53, 968.
- 206 Wang, L.; Flood, T. C. *J. Am. Chem. Soc.* **1992**, 114, 3169.
- 207 Wang, L.; Lu, R. S.; Bau, R.; Flood, T. C. *J. Am. Chem. Soc.* **1993**, 115, 6999.

- 208 Gibson, V. C.; Humphries, M. J.; Tellmann, K. P.; Wass, D. F.; White, A. J. P.; Williams, D.J. *Chem. Commun.* **2001**, 2252.
- 209 Kooistra, T. M.; Knijnenburg, Q.; Smits, J. M. M.; Horton, A. D.; Budzelaar, P. H. M.; Gal, A. W. *Angew. Chem. Int. Ed.* **2001**, 40, 4719.
- 210 Ittel, S. D.; Johnson, L. K.; Brookhart, M. *Chem. Rev.* **2000**, 100, 1169.
- 211 Gibson, V. C.; Spitzmesser, S. K. *Chem. Rev.* **2003**, 103, 283.
- 212 Strauch, J. W.; Erker, G.; Kehr, G.; Frohlich, R. *Angew. Chem. Int. Ed.* **2002**, 41, 2543.
- 213 Laine, T. V.; Klinga, M.; Leskela, M. *Eur. J. Inorg. Chem.* **1999**, 959.
- 214 Laine, T. V.; Lappalainen, K.; Liimatta, J.; Aitola, E.; Lofgren, B.; Leskela, M. *Macromol. Rapid Commun.* **1999**, 20, 487.
- 215 Laine, T. V.; Piironen, U.; Lappalainen, K.; Klinga, M.; Aitola, E.; Leskela, M. *J. Organomet. Chem.* **2000**, 606, 112.
- 216 Meneghetti, S. P.; Lutz, P. J.; Kress, J. *Organometallics* **1999**, 18, 2734.
- 217 Koppl, A.; Alt, H. G. *J. Mol. Catal. A: Chem.* **2000**, 154, 45.
- 218 McKenzie, P. B.; Moody, L. S.; Killian, C. M.; Ponasik Jr., J. A.; McDevitt, J. P.; Lavoie, G. G. (Eastman Chemical Co.) *US Patent 6103658*, **2000**.
- 219 Ponasik Jr.; J. A.; McKenzie, P. B.; Killian, C.M. (Eastman Chemical Co.) *US Patent 6117959*, **2000**.
- 220 Turner, S. R.; McKenzie, P. B.; Jones, A. S.; McDevitt, J. P.; Killian, C. M.; Ponasik Jr., J. A. (Eastman Chemical Co.) *US Patent 6090900*, **2000**.
- 221 Killian, C. M.; Ponasik Jr, J. A.; McDevitt, J. P.; McKenzie, P. B. (Eastman Chemical Co.) *US Patent 6174976*, **2001**.
- 222 Ponasik Jr, J. A.; McDevitt, J. P.; Killian, C. M.; McKenzie, P. B.; Lavoie, G. G.; Moody, L. S. (Eastman Chemical Co.) *US Patent 6200925*, **2001**.
- 223 Killian, C. M.; McKenzie, P. B.; Hyatt, J. A.; Moody, L. S.; Lavoie, G. G. (Eastman Chemical Co.) *US Patent 6350837*, **2002**.
- 224 Ponasik Jr, J. A.; McDevitt, J. P.; Killain, C. M.; McKenzie, P. B.; Moody, L. S. (Eastman Chemical Co.) *US Patent 6372682*, **2002**.
- 225 Cooley, N. A.; Green, S. M.; Wass, D. F.; Heslop, K.; Orpen, A. G.; Pringle, P. G. *Organometallics* **2001**, 20, 4769.
- 226 Liu, W.; Malinoski, J. M.; Brookhart, M. *Organometallics* **2002**, 21, 2836.

- 227 Heinicke, J.; He, M. Z.; Dal, A.; Klein, H. F.; Hetche, O.; Keim, W.; Florke, U.; Haupt, H.J. *Eur. J. Inorg. Chem.* **2000**, 431.
- 228 Heinicke, J.; Koesling, M.; Brull, R.; Keim, W.; Pritzkow, H. *Eur. J. Inorg. Chem.* **2000**, 299.
- 229 Soula, R.; Broyer, J. P.; Llauro, M. F.; Tomov, A.; Spitz, R.; Claverie, J.; Drujon, X.; Malinge, J.; Saudermont, T. *Macromolecules* **2001**, *34*, 2438.
- 230 Gibson, V. C.; Tomov, A.; White, A. J. P.; Williams, D. J. *Chem. Commun.* **2001**, 719
- 231 Komon, Z. J. A.; Bu, X. H.; Bazan, G. C. *J. Am. Chem. Soc.* **2000**, *122*, 1830.
- 232 Wang, C. M.; Friedrich, S.; Younkin, T. R.; Li, R. T.; Grubbs, R. H.; Bansleben, D. A.; Day, M. W. *Organometallics* **1998**, *17*, 3149.
- 233 Novak, B. M.; Tian, G.; Nodono, M.; Boyle, P. *PMSE-Preprints*, 223rd ACS national Meeting, Orlando, FL, April 7-11, 2002, American Chemical Society, Washington DC, **2002**, *86*, 326.
- 234 Hicks, F. A.; Brookhart, M. *Organometallics* **2001**, *20*, 3217.
- 235 Zhang, D.; Jin, G.-X. *Organometallics* **2003**, *22*, 2851.
- 236 Shim, C. B.; Kim, Y. H.; Lee, B. Y.; Dong, Y.; Yun, H. *Organometallics* **2003**, *22*, 4272
- 237 Kunrath, F. A.; de Souza, R. F.; Casagrande Jr., O. L.; Brooks, N. R.; Young, Jr., V. G. *Organometallics* **2003**, *22*, 4739.
- 238 Chen, H. -P.; Liu, Y. -H.; Peng, S. -M.; Liu, S. -T. *Organometallics* **2003**, *22*, 4893.
- 239 Tanabiki, M.; Tsuchiya, K.; Kumanomido, Y.; Matsubara, K.; Motoyama, Y.; Nagashima, H. *Organometallics* **2004**, *23*, 3976.
- 240 Ionkin, A. S.; Marshall, W. J. *Organometallics* **2004**, *23*, 3276.
- 241 Hu, T.; Tang, L. -M.; Li, X. -F.; Li, Y. -S.; Hu, N. -H. *Organometallics* **2005**, *24*, 2628.
- 242 Camacho, D. H.; Salo, E. V.; Ziller, J. W.; Guan, Z. *Angew. Chem. Int. Ed.* **2004**, *43*, 1821.
- 243 Camacho, D. H.; Salo, E. V.; Guan, Z.; Ziller, J. W. *Organometallics* **2005**, *24*, 4933.
- 244 Son, G. W.; Bijal, K. B.; park, D. -W.; Ha, C. -S.; Kim, I. *Catal. Today* **2006**, *11*, 412
- 245 Wang, W. -H.; Jin, G. -X. *Inorg. Chem. Commun.* **2006**, *9*, 548.
- 246 Chen, Q.; Yu, J.; Huang, J. *Organometallics* **2007**, *26*, 617.
- 247 Na, S. J.; Joe, D. J.; Sujith, S.; Han, W. -S.; Kang, S. O.; Lee, B. Y. *J. Organomet.*

- Chem.* **2006**, *691*, 611.
- 248 Zheng, L.; Brookhart, M.; White, P. S. *Organometallics* **2006**, *25*, 1868.
- 249 Carlini, C.; De Luise, V.; Galletti, A. M. R.; Sbrana, G. *J. Polym. Sci. Part A Polym. Chem.* **2006**, *44*, 20.
- 250 Okada, M.; Nakayama, Y.; Ikeda, T.; Shiono, T. *Macromol. Rapid Commun.* **2006**, *27*, 1418.
- 251 Benito, J. M.; de Jesus, E.; de la Mata, F. J.; Flores, J. C.; Gomez, R.; Gomez-Sal, P. *Organometallics* **2006**, *25*, 3876.
- 252 Gottker-Schnetmann, I.; Wehrmann, P.; Rohr, C.; Mecking, S. *Organometallics* **2007**, *26*, 2348.
- 253 Schrekker, H. S.; Kotov, V.; Preishuber-Pflugl, P.; White, P.; Brookhart, M. *Macromolecules* **2006**, *39*, 6341.
- 254 Johnson, L. K.; Mecking, S.; Brookhart, M. *J. Am. Chem. Soc.* **1996**, *118*, 267.
- 255 Mecking, S.; Johnson, L. K.; Wang, L.; Brookhart, M. *J. Am. Chem. Soc.* **1998**, *120*, 888.
- 256 Heinemann, J.; Mulhaupt, R.; Brinkmann, P.; Luinstra, G. *Macromol. Chem. Phys.* **1999**, *200*, 384.
- 257 Fernandes, S.; Marques, M. M.; Correira, S. G.; Mano, J.; Chien, J. C. W. *Macromol. Chem. Phys.* **2000**, *201*, 2566.
- 258 Marques, M. M.; Fernandes, S.; Correira, S. G.; Ascenso, J. R.; Coroco, S.; Gomes, P. T.; Mano, J.; Pereira, S. G.; Nunes, T.; Dias, A. R.; Rausch, M. D.; Chien, J. C. W. *Macromol. Chem. Phys.* **2000**, *201*, 2464.
- 259 Marques, M. M.; Fernandes, S.; Correira, S. G.; Coroco, S.; Gomes, P. T.; Mano, J.; Dias, A. R.; Rausch, M. D.; Chien, J. C. W. *Polym. Int.* **2001**, *50*, 579.
- 260 Gibson, V. C.; Tomov, A. *Chem. Commun.* **2001**, 1964.
- 261 Drent, E.; vN Dijk, R.; van Ginkel, R.; van Oort, B.; Pugh, R. I. *Chem. Commun.* **2002**, 744.
- 262 de Souza, R. F.; Casagrande, O. L. *Macromol. Rapid Commun.* **2001**, *22*, 1293.
- 263 Mota, F. F.; Mauler, R. S.; de Souza, R. F.; Casagrande, O. L. *Macromol. Chem. Phys.* **2001**, *22*, 1016.
- 264 Kunrath, F. A.; de Souza, R. F.; Casagrande, O. L. *Macromol. Rapid Commun.* **2000**,

- 21, 277.
- 265 Guan, Z.; Cotts, P. M.; McCord, E. F.; McLain, S. J. *Science* **1999**, 283, 2059.
- 266 Tempel, D. J.; Johnson, L. K.; Huff, R. L.; White, P. S., Brookhart, M. *J. Am. Chem. Soc.* **2000**, 122, 6686.
- 267 Luo, H. -K.; Yang, Z. -H.; Mao, B. -Q.; Yu, D. -S.; Tang, R. -G. *J. Mol. Catal. A: Chem.* **2002**, 177, 195.
- 268 Shultz, L. H.; Brookhart, M. *Organometallics* **2001**, 20, 3975.
- 269 Shultz, L. H.; Tempel, D. J.; Brookhart, M. *J. Am. Chem. Soc.* **2001**, 123, 11539.
- 270 Simon, L. C.; Williams, C. P.; Soares, J. B. P.; de Souza, R. F. *J. Mol. Catal. A: Chem.* **2001**, 165, 55.
- 271 Simon, L. C.; Williams, C. P.; Soares, J. B. P.; de Souza, R. F. *Chem. Eng. Sci.* **2001**, 56, 4181.
- 272 Woo, T. K.; Blochl, P. E.; Ziegler, T. *J. Phys. Chem. A* **2000**, 104, 121.
- 273 Michalak, A.; Ziegler, T. *Organometallics* **2000**, 19, 1850.
- 274 Michalak, A.; Ziegler, T. *J. Am. Chem. Soc.* **2001**, 123, 12266.
- 275 Michalak, A.; Ziegler, T. *J. Am. Chem. Soc.* **2002**, 124, 7519.
- 276 Musaev, D. G.; Froese, R. D. J.; Morokuma, K. *Organometallics* **1998**, 17, 1850.
- 277 Musaev, D. G.; Morokuma, K. *Topics Catal.* **1999**, 7, 107.
- 278 Froese, R. D. J.; Musaev, D. G.; Morokuma, K. *J. Am. Chem. Soc.* **1998**, 120, 1581.
- 279 Shibayama, K. *Pat. Appl. JP 11269214, JP 2000007719*, **2000**.
- 280 Shibayama, K.; Ogassa, M. *PCT Int.. Appl. WO 9835996*, Sekisui Chemical Co Ltd., Japan, **1998**.
- 281 Shibayama, K. *Pat. Appl. JP 2000103805*, **2000**.
- 282 Stibrany, R. T.; Schulz, D. N.; Kacker, S.; Patil, A. O. *PCT Int. Appl. WO 9930822*, Exxon, **1999**.
- 283 Stibrany, R. T.; Patil, A. O.; Zushma, S. *Polym. Mater. Sci. & Engg.* **2002**, 86, 323.
- 284 Stibrany, R. T.; Schulz, D. N.; Kacker, S.; Patil, A. O.; Baugh, L. S.; Rucker, S. P.; Zushma, S.; Berluce, E.; Sissano, J. A. *Polym. Mater. Sci. & Engg.* **2002**, 86, 325.
- 285 Stibrany, R. T.; Schulz, D. N.; Kacker, S.; Patil, A. O.; Baugh, L. S.; Rucker, S. P.; Zushma, S.; Berluce, E.; Sissano, J. A. *Macromolecules.* **2003**, 36, 8584.

- 286 Gibson, V. C.; Tomov, A.; Wass, D. F.; White, A. J. P.; Williams, D. J. *J. Chem. Soc., Dalton Trans.* **2002**, 2261.
- 287 Carlini, C.; Giaiacopi, S.; Marchetti, F.; Pinzino, C.; Galletti, A.M.R.; Sbrana, G. *Organometallics* **2006**, 25, 3659.
- 288 Chen, F. -T.; Tang, G. -R.; Jin, G. -X. *J. Polym. Sci. Part A. Polym. Chem.* **2007**, 692, 3435.
- .

CHAPTER 2
SCOPE AND OBJECTIVES

2.1. Introduction

Poly(olefin)s are of vast economic importance which is reflected by an annual production of more than 100 million tons of poly(ethylene)s and poly(propylene)s. Past two decades have witnessed tremendous advances in the preparation and application of organometallic complexes as olefin polymerization catalysts. Since the early 1980's there have been dramatic advances in a new class of catalysts, namely, metallocenes, which have impacted the polyolefins industry and resulted in a number of commercial processes for the preparation of polyolefinic materials with new or improved properties¹⁻⁴. In order to extend the range of properties of polyolefinic materials considerable effort has been devoted to the discovery of new families of catalysts. In pursuit of these efforts, particular importance has been paid either to gain greater control on polyolefin properties or to the preparation of new materials^{5,6}.

In recent years, there have been significant advances in the development of non-metallocene catalysts for olefin polymerization. Many novel ligands and metals have been explored in the design of organometallic complexes to be used as olefin polymerization catalysts. These include complexes based on early (Ti, Zr, Hf) as well as late (Ni, Pd, Fe, Co, Cu) transition metals.

An important advance in the late transition metal catalyzed polymerization processes was due to Brookhart and coworkers who showed that nickel(II) and palladium(II) complexes bearing bulky α -diimine ligands are capable of polymerizing ethylene and higher α -olefins to high molecular weight polymers⁷⁻¹¹. Hindered aryl groups on the α -diimine nitrogens block the axial coordination sites and retard chain transfer relative to propagation resulting in high molecular weight polymers. These complexes produce poly(ethylene)s with a microstructure ranging from almost linear to hyperbranched depending on the catalyst used and reaction variables. Nickel(II) and palladium(II) complexes also exhibit good functional group tolerance and, hence, can be used in the copolymerization of ethylene with polar comonomers such as acrylates. Gibson and coworkers^{12,13} reported iron and cobalt based catalysts based on bis(imino)pyridine ligands which are highly active in the

polymerization of ethylene and resulted in linear poly(ethylene)s.

Recently many copper based complexes have also been explored as olefin polymerization catalysts. Copper complexes based on benzamidinate¹⁴ and benzimidazole¹⁵⁻¹⁷ ligands are reported which exhibit relatively low activities. Gibson et al¹⁸ reported an α -diimine copper complex which produce very high molecular weight poly(ethylene)s with moderate activity. Vinyl addition polymerization of norbornene using copper(II) complexes has recently been reported.¹⁹⁻²⁰

Another class of catalysts that have been widely explored is the early transition metal complexes with bidentate ligands that combine two anionic functions such as cyclopentadienyl, indenyl or fluorenyl with alkoxide, amide or similar groups. In particular, complexes of bifunctional mono cyclopentadienyl ligands having an appended hetero atom donor have attracted considerable attention, as exemplified by “constrained geometry” catalysts(CGC)²¹⁻²³. These mono-cyclopentadienyl complexes are characterized by a covalently linked amide donor which stabilizes the metal center electronically, and a short bridging group which opens up one side of the complex. The Cp-M-N angle is less than 115°. The consequence of the open structure of these complexes is that they are capable of incorporating long chain α -olefins and sterically hindered monomers such as styrene into polyethylene chains. Constrained geometry catalysts produce polyolefins with narrow molecular weight and good comonomer distributions. Generally, narrow molecular weight distributions obtained with metallocene type catalysts tend to make melt processing of polymers more difficult. Constrained geometry catalysts produce polymers with good physical properties without sacrificing processability. Improved processability is due to the presence of small amounts of long chain branching resulting from the reincorporation of the α -olefins produced by the β -H transfer at higher temperatures.

Alt et al^{24,25} have reported several amido functionalized half sandwich complexes based on indenyl and fluorenyl ligands which show potential application as olefin polymerization catalysts.

2.2. Objectives of the present work

The objective of the present work was to explore organometallic complexes based on some novel ligands and metals as olefin polymerization catalysts.

1. A wide variety of late transition metal complexes based on iron, cobalt, nickel and palladium have been employed as olefin polymerization catalysts. While the iron and cobalt based complexes produce linear poly(ethylene)s, the nickel and palladium based complexes are characterized by the production of branched polyethylenes. However, reports on the polymerization of olefins using copper based catalysts are scarce. Few copper complexes based on benzamidinate, benzimidazole and α -diimine ligands are reported which exhibit either very low or moderate activities. The objective of this work was to synthesize several copper complexes based on α -diimine, bis(oxazoline) and bis(benzimidazole) ligands and explore them as olefin polymerization catalysts.
2. There are only very few reports on olefin polymerization using mono-cyclopentadienyl (or substituted cyclopentadienyl) complexes bearing pendant oxygen donor atom. Presence of metal-oxygen bond in these complexes was expected to provide enhanced thermal stability compared to bis(cyclopentadienyl) complexes. Therefore the objective of this work was to synthesize novel ansa- η^5 -mono-fluorenyl cyclohexanolato complexes of Group 4 metals (Ti, Zr, Hf) and study their behavior towards polymerization of ethylene.
3. Amido functionalized fluorenyl half-sandwich complexes of zirconium have recently been reported to be active catalysts for ethylene polymerization by Alt et al. All these complexes bear an alkyl group on the amido nitrogen. However, there are no reports on olefin polymerization using such complexes with an aryl group on the amido nitrogen. The objective was to synthesize Group 4 metal complexes of amido functionalized fluorenyl ligands bearing an aryl group on the amido nitrogen and investigate their behavior towards polymerization of ethylene.

2.3. References

- 1 Brintzinger, H. H.; Fischer, D.; Mulhaupt, R.; Rieger, B.; Waymouth, R. M. *Angew Chem. Int. Ed. Engl.* **1995**, *34*, 1143..
- 2 Bochmann, M. *J. Chem. Soc., Dalton Trans.* **1996**, 255.
- 3 Jordan, R. F. *Adv. Organomet. Chem.* **1991**, *32*, 325.
- 4 Thayer, A. M. *Chem Eng. News*, **1995**, Sept 11, 15.
- 5 Kaminsky, W.; Arndt, M. *Adv. Polym. Sci.* **1997**, *127*, 143.
- 6 Suhm, J.; Heinemann, J.; Worner, C.; Muller, P.; Stricker, F.; Kressler, J.; Okuda, J.; Mulhaupt, R. *Macromol. Symp.* **1998**, *129*, 1.
- 7 Johnson, I. K.; Killian, C. M.; Brookhart, M. *J. Am. Chem. Soc.* **1995**, *117*, 6414.
- 8 C. M. Killian, D. J. Tempel, L. K. Johnson, M. Brookhart, *J. Am. Chem. Soc.* **1996**, *118*, 11664.
- 9 Johnson, L. K.; Mecking, S.; Brookhart, M. *J. Am. Chem. Soc.* **1996**, *118*, 267.
- 10 Schleis, T.; Spaniol, T. P.; Okuda, J.; Heinemann, J.; Mulhaupt, R. *J. Organomet. Chem.* **1998**, *569*, 159.
- 11 Johnson, L. K.; Killian, C. M.; Arthur, S. D.; Feldman, J.; McCord, E. F.; McLain, S. J.; Kreutzer, K. A.; Bennett, M. A.; Coughlin, E. B.; Ittel, S. D.; Parthasarathy, A.; Tempel, D. J.; Brookhart, M. S. (DuPont) *PCT Int. Appl. WO 9623010*, **1996**.
- 12 Britovsek, G. J. P.; Gibson, V. C.; Kimberley, B. S.; Maddox, P. J.; McTavish, S. J.; Solan, G. A.; White, A. J. P.; Williams, D. J. *Chem. Commun.* **1998**, 849.
- 13 Britovsek, G. J. P.; Bruce, M.; Gibson, V. C.; Kimberley, B. S.; Maddox, P. J.; Mastroianni, S.; McTavish, S. J.; Redshaw, C.; Solan, G. A.; Stromberg, S.; White, A. J. P.; Williams, D. J. *J. Am. Chem. Soc.* **1999**, *121*, 8728.
- 14 Shibayama, K.; Ogassa, M. (Sekisui Chemical Company Ltd., Japan) *PCT Int. Appl. WO 9835996*, **1998**, Chemical Abstracts 1998, *129*, 203390.
- 15 Stibrany, R.T.; Patil, A. O.; Zushma, S. *PMSE-Preprints*, Vol. 86, 323-324.

- 16 Stibrany, R. T.; Schulz, D. N.; Kacker, S.; Patil, A. O. (Exxon Research and Engineering Co., USA). *PCT Int. Appl. WO 9930822*, **1999**; CA 1999, 131, 45236.
- 17 Stibrany, R. T.; Schulz, D. N.; Kacker, S.; Patil, A. O.; Baugh, L. S.; Rucker, S. P.; Zushma, S.; Berluche, E.; Sissano, J.A. *PMSE-Preprints*, Vol 86, 325.
- 18 Gibson, V. C.; Tomov, A.; Wass, D. F.; White, A. J. P.; Williams, D. J. *J. Chem. Soc. Dalton Trans.* **2002**, 2261.
- 19 Carlini, C.; Giaiacopi, S.; Marchetti, F.; Pinzino, C.; Galletti, A. M. R.; Sbrana, G. *Organometallics* **2006**, 25, 3659.
- 20 Chen, F. -T.; Tang, G. -R.; Jin, G. -X. *J. Polym. Sci. Part A. Polym. Chem.* **2007**, 692, 3435.
- 21 Canich, J. A. M. (Exxon Chemicals Patents Inc. Linden, N.J.), *Patent Appl. US 5227440*, **1993**.
- 22 Canich, J. A. M. (Exxon Chemicals Patents Inc. Linden, N.J.), *Patent Appl. US 5264405*, **1993**.
- 23 McKnight, A.L.; Waymouth, R.M. *Chem. Rev.* **1998**, 98, 2587.
- 24 Reb, A.; Alt, H. G. *J. Mol. Catal. A. Chem.* **2001**, 174, 35.
- 25 Alt, H. G.; Reb, A. *J. Mol. Catal. A. Chem.* **2001**, 175, 43.

CHAPTER 3

EXPERIMENTAL METHODS

3.1. Introduction

All the catalysts used are sensitive to air and/or moisture and the active centers in Ziegler-Natta polymerizations are susceptible to termination by protic sources. Hence, all reagents and solvents should be carefully purified and dried prior to use. All manipulations of air- and/or moisture-sensitive compounds were performed using high vacuum or Schlenk techniques. All manipulations involving solid, air and moisture sensitive compounds were performed inside an inert atmosphere glove box (M. Braun/labmaster 100) continuously purged with high purity nitrogen. Argon and nitrogen were purified by passage through columns of phosphorus pentoxide.

In this chapter, materials used, methods of purification and drying of reagents, polymerization procedures and polymer characterization techniques are discussed.

3.2. Materials

Table 3.1 List of chemicals used

Name of chemical	Formula/Abbreviation	Grade/purity	Source
Absolute ethanol	C ₂ H ₅ OH	GR	E-Merck, Germany
Acenaphthenequinone	C ₁₂ H ₆ O ₂	Tech.	Aldrich, USA
Acetone	C ₃ H ₆ O	LR	S.D.Fine Chem Ltd., India
Acetonitrile	CH ₃ CN	AR	S.D. Fine Chem Ltd., India
2-Amino-3-methyl-1-butanol	(CH ₃) ₂ CHCH(NH ₂)CH ₂ OH	97%	Aldrich, USA
2-Amino-2-methyl-1-propanol	(CH ₃) ₂ C(NH ₂)CH ₂ OH	95%	Aldrich, USA
Ammonium chloride	NH ₄ Cl	LR	Thomas Baker, India

Benzophenone	$(C_6H_5)_2CO$	99 %	Aldrich, USA
1-Bromobutane	$CH_3(CH_2)_2CH_2Br$	99%	Aldrich, USA
2- <i>tert</i> -Butylaniline	$(CH_3)_3CC_6H_4NH_2$	99%	Aldrich, USA
<i>n</i> -Butyl lithium	<i>n</i> -BuLi	2.5M solution in hexane	Aldrich, USA
Calcium hydride	CaH_2	95%	Aldrich, USA
Celite Filter agent	SiO_2	95%	Aldrich, USA
Copper(II)bromide	$CuBr_2$	99%	E-Merck, Germany
Copper(II)chloride	$CuCl_2$	99%	E-Merck, Germany
Decahydronaphthalene	$C_{10}H_{16}$	99+%, anhydrous	Aldrich, USA
1,2-Dichlorobenzene	$C_6H_4Cl_2$	ExtrapureAR	SISCO, India.
Dichlorodiphenylsilane	$(C_6H_5)_2SiCl_2$	97%	Aldrich, USA
Dichloromethane	CH_2Cl_2	LR	Merck, India.
Diethyl ether	$(C_2H_5)_2O$	LR	S.D. Fine Chem Ltd., India
Diethyl oxalate	$(COOC_2H_5)_2$	Synthesis	Merck, India
2,6-Diisopropylaniline	$[(CH_3)_2CH]_2C_6H_3NH_2$	90%	Aldrich, USA
2,6-Dimethylaniline	$(CH_3)_2C_6H_3NH_2$	99%	Aldrich, USA
1,2-Dimethoxyethane	$C_2H_4(OCH_3)_2$ (DME)	99+ %	Aldrich, USA
Epoxycyclohexane	$C_6H_{10}O$	Synthesis	Merck, India
Ethanolamine	$CH_2(OH)CH_2(NH_2)$	GR	Merck, India

Fluorene	$C_{13}H_{10}$	98%	Aldrich, USA
Formic acid	HCOOH	97%	Indian Drugs & Petrochemicals Ltd. India.
Glyoxal	OHC-CHO	LR	S.D. Fine Chem Ltd., India
Hafnium(IV) chloride	HfCl ₄	99.9+ %	Aldrich, USA
Hexane	$CH_3(CH_2)_4CH_3$	AR	S.D. Fine Chem Ltd, India
Hexene-1	$CH_3(CH_2)_3CH=CH_2$	97%	Aldrich, USA
Hydrochloric acid	HCl	LR	S.D.Fine Chem Ltd., India
Iodomethane	CH ₃ I	99%	Aldrich, USA
Irganox 1010	$C_{16}H_{24}N_{10}O_4$	antioxidant	Ciba-Giegy, Switzerland
<i>tert</i> -Leucinol	$(CH_3)_2CCH(NH_2)CH_2OH$	98%	Aldrich, USA
Malonic acid	$CH_2(COOH)_2$	99%	Aldrich, USA
Methanol	CH ₃ OH	LR	S.D.Fine Chem Ltd., India
Molecular Sieves	$Na_{12}[(AlO_2)_{12}(SiO_2)_{12}].$ xH_2O		S.D. Fine Chem.Ltd., India
Methylaluminoxane	MAO	30 wt % solution in toluene. Me/Al = 1.7	Witco GmbH, Germany.

		free TMA = 31 wt %. Al content = 10.9 %	
Nickel(II)Bromide	NiBr ₂	Anhydrous, 99.99+ %	Aldrich, USA
Octene-1	CH ₃ (CH ₂) ₅ CH=CH ₂	98%	Aldrich, USA
Pentane	CH ₃ (CH ₂) ₃ CH ₃	LR	S.D.Fine Chem. Ltd., India.
Petroleum ether		Synthesis	Merck, India
1,2-Phenylenediamine	C ₆ H ₄ (NH ₂) ₂	99.5%	Aldrich, USA
Potassium hydroxide	KOH	LR	S.D.Fine Chem Ltd., India
Sodium hydride	NaH	60% dispersion in mineral oil	Lancaster,
Sodium metal	Na	LR	S.D.Fine Chem. Ltd., India.
Sodium sulphate	Na ₂ SO ₄	Anhydrous LR	S.D.Fine Chem.Ltd., India.
1,1,2,2- Tetrachloroethane-d ₂	Cl ₂ CDCDCl ₂	99.5+atom % D	Aldrich, USA
Tetrahydrofuran	THF	Synthesis grade	Merck, India.
Thionyl chloride	SOCl ₂	Synthesis	Merck, India
Titanium(IV) chloride	TiCl ₄	99.9+ %	Aldrich, USA

Toluene	$C_6H_5CH_3$	Sulfur free, LR	S.D. Fine Chem. Ltd., India.
p-Toluenesulphonic acid	PTSA	AR	Merck, India
1,2,4-Trichlorobenzene	$C_6H_3Cl_3$	Spectroscopic grade	Aldrich, USA
Triethylorthoformate	$CH(OC_2H_5)_3$	98%	Aldrich, USA
Triisobutylaluminium	TIBAL		Witco GmbH, Germany.
Trimethylaluminium	TMA		Schering A.-G., Germany.
Zirconium(IV) chloride	$ZrCl_4$	99.9+ %	Aldrich, USA

3.3. Purification and drying

All solvents and reagents were purified and dried under dry nitrogen atmosphere by standard procedures.¹ Toluene, n-hexane, n-pentane, diethylether and tetrahydrofuran were distilled from sodium benzophenone ketyl radical. Dichloromethane, 1,2-dichlorobenzene, 2,6-diisopropylaniline, 2,6-dimethyl aniline and 2-tert-butyl aniline were dried and distilled from calcium hydride.

3.4. Polymerization techniques

3.4.1. Apparatus used for polymerization of ethylene at one bar pressure

A glass tube of 3 L capacity with a glass jacket, a three-way stopcock and a supporting glass tube was fabricated. The fabricated unit was mounted on a wooden platform. In order to calibrate the fabricated glass apparatus, graph sheets were pasted on the wooden frame. Upon calibration, it was found that one unit on the graph sheet corresponds to 30 mL of ethylene. The calibrated glass tube was used as a gas burette for measuring the differences in displacement of volume of ethylene during the polymerization. A three-neck

flat-bottomed jacketed vessel of capacity 100-150 mL was used as the polymerization reactor.

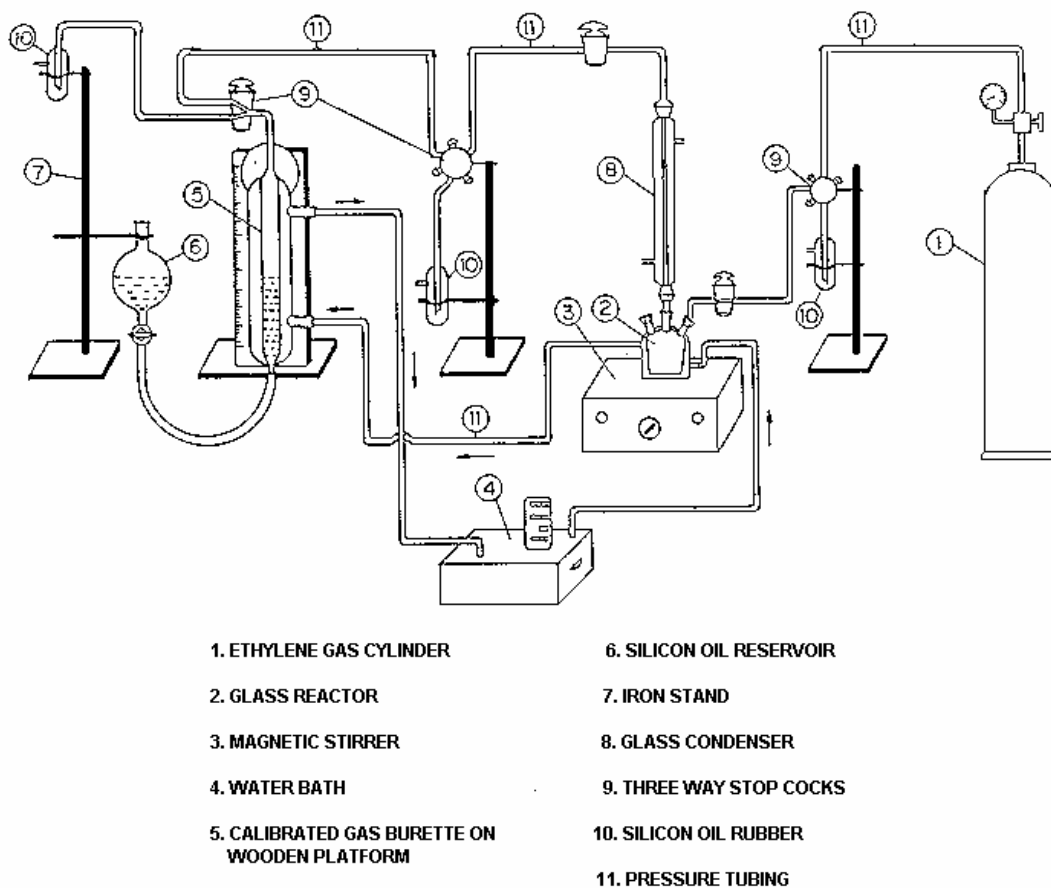


Figure 3.1 Set up for polymerization of ethylene at one bar pressure

A separating funnel of 4 L capacity filled with paraffin oil was connected to the gas burette through a PVC tubing. The reaction cell was mounted on a magnetic stirrer, which was connected to the gas burette through a T-shaped stopcock using pressure tubing. Two paraffin bubblers were also connected for purging purpose to the reaction assembly and gas burette as shown in the diagram. The reaction cell was dried at 200 °C overnight and thoroughly checked for leaks by running a blank experiment under one atmosphere pressure for 2-3 hours. The paraffin oil was saturated with ethylene gas before starting the experiment.

3.4.2. Polymerization of ethylene at 1 bar pressure

Polymerization was performed with the assembly described previously at one atmosphere pressure in toluene. Ethylene was continuously fed to the cell using a gas burette with a reservoir containing paraffin oil. The reaction cell, pre dried at 200 °C overnight was cooled under ethylene. The gas burette was flushed 2-3 times by passing ethylene. Solvent was introduced into the cell using a hypodermic syringe and saturated with ethylene. Toluene solution of the cocatalyst was added. Polymerization was initiated by the addition of the catalyst dissolved in suitable solvent (toluene in the case of titanium and zirconium complexes and o-dichlorobenzene in the case of copper catalysts). Polymerization temperature was maintained by circulating water from a thermostat through the jacket of the cell and the gas burette. Ethylene uptake was measured as a function of time from the gas burette. The reaction was terminated by the addition of acidified methanol (methanol containing 10 % HCl). The polymer was precipitated by the addition of acetone, filtered, washed with acetone and dried at 60 °C under vacuum.

3.4.3. Polymerization of ethylene at higher pressures

Polymerization of ethylene at high pressures was performed in a Buchi AG miniclave (**Figure 3.2**). The oven-dried glass reactor (heated at 200°C overnight) was cooled in an atmosphere of ethylene. Toluene (30 mL) was injected into the reactor through a hypodermic syringe and stirred for 10 minutes in order to achieve saturation with ethylene. This was followed by addition of the comonomer (in the case of copolymerizations). The cocatalyst was then added through a syringe. Finally the catalyst solution was added through a syringe and the reactor was pressurized with ethylene. After 60 min, polymerization was terminated by addition of methanol containing 15% dilute hydrochloric acid and the polymer was precipitated in methanol. The polymer was filtered, washed several times with methanol and dried at 60°C in vacuum.

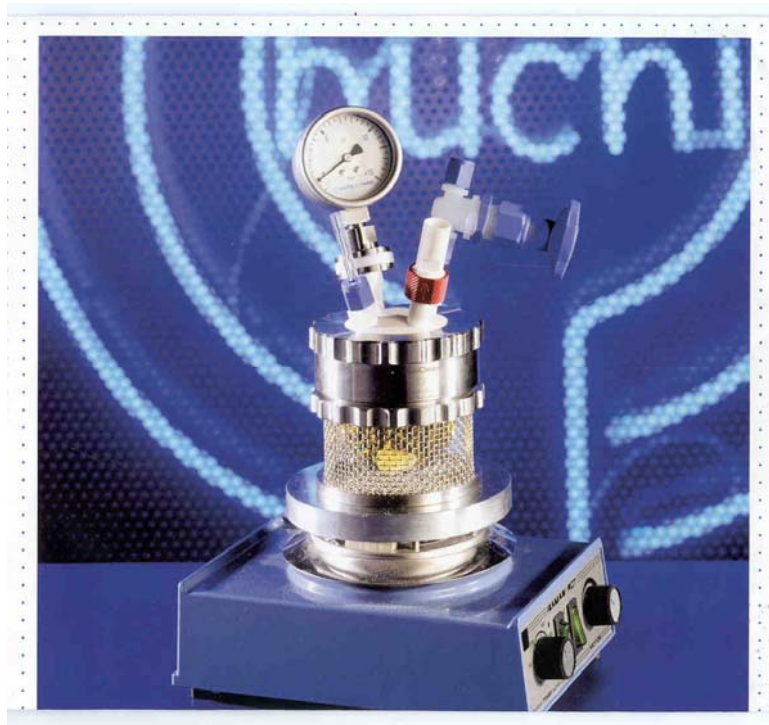


Figure 3.2 Buchi miniclave

3.5. Characterization techniques

3.5.1. Gel permeation chromatography (GPC)

The molecular weights and molecular weight distributions of the polymer samples were determined by high temperature GPC analysis. A GPC instrument, PL 220, equipped with a refractive index detector was employed using μ -styragel columns (10^6 , 10^5 , 10^4 , 10^3 , 500\AA) and 1,2,4-trichlorobenzene as the solvent at 160°C with a flow rate of $1\text{mL}/\text{min}$. Universal calibration method was used for analysis. The solvent was filtered through $0.45\ \mu$ membrane filter (Millipore) thrice prior to use.

3.5.2. Differential scanning calorimetry (DSC)

DSC of the homo- and copolymers were recorded on a Perkin Elmer DSC 7 instrument. The sample was initially heated upto $150\ ^\circ\text{C}$ at a heating rate of $10^\circ\text{C}/\text{min}$ and then rapidly cooled to $50\ ^\circ\text{C}$ at a rate of $100\ ^\circ\text{C}/\text{min}$. Finally the sample was again heated at a rate of $10\ ^\circ\text{C}/\text{min}$. The melting points reported were calculated from the second heating curve.

3.5.3. Intrinsic viscosity

Intrinsic viscosities of the polymer samples were determined in decahydronaphthalene at 135 °C using an Ubbelohde viscometer.

3.5.4. Infra red spectra

IR spectra were recorded on a Perkin Elmer 16 PC FT-IR Spectrometer.

3.5.5. NMR spectra

¹H NMR spectra of the ligands and complexes were recorded using a 200 MHz and 500 MHz Bruker NMR spectrometer. Deuterated solvents like CDCl₃, C₆D₆, 1,1,2,2-tetrachlorodideuterioethane were used.

Quantitative ¹³C NMR of the polymers were recorded on Bruker DRX-500 NMR spectrometer at 130°C under quantitative conditions (90° pulse followed by 10 seconds delay). Samples were prepared by dissolving about 200 mg of the polymer in 2 mL of 1,1,2,2-tetrachlorodideuterioethane or 1,2-dichlorobenzene/benzene-d₆ in a 10-mm-o.d. tube.

3.5.6. Cyclic voltametry

Electrochemical measurements were made in equimolar dichloromethane : acetonitrile solvent using tetraethylammonium perchlorate (TEAP) as the supporting electrolyte with the help of BAS cyclic voltammetric model CV-27 with automatic system under a dry and pure nitrogen atmosphere. The three-electrode system employed consisted of platinum working electrode, platinum wire (auxillary electrode) and SCE as the reference electrode.

3.5.7. Single crystal X-ray crystallography

Single crystal X-ray diffraction data were collected on a Bruker AXS Smart Apex CCD diffractometer at 297(2) K. The X-ray generator was operated at 50 kV and 30 mA. X-ray data collection was monitored by Bruker's SMART program (Bruker(1998) SMART Version 5.0. Bruker AXS Inc., Madison, Wisconsin, USA). All the data were corrected for Lorentzian polarization and absorption effects using Bruker's SAINT and SADABS programs (Bruker SMART (V5.628), SAINT (V6.45a), Bruker AXS Inc., Madison, Wisconsin, USA, 2004). XPREP was used to determine the space group. The initial structure was solved by SHELX-97 and refined by least squares methods based on F^2 (Sheldrick, G.M. SHELXS 97, SHELXL 97: University of Gottingen, Germany, 1997). Molecular diagrams were generated using XShell program embedded in SHELXTL. Geometrical calculations were done using SHELX-97. All the hydrogen atoms were treated as riding model and refined isotropically.

3.5.8. Electron paramagnetic resonance (EPR) spectra

EPR spectra of the complexes were recorded in dichloromethane solution on a Bruker EMX spectrometer operating at a frequency of 9.45 GHz (X-band). Samples were taken in Suprasil quartz aqueous cell and measurements were done at 77 K using 100 kHz field modulation and a modulation amplitude of 2 G_p .

3.6. References

1. L. F. Armarego and D. D. Perrin, *Purification of laboratory chemicals*, W. Eds., 4th Edn., Butterworth Heinemann **1996**.

CHAPTER 4
**POLYMERIZATION OF ETHYLENE USING (α -DIIMINE) COPPER(II)
COMPLEXES**

4.1. Introduction

In recent years many advances have been made in the field of late transition metal catalysts for olefin polymerization. A large variety of complexes based on iron, cobalt, nickel and palladium for polymerization of olefins are reported in the literature. However, with the exclusion of ATRP¹, there are only very few reports on polymerization catalysts based on copper. Copper presents an attractive candidate for olefin polymerization, as it may be more tolerant of polar comonomers than any of the previously used metals, thus offering new opportunities for preparing copolymers of ethylene with polar monomers.

Shibayama et al²⁻⁴ reported an amidinate-based copper complex, N, N'-bis (trimethylsilyl benzamidinato) copper (II) chloride, which when activated with methylaluminumoxane, produced poly(ethylene)s with M_w of 820,000 and T_m of 138°C.

Several bis(benzimidazole) copper complexes have been reported by Stribany et al⁵⁻¹⁵ that, when activated with MAO, homopolymerize ethylene and acrylates and also copolymerize these two monomers. They also exhibit activities towards vinyl ethers^{5,6} and α -olefins¹⁰. Poly(ethylene)s produced by these catalyst systems at 80°C and 50 bar ethylene pressure possess high molecular weights ($M_w = 150000$), narrow molecular weight distributions ($M_w/M_n = 2.5$) and high melting point ($T_m = 138^\circ\text{C}$)¹². ¹³C NMR spectrum of poly(ethylene)s confirmed their linear nature. These observations suggest a single site coordination/insertion mechanism for these catalyst systems. This was further supported by mechanistic studies using ¹⁹F labeled copper catalysts¹³.

Homopolymerization of acrylates was also studied using copper bis(benzimidazole)/MAO catalysts⁸. Monomer reactivity was found to follow the order t-butyl acrylate > n-butyl acrylate > methyl methacrylate. An increase in Al/Cu ratio and longer reaction times were found to increase the polymer conversion. The resulting polymers possess high molecular weights and narrow molecular weight distributions. Tacticities of these polymers were different from poly(acrylate)s prepared by free radical mechanism. Moreover these catalysts do not polymerize monomers like styrene, butadiene and vinyl acetate and failed to induce atom transfer radical polymerization with PhEtCl or reverse atom radical transfer

polymerization with AIBN. This led to the conclusion that homopolymerization of acrylates using these copper bis (benzimidazole)/MAO catalysts do not proceed via free radical or ATRP mechanisms.

Copolymerization of ethylene with t-butyl acrylate was studied using copper bis(benzimidazole)/MAO catalysts at 80°C and 40-55 bar ethylene pressure^{8,14}. The copolymers possess high molecular weight, narrow molecular weight distribution and low levels of branching. High levels of acrylate incorporation (45-100 mol %) can be achieved by these catalysts⁸. A typical copolymer with 67 mol% t-butyl acrylate showed a M_w of 108,000 and M_w/M_n of 1.8¹⁴.

Recently Baugh et al¹⁵ reported several copper bis(benzimidazole) complexes with perfluorinated carbon spacers. Introduction of perfluorinated two carbon spacer in the ligand backbone instead of one carbon spacer was found to reduce the bite angle slightly. However no obvious correlation between ligand structure and copolymer composition was observed. Ethylene copolymerization with t-butyl acrylate, methyl acrylate, methyl methacrylate and t-butyl methacrylate were studied using these complexes/MAO. The lowest acrylate incorporations were obtained with t-butyl methacrylate (37-69 mol %) while the highest incorporations were obtained with methyl acrylate (>85 mol%). Copolymers of ethylene with methyl acrylate and methyl methacrylate showed presence of unusual γ -keto ester structures at low acrylate feeds, that may arise from chain termination or transfer processes. This type of structures may result from 1,2 -insertion of acrylate followed by the attack of the resultant, less stable chain end at a pendant carbonyl site.

(α -diimine) copper complexes active for the polymerization of ethylene were reported by Gibson et al¹⁶. The *ortho*-phenyl substituted catalyst showed an activity of 22.5 g PE $\text{mmol}^{-1} \text{Cu h}^{-1}$ at 4.5 bar ethylene pressure whereas the *ortho*-isopropyl substituted catalyst gave only traces of polymer at 5 bar pressure. Activity of the *ortho*-phenyl substituted catalyst increased to 300 g PE $\text{mmol}^{-1} \text{Cu h}^{-1}$ when ethylene pressure was increased to 30 bar. Higher activity of the *ortho*-phenyl substituted catalyst was explained to be due to stabilization of the active species through weak interactions with *ortho*-phenyl substituents.

Several bis(salicylaldiminato) copper(II) complexes¹⁷ when activated with MAO (containing 15% TMA) were reported to be active for vinyl-type polymerization of norbornene. No catalyst activity was observed with TMA alone or with TMA-free MAO indicating that both TMA and MAO are necessary for catalyst activity. Moreover complete deactivation of the catalyst occurred when MAO containing 28 mol% TMA was employed as cocatalyst. The catalysts were active even at 80°C but slight deactivation was observed at 100°C. Presence of electron withdrawing nitro groups on phenol moiety of the catalyst played an important role in the activation. FT-IR and NMR analysis showed the non-stereoregular vinyl-type structure of the poly(norbornene)s. High molecular weight and non-stereoregular vinyl-type structure of poly(norbornene)s also indicates that a non-radical mechanism is operating in the case of these catalysts. ESR studies on the polymerization system supported the formation of a Cu (I) active species. Vinyl addition polymerization of norbornene using copper (II) complexes based on bis{{2'-(4',6'-di-*t*-butylhydroxy-phenyl)-1,4,5-triphenylimidazole}} has been reported recently that resulted in high catalyst activities and high molecular weight atactic poly(norbornene)s¹⁸.

In this chapter, synthesis and characterization Cu (II) and Cu(I) complexes containing α -diimine, bis (oxazoline) and bis(benzimidazole) ligands are described and their efficacy in the polymerization of ethylene explored. The (α -diimine) copper complex with acenaphthene based chelating ligand framework was selected for the study. The analogous nickel complex has been reported to be active for polymerization of ethylene. The objective was to compare the polymerization behaviour of copper complexes with that of nickel complexes. Bis(oxazoline) and bis(benzimidazole)copper(II) complexes were explored for the polymerization of ethylene as they possess the diimine structure with an oxygen or nitrogen atom linked to the imine moiety.

4.2. Experimental

4.2.1. Materials and their purification

This has been described in Chapter 3, Section 3.2 and 3.3

4.2.2. Synthesis of (α -diimine) copper complexes

4.2.2.1. Synthesis of [(N,N'-diisopropylbenzene)-2,3-naphthyl-(1,4-diazabutadiene)] dichlorocopper(II) (2a)

4.2.2.1.1. Synthesis of [(N,N'-diisopropylbenzene)-2,3-naphthyl-(1,4-diazabutadiene)] (1a)

The ligand was prepared according to literature procedure¹⁹.

Analysis for C₃₆H₄₀N₂:

Calcd., % C 86.40 H 8.00 N 5.60

Found, % C 86.13 H 7.52 N 5.68

¹H NMR (CDCl₃, 200 MHz): δ ppm 7.9(d,2H), 7.4(t, 2H), 7.25(s, 6H), 6.15 (d, 2H), 3.05(septet, 4 H), 1.25(d, 12 H), 1.0(d, 12 H).

¹³C NMR (CDCl₃, 50 MHz): δ ppm 23.1, 23.3, 28.6, 123.4, 127.8, 128.8, 129.5, 131, 135.3, 140.8, 147.5, 160.9.

IR(nujol mull): cm⁻¹ 1672 w, 1650 w, 1588 w, 1378 s, 1342 w, 1272 w, 1178 w, 1106 w, 1084 w, 1060 w, 1034 w, 938 w, 922 w, 834 w, 786 w, 748 m, 724 m, 590 w, 532 w, 500 w, 478 w, 464 w, 456 w.

4.2.2.1.2. Synthesis of 2a

Anhydrous copper (II) chloride (0.1345 g, 1.0 mmol) was taken in a 100 mL round-bottomed flask and absolute ethanol was added to it to form a green solution. Ligand **1a** (0.525 g, 1.05 mmol) dissolved in dichloromethane was added to this solution and the mixture was stirred overnight. A brown-colored crystalline precipitate was formed which was filtered, washed with ethanol and dried. Yield : 0.54 g (85%)

Analysis for C₃₆H₄₀N₂CuCl₂ :

Calcd., C % 68.09 H 6.30 N 4.41

Found, C % 67.69 H 6.02 N 4.20

IR (nujol mull) : cm⁻¹ 1630 m, 1582 m, 1378 s, 1292 w, 1256 w, 1222 w, 1182 w, 1132 w, 1104 w, 1048 w, 936 w, 836 w, 782 w, 756 w, 722 w.

EPR: g_{||} = 2.19, g_⊥ = 2.05.

4.2.2.2. Synthesis of [(N,N'-diisopropylbenzene)-2,3-naphthyl-(1,4-diazabutadiene)] dibromocopper(II) (2b)

The complex was prepared by the same procedure as complex **2a** using ligand **1a** and CuBr₂ in ethanol/dichloromethane. Yield: 1.2 g (85 %).

Analysis for $C_{36}H_{40}N_2CuBr_2$:

Calcd., C % 59.71 H 5.53 N 3.87

Found, C % 59.81 H 5.48 N 3.92

IR(nujol mull): cm^{-1} 1648 s, 1624 s, 1578 w, 1416 s, 1378 w, 1364 w, 1320 m, 1288 w, 1254 w, 1220 w, 1180 m, 1148 w, 1128 w, 1086 w, 1056 w, 1044 m, 938 m, 848 s, 834 s, 800 s, 780 s, 758 w, 612 m, 542 m, 512 m, 478 m, 460 m, 452 m.

EPR: $g_{||} = 2.27$, $g_{\perp} = 2.14$.

4.2.2.3. Synthesis of [(N,N'-2-*tert*-butylbenzene)-2,3-naphthyl-(1,4-diazabutadiene)] dichloro copper(II) (2c)

4.2.2.3.1. Synthesis of [(N,N'-2-*tert*-butylbenzene)-2,3-naphthyl -(1,4-diazabutadiene)] (1b)

The ligand was prepared according to literature procedure¹⁹.

Analysis for $C_{32}H_{32}N_2$:

Calcd., % C 86.49 H 7.21 N 6.34

Found, % C 86.61 H 7.83 N 6.31

1H NMR ($CDCl_3$, 200 MHz): δ ppm 7.84 (d, 2 H) 7.51 (m, 2 H), 7.36 (t, 2H), 7.19 (m, 4 H), 6.96(m, 2 H), 6.84(d, 2 H), 1.39(s, 18 H).

^{13}C NMR ($CDCl_3$, 50 MHz): δ ppm 160.1, 150.8, 142.05, 139.55, 131.43, 129.41, 128.97, 127.94, 126.98, 124.85, 124.11, 119.19, 35.75, 30.05

4.2.2.3.2. Synthesis of 2c

Anhydrous copper (II) chloride (0.150 g, 1.126 mmol, 1 eqv) was weighed into a round-bottomed flask. Ethanol was added to it and a green solution formed. Ligand **1b** (0.55 g, 1.23 mmol, 1.1 eqv) dissolved in dry dichloromethane was added with stirring. A precipitate formed after a few minutes. The reaction mixture was stirred overnight. Solvents were removed through a cannula; the complex was washed with dry n-hexane and dried in vacuum. Yield: 0.56 g (86%)

Analysis for $C_{32}H_{32}N_2CuCl_2 \cdot CH_2Cl_2$:

Calcd., % C 59.63 H 5.12 N 4.22

Found, % C 59.87 H 4.96 N 4.15

4.2.2.4. Synthesis of [(N,N'-diisopropylbenzene)-2,3-naphthyl-(1,4-diazabutadiene)] chloro copper(I) (3a)

The complex was prepared by the same procedure as complex **2a** using CuCl and ligand **1a** in ethanol. Yield : 0.72 g (80 %).

Analysis for C₃₆H₄₀N₂CuCl. C₂H₅OH :

Calcd., % C 70.69 H 7.14 N 4.34

Found, % C 70.96 H 6.49 N 4.32

IR(nujol mull): cm⁻¹ 1642 m, 1434 w, 1380 s, 1362 w, 1280 m, 1254 w, 1218 w, 1178 m, 1120 w, 1088 w, 1042 m, 938 w, 830 m, 796 s, 778 s, 752 w, 622 w, 540 w, 512 w, 486 w, 474 w, 464 w.

4.2.2.5. Synthesis of [(N,N'-diisopropylbenzene)-2,3-naphthyl-(1,4-diazabutadiene)] bromo copper(I) (3b)

The complex was prepared by the same procedure as complex **3a** using CuBr(0.143 g) and ligand **1a** (0.50 g) in ethanol. Yield: 0.53 g (82 %).

Analysis for C₃₆H₄₀N₂CuBr :

Calcd., % C 67.1 H 6.21 N 4.35

Found, % C 66.5 H 6.09 N 4.14

IR(nujol mull): cm⁻¹ 1644 m, 1378 s, 1280 m, 1120 m, 1088 w, 1042 w, 938 m, 830 m, 778 s, 754 s

4.2.2.6. Synthesis of [(N,N'-diisopropylbenzene)-2,3-naphthyl-(1,4-diazabutadiene)] dibromo nickel(II) (4)

The complex was prepared by the literature procedure¹⁹ using ligand **1a** and NiBr₂(DME).

Analysis for C₃₆H₄₀N₂NiBr₂

Calcd., % C 60.12 H 5.61 N 3.89

Found, % C 59.98 H 5.45 N 3.73

4.2.2.7. Synthesis of [(N,N'-diisopropylbenzene)(1,4-diazabutadiene)] dichloro copper(II) (6)

4.2.2.7.1. Synthesis of [(N,N'-diisopropylbenzene)(1,4-diazabutadiene)] (5)

In a 100 mL round-bottomed flask, 20 mL of methanol and a few drops of formic acid were added. 7 mL (34.5 mmol) of 2,6-diisopropylaniline was added to it and the flask was cooled to 0 °C. To this, 2.5 mL (17.25 mol) of glyoxal (40% aqueous solution) was added dropwise. After 5-10 min, a yellow precipitate formed and the reaction mixture turned yellow. It was stirred overnight. The precipitate was filtered and washed with cold methanol. The compound was recrystallized from hexane/methanol mixture and redissolved in hexane to which methanol was added and kept in a freezer. Crystals of the compound were collected in a Buchner funnel and washed with cold methanol and dried. Yield: 0.40 g (60%)

Analysis for C₂₆H₃₆N₂:

Calcd., % C 82.97 H 9.57 N 7.45

Found, % C 83.30 H 10.17 N 7.33

¹H NMR (CDCl₃, 200 MHz) δ ppm 8.1 (s, 2, CH=N), 7.2 (m, 6, H aryl), 2.9 (m, 4, CHPh), 1.25 (d, 24, CH (CH₃)₂)

4.2.2.7.2. Synthesis of 6

Anhydrous copper(II) chloride (0.300 g, 2.2 mmol, 1 eqv) was weighed into a round-bottomed flask inside the glove box. Ethanol and triethylorthoformate were added to it and a green solution formed. Ligand **5** (1 g, 2.6 mmol, 1.2 eqv) dissolved in dry dichloromethane was added with stirring. A precipitate formed after a few minutes. The reaction mixture was kept stirring for 18 h. Solvents were removed through a cannula; the complex was washed with dry n-hexane and dried in vacuum. Yield: 0.90 g (80%)

Analysis for C₂₆H₃₆N₂CuCl₂ :

Calcd., % C 61.12 H 7.0 N 5.48

Found, % C 61.11 H 6.81 N 5.37

4.2.3. Synthesis of bis(oxazoline) copper(II) complexes

4.2.3.1. Synthesis of 2,2'-bis(1,3-oxazoline) dichlorocopper(II) (10a)

4.2.3.1.1. Synthesis of 2, 2'-bis (1, 3-oxazoline) (9a)

The ligand was synthesized by a modification of literature procedure²⁰.

Diethyl oxalate (2 mL, 16.5 mmol) was added to ethanolamine (2 mL, 33.0 mmol) in a 100 mL R.B. flask and stirred at room temperature for 2 h. An exothermic reaction was observed and a white solid formed. The solid, N,N'-bis(1-hydroxyethyl)1,2-ethane diamide (**7a**) was dried in vacuum. Yield: 2.5 g (87%)

Analysis for C₆H₁₂N₂O₄

Calcd., % C 40.90 H 6.82 N 15.91

Found, % C 41.22 H 6.68 N 15.45

7a (2 g, 11.3 mmol) was added to freshly distilled thionyl chloride (10 mL) and refluxed for 4 h. The reaction mixture was cooled and excess thionyl chloride was removed under vacuum. The last traces were removed by washing with toluene. N,N'-bis(1-chloroethyl)1,2-ethane diamide (**8a**) obtained was dried in vacuum. Yield: 1.9 g (80%)

Analysis for C₆H₁₀N₂O₂Cl₂

Calcd., % C 33.80 H 4.69 N 13.15

Found, % C 34.22 H 4.68 N 13.45

In a 100 mL round-bottomed flask, **8a** and KOH were taken and methanol was added to it and refluxed for about 6 h. The solution became clear and KCl settled at the bottom. The solution was filtered and methanol was evaporated under vacuum to obtain **9a** as a white solid. Yield: 1.7 g (75%)

Analysis for C₆H₈N₂O₂

Calcd., % 51.43 H 5.71 N 20.00

Found, % 50.81 H 6.19 N 19.83

4.2.3.1.2. Synthesis of 10a

A 100 mL Schlenk flask was cooled under vacuum and charged with argon. Anhydrous copper(II) chloride (0.269 g, 2 mmol) and **9a** (0.280 g, 2 mmol) were added to the flask and dichloromethane was added through a canula. The mixture stirred for about 12 h. Complex **10a** was obtained as a green-colored solid which was filtered and dried in vacuum. Yield: 0.25 g (45%).

Analysis for $C_6H_8N_2O_2CuCl_2$:

Calcd., % C 26.23 H 2.91 N 10.20

Found, % C 25.97 H 3.11 N 10.34

4.2.3.2. Synthesis of 2,2'-bis[(4,4-dimethyl)-1,3-oxazoline]dichlorocopper(II) (10b)

4.2.3.2.1. Synthesis of 2,2'-bis[(4,4-dimethyl)-1,3-oxazoline] (9b)

In a 100 mL round-bottomed flask, diethyl oxalate (3.8 mL, 0.028 mole) was taken and to this was added 2-amino-2-methyl-1-propanol (5.4 mL, 0.056 mole) with stirring. An exothermic reaction was observed and after some time the whole reaction mixture solidified. The flask was cooled; the solid was washed with hexane and dried under vacuum to yield the bisamide **7b**. Yield: 7.0 g (90%)

Analysis for $C_{10}H_{20}N_2O_4$:

Calcd., % C 51.72 H 8.62 N 12.07

Found, % C 52.04 H 8.71 N 12.45

7b (2.0 g, 8.62 mmol) was added to freshly distilled thionyl chloride (10 ml, excess) in a 100 mL round-bottomed flask and refluxed for 4 h. The reaction mixture was cooled and excess thionyl chloride was removed by distillation. The last traces were removed by washing with toluene. The resultant solid was recrystallized from ethyl acetate-hexane to afford **8b**. Yield : 1.7 g (74 %)

Analysis for $C_{10}H_{18}N_2O_2Cl_2$:

Calcd., % C 44.61 H 6.69 N 10.41

Found, % C 44.52 H 6.90 N 10.81

KOH (0.413 g, 7.38 mmol) was dissolved in methanol. **8b** (1 g, 3.69 mmol) was added into this solution and the reaction mixture was stirred for 6 h at reflux. The mixture was cooled to room temperature, KCl formed was filtered off and the methanol evaporated to yield **9b**

as a white solid which was recrystallized from dichloromethane-hexane mixture. Yield: 0.4 g (80%).

Analysis for $C_{10}H_{16}N_2O_2$

Calcd., % C 61.22 H 8.16 N 14.29

Found, % C 60.86 H 7.82 N 13.74

1H NMR ($CDCl_3$, 200 MHz): δ ppm 1.34 (12 H), 4.10 (4 H)

4.2.3.2.2. Synthesis of **10b**

A 100 mL Schlenk flask was cooled under vacuum and filled with argon. Anhydrous $CuCl_2$ (0.342 g, 2.55 mmol) and **9b** (0.50 g, 2.55 mmol) were added into the flask under argon. Dichloromethane was added through a canula and the mixture was stirred for 4 h. During this time, $CuCl_2$ reacted completely. The reaction mixture was further stirred for 12 h to obtain **10b** as a yellow-colored solid which was filtered and dried in vacuum. Yield: 0.40 g (47%).

Analysis for $C_{10}H_{16}N_2O_2CuCl_2$:

Calcd., % C 36.31 H 4.84 N 8.47

Found, % C 35.98 H 4.70 N 8.30

4.2.3.3. Synthesis of 2,2'-bis[(4-isopropyl)-1,3-oxazoline]dichlorocopper(II) (**10c**)

4.2.3.3.1. Synthesis of 2,2'-bis[(4-isopropyl)-1,3-oxazoline] (**9c**)

Diethyl oxalate (0.62 mL, 4.536 mmol) was added to 2- amino-3- methyl-1-butanol (1 mL, 9.072 mmol) and stirred for 1 h during which the reaction mixture solidified. The mixture was cooled, washed with hexane, powdered and dried under vacuum to yield N,N'-bis[2 - isopropyl-1-hydroxyethyl]-1,2-ethanediamide **7c**. Yield: 1.1 g (93%)

Analysis for $C_{12}H_{24}N_2O_4$:

Calcd., % C 55.38 H 9.23 H 10.77

Found, % C 54.93 H 9.58 H 10.65

Bisamide 7c (0.5 g, 1.923 mmol) was added to freshly distilled thionyl chloride (5 mL) and refluxed for 3 h. The reaction mixture was cooled and excess thionyl chloride was removed by distillation. The last traces were removed by washing with toluene. The resultant solid was recrystallized from ethyl acetate-hexane to yield N,N'-bis-[2

isopropyl-1-chloroethyl]-1,2-ethanediamide 8c. Yield: 0.52 g (90%)

Analysis for C₁₂H₂₂N₂O₂Cl₂:

Calcd., % C 48.48 H 7.41 N 9.43

Found, % C 47.98 H 7.63 N 9.31

KOH (0.188 g, 3.37 mmol) was dissolved in methanol. **8c** (0.5 g, 1.68 mmol) was added to this solution and the reaction mixture was stirred for 6 h at reflux. The mixture was cooled to room temperature, KCl formed was filtered off and methanol evaporated to yield **9c** as a white solid which was recrystallized from dichloromethane-hexane mixture. Yield: 0.4 g (80%).

Analysis for C₁₂H₂₀N₂O₂:

Calcd., % C 64.29 H 8.93 N 12.50

Found, % C 64.04 H 9.08 N 11.93

¹H NMR (CDCl₃, 200 MHz): δ 0.92(12 H), 1.85(2 H), 4.11(4 H), 4.44(2 H)

4.2.3.3.2. Synthesis of 10c

In a 100 mL Schlenk flask, vacuum dried and filled with argon was taken anhydrous copper(II) chloride (0.240 g, 1.79 mmol) and ligand **9c** (0.40 g, 1.79 mmol) and dichloromethane was added. The reaction mixture was stirred for about 4 h. During this time, all the CuCl₂ reacted completely. The reaction mixture was stirred for another 8 h to obtain **10c** as a green-colored solid which was filtered and dried in vacuum. Yield: 0.30 g (48%).

Analysis for C₁₂H₂₀N₂O₂CuCl₂:

Calcd., % C 40.17 H 5.58 N 7.81

Found, % C 39.32 H 5.50 N 7.19

4.2.3.4. Synthesis of 2,2'-bis[(4-tert-butyl)-1,3-oxazoline]dichlorocopper(II) (10d)

4.2.3.4.1. Synthesis of 2,2'-bis[(4-tert-butyl)-1,3-oxazoline] (9d)

Diethyl oxalate (0.29 mL, 2.137 mmol) was added to tert-Leucinol(0.5 g, 4.274 mmol) and the reaction mixture was stirred for 1 h. The reaction mixture solidified during this time. The mixture was cooled, washed with hexane, powdered and dried under vacuum to yield the N,N'-bis[2 -t-butyl-1-hydroxyethyl]-1,2-ethanediamide **7d**. Yield: 0.55 g (90%)

Analysis for C₁₄H₂₈N₂O₄

Calcd., % C 58.33 H 9.72 N 9.72

Found % C 57.68 H 9.73 N 10.02

Bisamide **7d** (0.5 g, 1.736 mmol) was added to freshly distilled thionyl chloride (5 mL, excess) and refluxed for 3 h. The reaction mixture was cooled and thionyl chloride was removed by distillation. The last traces were removed by washing with toluene. The resultant solid was recrystallized from ethylacetate-hexane to yield N,N'-bis-[2 t-butyl-1-chloroethyl]-1,2-ethanediamide **8d**. Yield: 0.50 g (89%)

Analysis for C₁₄H₂₆N₂O₂Cl₂:

Calcd., % C 51.69 H 8.00 N 8.62

Found, % C 51.35 H 7.88 N 8.84

8d (0.120 g, 0.3692 mmol) and KOH (0.041 g, 0.7385 mmol) were refluxed in methanol for 6 h. The resultant clear solution was filtered from KCl and methanol removed under vacuum to obtain a white solid, 2,2'-bis(4,-tert-butyl)-1,3-oxazoline (**9d**) which was recrystallized from dichloromethane-hexane. Yield : 0.06 g (65%)

Analysis for C₁₄H₂₄N₂O₂

Calcd., % C 66.67 H 9.52 N 11.11

Found, % C 67.02 H 9.35 N 11.45

¹H NMR (CDCl₃, 200 MHz) : δ 1.34 (18 H, CMe₃), 4.09(2 H, CH₂)

4.2.3.4.2. Synthesis of **10d**

A 100 mL Schlenk flask (dried in oven at 200°C) was dried under vacuum and filled with argon. Anhydrous CuCl₂ (0.133 g, 0.992 mmol) and **9d** (0.25 g, 0.992 mmol) were added into the flask and dichloromethane was added through a canula. The reaction mixture was allowed to stir for 12 h. It was then allowed to settle, solvent was removed through a canula, and the greenish blue-colored solid **10d** was washed with ethanol and dried under vacuum. Yield: 0.18 g (47%).

Analysis for $C_{14}H_{24}N_2O_2CuCl_2$:

Calcd., % C 43.47 H 6.21 N 7.24

Found, % C 42.98 H 6.45 N 7.46

4.2.4. Synthesis of bis(benzimidazole) copper(II) complexes

4.2.4.1. Synthesis of [1,1'-bis(benzimidazolyl)ethane]dichlorocopper(II) (13a)

4.2.4.1.1. Synthesis of [1,1'-bis(benzimidazolyl)ethane] (12a)

Malonic acid (5.0 g, 48 mmol) and 1,2-phenylenediamine (10.4 g, 96 mmol) were refluxed in 100 mL of 4 N HCl for 24 h. The reaction mixture was cooled to room temperature, made alkaline with ammonia solution, filtered, washed with water and dried. Yield: 7.0 g (60 %)

1H NMR (DMSO- d_6 , 200 MHz): δ 4.50 (s, 2 H), 7.18(m, 4 H), 7.50 (m, 4 H)

A 250 mL Schlenk flask (dried in oven at 200°C) was cooled under vacuum and charged with argon. Sodium hydride (60% dispersion in mineral oil, 2.6 g, 64.5 mmol, 8 eqv) was added to the flask, washed with dry hexane and dried in vacuum. To this, dry THF (80 mL) was transferred through a canula. The flask was cooled in an ice bath and 2,2'-bis(benzimidazol-2-yl) methane (2.0 g, 8.065 mmol, 1 eqv) was added slowly to this suspension with stirring under argon atmosphere. After the addition is complete, the mixture was stirred for 15 min. Iodomethane (4 mL, 64.5 mmol, 8 eqv) was added through a syringe. The reaction mixture was stirred at room temperature for 36 h. The reaction was quenched with ice, THF was removed under vacuum and the product extracted with dichloromethane. Dichloromethane layer was washed with water, dried over anhydrous sodium sulphate and concentrated to obtain a yellow solid which was purified by column chromatography. Yield: 1.0 g (45 %)

1H NMR ($CDCl_3$, 200 MHz): δ 2.10 (3H, HCMe), 3.64 (6 H, N-Me), 5.05 (1H, CHMe), 7.28 (6H, aromatic), 7.79(2 H, aromatic)

4.2.4.1.2. Synthesis of 13a

In a 100 mL Schlenk flask, cooled under vacuum and filled with argon, was added anhydrous copper(II) chloride (0.067 g, 0.5 mmol). To it absolute ethanol was added to form a green solution. Ligand **12a** (0.145 g, 0.5 mmol) dissolved in ethanol was transferred into the green solution through a canula. An yellow-colored solid started

precipitating. The reaction mixture was stirred for 12 h. The solid was then filtered and washed with dichloromethane and dried in vacuum. Yield: 0.15 g (70 %)

Analysis for $C_{18}H_{18}N_4CuCl_2$

Calcd., % C 50.88 H 4.24 N 13.04

Found, % C 50.67 H 4.09 N 13.19

4.2.4.2. Synthesis of [1,1'-bis(benzimidazolyl)ethane]dibromocopper(II) (13c)

In a 100 mL Schlenk flask (dried in oven at 200°C) cooled under vacuum and filled with argon was added anhydrous copper (II) bromide (0.111 g, 0.5 mmol). To it absolute ethanol was added to form an orange brown solution. Ligand **12a** (0.145 g, 0.5 mmol) dissolved in ethanol was transferred into the solution through a canula. An orange-colored solid started precipitating. The reaction mixture was stirred for 12 h. The solid was then filtered and washed with dichloromethane and dried in vacuum. Yield: 0.16 g (60 %)

Analysis for $C_{18}H_{18}N_4CuBr_2$:

Calcd., % C 42.22 H 3.12 N 10.95

Found, % C 42.25 H 3.30 N 10.59

4.2.4.3. Synthesis of [1,1'-bis(benzimidazolyl)pentane]dibromocopper(II) (13b)

4.2.4.3.1. Synthesis of [1,1'-bis(benzimidazolyl)pentane] (12b)

A 250 mL Schlenk flask was cooled under vacuum and charged with argon. Sodium hydride (60% dispersion in mineral oil, 0.65 g, 8 eqv) was added to the flask, washed with dry hexane and dried in vacuum. To this, dry THF (50 mL) was transferred through a canula. The flask was then cooled in an ice bath and 2,2'-bis(benzimidazol-2-yl) methane (0.5 g, 2.03 mmol, 1 eqv) was added slowly to this suspension with stirring under argon atmosphere. After the addition is complete, the mixture was stirred for 30 min. n-Butyl bromide (1.7mL, 8 eqv) was added through a syringe. The reaction mixture was stirred at room temperature for about 12 h. No reaction was observed on checking the TLC. The reaction mixture was then refluxed for another 6 h. The mixture was then quenched with ice, THF was removed by rotary evaporation and the product extracted with dichloromethane. Dichloromethane layer was then washed with water, dried over

anhydrous sodium sulphate and concentrated to obtain a yellow solid which was purified by column chromatography. Yield : 0.28 g (33 %)

4.2.4.3.2. Synthesis of 13b

In a 100 mL Schlenk flask cooled under vacuum and filled with argon was added anhydrous copper(II) bromide (0.13 g, 0.6 mmol). To it absolute ethanol was added to form an orange brown solution. Ligand **12b** (0.25 g, 0.6 mmol) dissolved in ethanol was transferred into the solution through a canula. A reddish brown colored solid started precipitating. The reaction mixture was stirred for 12 h. The solid was then filtered and dried in vacuum. Yield: 0.20 g (52 %)

Analysis for $C_{27}H_{36}N_4CuBr_2$

Calcd., % C 50.66 H 5.63 N 8.76

Found, % C 51.39 H 6.11 N 8.59

4.3. Results and Discussion

4.3.1. Synthesis and characterization of (α -diimine) copper complexes

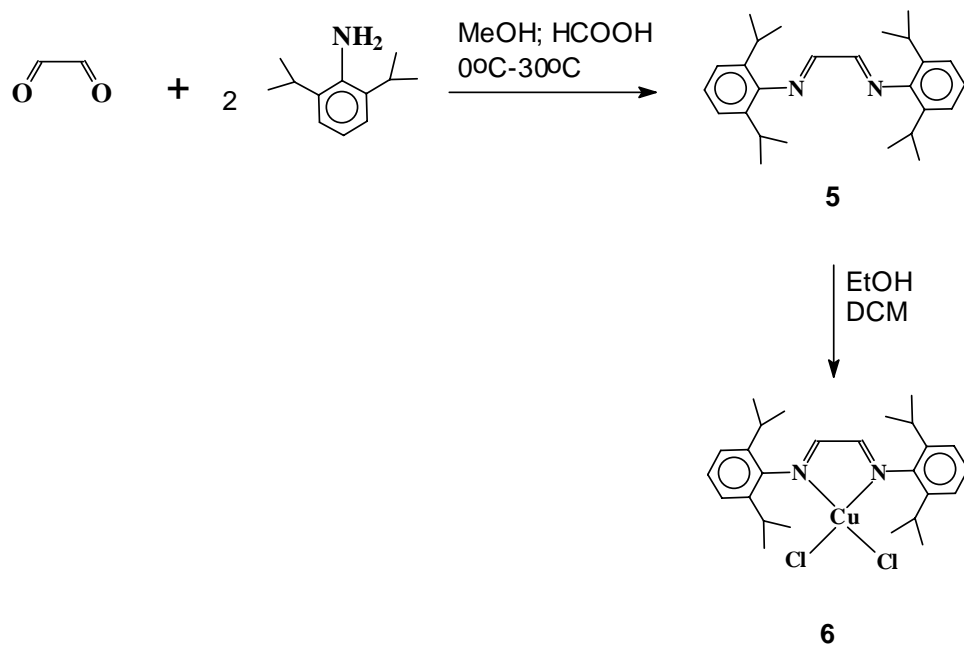
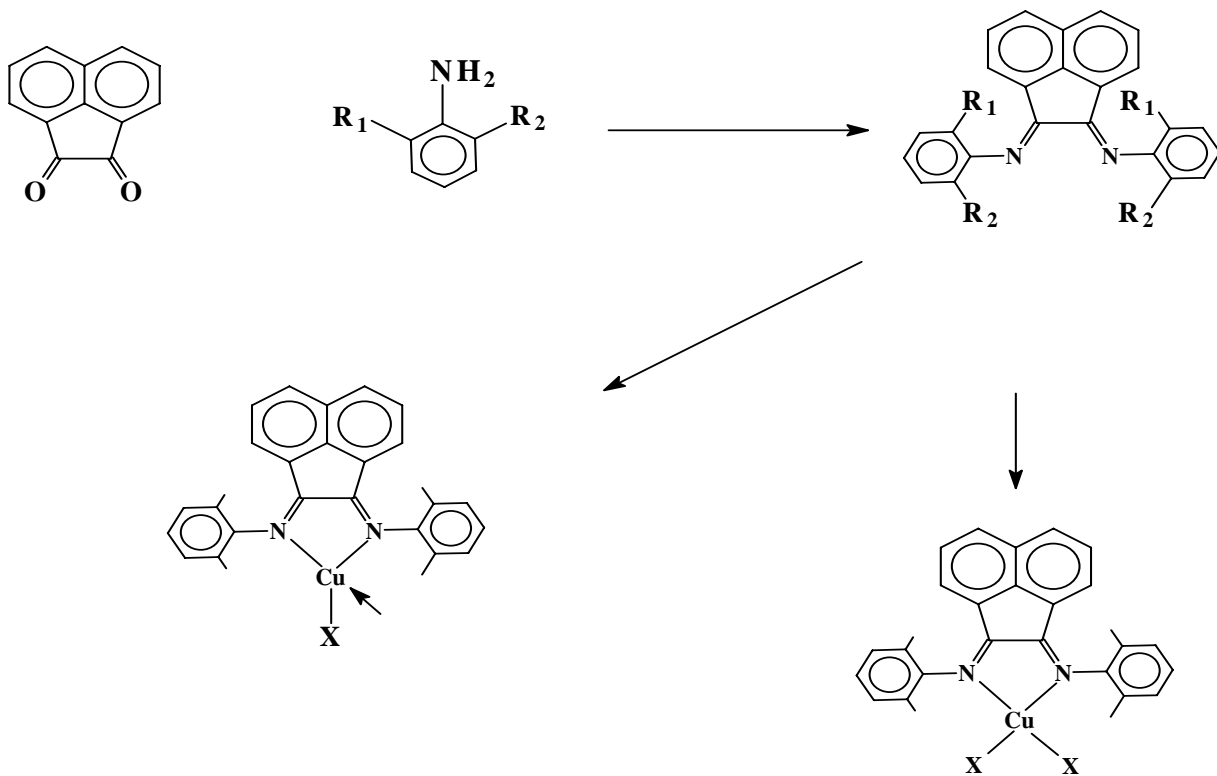
Synthetic routes for the preparation of (α -diimine) copper complexes employed in the present study are shown in **Scheme 4.1**. The ligands **1a**, **1b**, and **5** were prepared in good yields (> 80%) according to literature procedures. Upon reacting with copper halides in ethanol/dichloromethane the corresponding metal complexes **2a-2c**, and **6** could be obtained. The complexes were readily soluble in polar solvents like dichloromethane and 1,2-dichlorobenzene, but sparingly soluble in toluene.

Copper (I) complexes **3a** and **3b** were synthesized by the reaction of copper (I) halide with the corresponding ligand. Complex **3a** was found to have an ethanol molecule coordinated to the metal as revealed by elemental analysis.

4.3.1.1. Crystal structure of copper complexes 2a-2c

Structures of copper complexes **2a-2c** with the numbering scheme of atoms are shown in **Figure 4.1-4.3** while selected bond distances and angles are included in **Table 4.1**. X-ray crystal data and structure refinement for complexes **2a-2c** are listed in **Appendix A**.

Inspection of the structures of metal complexes **2a-2c** reveal that they are mononuclear compounds where the Schiff base ligands are acting as bidentate N, N donors. The geometry around copper is distorted square planar. The coordination sphere around the copper atom in each of these complexes consists of two imine nitrogens and two halide atoms. The equatorial plane comprising of these donors atoms is slightly distorted as indicated by the unequal bond angles observed for the complex **2a** as N (1) – Cu (1) – Cl (1) [147.8°] and N (2) – Cu (1) – Cl (2) [143.0°] respectively. Similar arrangement also prevails in compounds **2b** and **2c**. The metal-nitrogen (imine) distances are found to remain nearly identical in all compounds (2.02 – 2.08Å) due to rigid orthoquinone moiety while the metal halogen distances are observed to be longer and vary between 2.18 and 2.31 Å respectively. The steric hindrance offered by the bulky bromide atoms to iso-propyl groups results in opening of the N (1) – C (13) – C (14) angle from 116° (in chloro complex) to 120° (in bromo complex). One molecule of dichloromethane was observed in the crystal lattice of complex **2c**.



Scheme 4.1 Synthesis of (α -diimine) copper (II) and copper(I) complexes

Table 4.1 Selected bond lengths and bond angles for complexes 2a-2c

	2a	2b	2c
Bond lengths (Å)		2.072(5)	2.059(2)
Cu (1) – N (1)	2.082(3)	2.042(5)	2.088(2)
Cu (1) – N (2)	2.021(3)	-	2.220(10)
Cu (1) – Cl (1)	2.193(12)	-	2.246(10)
Cu (1) – Cl (2)	2.185(12)	2.317(12)	-
Cu (1) – Br (1)	-	2.316(12)	-
Cu (1) – Br (2)	-	1.444(8)	1.448(3)
N (1) – C (13)	1.449(5)	-	1.448(3)
N (2) – C (23)	-	1.433(9)	-
N (2) – C (25)	1.445(5)		
Bond angles (°)		-	-
N(1)-Cu(1)-Cl(1)	147.78(10)	-	-
N(2)-Cu(1)-Cl(2)	143.00(10)	120.40(7)	113.90(2)
C(14)-C(13)-N(1)	116.40(3)	116.60(6)	124.20(3)
C(18)-C(13)-N(1)	121.00(3)	118.10(7)	-
C(26)-C(25)-N(2)	117.70(4)	118.40(7)	-
C(30)-C(25)-N(2)	119.60(4)	147.40(17)	-
N(1)-Cu(1)-Br(1)	-	142.08(19)	-
N(2)-Cu(1)-Br(2)	-	-	161.66(8)
N(1)-Cu(1)-Cl(2)	-	-	151.58(7)
N(2)-Cu(1)-Cl(1)	-	-	114.50(2)
C(24)-C(23)-N(2)	-	-	123.30(3)
C(28)-C(23)-N(2)	-		

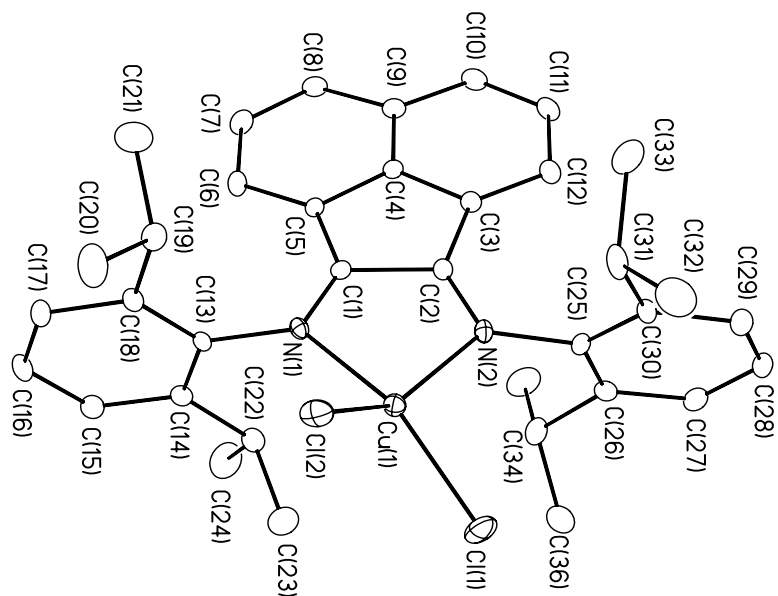


Figure 4.1 Molecular structure and numbering scheme for 2a

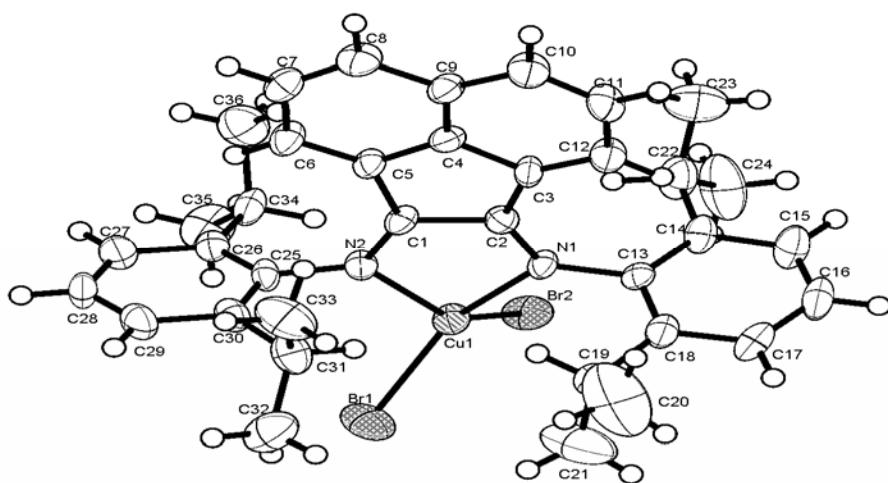


Figure 4.2 Molecular structure and numbering scheme for 2b

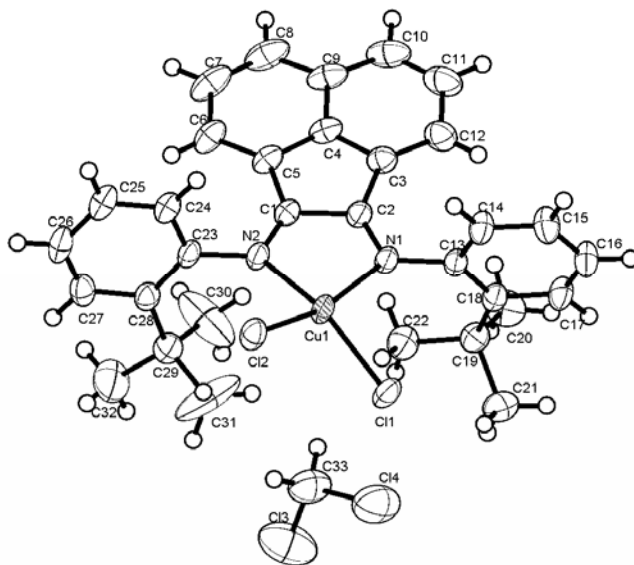


Figure 4.3 Molecular structure and numbering scheme for 2c

X-ray crystal structure of the analogous nickel (II) complex with ortho-isopropyl or t-butyl substituents are not reported in literature as they were poorly soluble in common organic solvents. However crystal structure of nickel complex with ortho-C₆F₅ substituent shows the geometry around the nickel atom to be tetrahedral.²¹

4.3.1.2. Spectroscopy

Infrared spectra of the ligands exhibit an absorption in the range 1645-1673 cm⁻¹ corresponding to imino (C=N) stretch which upon metal complexation shifted to lower wavenumbers indicating involvement of diimine nitrogens in copper coordination. In the case of ligand **1a**, C=N stretching is observed at 1673 cm⁻¹ and 1652 cm⁻¹ which shifted to 1652 and 1629 cm⁻¹ in **2a** and 1652 and 1626 cm⁻¹ in **2b**. El-Ayaan et al reported similar shifts of 10-17 cm⁻¹ in the case of the mixed-ligand cupric complex containing acetylacetonate ligand²².

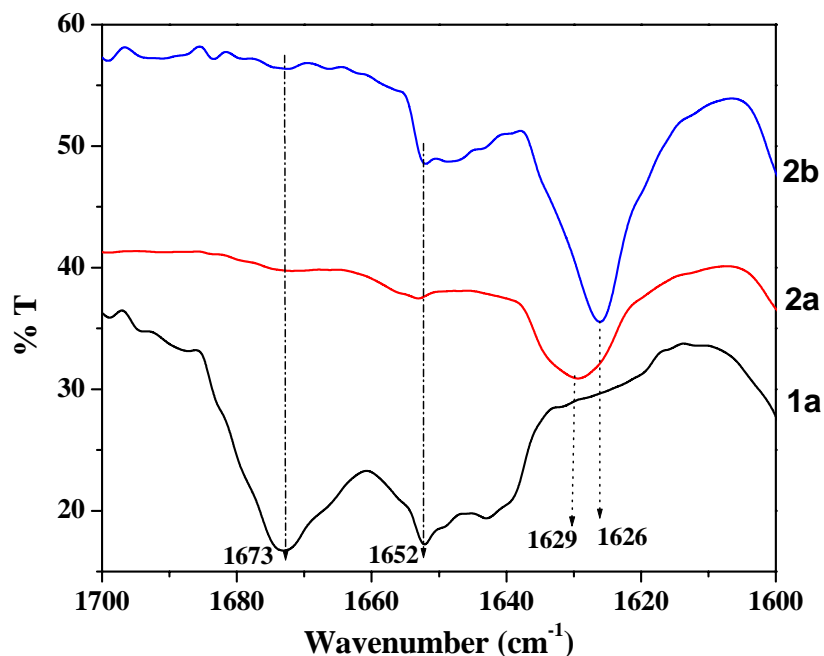


Figure 4.4 IR spectra of 1a, 2a and 2b

Electronic spectra (**Figure 4.5**) of copper complexes **2a-2c** show absorption bands below 350 nm that can be assigned to intra-ligand transitions while an intense band around 440 nm (for **2a** and **2b**) and 415 nm (for **2c**) which can be ascribed to metal-to-ligand charge transfer transition²². This shift to a much longer wavelength compared to other diimine ligands, such as, 2,2'-bipyridine and 1,10-phenanthroline can be attributed to the presence of low energy π^* orbitals in diimine ligands **1a** and **1b** which results in increased overlap with metal (d) orbitals and, consequently, in a stronger π - bonding interaction. The absorption in the visible region around 600-640 nm is due to metal-based transitions characteristic of the distorted square planar geometries of such complexes²³.

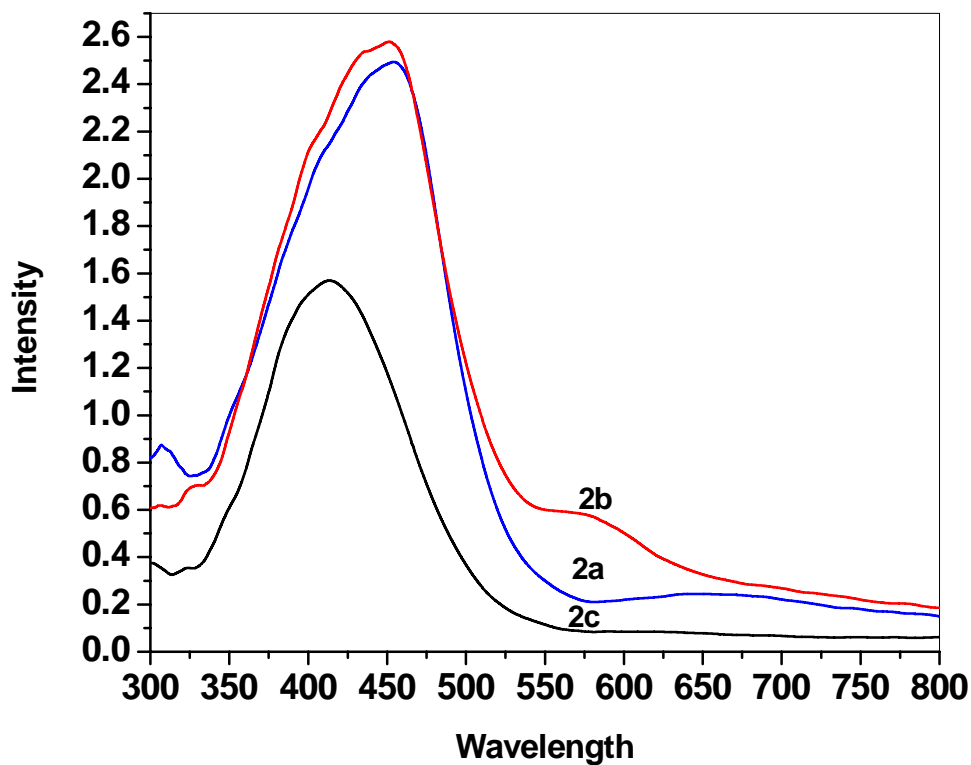


Figure 4.5 UV –visible spectra of complexes 2a-2c

Polycrystalline X-band EPR spectra of the copper complexes (**Figure 4.6**) at 77 K indicates an axial symmetry and resolve into parallel and perpendicular components. The calculated parameters suggest a trend $g_{||} > g_{\perp} > 2.0$ which is consistent with the distorted square planar geometry and localization of the unpaired electron in the $d_{x^2 - y^2}$ ground state.

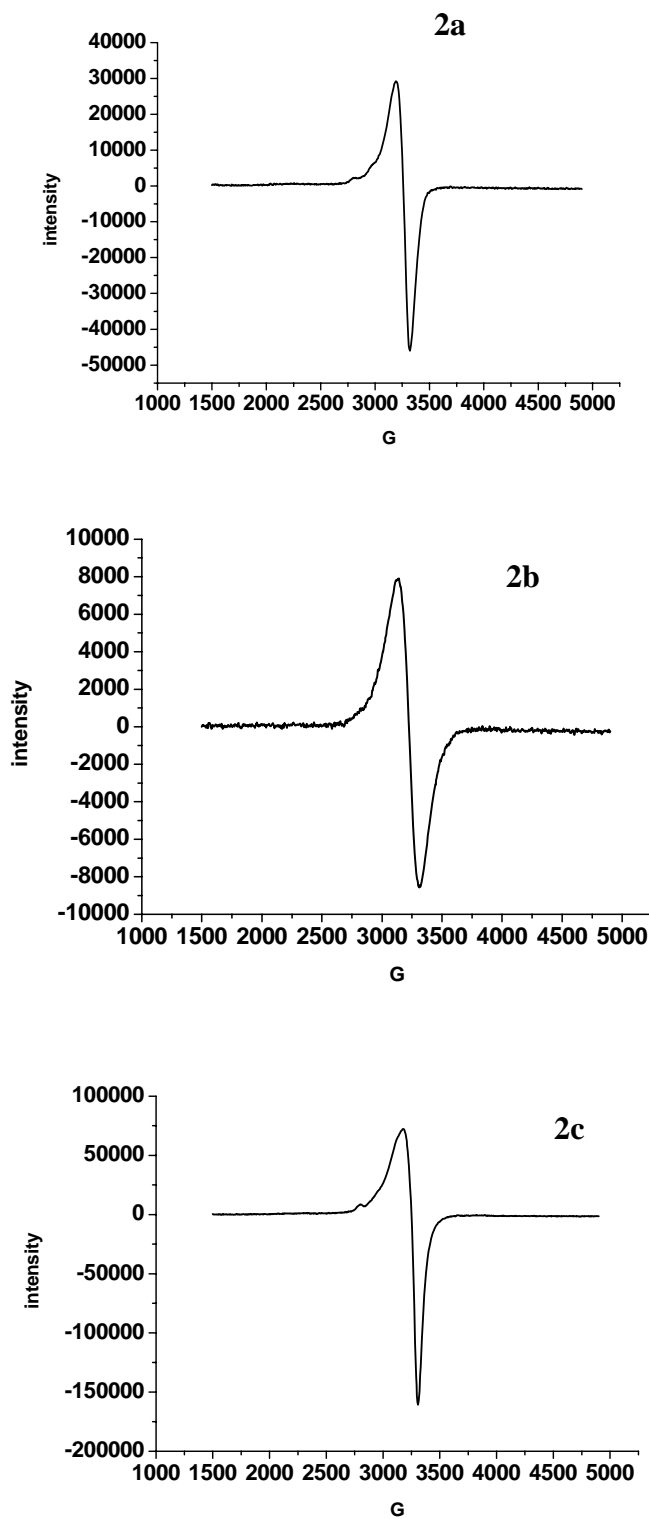


Figure 4.6 EPR spectra of complexes 2a-2c

4.3.1.3. Electrochemical studies

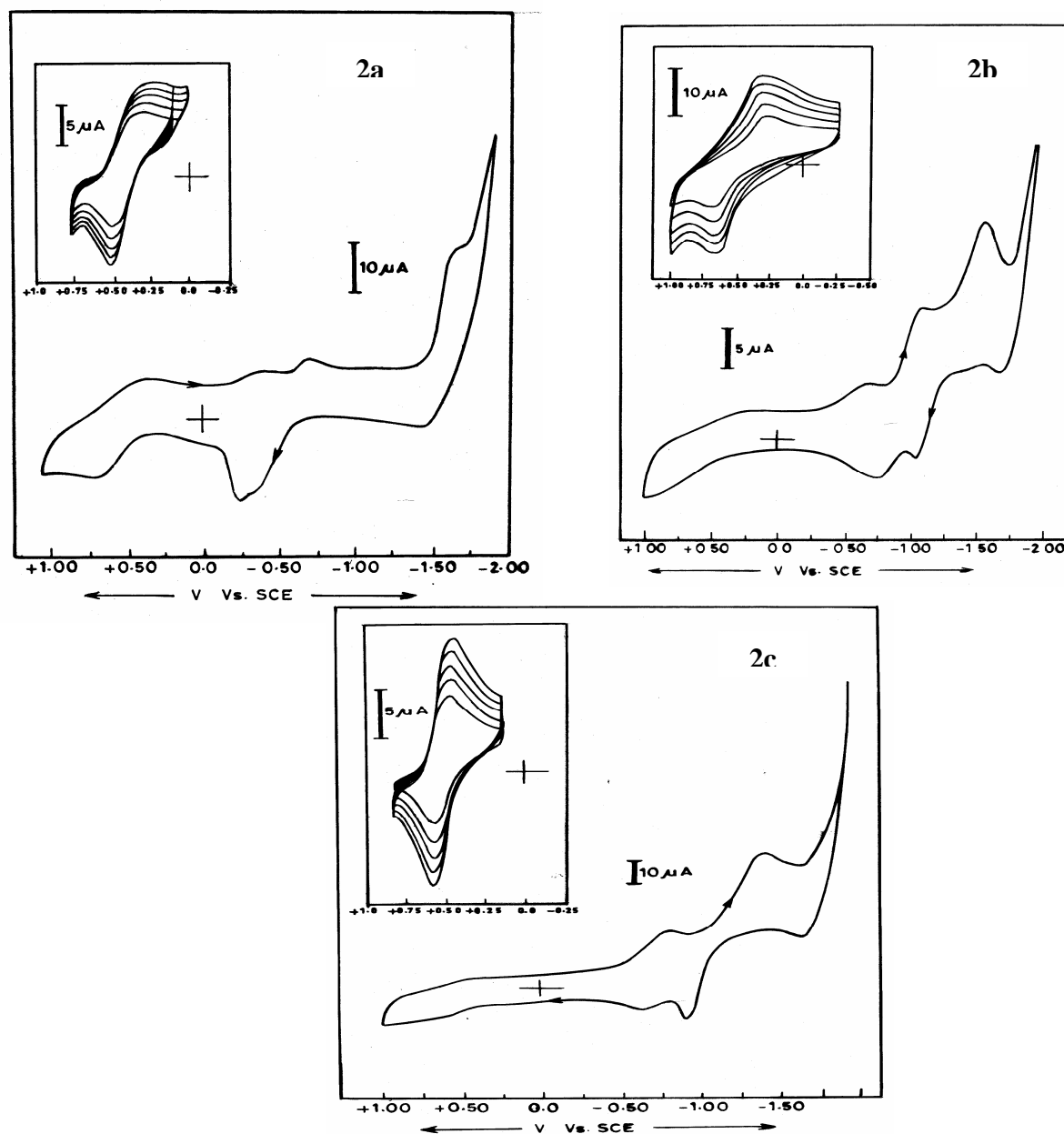


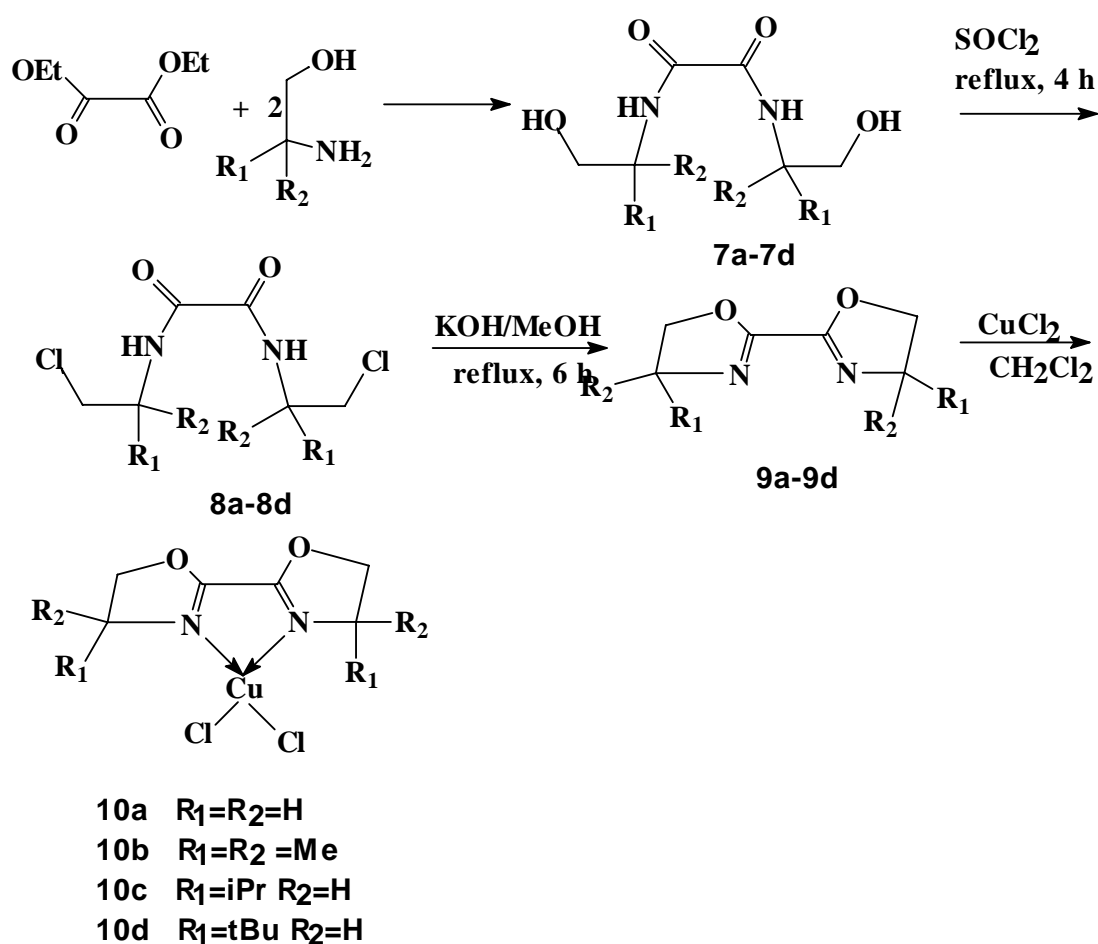
Figure 4.7 Cyclic voltammograms of complexes 2a-2c

Cyclic voltammogram of complex **2a** in equimolar dichloromethane : acetonitrile solvent mixture (**Figure 4.7**) showed a reversible reduction wave at +0.42V which can be assigned to $\text{Cu}^{+2/+1}$ redox couple while the irreversible reduction wave observed at -1.50 V is assigned to reduction of the azomethine linkage. The other two reduction waves observed

are the ligand-based peaks. A similar pattern was observed in the cyclic voltammograms of complexes **2b** and **2c**.

4.3.2. Synthesis and characterization of bis(oxazoline)copper(II) complexes

Bis(oxazoline) copper complexes **10a-10d** were prepared by a modified literature procedure²⁰ as shown in **Scheme 4.2**. The complexes were obtained in good yields as green or yellow microcrystalline solids. These complexes were soluble in dichloromethane, but sparingly soluble in toluene.

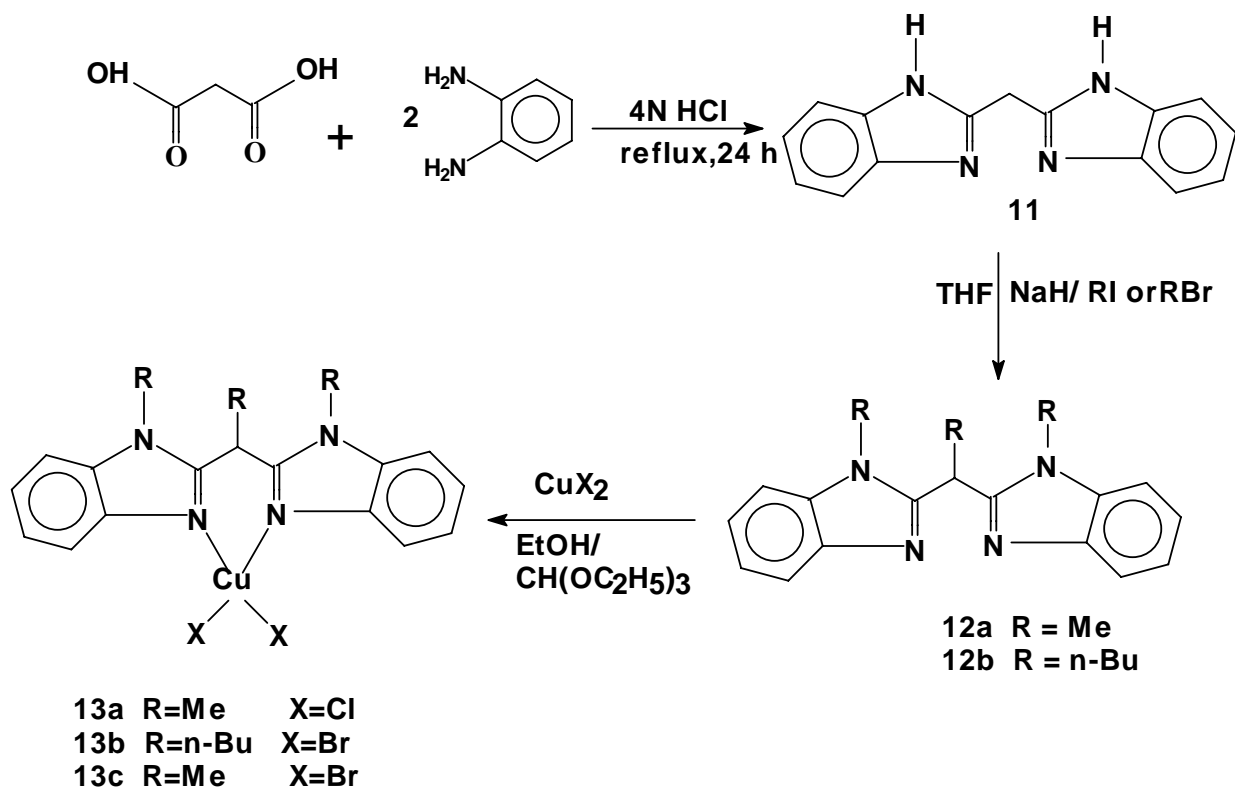


Scheme 4.2 Synthesis of bis(oxazoline) ligands and copper(II) complexes

Substituents R_1 and R_2 on the bis(oxazoline)s were varied in order to study the effect of these substituents on their catalytic behaviour towards the polymerization of ethylene. Attempts to prepare single crystals of these complexes were not successful.

4.3.3. Synthesis and characterization of bis(benzimidazole)copper(II) complexes

Bis(benzimidazole) ligands and complexes were prepared using the procedure⁵ shown in **Scheme 4.3**. Copper complexes **13a** and **13c** were obtained as yellow and reddish brown powder respectively. They were insoluble in almost all organic solvents, both polar and nonpolar. Tri-*n*-butyl substituted complex **13b** was obtained as a dark brown powder and was soluble in dichloromethane



Scheme 4.3 Synthesis of bis(benzimidazole) ligands and copper (II) complexes

4.3.4. Polymerization of ethylene using copper complexes

4.3.4.1. Polymerization of ethylene using α -diimine copper complexes (**2a-2c**, **3a**, **3b**, **6**)

4.3.4.1.1. Polymerization of ethylene at 1 bar ethylene pressure

Polymerization of ethylene was performed at 1 bar ethylene using complexes **2a-2c**, **3a-3b** and **6** with MAO as cocatalyst and toluene as diluent. Colour of all the complexes in solution changed from yellow to orange-red upon mixing with MAO in presence of ethylene. Several experimental conditions were explored. Catalyst concentration was varied from 8 to 32 μmol , Al/Cu ratio was varied from 500-2000 and temperature varied from 25 to 80°C. Under none of these conditions there was any appreciable uptake of ethylene. Consequently polymerization studies were attempted at higher pressures.

4.3.4.1.2. Polymerization of ethylene at 3 and 5 bar ethylene pressures

Polymerization of ethylene was performed with complexes **2a-2c** and **6** at 3 and 5 bar ethylene pressures (**Table 4.2**). Complex **2a** and **2b** exhibited polymerization activity at 5 bar ethylene pressure. Catalyst activity was higher for **2a** than **2b**. Only traces of polymer were formed with **2c** while with **6** no reaction was observed. Polymerization using **2a** at 3 bar ethylene pressure led to a decrease in catalyst activity.

Table 4.2 Polymerization of ethylene using the complexes **2a-2c** and **6**/MAO ^a

Entry	Complex	P _{C₂H₄} (bar)	Yield (g)	Activity g PE mmol ⁻¹ Cu.h ⁻¹	Mw	Mw/ Mn	Tm (°C)
1	2a	3	0.08	5.0	231000	1.9	130
2	2a	5	0.20	12.5	209 000	1.9	131
3	2b	5	0.06	4.5	259 000	2.4	133
5	2c	5	traces	--	-	--	--
6	6	5	No reaction	-	-	-	-

^a Cu, 16 μmol ; toluene, 30 mL; Tp: 60°C, time = 60 min.

The analogous α -diimine nickel complexes are reported to be active for polymerization of ethylene²⁴. In order to confirm that the observed activity of the copper (II) complexes is not due to trace nickel impurities, nickel content in the copper chloride used for the

preparation of the complexes was determined using inductively coupled plasma (ICP) analysis. The nickel content in copper(II) chloride was found to be 0.4 ppm. This corresponds to a nickel content of 1.4×10^{-5} μmol in the catalyst concentration used for polymerization (16 μmol). This level of nickel should contribute to a polymerization activity of 10^{-4} g PE $\text{mmol}^{-1}\text{Ni h}^{-1}$ which is significantly less than the activity observed for copper complexes **2a-2c**. Hence, it can be concluded that the observed activity of copper(II) complexes was not because of trace nickel impurities in copper.

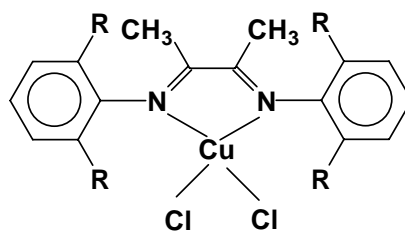
Further studies were performed using **2a** as it was the most active among all the complexes.

Effect of temperature

Polymerization using catalyst **2a**/MAO was carried out at 40, 60 and 80° and results are summarized in **Table 4.3**. Maximum catalyst activity was observed at 40°C and decreased thereafter. Polymer molecular weight decreased with increase in temperature.

Poly(ethylene)s obtained with **2a**/MAO show melting peaks at 131-133°C (**Figure 4.8**) and only a single peak at 29.9 ppm in ^{13}C NMR (**Figure 4.9**). Molecular weight distribution curves of the polymers are shown in **Figure 4.10**. In all cases molecular weight distribution was close to 2.0.

Polymerization behavior of the catalyst **2a**/MAO was compared with that of complexes **14a-14b**/MAO reported previously by Gibson et al¹⁶. Catalyst activity of **2a**/MAO was comparable to **14a**/MAO (**Table 4.3**). Catalyst **14b**/MAO resulted in only traces of polymer even at 5 bar ethylene pressure. Similar observations were made in the case of catalyst **6**/MAO in the course of the present study (**Table 4.2, entry 6**). Gibson et al attributed the higher activity of **14a** to the stabilization of active species by the *ortho*-phenyl substituents. However, **2a** bearing an *ortho*-isopropyl substituent but having an aromatic chelating ligand framework was active for polymerization of ethylene. This implies that nature of the chelating ligand also plays a major role in stabilizing the active species.



14a R = Ph

14b R = iPr

**Table 4.3 Effect of temperature on catalyst activity and polymer properties using
2a/MAO^a**

Entry	Complex	Al/Cu	Temp (°C)	Yield (g)	Activity g PE mmol ⁻¹ Cu.h ⁻¹	Mw	Mw/Mn	Tm (°C)
1	2a	1000	40	0.50	32	458,000	2.2	132
2	2a	1000	60	0.20	12.5	209,000	1.9	131
3	2a	1000	80	0.19	11	204,000	2.0	133
4	14a ^b	500	room temp.	0.40	22.5	n.r ^c	n.r	n.r
5	14b ^b	500	70	Traces	n.r	n.r	n.r	n.r

^a Cu, 16 μmol; toluene, 30 mL; Al/Cu : 1000; P_{C₂H₄}: 5 bar; time : 60 min.

^b data from reference 16

^c not reported

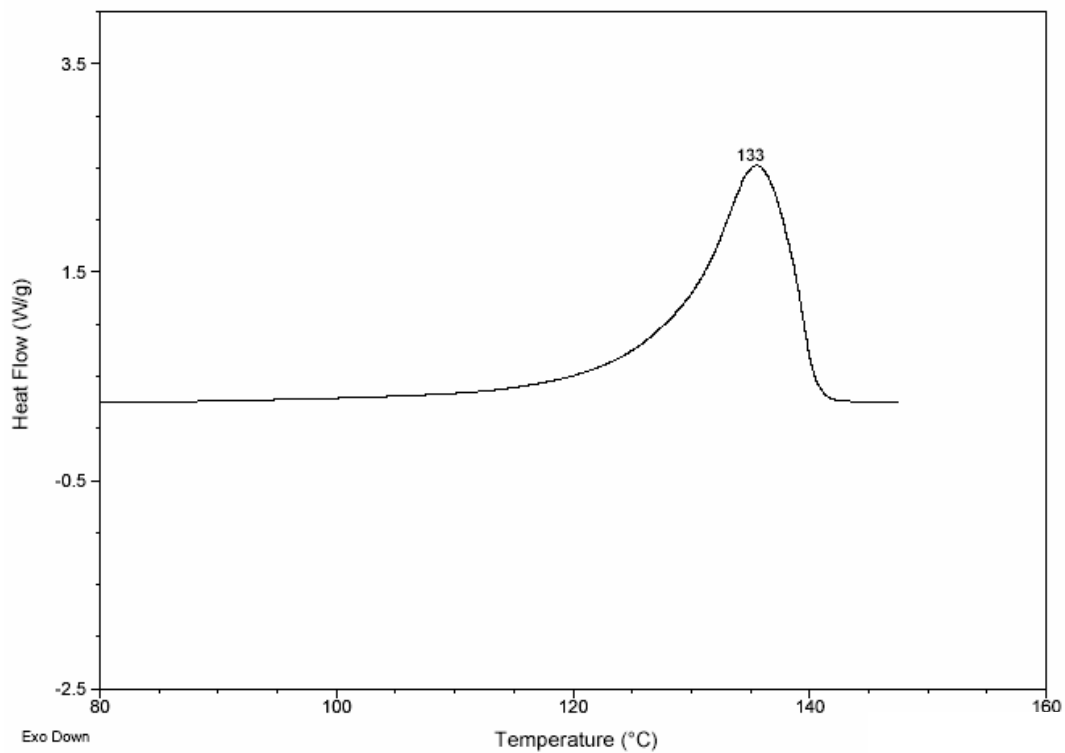


Figure 4.8 DSC thermogram of poly(ethylene)s obtained with 2a/MAO (entry 3, Table 4.3)

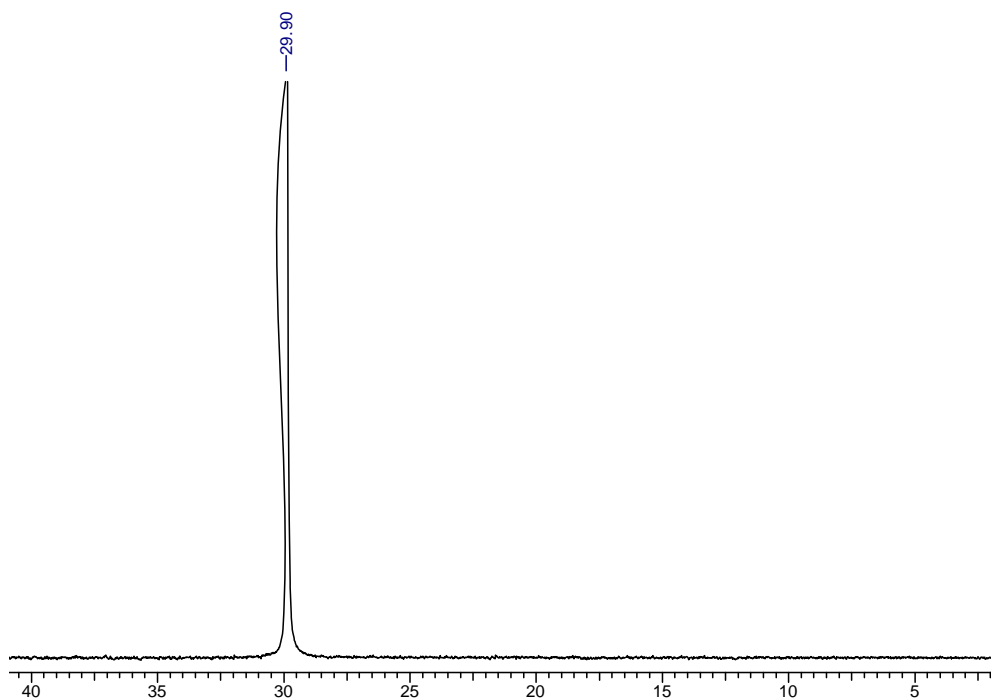


Figure 4.9 ¹³C NMR spectrum of poly(ethylene)s prepared using 2a/MAO at 40°C (entry 1, Table 4.3)

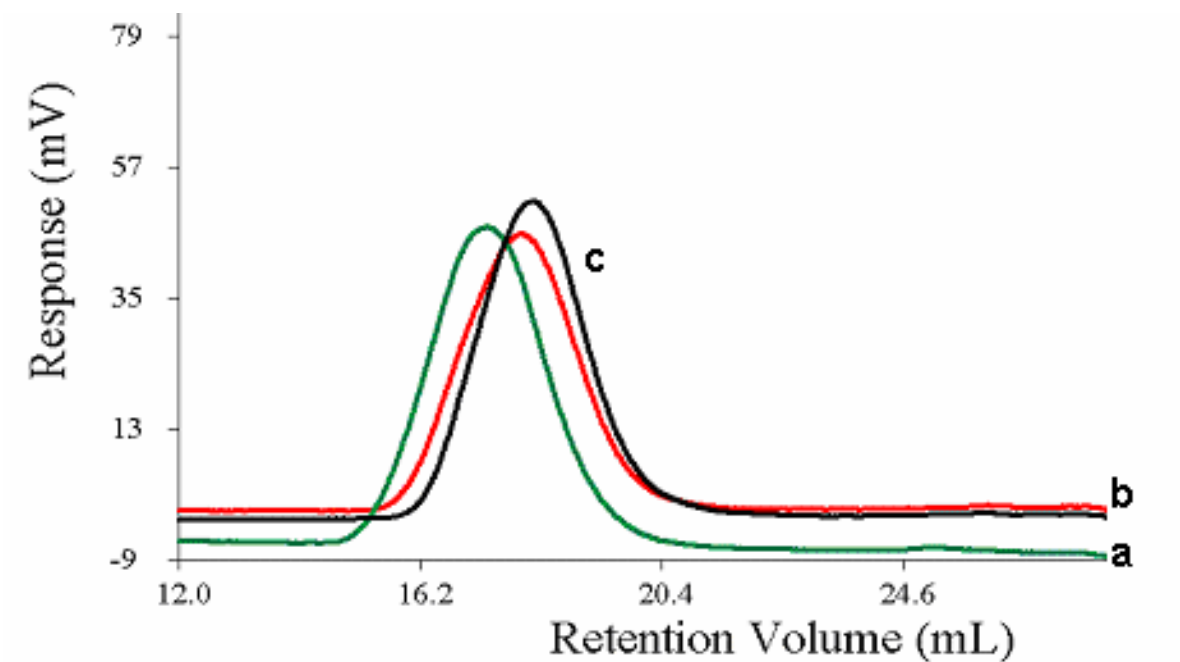


Figure 4.10 GPC of poly(ethylene)s obtained using **2a/MAO** (a) entry1 (b)entry2 (3)entry 3; **Table 4.3**

Effect of Al/Cu ratio

Catalyst activity was found to increase with increase in Al/Cu ratio. Molecular weight distributions were not significantly influenced by Al/Cu ratio (**Table 4.4**).

Table 4.4 Effect of Al/Cu ratio on catalyst activity and polymer properties using **2a/MAO**^a

Entry	MAO/Cu	Yield (g)	Activity gPEmmol ⁻¹ Cu.h ⁻¹	Mw	Mw/Mn	Tm (°C)
1	500	0.08	5	247,000	2.0	130
2	1000	0.20	12.5	209,000	1.9	131
3	1500	0.42	27	285,000	2.1	133

^a Cu, 16 μmol; toluene, 30 mL; T_p: 60°C; P_{C₂H₄}: 5 bar; time: 60 min

Effect of nature of diluent

Polymerization was carried out in toluene as well as in 1,2-dichlorobenzene using **2a/MAO** (**Table 4.5**). Higher catalyst activity was observed in 1,2-dichlorobenzene compared to

toluene. Molecular weights of the polymers were found to be higher in 1,2-dichlorobenzene.

Table 4.5 Effect of diluent on catalyst activity and polymer properties ^a

Solvent	Yield (g)	Activity g PE mmol ⁻¹ Cu h ⁻¹	Mw	Mw/Mn	Tm (°C)
Toluene	0.05	3.2	265000	2.3	130
1,2-Dichlorobenzene	0.20	12.5	303000	2.3	132

^a Solvent (30mL); MAO; Cu :16μmol; Tp:60°C; P_{C₂H₄}:5bar; time: 1 h

Effect of oxidation state of the metal

In order to study the effect of oxidation state of the metal on polymerization behaviour, copper (I) complexes **3a** and **3b** were also tested for polymerization of ethylene. However no polymerization was observed indicating that copper in +1 oxidation state is not active in initiating polymerization of ethylene.

Comparison of copper and nickel diimine catalysts

A comparative study of polymerization of ethylene using (α-diimine) copper(II) complex (**2b**) and nickel (II) complex (**4**) was made.

Table 4.6 Comparison of (α-diimine) copper and nickel catalysts ^a

Entry	Complex	Activity g PE mmol ⁻¹ metal h ⁻¹	Mw	Mw/Mn	Tm (°C)
1	2b	4.5	259000	2.4	133
2	4	110 (6440) ^b	86300 (279000)	11 (1.8)	125(110)

^a Toluene(30 mL); Cat:16μmol; MAO; Al/M :1000; Tp:60°C; P_{C₂H₄}: 5 bar; time: 1h

^b values in parentheses as per as per reference 21 (at 15 bar; 60°C; time: 10 min)

Activity of copper complex **2a** was found to be significantly lower than that of the corresponding nickel complex **4** (Table 4.6). While nickel complex results in branched poly(ethylene)s with broad molecular weight distributions, **2a** produces linear poly(ethylene)s with narrow molecular weight distributions (Figure 4.11)

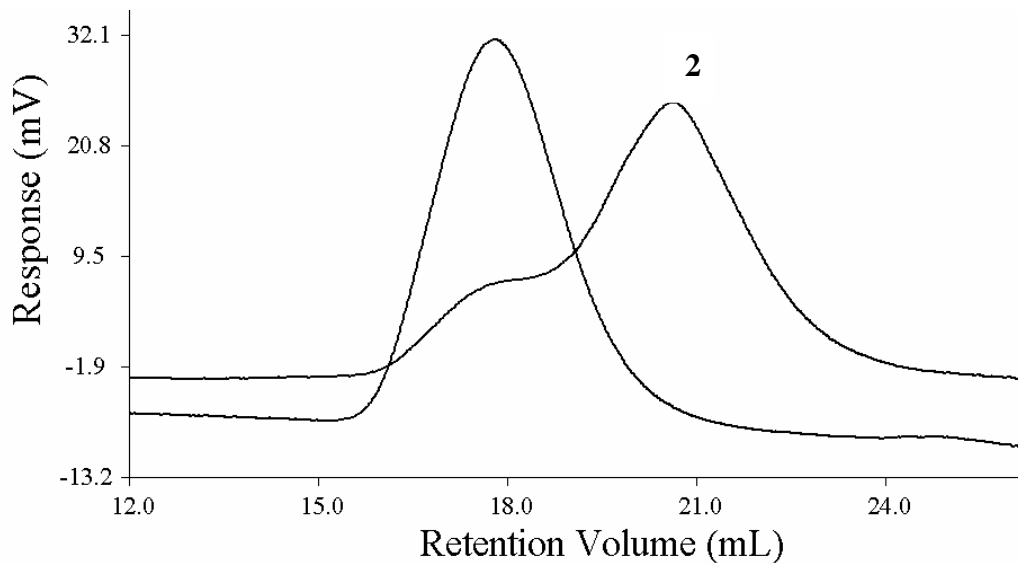


Figure 4.11. GPC of poly(ethylene)s prepared using (α -diimine) copper and nickel complexes/MAO (1) entry1 (2) entry 2; Table 4.6

Copolymerization of ethylene with hexene-1

Copolymerization of ethylene with hexene-1 was carried out using **2a**/MAO (Table 4.7).. There was no significant change in catalyst activity in presence of hexene-1 comonomer. However, there was a decrease in polymer molecular weight and melting point. Comonomer content was calculated from the ratio of integral of peak at 23.26 (characteristic of butyl branch) to the total integral.

Table 4.7 Copolymerization of ethylene and hexene-1 using 2a/MAO^a

Entry	[hexene-1] mol/L	Yield (g)	Activity g polymer mmol ⁻¹ Cu. h ⁻¹	Comonomer content (mol%)	Mw	M _w /M _n	T _m (°C)
1	0	0.5	32	-	458,000	2.2	132
2	0.27	0.45	28	0.28	260,000	2.6	126

^aToluene(30 mL); MAO; Al/Cu:1000; Tp:40°C; P_{C₂H₄}:5 bar; time:1 h

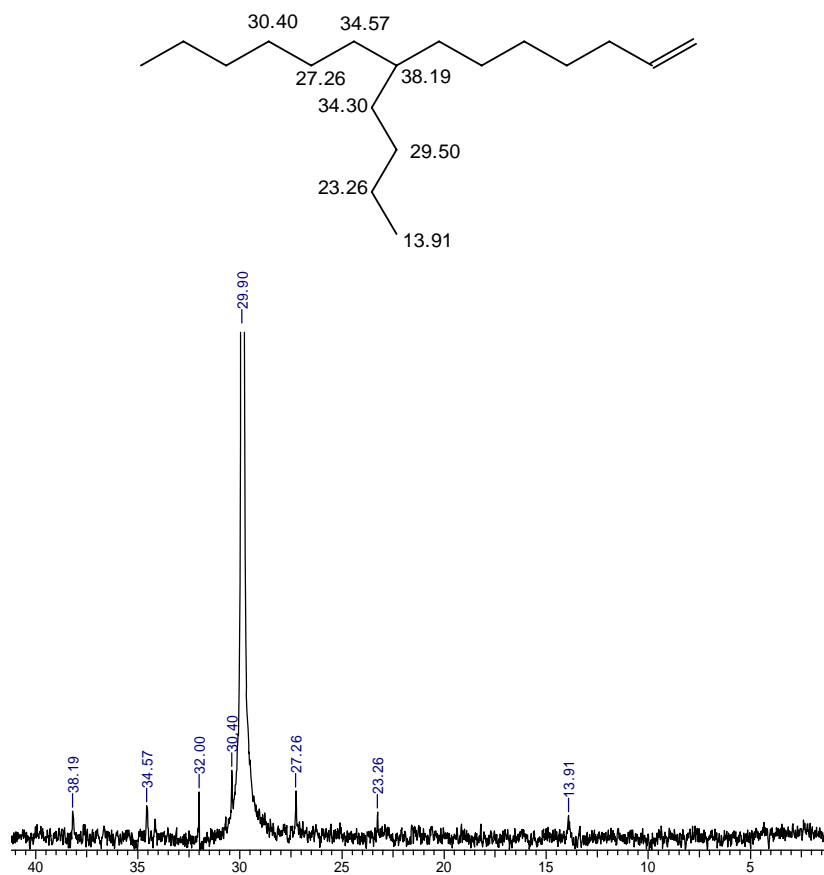


Figure 4.12 Quantitative ^{13}C NMR spectrum of ethylene/hexene-1 copolymer prepared using 2a/MAO (entry 2, Table 4.7)

4.3.4.2. Polymerization of ethylene using bis(oxazoline) (10a-10d) and bis(benzimidazole) (13a-13c) copper(II) complexes

Bis(oxazoline) copper(II) complexes (**10a-10d**) and bis(benzimidazole) copper(II) complexes (**13a-13c**) were used for the polymerization of ethylene in conjunction with MAO as cocatalyst. These complexes were not active for polymerization upto 5 bar ethylene pressure. Polymerization at pressures higher than 5 bar was not attempted.

Following are the salient observations which characterize the behavior of (α -diimine) copper (II) complexes in the polymerization of ethylene:

- (α -Diimine) copper(II) complexes **2a-2c** show a distorted square planar structure, with the bulky *ortho*-substituents offering substantial steric shielding to the metal atom. This structure is also evident in solution by UV-visible and EPR spectroscopy.
- (α -Diimine) copper(II) complex **2c** has a molecule of dichloromethane associated with the crystalline structure.
- Complexes **2a-2c** when activated using MAO show moderate activity for polymerization of ethylene at 5 bar ethylene pressures. The order of catalyst activity followed the order **2a>2b>2c**.
- Complex **6** was inactive for polymerization of ethylene both at 1 bar and 5 bar ethylene pressures
- Copper (II) bis(oxazoline) complexes (**10a-10d**) and copper (II) bis(benzimidazole) complexes (**13a-13c**) were also inactive for polymerization of ethylene at 1 and 5 bar ethylene pressures.
- (α -diimine) copper (I) complexes **3a-3b** failed to polymerize ethylene under conditions where the corresponding copper (II) complexes were active.
- Polymers resulting from (α -diimine) copper (II) complexes were linear poly(ethylene)s and exhibited high molecular weights, molecular weight distributions close to 2.0 and T_m : 130-133°C. Under similar conditions the analogous nickel(II) complexes produced poly(ethylene)s which exhibit lower molecular weights, a branched polymer structure and lower melting points.

The observation that copper complexes **2a-2c** are able to polymerize ethylene only at higher pressures and with low activity is indicative of either low concentration of active centres and/or low rate of insertion of ethylene at the active centre. Experimental results appear to support both. Cationic copper(II) species (**15**) are likely to be less coordinatively unsaturated and less electrophilic (d^9 system) compared to other late transition metal complexes, resulting in lower rates of monomer coordination/insertion. Low active centre

concentration may also be responsible for the unusually high molecular weights of poly(ethylene)s obtained with α -diimine copper(II) complexes.

The nature of halogen on copper also determines catalyst activity with **2a**>**2b**. This is contra-intuitive since generally M-Br bond is easy to alkylate than M-Cl bond.

Nature of ligand and substitution in the aryl ring also appear important. Gibson et al had earlier shown that with certain α -diimine ligands, *ortho*-diphenyl substitution was more effective than 2,6-diisopropyl substitution.¹⁶ Use of an acenaphthene based α -diimine ligand results in complexes (**2a-2b**) where, 2,6-diisopropyl substituent is effective as a catalyst in conjunction with MAO. Thus, both the nature of the ligand as well as the substitution in the aryl ring are important in determining catalyst activity.

Substitution of the aryl group with a single *t*-butyl group (**2c**) results in loss of activity in polymerization. It is likely that the *ortho-t*-butyl substituent, in its preferred conformation (away from the acenaphthyl ring), effectively blocks the active centre from coordinating with ethylene.

Bis(oxazoline) copper complexes **10a-10d** and bis(benzimidazole) complexes (**13a-13c**) were not active for polymerization of ethylene upto 5 bar pressure. The inactivity of **10a - 10d** may be attributed to the presence of an oxygen atom adjacent to the imine moiety that can donate electrons to the metal through resonance and decrease the electron deficiency at the metal center. However, complexes **13a-13c** have been reported to be active for the polymerization of ethylene at 50 bar pressure⁵. Apparently, even in these cases, active centres are formed only in low concentration.

4.3.4.3. Nature of active species in the polymerization of ethylene using copper(II) complexes

Precise nature of the oxidation states responsible for polymerization of ethylene using (α -diimine) copper (II) complexes is a matter of speculation. Stribany suggested based on Near Edge X-ray Absorption Fine Structure Spectroscopy (NEXAFS) and EPR studies that

only diamagnetic Cu(I) and Cu(III) species were present during the polymerization of ethylene using bis(benzimidazole)copper complexes/MAO¹³. In the present study, cyclic voltametry was used to estimate the redox potentials of complexes **2a-2c**. **Figure 4.13** attempts a correlation between the redox potential of the metal complexes **2a-2c** and their polymerization activity. Amongst the complexes studied **2a** possesses the least positive redox potential and also exhibits highest activity. This can be related to the nature of *ortho*-substituents which affect the electronic environment around the metal center. Lower redox potential implies that complex **2a** is more resistant to reduction or more easily oxidized relative to complexes **2b** and **2c**. Thus, the ability to reduce Cu(II) to Cu(I) is not the determining factor for activity in polymerization. The fact that Cu(I) complexes **3a** and **3b** were not active for the polymerization of ethylene supports this argument. Oxidation of Cu(II) to Cu(III) is also less likely. Consequently, the active species is proposed to be a copper(II) center with μ -Cl or μ -Me bridges (**Figure 4.14**). Similar μ -Me bridged Fe(II) species are implicated as active sites in bis(imino)pyridine iron catalysts by Bryliakov et al^{25, 26}.

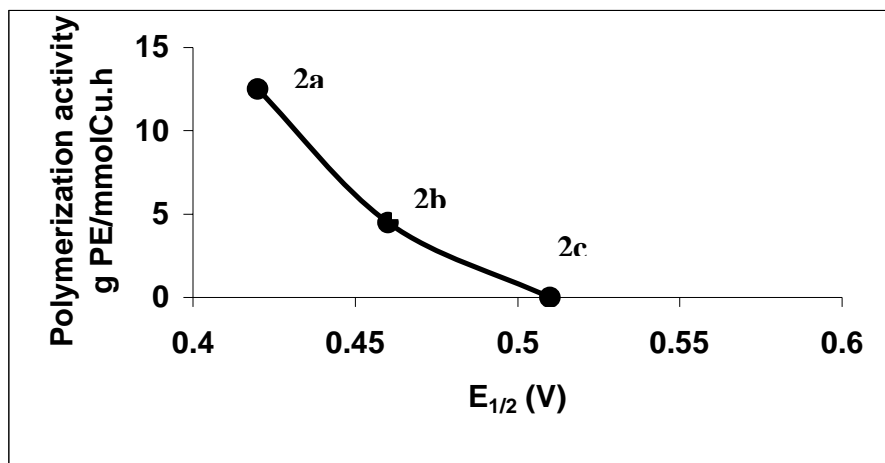
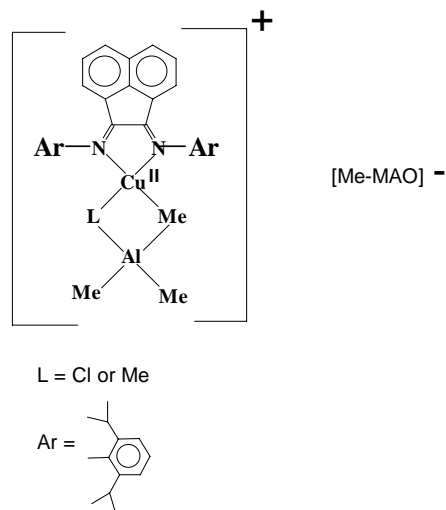


Figure 4.13 Correlation between redox potential of the complexes **2a-2c** and polymerization activity



15

Figure 4.14 Probable active species in the polymerization of ethylene with 2a/MAO

4.4. Conclusions

Several copper complexes based on α -diimine, bis(oxazoline) and bis(benzimidazole) ligands were synthesized and studied as ethylene polymerization catalysts. α -Diimine copper(II) complexes **2a-2c** were characterized by single crystal XRD, IR, UV, EPR and cyclic voltametry. Complexes **2a-2c** show a distorted square planar structure, with the bulky *ortho*-substituents offering substantial steric shielding to the metal atom. Complexes **2a-2b** exhibited moderate activity for polymerization of ethylene when activated with MAO at 5 bar ethylene pressure, while complex **2c** was inactive. Both **2a** and **2b** resulted in linear high molecular weight poly(ethylene)s with narrow molecular weight distributions indicative of single site nature of the active center. Complex **6** bearing an aliphatic diimine ligand framework was inactive for polymerization of ethylene at 5 bar pressure indicating that nature of the chelating ligand plays a significant role in the stabilization of the active species. Copper(I) complexes **3a** and **3b** were not active in polymerizing ethylene. The active species is proposed to be a copper(II) species with μ -Cl or μ -Me bridges. **2a/MAO** also copolymerized ethylene with hexene-1 resulting in about 0.28 mol% comonomer incorporation. Bis(oxazoline) complexes **10a-10d** and bis(benzimidazole) complexes (**13a-13c**) were not active in ethylene polymerization even at 5 bar pressure.

4.5. References

1. Matyjaszewski, K.; Xia, J. *Chem. Rev.* **2001**, *101*, 2921.
2. Shibayama, K.; Ogassa, M (Sekisui Chemical Co.). *PCT Int. Appl. WO 9835996 (CA No.129:203390)*, **1998**.
3. Shibayama, K (Sekisui Chemical Co.). *JP 2000007719 (CA No. 132:64658)*, **2000**.
4. Shibayama, K (Sekisui Chemical Co.). *JP 2000103805 (CA No.132:265594)*, **2000**.
5. Stibrany, R. T.; Schulz, D. N.; Kacker, S.; Patil, A. O (Exxon). *PCT Int. Pat. WO 9930822 (CA No.131:45236)*, **1999**.
6. Stibrany, R. T.; Schulz, D. N.; Kacker, S.; Patil A. O. (Exxon-Mobil), *US patent 6037297(CA No.132:223042)*, **2000**.
7. Stibrany, R. T. (Exxon) *US patent 6180788 (CA No. 134:131949)*, **2001**.
8. Stibrany, R. T.; Schulz, D. N.; Kacker, S.; Patil A. O. (Exxon), *US patent 6417303 (CA No.137:79388)*, **2002**.
9. Stibrany, R. T.; Patil, A. O.; Zushma, S. *Polym. Mater. Sci. & Engg.* **2002**, *86*, 323.
10. Stibrany, R. T.; Schulz, D. N.; Kacker, S.; Patil, A. O.; Baugh, L. S.; Rucker, S. P.; Zushma, S.; Berluce, E.; Sissano, J. A. *Polym. Mater. Sci. & Engg.* **2002**, *86*, 325.
11. Stibrany, R. T.; Schulz, D. N.; Kacker, S.; Patil, A. O.; Baugh, L. S.; Rucker, S. P.; Zushma, S.; Berluce, E.; Sissano, J. A. *Macromolecules.* **2003**, *36*, 8584.
12. Stibrany, R. T.; Patil, A. O.; Zushma, S. *In Beyond Metallocenes: Next Generation Polymerization Catalysts*; Patil, A.O; Hlatky, G.G., Eds.; ACS Symposium Series 857; American Chemical Society: Washington DC, **2003**, pp 194-208.
13. Stibrany, R. T. *In Beyond Metallocenes: Next Generation Polymerization Catalysts*; Patil, A. O; Hlatky, G. G., Eds.; ACS Symposium Series 857; American Chemical Society: Washington DC, **2003**, pp 210-221.
14. Stibrany, R. T.; Schulz, D. N.; Kacker, S.; Patil, A. O.; Baugh, L. S.; Rucker, S. P.; Zushma, S.; Berluce, E.; Sissano, J.A. *In Beyond Metallocenes: Next Generation Polymerization Catalysts*; Patil, A.O; Hlatky, G.G., Eds.; ACS Symposium Series 857; American Chemical Society: Washington DC, **2003**, pp 222-229.
15. Baugh, L.S.; Sissano, J.A.; Kacker, S.; Berluce, E.; Stibrany, R.T.; Schulz, D.N.; Rucker, S. P. *J.Polym. Sci. Part A. Polym. Chem.* **2006**, *44*, 1817.

16. Gibson, V. C.; Tomov, A.; Wass, D. F.; White, A. J. P.; Williams, D. J. *J. Chem. Soc., Dalton Trans.*, **2002**, 2261.
17. Carlini, C.; Giaiacopi, S.; Marchetti, F.; Pinzino, C.; Galletti, A. M. R.; Sbrana, G. *Organometallics* **2006**, *25*, 3659.
18. Chen, F. -T.; Tang, G. -R.; Jin, G. -X. *J. Polym. Sci. Part A. Polym. Chem.* **2007**, *692*, 3435.
19. Killian, C. M.; Tempel, D. J.; Johnson, L. K.; Brookhart, M. *J. Am. Chem. Soc.* **1996**, *118*, 11664.
20. Denmark, S. E.; Nakajima, N.; Nicaise, O. J. -C.; Faucher, A. -M.; Edwards, J. P. *J. Org. Chem.* **1995**, *60*, 4884.
21. Gates, D. P.; Svejda, S. A.; Enrique Onate, E.; Killian, C. M.; Johnson, L. K.; White, P. S.; Brookhart, M. *Macromolecules* **2000**, *33*, 2320.
22. El-Ayaan, U.; Paulovicova, A.; Fukuda, Y. *J. Mol. Str.*, **2003**, *645*, 205-212.
23. Sutton, D; *Electronic Spectra of Transition Metal complexes*, McGraw Hill, London, **1968**.
24. Johnson, L. K.; Killian, C. M.; Brookhart, M. *J. Am. Chem. Soc.* **1995**, *117*, 6414
25. Bryliakov, K. P.; Semikolenova, N. V.; Zudin, V. N.; Zakharov, V. A.; Talsi, E. P. *Catal. Commun.* **2004**, *5*, 45.
26. Bryliakov, K. P.; Semikolenova, N. V.; Zakharov, V. A.; Talsi, E. P. *Organometallics* **2004**, *23*, 5375.

CHAPTER 5

POLYMERIZATION OF ETHYLENE USING *ansa*- η^5 - MONOFLUORENYL COMPLEXES OF GROUP IV METALS

5.1. Introduction

There is growing interest in early transition metal complexes with bidentate ligands that combine two anionic functions such as cyclopentadienyl, indenyl or fluorenyl with built-in alkoxide, amide or similar groups as catalysts for oligomerization or polymerization of olefins. Such ligands have led to the development of new “single site” group 4 metallocene complexes which provide control over stereoregularity, molecular weight, thermal/rheological characteristics, ability to incorporate bulky and polar comonomers and microstructure¹⁻⁴. In particular, complexes of bifunctional monocyclopentadienyl ligands having an appended hetero atom donor have attracted considerable attention, as exemplified by “constrained geometry” catalysts. However, there are only very few reports on olefin polymerization catalyzed by oxygen containing complexes such as Cp'M(OR)X₂. These types of complexes are of interest because of ease of synthesis and their similarity to the half-metallocene analogues.

Rieger⁵ reported the synthesis and characterization of zirconium complexes based on *trans*-2-[9-(H)-fluorenyl] cyclopentanol and *trans*-2-[9-(H)-fluorenyl] cyclohexanol. Although it was reported that these complexes along with MAO or TMA exhibited catalytic activity for polymerization of ethylene, no experimental data were reported.

A novel cyclopentadienyl phenolate titanium catalyst system active in the polymerization of olefins was reported by Marks and coworkers⁶. This complex when activated with [Ph₃C]⁺[B(C₆F₅)₄]⁻ exhibited high activity for polymerization of ethylene, propylene and styrene producing high molecular weight (> 10⁶) poly(ethylene)s with high T_m (142°C) as well as atactic PP and PS. Poly (ethylene)s produced had a broad molecular weight distribution of greater than 10.0 while poly(propylene)s showed MWD of 1.85. The reason for broad molecular weight distribution of poly(ethylene)s was attributed to rapid decomposition of the cationic species at room temperature or slow initiation with respect to fast propagation and significant inhomogeneity during the course of the catalytic reaction. Observed narrow molecular weight distribution in the case of PP may be due to the structurally open nature of the cationic metal coordination sphere and apparently greater stabilization of the active sites in presence of propylene.

Gielens et al⁷ reported a titanium hydrocarbyl complex with a linked Cp-alkoxide ancillary ligand which exhibited an activity of 263 g PP mmol⁻¹Ti.h⁻¹ for polymerization of propylene. Poly(propylene)s formed were atactic with a noticeable amount of 2,1-misinsertions. The polymer had a Mw of 41,000 and molecular weight distribution of 2.1 indicative of a single active species.

Objective of the present study was to synthesize Group 4 metal complexes (Ti, Zr, Hf) of *trans*-2-[9-(H) fluorenyl] cyclohexanol and study their behavior towards polymerization of ethylene. The idea behind selecting these complexes was to explore the contribution of a metal-oxygen bond towards improving thermal stability of the complexes which in turn may make them suitable for high temperature catalysis. Moreover, the open nature of the complexes may allow easier incorporation of α -olefins into the growing polymer chain. Towards these objectives several complexes were synthesized and the effect of various reaction conditions such as nature of metal, cocatalysts, cocatalyst concentration, polymerization temperature and ethylene pressure on catalyst activity and the resulting polymer properties was explored. Polymerization behavior of these complexes was compared with similar catalyst systems reported in the literature.

5.2. Experimental

5.2.1. Materials

This is described in chapter 3, Section 3.2 and 3.3

5.2.2. Synthesis of complexes 3a-3c

5.2.2.1. Synthesis of *ansa*-(η 5-fluorenyl cyclohexanolato) bis(tetrahydrofuran) titanium(IV)dichloride(3a)

5.2.2.1.1. Synthesis of *trans*-2-[9-(H)-fluorenyl] cyclohexanol (2)

An oven-dried 250 mL Schlenk flask was cooled under vacuum and charged with argon. Fluorene (2 g, 12 mmol) was taken in it and dissolved in dry diethyl ether. An ethereal solution of n-BuLi (5 mL, 12.5 mmol of 2.5 M solution in hexane) was added to this solution at 0°C over a period of 45 min. It was stirred for 1 h and epoxycyclohexane (1.2 mL, 12 mmol) was added dropwise to it at 0°C over a period of 1 h. The mixture was

stirred at 25°C for 12 h. The product was hydrolyzed with aqueous ammonium chloride solution. Ether layer was separated, dried over anhydrous sodium sulphate and concentrated to obtain **2** as a pale yellow solid. The compound was further purified by column chromatography. Yield: 2.70 g (85 %)

Analysis for C₁₉H₂₀O :

Calcd., % C 86.34 H 7.63

Found, % C 86.25 H 7.52

¹H NMR (CDCl₃, 400 MHz): δ ppm 7.2-7.9(m, 8 H), 4.55(d, 1 H), 3.95(m, 1 H), 0.57-2.2(m, 10 H)

¹³C NMR (CDCl₃, 100 MHz): δ ppm 24.47, 24.84, 25.32, 36.49, 47.30, 49.65, 72.22, 119.35, 119.68, 123.76, 125.48, 126.40, 126.59, 126.77, 141.40, 141.66, 145.08, 147.06

5.2.2.1.2. Synthesis of TiCl₄(thf)₂

An oven-dried 250 mL Schlenk flask was cooled under vacuum and charged with argon. Dichloromethane (50 mL) was transferred to it through a cannula and TiCl₄ (2.9 mL, 26.4 mmol) was added through a syringe. THF (8.5 mL, 105.6 mmol) was added dropwise. A yellow solution was obtained which was stirred for 1 h. Pentane (50 mL) was added and the solution chilled to -25°C for 1 h. A bright yellow crystalline solid was obtained which was filtered through a sintered filter, washed twice with dry pentane and dried under vacuum.

5.2.2.1.3. Synthesis of **3a**

In an oven-dried 250 mL Schlenk flask, cooled under vacuum and charged with argon was taken **2** (0.264 g, 1 mmol) and dissolved in THF. n-BuLi (0.8 mL, 2 mmol) was added to it at 0°C slowly and stirred for 30 min. The flask was then cooled to -78°C and TiCl₄(thf)₂ (0.334 g, 1 mmol) dissolved in THF was added drop wise. The reaction mixture was stirred at room temperature for 12 h. THF was evaporated, dichloromethane was added and the solution filtered through a celite bed to remove LiCl. Dichloromethane solution on evaporation gave a reddish brown solid, which was washed with hexane and dried in vacuum. Elemental analysis showed the presence of 2 THF molecules in the complex. Yield: 0.40 g (76 %)

Analysis for $C_{19}H_{18}OTiCl_2 \cdot 2C_4H_8O$

Calcd., % C 61.81 H 6.48

Found, % C 61.87 H 6.74

5.2.2.2. Synthesis of *ansa*-(η^5 -fluorenyl cyclohexanolato) bis(tetrahydrofuran) zirconium(IV)dichloride (3b)

5.2.2.2.1. Synthesis of $ZrCl_4$ (thf)₂

An oven-dried 250 mL Schlenk flask was cooled under vacuum and charged with argon. $ZrCl_4$ (2.33 g, 10 mmol) was taken in the flask and suspended in dichloromethane (30 mL). THF (1.6 mL, 20 mmol) was added dropwise. The reaction mixture was stirred at room temperature for 4 h. A colorless turbid solution was obtained. The solution is filtered through a sintered filter, pentane (50 mL) was added and the solution chilled to $-25^\circ C$ for 2 h. A white crystalline solid was obtained which was filtered through a sintered filter, washed twice with dry pentane and dried under vacuum.

5.2.2.2.2. Synthesis of 3b

In an oven-dried 250 mL Schlenk flask, cooled under vacuum and charged with argon was taken compound **2** (0.264 g, 1 mmol) and dissolved in THF. *n*-BuLi (0.8 mL, 2 mmol) was added to it at $0^\circ C$ slowly and stirred for 30 min. The flask was cooled to $-78^\circ C$ and $ZrCl_4$ (thf)₂ (0.377 g, 1 mmol) dissolved in THF was added dropwise. The reaction mixture was refluxed for 6 h. THF was evaporated, dichloromethane was added and the solution filtered through a celite bed to remove LiCl. Dichloromethane solution on evaporation gave a yellow solid, which was washed with hexane and dried in vacuum. Elemental analysis of the complex showed the presence of 2 THF molecules coordinated to the metal center. Yield: 0.38 g (67 %)

Analysis for $C_{19}H_{18}OZrCl_2 \cdot 2 C_4H_8O$:

Calcd., % C 57.02 H 5.98

Found, % C 56.76 H 6.06

5.2.2.3. Synthesis of *ansa*-(η 5-fluorenyl cyclohexanolato) bis (tetrahydrofuran) hafnium (IV)dichloride (3c)

5.2.2.3.1. Synthesis of $\text{HfCl}_4(\text{thf})_2$

An oven-dried 250 mL Schlenk flask was cooled under vacuum and charged with argon. HfCl_4 (5.0 g, 15.6 mmol) was taken in the flask and suspended in dry dichloromethane (50 mL). Dry THF (10 mL, 62.4 mmol) was added dropwise. The reaction mixture was stirred at room temperature for 2 h. A colorless turbid solution was obtained. The solution was filtered through a sintered filter, dry pentane (50 mL) was added and the solution chilled to -35°C for 2 h. A white crystalline solid was obtained which was filtered through a sintered filter, washed twice with dry pentane and dried under vacuum.

5.2.2.3.2. Synthesis of 3c

An oven dried 250 mL Schlenk flask was dried under vacuum and filled with argon. Compound **2** (1.0 g, 3.78 mmol) was added into the flask and dissolved in THF. The flask was cooled to -78°C and n-BuLi (4.7 mL, 7.56 mmol of 1.6 M solution in hexane) was added dropwise. A red-colored solution was observed which was stirred for 30 min. To this solution, $\text{HfCl}_4(\text{thf})_2$ (1.74 g, 3.78 mmol) dissolved in THF was added dropwise at -78°C . After the addition is complete, the reaction mixture was allowed to attain room temperature and then refluxed under argon for 6 h. The solvent was then removed under vacuum, the residue dissolved in dry dichloromethane and filtered through a celite bed to remove the LiCl. The dichloromethane solution upon evaporation yielded a yellow solid. Elemental analysis of the complex showed the presence of two coordinated THF molecules. Yield: 1.7 g (70 %)

Analysis for $\text{C}_{19}\text{H}_{18}\text{OHfCl}_2 \cdot 2 \text{C}_4\text{H}_8\text{O}$

Calcd., % C 49.64 H 5.18

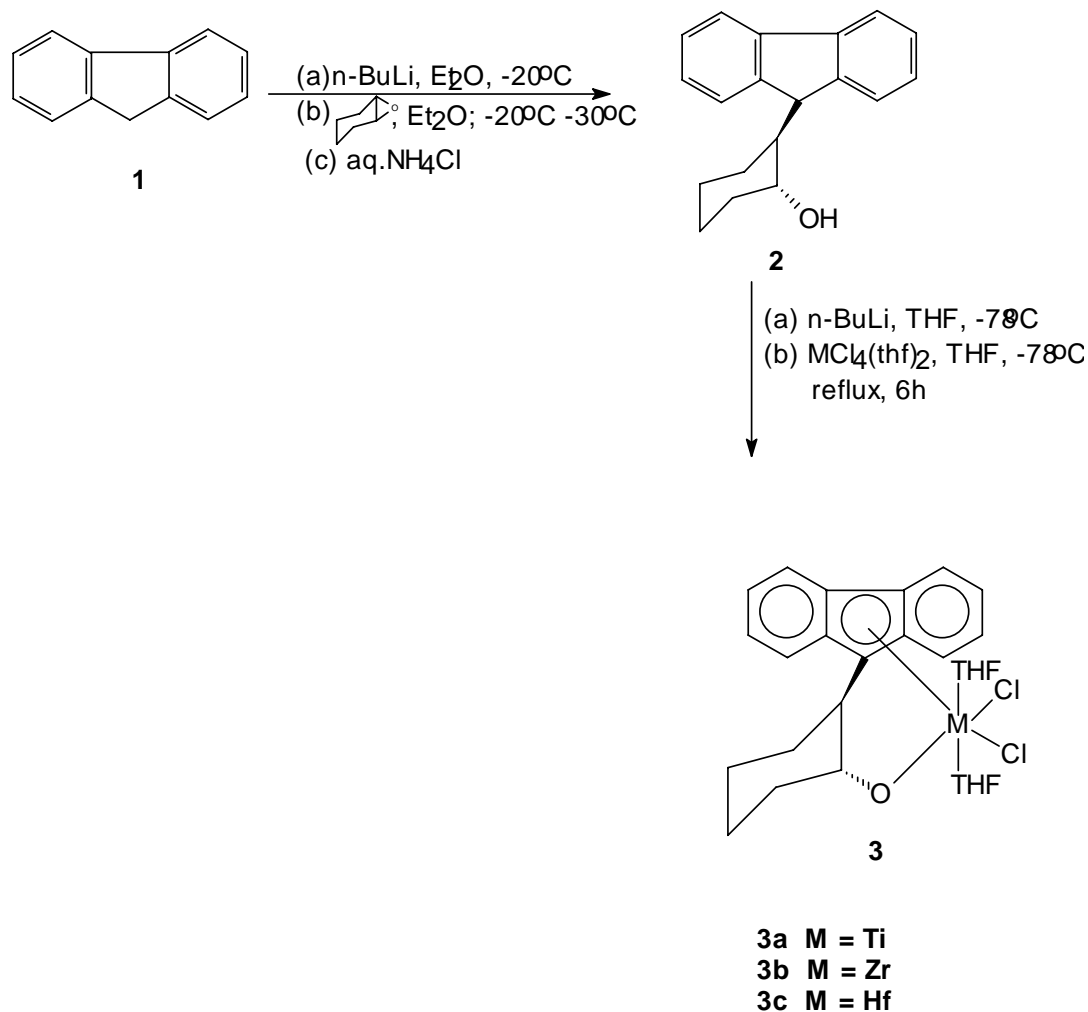
Found, % C 49.43 H 5.28

5.3. Results and Discussion

5.3.1. Synthesis of *trans*-2-[9-(H)-fluorenyl cyclohexanol and its metal complexes

Synthetic scheme for *trans*-2-[9-(H)-fluorenyl cyclohexanol and its metal complexes is

shown in **Scheme 5.1**. Fluorene upon treatment with *n*-BuLi in diethyl ether at -20°C gave fluorenyl lithium which in turn caused the opening of epoxide ring in epoxy-cyclohexane.



Scheme 5.1 Synthesis of *trans*-2-[9-H]-fluorenyl cyclohexanol and the metal complexes

Unambiguous assignment of all protons and carbons of 2-[9-H]-fluorenyl cyclohexanol (**2**) was achieved by a combination of ^1H , ^{13}C 1D and 2D NMR techniques. COSY, ^1H - ^{13}C HSQC and ^1H - ^{13}C HMBC spectra were analyzed to identify the protons in the cyclohexyl and aromatic rings. ^1H and ^{13}C NMR spectra of **2** are shown in **Figure 5.1-5.2** and ^{13}C DEPT spectrum shown in **Figure 5.3**.

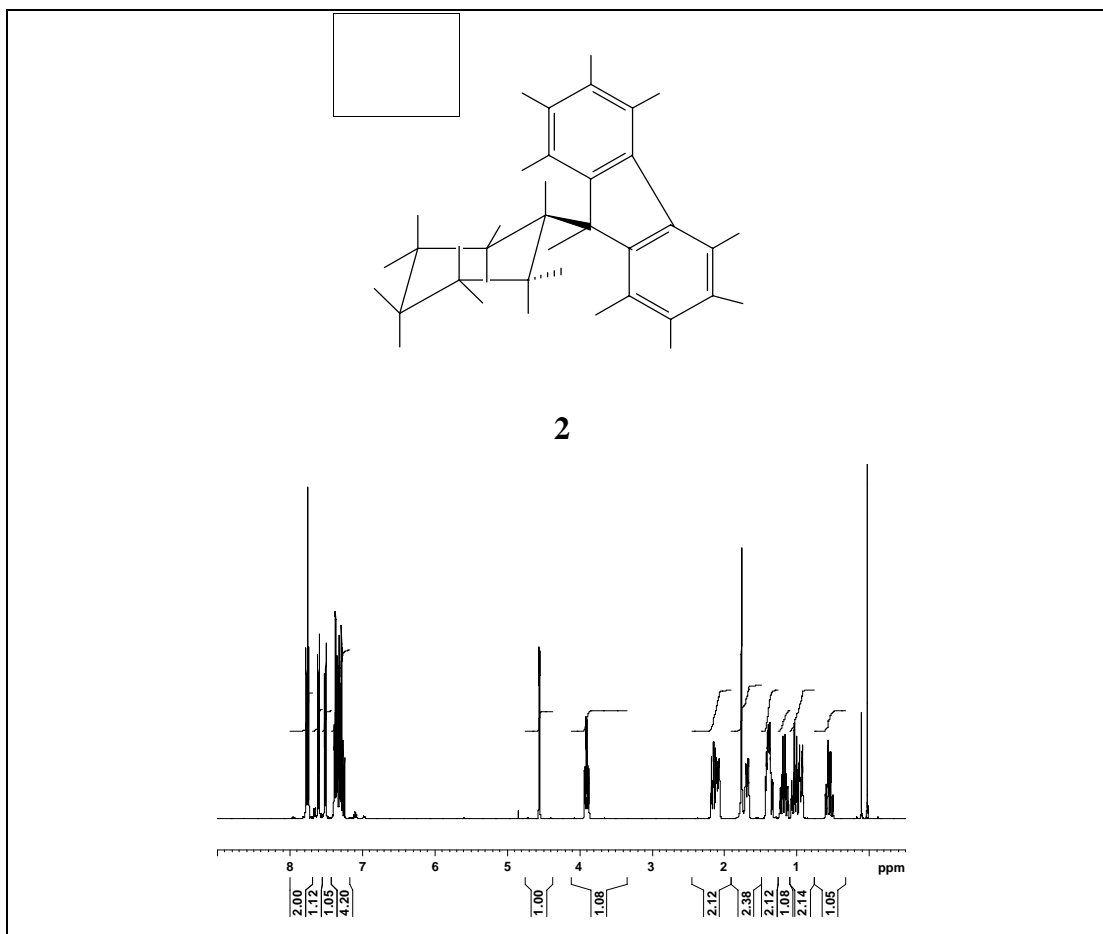


Figure 5.1 ^1H NMR spectrum (in CDCl_3 , 400 MHz) of **2**

The ^1H assignments are given in **Table 5.1**. Further, the ^1H - ^1H scalar coupling and NOESY data were used for the determination of the stereochemistry.

Table 5.1 ^1H NMR assignment for **2**

δ (ppm)	Assignment	δ (ppm)	Assignment	δ (ppm)	Assignment
0.58	H_3	2.14	H_2	7.60	H_h
0.98	H_4	3.98	H_1	7.75	H_d, H_e
1.04	H_5	4.55	H_{11}		
1.17	H_7	7.28	H_g		
1.39	H_6, H_9	7.32	H_b		
1.69	H_8	7.37	H_c, H_f		
2.08	H_{10}	7.51	H_a		

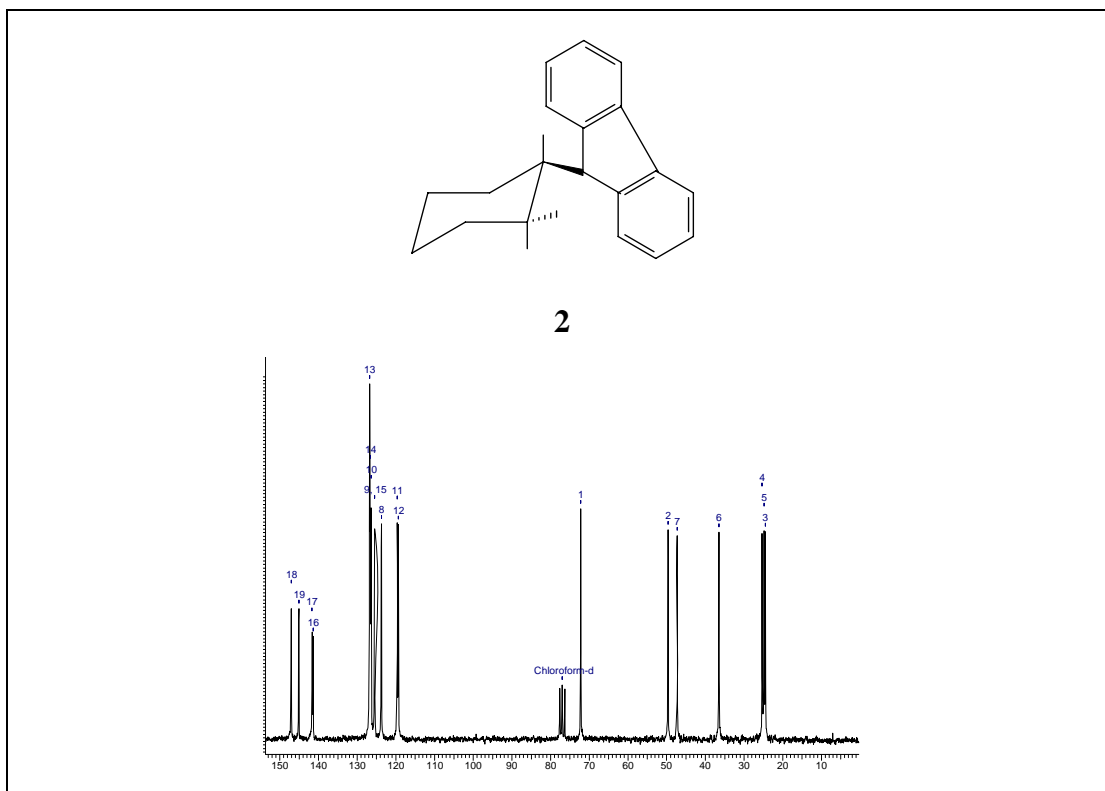


Figure 5.2 ^{13}C NMR spectrum (in CDCl_3 , 100 MHz) of **2**

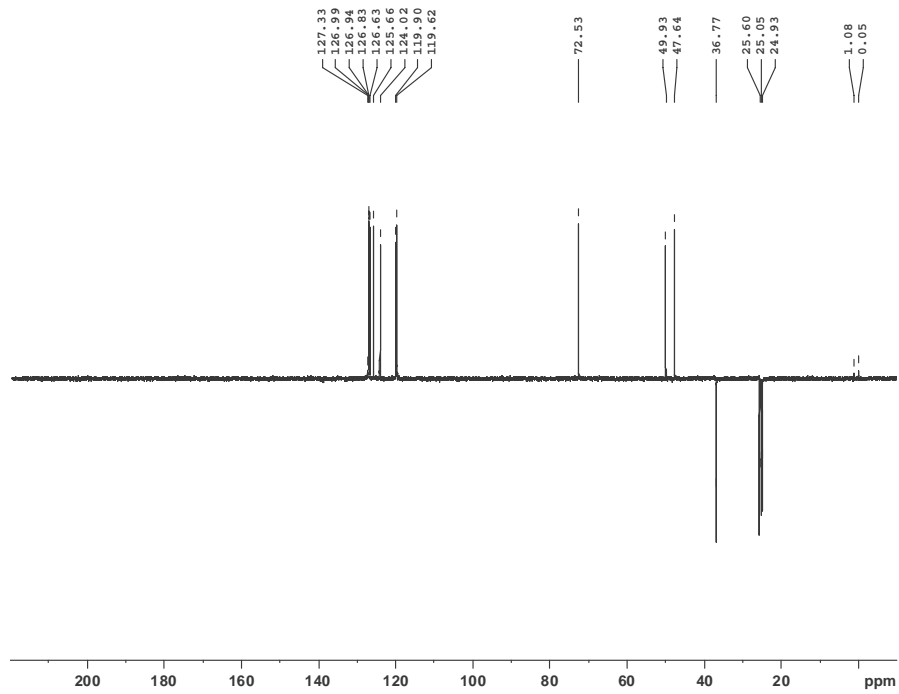


Figure 5.3 ^{13}C -DEPT spectrum (in CDCl_3 , 100 MHz) of **2**

A COSY spectrum shows the coupling interactions between the same type of nuclei in a compound in the form of a two-dimensional contour plot. The contours on the 45° diagonal line of the plot correspond to an overhead view of the peaks in the 1D NMR spectrum and those which lie away from the diagonal represent coupling interactions between the protons. The top end of the diagonal represents the upfield region and the lower end represents the downfield region. In order to find out the coupling between protons, two lines are drawn at 90° from each other starting at the contour cross peak and ending at the diagonal line. The two points on the diagonal where the two lines cross it correspond to the chemical shifts of the two coupled nuclei. For example, in **Figure 5.4** the diagonal line passes through contours numbered 1,2,3,4 etc. There are cross peaks represented as A, B etc. Now if a line is drawn straight down from cross peak A, it meets the diagonal line at point 2. If another line is drawn from the same peak A horizontally, it meets the diagonal at point 3. This indicates that proton at point 2 (3.98 ppm) is coupled to the proton at point 3 (2.14 ppm). Similarly coupling between other protons can be found out from the COSY spectrum.

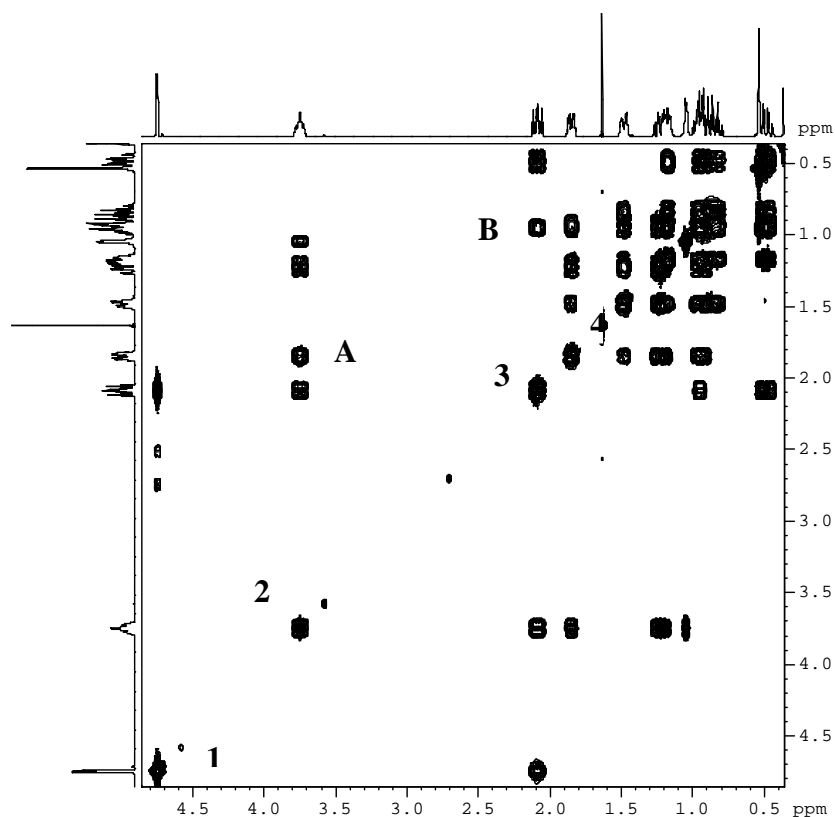


Figure 5.4 COSY spectrum of 2

Coupling constants of protons of H₁ and H₂ are given in Table 5.2.

Table 5.2 Coupling constants of protons H₁ and H₂

H ₁ (3.98 ppm)	J _{H1-H2} - 10.5 Hz J _{H1-H9} - 10.5 Hz J _{H1-H10} - 3.3 Hz
H ₂ (2.14 ppm)	J _{H2-H1} - 10.5Hz J _{H2-H3} - 12.5 Hz J _{H2-H4} - 3.3 Hz J _{H2-H11} - 3.3 Hz

Coupling pattern of proton H₁ showed two strong axial-axial couplings (10.5Hz) and a weak axial-equatorial coupling (3.3Hz) with adjacent protons and appears as a doublet of a triplet. This pattern is possible only when H₁ and H₂ are in the axial positions and the hydroxyl and fluorenyl groups are at the equatorial positions. The axial position of H₁ (2.14ppm) also can be inferred from the coupling pattern observed.

Trans-geometry of **2** was also confirmed by NOESY spectrum (**Figure 5.5**) wherein a strong NOE was observed between the aromatic proton H_a and cyclohexyl proton H₂ and between H_h and H₁ (**Figure 5.6**). This is also supported by the fact that a strong NOE is absent between protons H₁ and H₂.

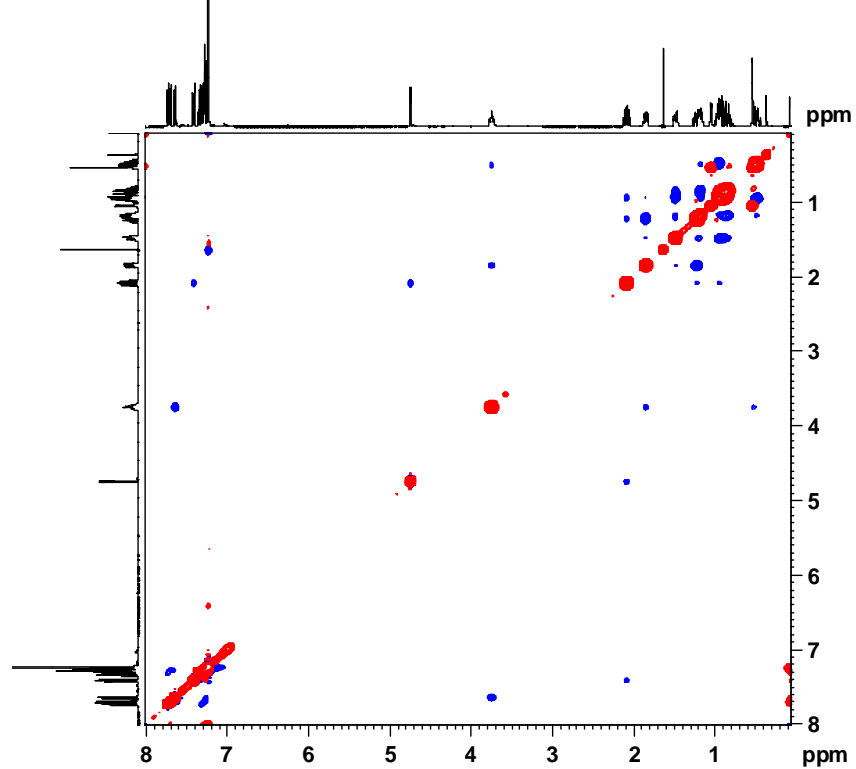


Figure 5.5 NOESY spectrum of 2

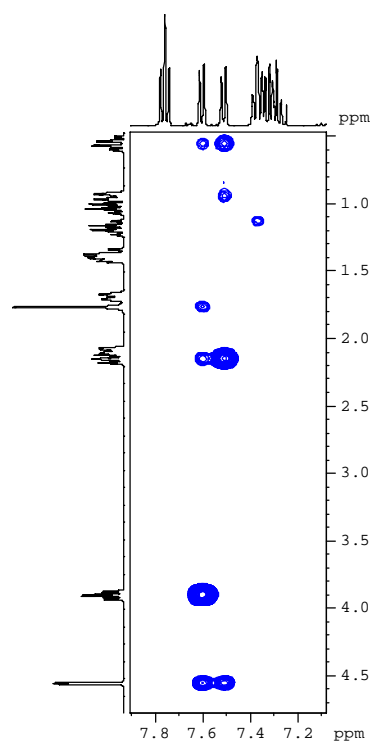


Figure 5.6 NOESY spectrum of 2 showing strong NOE between aromatic and cyclohexyl ring protons

Complexes **3a-3c** were found to contain two molecules of THF coordinated to the metal center as reported by Rieger⁵. NMR spectroscopy (**Figure 5.7**) and elemental analysis also confirmed this observation. The presence of coordinated donor molecules in the complexes is determined by steric and electronic factors around the metal center. It is known that fluorenyl based complexes are more prone to donor molecule coordination than the cyclopentadienyl and indenyl based systems as the metal center is more electrophilic due to the delocalization of the π electrons over two aromatic rings. Presence of fluorenyl ligand and more open nature of the complexes may be responsible for the presence of THF molecules in the coordination sphere of these complexes.

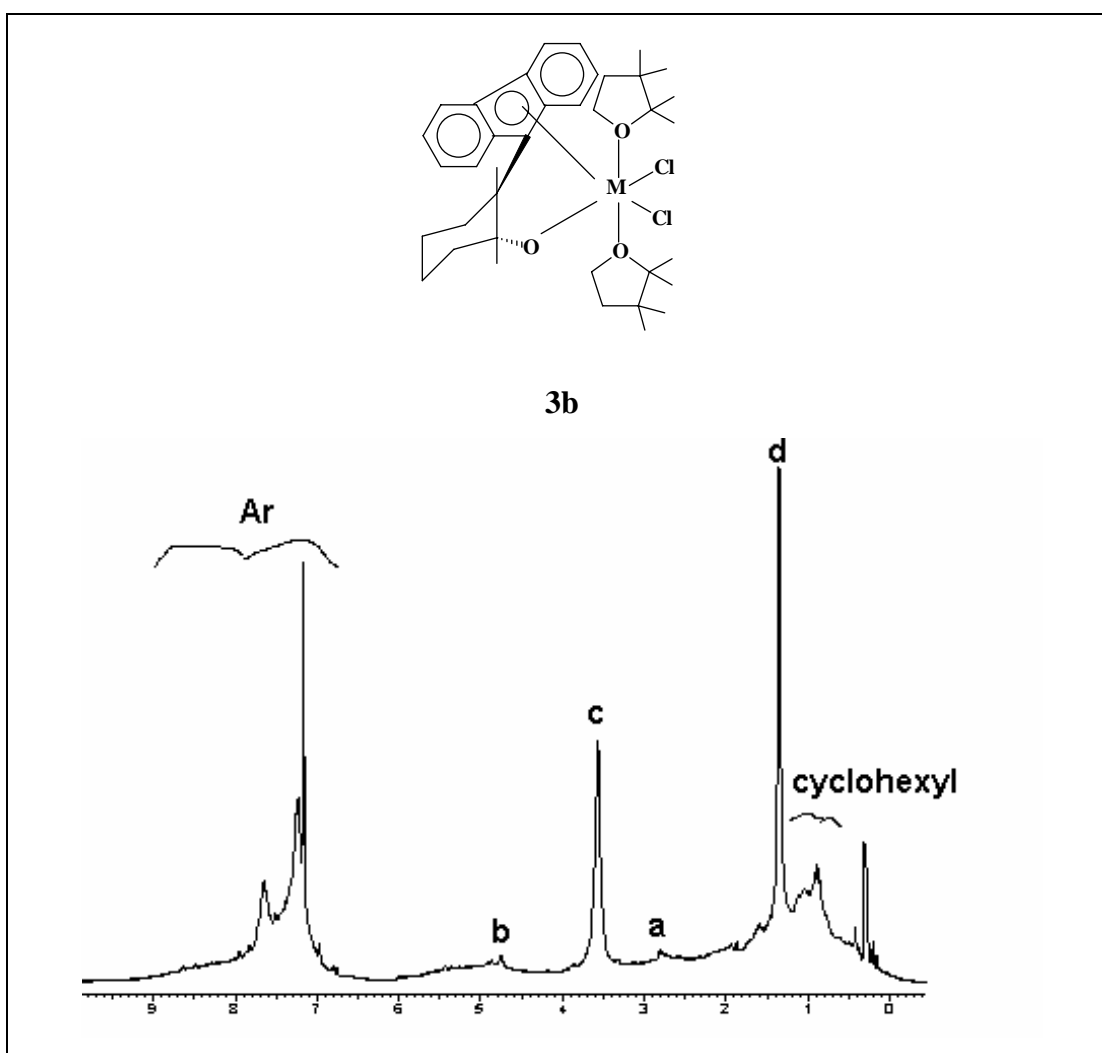


Figure 5.7 ¹H NMR spectrum (in C₆D₆, 500 MHz) of zirconium complex **3b**

Several attempts to prepare single crystals of complexes were not successful; hence they were used as powder for ethylene polymerization studies.

5.3.2. Polymerization of ethylene using complexes 3a-3c

5.3.2.1. Polymerization of ethylene at 1 bar ethylene pressure

The red colored solution of complex **3a-3c** upon addition to toluene solution of MAO saturated with ethylene resulted in an yellow colored solution. No polymer formation was observed at 25°C and 1 bar ethylene pressure. When the polymerization temperature was increased to 60°C, only traces of polymer was formed.

5.3.2.2. Polymerization of ethylene at 5 bar pressure

5.3.2.2.1. Effect of nature of the metal

Effect of metal on catalyst activity and polymer properties were investigated at two different temperatures. Results are summarized in **Table 5.3**.

Table 5.3 Effect of metal on catalyst activity and polymer properties using 3a-3c/MAO^a

Entry	Complex	Complex (μmol)	Tp (°C)	Yield (g)	Activity g PE mmo ⁻¹ M.h ⁻¹	[η] ^b dL/g	Mw (x10 ⁴)	M _w /M _n	Tm (°C)
1	3a	19.0	25	0.20	10	5.2	n.d ^c	n.d ^c	142
2	3b	17.6	25	1.0	57	5.1	n.d	n.d	134
3	3c	15.5	25	0.04	2.6	2.8	n.d	n.d	133
4	3a	19.0	80	0.30	16	2.5	n.d	n.d	140
5	3b	17.6	80	3.7	210	0.9	12.2	25.5	122
6	3c	15.5	80	0.07	4.5	2.0	n.d	n.d	134

^a Toluene(30 mL); MAO; Al/M: 2000; P_{C₂H₄}: 5 bar; time: 1 h

^b measured in decahydronaphthalene at 135°C

^c n.d : not determined

Zirconium complex **3b** was found to be significantly more active than titanium (**3a**) and hafnium analogues (**3c**). Catalyst activities were higher for all three complexes at 80°C. Intrinsic viscosities were higher for titanium and hafnium complexes than zirconium complex. Titanium complex **3a** resulted in poly(ethylene)s with exceptionally high

crystalline melting points (140-142°C) (**Figure 5.8**) Attempts to analyze the polymers by GPC were not successful in view of the high viscosities of their solutions. Hence the molecular weights and molecular weight distributions of only a few lower molecular weight samples are reported.

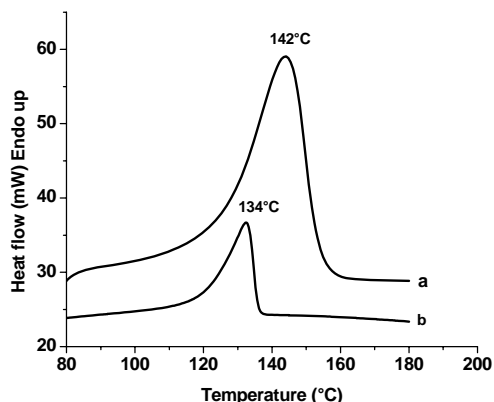


Figure 5.8 DSC thermogram of poly(ethylene)s obtained by 3a and 3b/MAO (a) entry 1 (b) entry 2, Table 5.3

5.3.2.2.2. Effect of MAO concentration on catalyst activity and polymer properties

Catalyst activity was found to be independent of MAO concentration in the range of 500-2000 at 25°C (**Table 5.4**). At 80°C marginal increase in activity was observed with increase in MAO concentration. Polymer molecular weights decreased with increase in MAO concentration.

Table 5.4 Polymerization of ethylene using 3b/MAO: Effect of Al/Zr ratio ^a

Entry	Al/Zr	T _p (°C)	Yield(g)	Activity g PE mmol ⁻¹ Zr.h ⁻¹	[η] ^b dL/g	T _m (°C)
1	500	25	0.9	51	6.55	132
2	1000	25	0.96	55	6.30	132
3	2000	25	1.0	57	5.13	130
4	500	80	2.5	142	1.25	127
5	1000	80	2.8	159	1.35	122
6	2000	80	3.7	210	0.93	122

^a Toluene(30 mL); Zr: 17.6 μmol; MAO; P_{C₂H₄}: 5 bar; time: 1 h

^b measured in decahydronaphthalene at 135°C

5.3.2.2.3. Effect of cocatalyst on polymerization of ethylene using complex 3b

Activators such as triethyl aluminium and diethylaluminium chloride were also studied for ethylene polymerization using **3b** and were found to be inefficient.

5.3.2.2.4. Effect of added TMA

Polymerization of ethylene using **3b/MAO** was studied in presence of TMA. The results are summarized in **Table 5.5**. It is seen from the data that TMA alone is not an efficient activator for the catalyst. However, there was a significant increase in the catalyst activity when the catalyst was pretreated with TMA for 30 min before introducing into the reactor.

Table 5.5 Ethylene polymerization using 3b: Effect of TMA^a

Entry	MAO/Zr	TMA/Zr	Yield(g)	Activity g PE _{mmol} ⁻¹ Zr.h ⁻¹	[η] dL/g	T _m (°C)
1	1000	0	0.95	55	6.30	134
2	0	1000	traces	-	-	-
3 ^b	1000	250	1.1	63	6.18	135
4 ^c	1000	250	1.7	97	4.93	133

^a Toluene(30 mL); Zr: 17.6 μmol; P_{C₂H₄}: 5 bar; T_p:25°C; time: 1 h

^b **3b** was treated with TMA for 10 min inside the reactor before addition of MAO

^c **3b** was pretreated with TMA for 30 min before introducing into the reactor

5.3.2.2.5. Effect of temperature

Polymerization of ethylene was conducted using **3b/MAO** in the temperature range 25-100°C. The results of the polymerization are tabulated in Table 5.6. Catalyst system **3b/MAO** exhibited high activities even at 100°C. Poly(ethylene)s obtained above 60°C were sticky. Therefore, following method was used for recovery of the polymer and its purification. The solid obtained after filtration, upon washing several times with boiling acetone, yielded a solid polymer (designated as **Fraction A**). The acetone solution upon evaporation resulted in a waxy material (designated as **Fraction B**). Toluene-methanol layer (after precipitation and filtering of the solid) was neutralized with aqueous sodium bicarbonate solution, organic layer separated and concentrated to obtain liquid oligomers (designated as **Fraction C**). Thus, a mixture of insoluble solid polymer and soluble liquid oligomers was obtained using **3b/MAO** at temperatures above 60°C.

Table 5.6 Effect of temperature on polymerization of ethylene using 3b/MAO ^a

Entry	Tp (°C)	Total yield (g)	Acetone insoluble fraction (Fraction A) (g)	Acetone soluble fraction (Fraction B) (g)	Toluene soluble fraction (Fraction C) (g)	Activity g PE mol ⁻¹ Zr.h ⁻¹
1	25	1.0	1.0	nil	nil	57
2	40	0.96	0.96	nil	nil	55
3	60	3.9	1.9	1.1	0.9	222
4	80	3.7	1.8	1.1	0.8	210
5	100	2.8	1.7	0.5	0.6	159

^a Toluene (30 mL); Zr: 17.6 μmol; MAO; Al/Zr: 2000; P_{C₂H₄} : 5 bar; time : 1 h

5.3.2.3. Characterization of polymer and oligomer fractions

All the three fractions were separately characterized for their structure and melting behaviour.

5.3.2.3.1. Characterization of Fraction A

Intrinsic viscosities and melting points of **Fraction A** obtained using **3b/MAO** is shown in **Table 5.7**. A gradual decrease in molecular weights and melting points was observed upon increasing the polymerization temperature (**Figure 5.9**). GPC of poly(ethylene)s appeared similar for fraction **A** produced at 80 and 100°C (**Figure 5.10**). Very broad bimodal molecular weight distributions were observed.

Table 5.7 Characterization of Fraction A obtained with 3b/MAO

Entry	Tp (°C)	[η] dL/g	Mw (x10 ⁴)	Mw/Mn	Tm (°C)
1	25	5.1	n.d	n.d	132
2	40	4.7	n.d	n.d	130
3	60	1.04	n.d	n.d	125
4	80	0.93	12.2	25.5	121
5	100	0.59	7.7	17.5	123

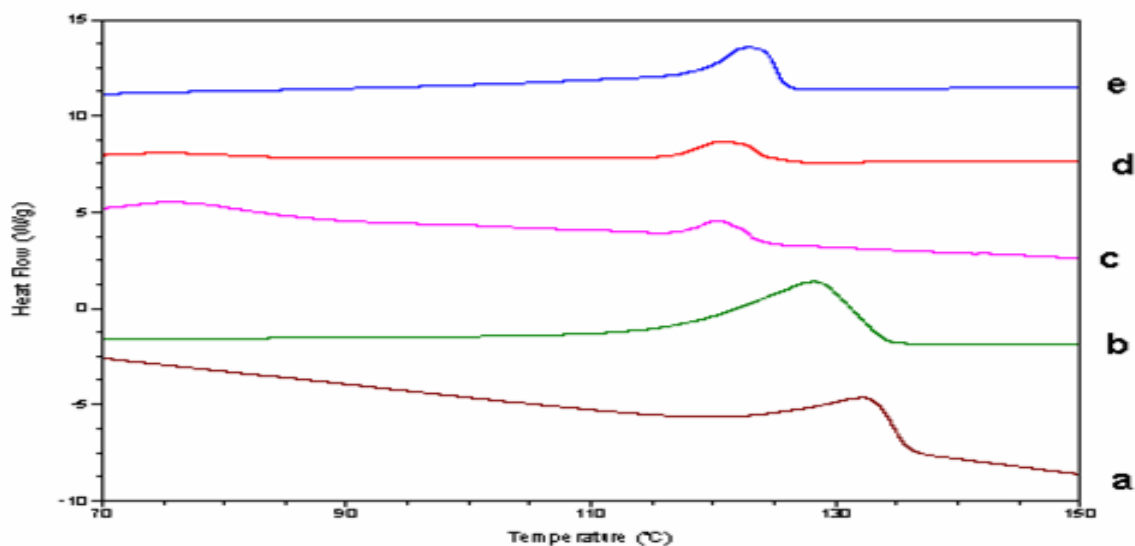


Figure 5.9 DSC thermograms of Fraction A produced with catalyst 3b/MAO at different temperatures (a) entry 1 (b) entry 2 (c) entry 3 (d) entry 4 (e) entry 5 in Table 5.7.

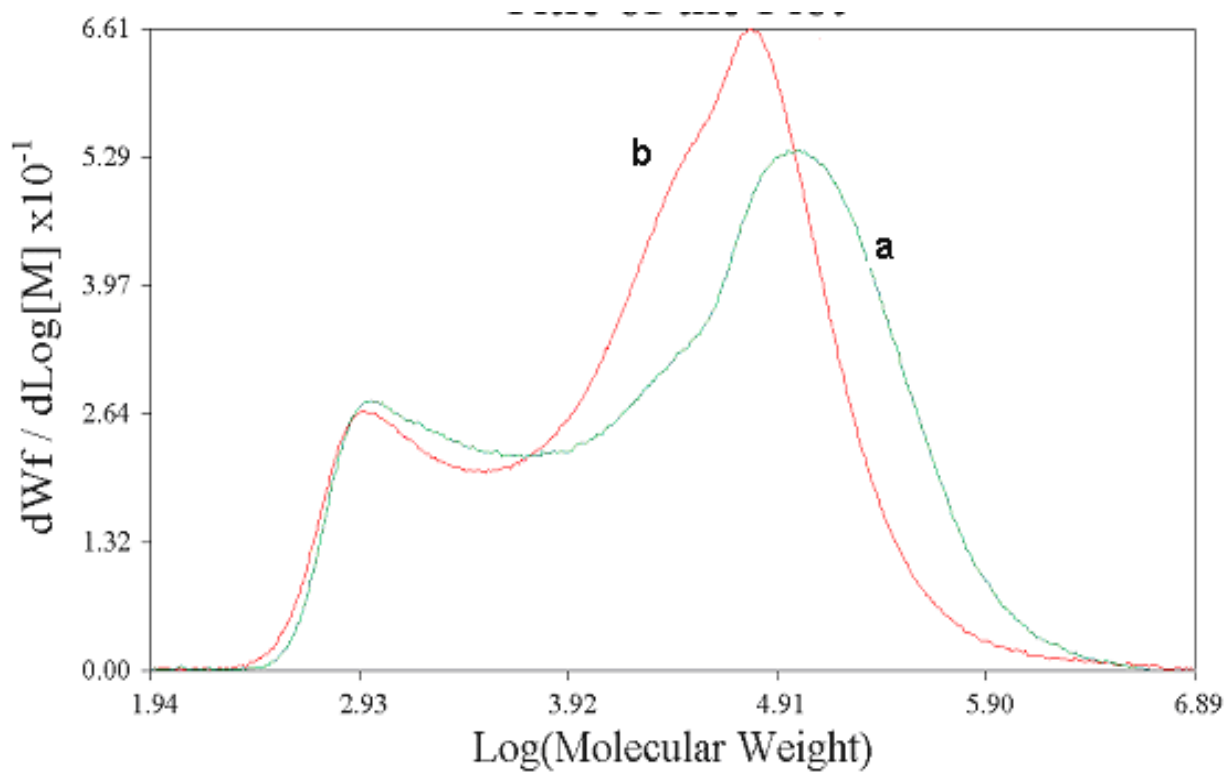


Figure 5.10 GPC of Fraction A produced by 3b/MAO (a) entry 4 (b) entry 5, Table 5.5.

5.3.2.3.2. Characterization of Fraction A by ^{13}C NMR spectroscopy

Solid polymers (**Fraction A**) obtained using the catalyst **3b**/MAO in the temperature range 25-100°C were characterized by ^{13}C NMR spectroscopy (**Figure 5.11 – 5.15**). Nomenclature according to Usami and Takayama⁸ for isolated branches was used in this work (**Figure 5.16**).

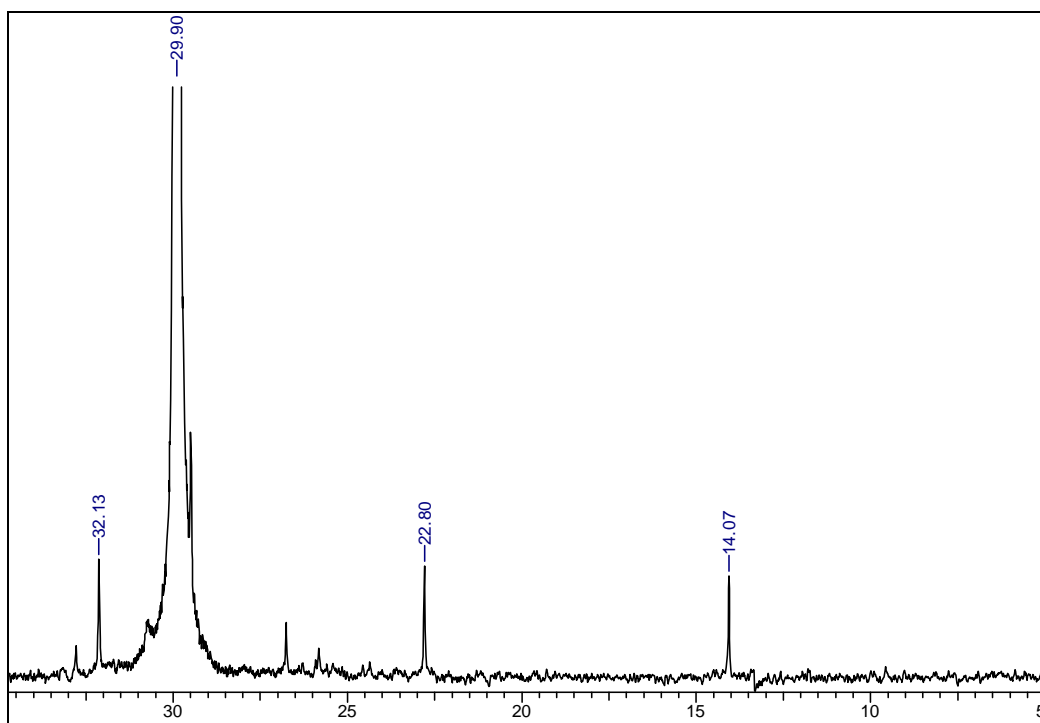


Figure 5.11 Quantitative ^{13}C NMR spectrum (in $\text{C}_2\text{D}_2\text{Cl}_4$) of Fraction A obtained from **3b**/MAO at 25°C

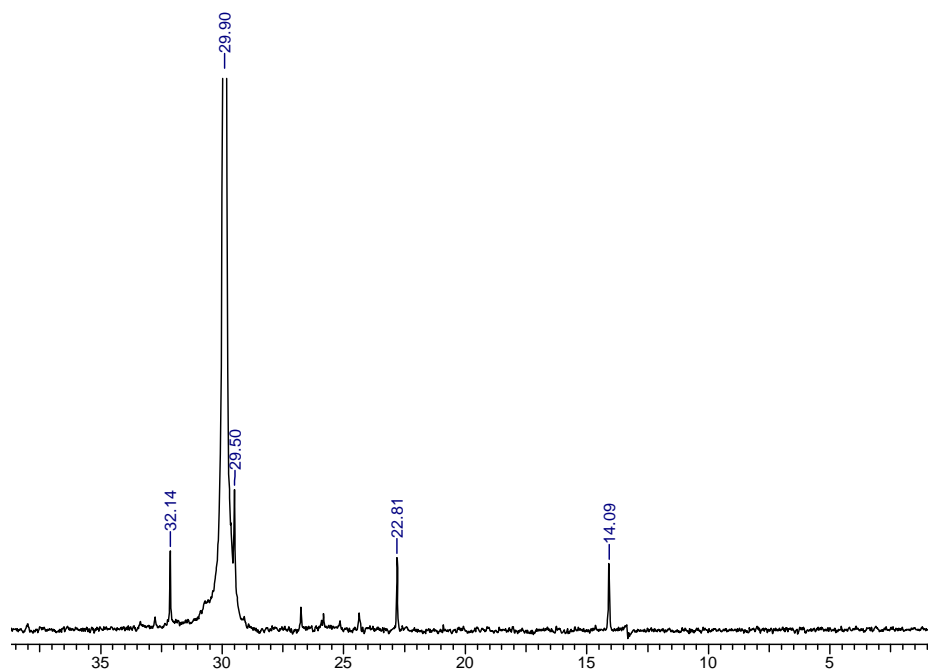


Figure 5.12 Quantitative ^{13}C NMR spectrum (in $\text{C}_2\text{D}_2\text{Cl}_4$) of Fraction A obtained from 3b/MAO at 40°C

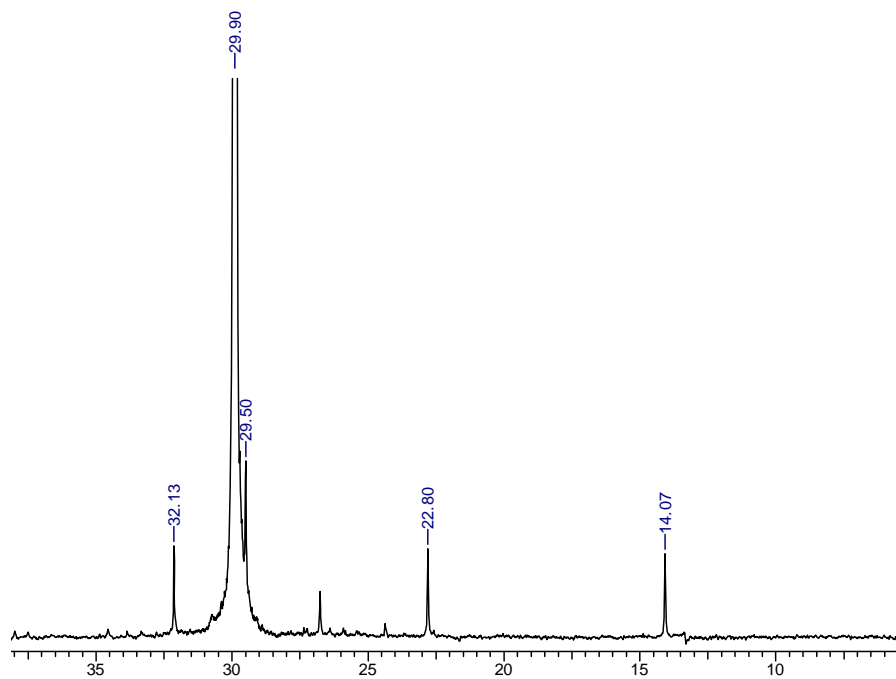


Figure 5.13 Quantitative ^{13}C NMR spectrum (in $\text{C}_2\text{D}_2\text{Cl}_4$) of Fraction A obtained from 3b/MAO at 60°C

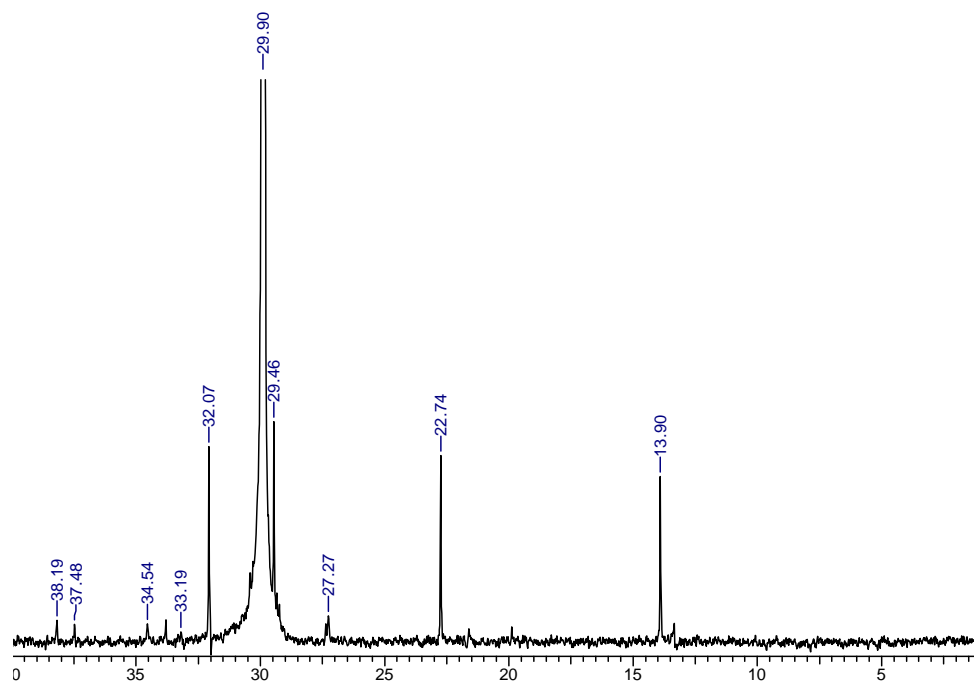


Figure 5.14 Quantitative ^{13}C NMR spectrum ($\text{C}_6\text{H}_4\text{Cl}_2/\text{C}_6\text{D}_6$) of Fraction A obtained from 3b/MAO at 80°C

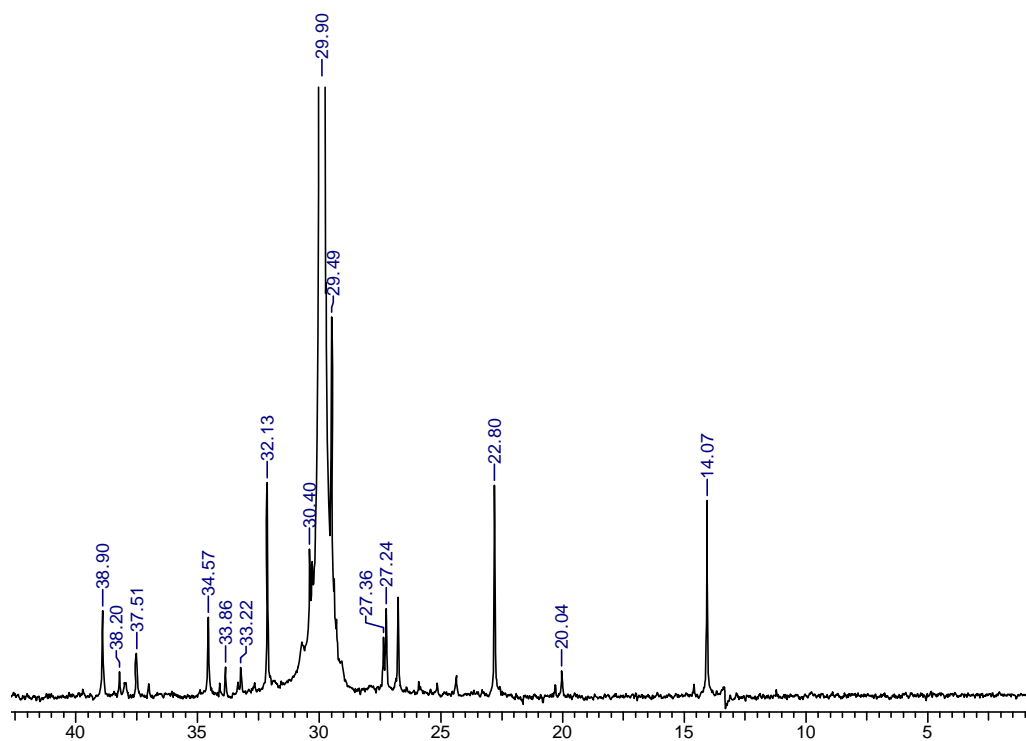


Figure 5.15 Quantitative ^{13}C NMR spectrum (in $\text{C}_2\text{D}_2\text{Cl}_4$) of Fraction A obtained from 3b/MAO at 100°C

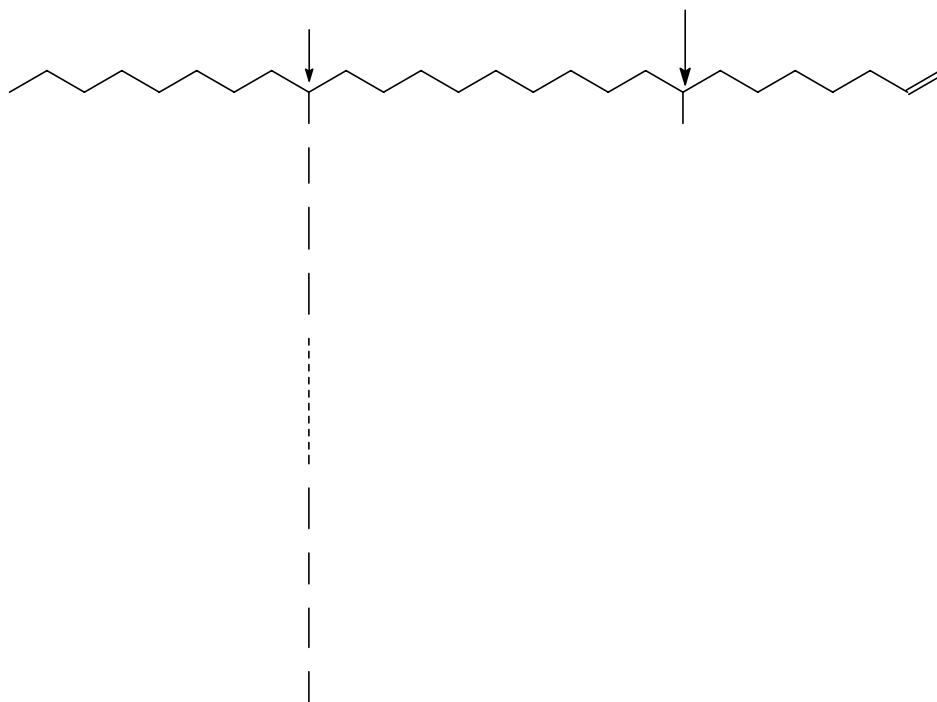


Figure 5.16 Nomenclature for branched poly(ethylene)s (according to ref.8)

Table 5.8 ¹³C Chemical Shifts and Assignments for branched poly(ethylene)s

Peak No.	Chemical shift exptl(ppm) in		Assignment
	1,1,2,2-tetrachloroethane-d ₂	1,2-dichlorobenzene/benzene-d ₆	
1	14.07	13.90	1Bn + 1s
2	20.04	19.87	1B1
3	22.80	22.74	2Bn + 2s
4	26.82		Unassigned
5	27.25	27.27	βBn
6	27.36	27.42	βB ₁
7	29.90	29.90	δδCH ₂ (main chain)
8	30.40		γB ₁
9	32.13	32.07	3Bn + 3s
10	33.22	33.19	brB ₁
11	33.92		CH ₂ -CH=CH ₂
12	34.57	34.54	αBn, nBn
13	37.47	37.48	αB1
14	38.19	38.19	brBn, brB1
15	38.90		unassigned
16	114.4	114.4	CH=CH ₂
17	139.5	139.5	CH=CH ₂

^{13}C NMR spectra of **Fraction A** obtained at 25, 40 and 60°C showed peaks only at 14.07, 22.80, 32.13 and 29.90 ppm corresponding to 1s, 2s, 3s and main chain carbons respectively. There are no peaks due to branched carbon atom at 38.19 ppm. Absence of peaks at 114.4 and 139.5 ppm corresponding to unsaturation indicates that the polymer chains contain predominantly saturated end groups.

Poly(ethylene)s prepared at 80 and 100°C exhibit peak at 38.19 ppm indicating the presence of branching. Moreover peaks at 14.07, 22.80, 32.13, 29.50, 34.57, 27.25, 30.48 are characteristic of long chain branching (more than six carbons).

^{13}C NMR spectrum of **Fraction A** obtained at 100°C showed, in addition to the long chain branches, signals at 20.04, 30.40, and 37.47 ppm. These peaks may be assigned to the presence of methyl pendants in the polymer.

Amount of long chain branching was calculated with respect to the signal at 34.57 ppm since the peak at 14.07 ppm (corresponding to methyl resonance) includes contribution also from saturated chain ends. Signal at 20.04 ppm is due to exclusively to a methyl branch and hence amount of methyl branches was calculated with respect to this signal.

Amount of branching in these poly(ethylene) samples was calculated by the following method:

No. of methyl branches, N_M = Integral value of the peak at 20.04 ppm

No. of long chain branches, N_L = Integral value of the peak at 34.57 ppm

Percentage of methyl branches with respect to total branching = $N_M / (N_M + N_L) \times 100$

Percentage of long chain branches with respect to total branching = $N_L / (N_M + N_L) \times 100$

Degree of branching was calculated by dividing the integral value of area for a single branch point by the total integral value of area for all the peaks and multiplying by 1000.

The results are summarized in **Table 5.9**.

Table 5.9 Nature of branching and branching distribution of Fraction A obtained using 3b/MAO

Temp.	Total branching/1000 C	Branching with respect to total	
		Methyl (%)	Long chain (%)
25	0	0	0
40	0	0	0
60	0	0	0
80	1.4	0	100
100	2.6	60	40

5.3.2.3.3 Characterization of Fractions B and C by ^1H and ^{13}C NMR spectroscopy

^1H and ^{13}C NMR of **Fractions B** and **C** showed the presence of linear α -olefins along with long chain alkanes (**Figure 5.17 and 5.18, Table 5.10**).

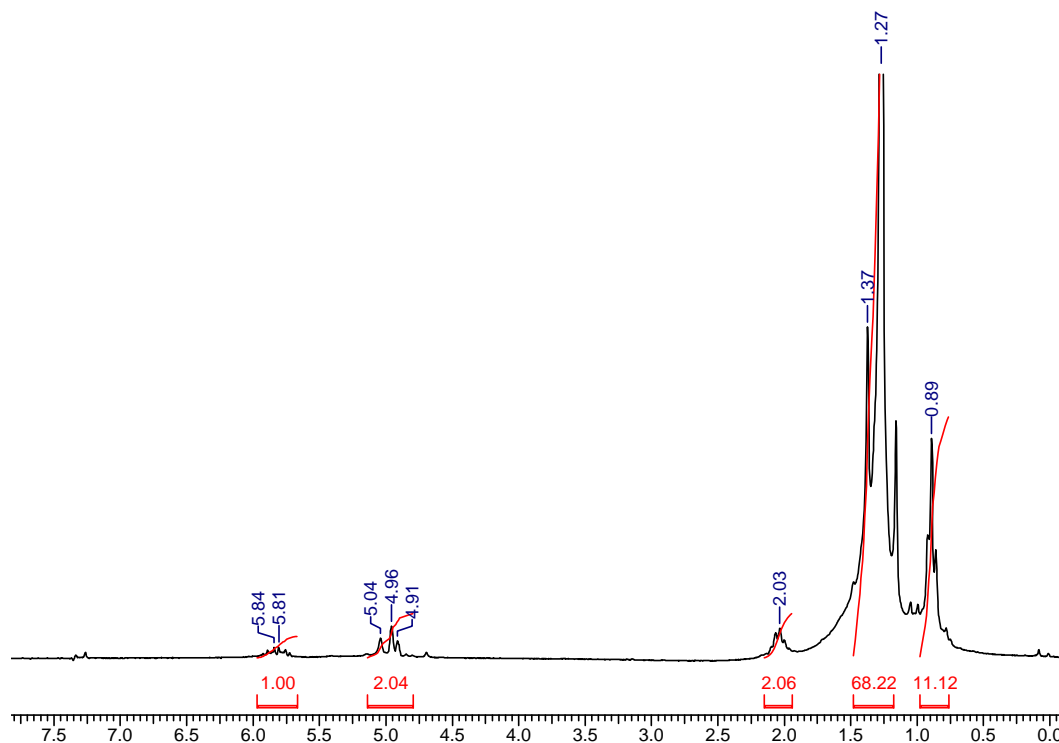


Figure 5.17 ^1H NMR spectrum (in CDCl_3 , 200 MHz) of Fraction B obtained by 3b/MAO at 100°C

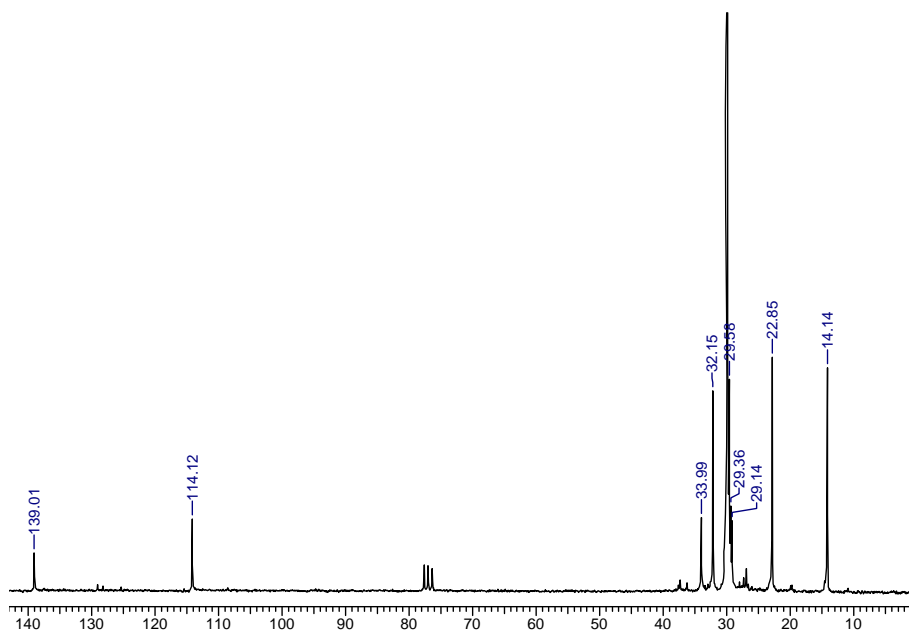


Figure 5.18 ^{13}C NMR spectrum (in CDCl_3 , 50 MHz) of Fraction B obtained by 3b/MAO at 100°C

Table 5.10 ^1H NMR chemical shifts and their assignments for Fractions B and C

Peak No.	Chemical shift (ppm)	Assignments
1	0.89	$-\text{CH}_3$
2	1.27-1.37	$-(\text{CH}_2)_n$
3	2.04	$-\text{CH}_2-\text{CH}=\text{CH}_2$
4	4.91-5.06	$-\text{CH}_2=\text{CH}$
5	5.70-5.78	$-\text{CH}_2=\text{CH}-$

Relative percentage of alkanes with respect to α -olefins was calculated by using the following relationship⁹:

Intensity corresponding to one proton of α -olefin, $I_{\text{H } \alpha\text{-olefin}} = (I_3/2 + I_4/2 + I_5)/3$

Intensity corresponding to one proton of alkane, $I_{\text{H alkane}} = (I_1 - 3 I_{\text{H } \alpha\text{-olefin}})/6$

Where I corresponds to the intensity of the peak and the subscript refers to the peak number in **Table 5.10**.

$$\% \text{ of alkane} = I_{\text{H alkane}} / (I_{\text{H alkane}} + I_{\text{H } \alpha\text{-olefin}}) \times 100$$

Number average molecular weight (M_n) determination from ^1H NMR

The integral corresponding to total protons is given by

$$I_{\text{Total H}} = I_2 + 8 I_{\text{H } \alpha\text{-olefin}} + 6 I_{\text{H alkane}}$$

I_2 is the integral that corresponds to the total methylene protons of the α -olefin and the alkane.

$$\text{Total number of protons in the oligomer} = I_{\text{Total H}} / (I_{\text{H } \alpha\text{-olefin}} + I_{\text{H alkane}})$$

M_n can be determined from the product of the number of CH_2 present and the mass of CH_2 (14 g). The number of methylene units can be obtained by dividing the total number of protons by 2.

$$M_n \text{ of oligomer} = (I_{\text{Total H}} / I_{\text{H } \alpha\text{-olefin}} + I_{\text{H alkane}}) / 2 \times 14$$

In summary, **Fractions B and C** are low molecular weight oligomers (DP ~10), comprising a mixture of n-alkanes and α -olefins. As the temperature increases, the content of α -olefins in the mixture also increases (**Table 5.11**). There are no peaks corresponding to branched carbon in the ^{13}C NMR spectrum indicating that the oligomers are linear in nature. Presence of peaks at 4.91-5.04 ppm and 5.81-5.84 ppm in ^1H NMR spectra also confirms the presence of vinyl end groups in these oligomers.

Table 5.11 Characterization of Fractions B and C

Tp ($^{\circ}\text{C}$)	% alkanes		Mn	
	Fraction B	Fraction C	Fraction B	Fraction C
60	76	78	320	300
80	69	61	310	250
100	50	57	280	200

5.3.2.4. Copolymerization of ethylene with higher α -olefins

Ethylene was copolymerized with hexene-1 and octene-1 using **3b**/MAO. A decrease in catalyst activity was observed in presence of added comonomers (**Table 5.12**). ^{13}C NMR spectrum of ethylene/hexene-1 copolymer (**Figure 5.19**) shows all the peaks found in the homopolymer (**Figure 5.12**) and an additional peak at 23.32 ppm that is characteristic of

2B₄ carbon of butyl branch. Hexene-1 incorporation in the copolymer was calculated to be 0.67 mol%.

Table 5.12 Polymerization of ethylene with higher α -olefins using 3b/MAO ^a

Entry	α -olefin	[α -olefin] mol/L	Yield (g)	Activity g polymer mmol ⁻¹ Zr.h ⁻¹	T _m (°C)
1	-	-	3.7	210	121
2	Hexene-1	1.60	1.6	91	120
3	Octene-1	1.13	1.8	102	119

^a Toluene (30 mL); Zr: 17.6 μ mol; Al/Zr:2000; P_{C₂H₄}: 5 bar; T_p: 80°C; time: 1h

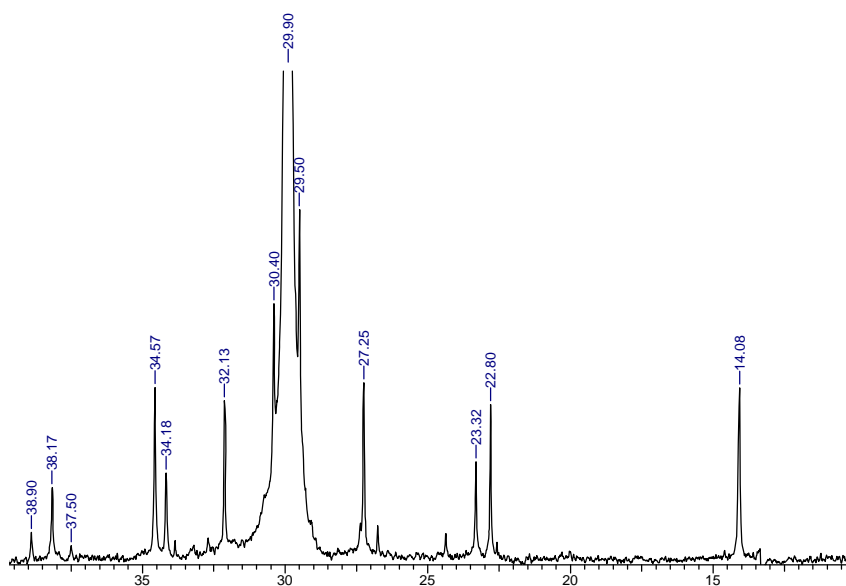


Figure 5.19 ¹³C NMR spectrum (in C₂D₂Cl₄) of ethylene/hexene-1 copolymer

¹³C NMR spectrum of ethylene/octene-1 copolymer (**Figure 5.20**) does not provide unequivocal evidence of a hexyl branch since it is difficult to distinguish these from the long chain branches found in the corresponding homopolymer.

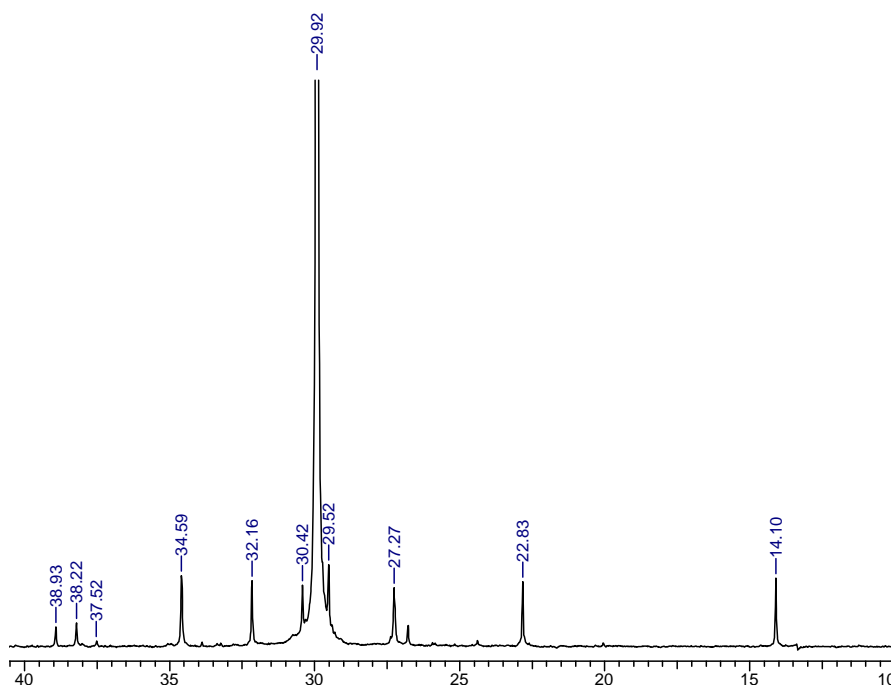


Figure 5.20 ^{13}C NMR spectrum (in $\text{C}_2\text{D}_2\text{Cl}_4$) of ethylene/octene-1 copolymer

In summary, following observations are significant in the context of the present study

- **3a-3c** when activated with MAO were found to be inactive for polymerization of ethylene at 25°C and 1 bar pressure.
- At 5 bar ethylene pressure, **3a-3c** exhibited moderate polymerization activity which decreased in the order **3b** > **3a** > **3c**
- **3a**/MAO produced poly(ethylene)s with exceptionally high melting points (142°C) whereas for **3b**, melting points were in the range 121-134°C.
- Catalyst activity of **3b**/MAO was found to increase in presence of added TMA. When TMA-pretreated **3b** was used for polymerization, even higher activity was observed.
- Complex **3b**/MAO polymerized ethylene to linear poly(ethylene)s at 25 and 40°C and no soluble oligomers were produced at these temperatures.
- At temperatures above 60°C, **3b**/MAO resulted in a mixture of insoluble solid polymer (**Fraction A**) and soluble oligomers (**Fractions B and C**).

- ^{13}C NMR spectra of **Fraction A** obtained at 25, 40 and 60°C showed only peaks corresponding to the saturated chain ends and the main chain carbon. Peaks corresponding to branched carbons were absent at these temperatures. Presence of peaks due to long chain branches (>6 carbons) was observed in the case of **Fraction A** produced at 80 and 100°C.
- **Fraction A** obtained at 100°C showed peaks at 20.04, 30.40 and 37.47 ppm in addition to the peaks due to long chain branches. These peaks correspond to methyl branches in the polymer
- NMR spectra of **Fractions B and C** indicate them to be a mixture of linear α -olefins and long chain alkanes
- In all cases **Fractions B and C** were rich in long chain alkanes (50-78 %). Linear nature of the oligomers was confirmed by the absence of peak at 38.19 ppm due to branched carbon in ^{13}C NMR spectrum.
- Peaks at 4.91-5.06 ppm and 5.70-5.78 ppm in ^1H NMR spectrum indicate the presence of vinyl end groups in the oligomers.
- Broad molecular weight distributions were observed for **Fraction A** at temperatures above 80°C
- Copolymerization of ethylene with hexene-1 using **3b**/MAO showed all the peaks of the homopolymer and an additional peak at 23.32 ppm characteristic of butyl branch.

Lower catalyst activity of hafnium complex **3c** when compared to **3a** and **3b** can be attributed to stronger Hf-C bond which slows down monomer insertion and chain propagation. Poor thermal stability of titanium species may be responsible for the observed lower activity of **3a** when compared to **3a** at higher temperatures.¹¹

Titanium complex **3a** produced poly(ethylene)s with exceptionally high melting point(142°C). Such high melting points (142.5°C) are also reported for poly(ethylene)s obtained from titanium complexes based on tetramethyl cyclopentadienyl phenolate ligand⁶. Certain half sandwich amido fluorenyl zirconium complexes¹⁰ also result in poly(ethylene)s with melting point of greater than 140°C. Crystalline nanofibers of linear

poly(ethylene)s with melting point of 140°C have been reported by extrusion polymerization using titanocene complex supported on mesoporous silica and MAO¹².

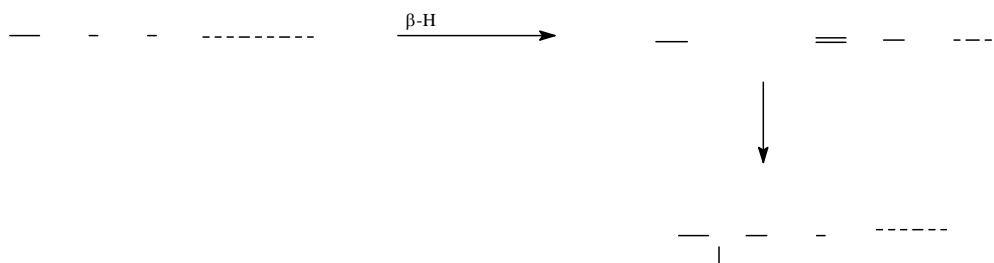
Increase in the catalyst activity of **3b**/MAO in presence of TMA can be attributed to the fact that TMA removes the coordinated THF molecules from the metal center via the formation of a TMA-THF complex. A similar type of complex formation has been reported in the literature¹³.

Formation of oligomers at temperatures higher than 60°C using **3b**/MAO implies enhanced rate of chain transfer reactions. These oligomers consist of a mixture of linear α -olefins and long chain alkanes that result from β -H transfer and chain transfer to aluminium respectively. The oligomers were rich in long chain alkanes (50-78 %) which implies that chain transfer to aluminium is dominant. As the temperature increased from 60 to 100°C, α -olefin content in the oligomers increased from 22 to 50 %. The rate of β -H transfer becomes competitive with chain transfer to aluminium at higher temperatures. Iron(II)bis(imino)pyridyl complex⁹ /MAO is also reported to oligomerize ethylene to a mixture of linear α -olefins and long chain alkanes.

Insoluble solid polymer (**Fraction A**) produced using **3b**/MAO at 80 and 100°C showed peaks corresponding to long chain branches (> 6 carbon atoms). This may be due to the fact that more open nature of **3b** allows easier reincorporation of α -olefins (formed by β -H transfer) into the growing polymer chains. Such a mechanism for long chain branching has been reported for constrained geometry catalysts¹⁴. Certain bis(phenolate) titanium complexes are also reported to polymerize ethylene to branched poly(ethylene)s consisting of ethyl, butyl and long chain branches¹⁵.

¹³C NMR spectrum of poly(ethylene)s produced at 100°C showed peaks due to long chain branching, and additional peaks due to isolated methyl branches. These methyl branches may result from β -H elimination followed by 2,1-insertion of the α -olefin into the [Zr]-H species (**Scheme 5.2**). Appearance of these signals only at higher temperatures implies that

the rate of 2,1-insertion increases with increase in polymerization temperature. Similar observation has been reported for a monocyclopentadienyl tribenzyloxy titanium complex that produced long chain branched poly(ethylene)s at lower temperatures but resulted in exclusively methyl branched polymer at 60°C¹⁶.



Scheme 5.2 Mechanism for the formation of methyl branches

Broad molecular weight distributions for poly(ethylene)s produced by **3b**/MAO may be due to chain transfer to aluminum as evident from the presence of saturated chain ends in the polymer.

5.4 Conclusions

ansa- η^5 -monofluorenyl Group 4 metal complexes (**3a-3c**) exhibited moderate activity for the polymerization of ethylene at 5 bar pressure. Zirconium complex **3b** showed better activity than the titanium (**3a**) and hafnium (**3c**) analogues. The complexes were active even at elevated temperature as high as 100°C that may be due to the thermal stability imparted by the metal-oxygen bond. Complex **3b**/MAO produced linear poly(ethylene)s with saturated chain ends at temperatures of 25-60°C. However at 80 and 100°C, a mixture of insoluble solid polymer and soluble liquid oligomers was obtained. The solid polymer consists of exclusively long chain branches (> 6 carbons) at 80°C whereas at 100°C, methyl branches were observed in addition to the long chain branches. The methyl branches may result from β -H elimination followed by 2,1-insertion of the α -olefin into the [Zr]-H species. The soluble oligomer was found to be a mixture of linear α -olefins and long chain alkanes. Long chain branches may be formed as a result of β -H transfer reaction followed by reincorporation of the resulting macromonomers into the growing polymer

chains due to the open nature of the complex. Presence of long chain alkanes in the soluble fractions can be attributed to chain transfer to aluminium. Molecular weight distributions of the poly(ethylene)s were broad presumably due to chain transfer to aluminium. In conclusion, complex **3b**/MAO results in a mixture of long chain branched poly(ethylene)s, linear α -olefins and long chain alkanes.

5.5. References

- 1 Kaminsky, W.; Arndt, M. *Adv. Polym. Sci.* **1997**, *127*, 144
- 2 Bochmann, M. *J. Chem. Soc., Dalton Trans.* **1996**, 255
- 3 Brintzinger, H. H.; Fischer, D.; Mulhaupt, R.; Rieger, B.; Waymouth, R. M. *Angew. Chem. Int. Ed. Engl.* **1995**, *34*, 1143
- 4 Marks, T. J. *Acc. Chem. Res.* **1992**, *25*, 57
- 5 Rieger, B. *J. Organomet. Chem.* **1991**, *420*, C17
- 6 Chen, Y. -X.; Fu, P. -F.; Stern, C. L.; Marks, T. J. *Organometallics* **1997**, *16*, 5958
- 7 Gielens, E. E. C. G.; Tiesnitsch, J. Y.; Hessen, B.; Teuben, J. H. *Organometallics* **1998**, *17*, 1652
- 8 Usami, T.; Takayama, S. *Macromolecules* **1984**, *17*, 1756
- 9 Galland, G. B.; Quijada, R.; Rojas, R.; Bazan, G. C.; Komon, Z. J. A. *Macromolecules* **2002**, *35*, 339
- 10 Alt, H. G.; Reb, A. *J. Mol. Catal. A. Chem.* **2001**, *175*, 43
- 11 (a) Alt, H. G.; Koppl, A. *Chem. Rev.* **2000**, *100*, 1205 (b) Resconi, L.; Cavallo, L.; Fait, A.; Piemontesi, F. *Chem. Rev.* **2000**, *100*, 1253
- 12 Kageyama, K.; Tamazawa, J.; Aida, T. *Science*, **1999**, *285*, 2113
- 13 Hill, M. S.; Hitchcock, P. B. *Organometallics*, **2002**, *21*, 3258
- 14 Lai, S. Y.; Wilson, J. R.; Knight, G. W.; Stevens, J. C.; Chum, P. W. S. *US Patent* 5272236, **1993**
- 15 Capacchione, C.; Proto, A.; Okuda, J. *J. Polym. Sci. Part A. Polym. Chem.* **2004**, *42*, 2815
- 16 Zhu, F.; Fang, Y.; Chen, H.; Lin, S. *Macromolecules* **2000**, *33*, 5006

CHAPTER 6

POLYMERIZATION OF ETHYLENE USING AMIDO FUNCTIONALIZED HALF-SANDWICH COMPLEXES OF GROUP IV METALS

6.1. Introduction

Amido functionalized half-sandwich complexes have evoked increasing interest in academic and industrial research since they were first reported by Bercaw et al¹. Catalyst activity and polymer properties are strongly dependent on molecular structure of the catalyst. Sterically less demanding nature of amido functionalized half-sandwich complexes makes them excellent candidates for copolymerization of ethylene with other α -olefins²⁻³. There are many reports on amido functionalized cyclopentadienyl and indenyl based complexes as catalyst precursors for olefin polymerization⁴⁻¹¹. However reports on fluorenyl based complexes are relatively rare. Okuda et al¹² reported the synthesis and characterization of zirconium complex based on (t-butylamino) dimethyl (fluorenyl) silane. However the ability of this complex to catalyze olefin polymerization was not reported. Alt et al¹³ investigated ethylene polymerization behavior of various amido functionalized *ansa*-fluorenylidene half sandwich complexes of zirconium. All these complexes contain alkyl substituents on the amido nitrogen. However, there are no reports of fluorenyl amido complexes bearing aromatic substituents on the nitrogen.

This chapter discusses the synthesis, characterization and polymerization of ethylene using titanium and zirconium complexes based on [(2, 6-diisopropylphenylamido) (fluorenyl) diphenylsilane] and [(2, 6-dimethylphenylamido) (fluorenyl) diphenylsilane]. It was anticipated that the presence of an aromatic substituent on the amido nitrogen will modify the electronic and steric environment at the metal center. Thus, -I effect of aromatic group should make the metal centre more electron deficient, whereas, resonance effect should contribute towards enhanced electron density at the metal centre. Moreover, presence of bulky *ortho*-substituents may also subtly modify the steric environment around the metal center. Since the overall catalytic activities of these complexes are determined by a balance of steric and electronic factors, they may show interesting polymerization behavior.

6.2. Experimental

6.2.1. Materials

This is described in chapter 3, Section 3.2 and 3.3.

6.2.2. Synthesis of complexes 3a-3d

6.2.2.1 Synthesis of [(2,6-diisopropylphenylamido) (fluorenyl) diphenylsilane] titanium(IV) dichloride (3a)

6.2.2.1.1. Synthesis of [(2,6-diisopropylphenylamido) (fluorenyl) diphenylsilane] (2a)

Synthesis of 9-fluorenyl diphenyl chlorosilane

A 250 mL oven-dried Schlenk flask was cooled under vacuum and filled with argon. Fluorene (2.0 g, 12 mmol) was transferred to the flask and dissolved in dry diethyl ether (20 mL). The flask was then cooled to -20°C and a solution n-BuLi (4.8 mL of 2.5 M solution in hexane) in ether was added drop wise to it with stirring over a period of 45 min. The mixture was stirred at 30°C for 6 h. An orange-colored solution of fluorenyl lithium was obtained.

A 250 mL oven-dried Schlenk flask was cooled under vacuum and filled with argon. Dichlorodiphenyl silane (2.5 mL, 12 mmol) was added into the flask and dissolved in dry diethyl ether. The flask was cooled to -30°C and a solution of fluorenyl lithium (prepared above) in ether was added into it drop wise with stirring over a period of 45 min. The reaction mixture was stirred at 30°C for 12 h. The solvent was evaporated, dichloromethane added and the solution filtered to remove lithium chloride. Dichloromethane was evaporated to obtain a yellow solid.

¹H NMR(CDCl₃, 500 MHz): δ ppm 4.02 (s, 1H), 7.16-7.93 (m, 18 H)

Synthesis of (2, 6-diisopropylphenylamido) (9-fluorenyl) diphenylsilane

An oven-dried 250 mL Schlenk flask was cooled under vacuum and charged with argon. Dry distilled 2, 6-diisopropylaniline (3 mL, 15.9 mmol, 1 eqv) was transferred to the flask and dissolved in dry hexane and diethyl ether (1:1). The flask was cooled to -78°C and a solution of n-BuLi (6.4 mL, 15.9 mmol of 2.5 M solution in hexane) in diethyl ether was

added dropwise. The reaction mixture was stirred at -20°C for 30 min. A white solid was obtained. An ether solution of (9-fluorenyl)diphenylchlorosilane (6.09 g, 15.9 mmol, 1 eqv) was added dropwise over a period of 45 min. The reaction mixture was stirred at 30°C for 10 h. Solvents were removed under vacuum, and the residue was dissolved in dichloromethane and the solution was filtered through a celite bed to remove LiCl. Dichloromethane was removed under vacuum to obtain **2a** as a yellow solid. The solid was washed several times with n-hexane to yield a pale yellow solid. The solid was recrystallized from dichloromethane to afford pale yellow crystals. Yield: 6.3 g (75%)

Analysis for C₃₇H₃₇NSi

Calcd., % C 84.89 H 7.07 N 2.67

Found, % C 84.39 H 7.11 N 2.56

¹H NMR (CDCl₃, 200 MHz): δ ppm 7.85(d, 2 H), 7.49(d, 4 H), 7.30-7.44(m, 8 H), 7.1(t, 2 H), 6.84(s, 2 H), 6.79(s, 3 H), 4.36(s, 1 H), 2.70(septet, 2 H), 0.71(d, 12 H)

¹³C NMR (CDCl₃, 50 MHz): δ ppm 143.86, 141.07, 138.72, 135.78, 132.76, 129.82, 127.27, 125.92, 125.78, 124.90, 122.80, 122.10, 119.82, 43.81, 28.33, 23.33

6.2.2.1.2. Synthesis of **3a**

An oven-dried 250 mL Schlenk flask was dried under vacuum and filled with argon. **2a** (0.5 g, 0.96 mmol) was added to the flask and dissolved in dry THF. The flask was cooled to -78°C and n-BuLi (1.4 mL of 1.4 M solution in hexane, 1.92 mmol) was added dropwise. After the addition was complete, the reaction mixture was stirred at 30°C for 6 h. The flask was again cooled to -78°C and TiCl₄ (thf)₂ (0.32 g, 0.96 mmol) dissolved in THF was added dropwise. The reaction mixture was stirred at 30°C for 12 h. Solvents were removed under vacuum. The residue was dissolved in dichloromethane and filtered through a celite bed to remove LiCl. Dichloromethane was removed under vacuum to yield an orange-colored solid, which was washed with n-hexane and dried under vacuum. Yield: 0.45 g (74 %)

Analysis for C₃₇H₃₅NSiTiCl₂

Calcd., % C 69.46 H 5.48 N 2.19

Found, % C 68.89 H 5.89 N 2.06

¹H NMR (C₆D₆, 500 MHz): 6.82-7.80 (m, 21 H), 2.91(m, 2 H), 1.21 (12 H)

6.2.2.2. Synthesis of [(2,6-diisopropylphenylamido) (fluorenyl) diphenylsilane] zirconium (IV) dichloride (3b)

An oven-dried 250 mL Schlenk flask was dried under vacuum and filled with argon. **2a** (1.2 g, 2.29 mmol) was added into the flask and dissolved in dry diethylether. The flask was cooled to -78°C and n-BuLi (1.9 mL of 2.5 M solution in hexane, 4.58 mmol) was added dropwise. After the addition was complete, the reaction mixture was stirred at 30°C for 6 h. The flask was cooled to -78°C and $\text{ZrCl}_4(\text{thf})_2$ (0.863 g, 2.29 mmol) dissolved in THF was added dropwise. The reaction mixture was stirred at 30°C for 12 h. Solvents were removed under vacuum. The residue was dissolved in dichloromethane and filtered through a celite bed to remove LiCl. Dichloromethane was removed under vacuum to yield an orange-colored solid, which was washed with hexane and dried under vacuum. Yield: 1.3 g (83 %)

Analysis for $\text{C}_{37}\text{H}_{35}\text{NSiZrCl}_2$

Calcd., % C 64.98 H 5.12 N 2.05

Found., % C 65.39 H 5.49 N 1.87

^1H NMR (C_6D_6 , 500 MHz): δ ppm 6.82-7.80 (m, 21 H), 2.91(m, 2 H), 1.21 (d, 12 H)

6.2.2.3. Synthesis of [(2,6-dimethylphenylamido) (9-fluorenyl) diphenylsilane] titanium (IV) dichloride (3c)

6.2.2.3.1 Synthesis of [(2,6-dimethylamido) (fluorenyl) diphenylsilane] (2b)

An oven-dried 250 mL Schlenk flask was cooled under vacuum and charged with argon. Dry distilled 2,6-dimethylaniline (1.6 mL, 13.1 mmol, 1 eqv)) was transferred to the flask and dissolved in dry hexane and diethyl ether(1:1). The flask was cooled to -78°C and a solution of n-BuLi (5.2 mL, 13.1 mmol of 2.5 M solution in hexane) in diethyl ether was added dropwise. The reaction mixture was stirred at -20°C for 30 min. A white solid was obtained. To this was added dropwise at -78°C a solution of (9-fluorenyl) diphenylchlorosilane (5.0 g, 13.1 mmol, 1 eqv) in diethyl ether over a period of 45 min. The reaction mixture was stirred at 30°C for 10 h. Solvents were removed under vacuum, dichloromethane was added and the solution filtered through a celite bed to remove LiCl. Dichloromethane was removed under vacuum to obtain an yellow solid which was washed

several times with n-hexane to yield **2b** as a pale yellow solid. The solid was recrystallized from dichloromethane to afford pale yellow crystals. Yield: 4.0 g (65%)

Analysis for C₃₃H₂₉NSi

Calcd., % C 84.75 H 6.21 N 3.00

Found, % C 84.48 H 6.15 N 2.87

¹H NMR (CDCl₃, 200 MHz): δ ppm 1.66 (s, 6 H); 4.36 (s, 1 H); 6.55-7.81 (m, 21 H)

¹³C NMR (CDCl₃, 50 MHz) δ ppm 20.08, 43.74, 119.82, 120.54, 125.01, 125.79, 127.54, 128.38, 128.92, 129.89, 133.82, 135.49, 141.05, 142.25, 143.76

6.2.2.3.2. Synthesis of **3c**

An oven-dried 250 mL Schlenk flask was dried under vacuum and filled with argon. **2b** (0.40 g, 0.86 mmol) was transferred into the flask and dissolved in dry diethylether. The flask was cooled to -78°C and n-BuLi (0.7 mL of 2.5 M solution in hexane, 1.72 mmol) was added dropwise. After the addition was complete, the reaction mixture was stirred at 30°C for 6 h. The flask was cooled to -78°C and TiCl₄ (thf)₂ (0.286 g, 0.86 mmol) dissolved in THF was added dropwise. The reaction mixture was stirred at 30°C for 12 h. Solvents were removed under vacuum, the residue dissolved in dichloromethane and filtered through a celite bed to remove LiCl. Dichloromethane was removed under vacuum to yield an orange-colored solid, which was washed with hexane and dried under vacuum. Yield: 0.36 g (70 %)

Analysis for C₃₃H₂₇NSiTiCl₂

Calcd., % C 67.90 H 4.63 N 2.40

Found, % C 67.39 H 4.89 N 2.06

¹H NMR (C₆D₆, 500 MHz) δ ppm 1.8 (6 H), 6.7-7.8 (21H, Ar)

6.2.2.4. Synthesis of [(2,6-dimethylphenylamido) (fluorenyl) diphenylsilane] zirconium(IV) dichloride (**3d**)

An oven-dried 250 mL Schlenk flask was dried under vacuum and filled with argon. Compound **2b** (1.0 g, 2.14 mmol) was transferred into the flask and dissolved in dry diethylether. The flask was cooled to -78°C and n-BuLi (1.7 mL of 2.5 M solution in hexane, 4.28 mmol) was added dropwise. After the addition was complete, the reaction

mixture was stirred at 30°C for 6 h. The flask was cooled to -78°C and ZrCl₄ (thf)₂ (0.807 g, 2.14 mmol) dissolved in THF was added dropwise. The reaction mixture was stirred at 30°C for 12 h. Solvents were removed under vacuum, the residue dissolved in dichloromethane and filtered through a celite bed to remove LiCl. Dichloromethane was removed under vacuum to yield an orange-colored solid, which was washed with hexane and dried under vacuum. Yield: 1.0 g (75%)

Analysis for C₃₃H₂₇NSiZrCl₂

Calcd., % C 63.13 H 4.30 N 2.23

Found, % C 62.88 H 4.55 N 1.87

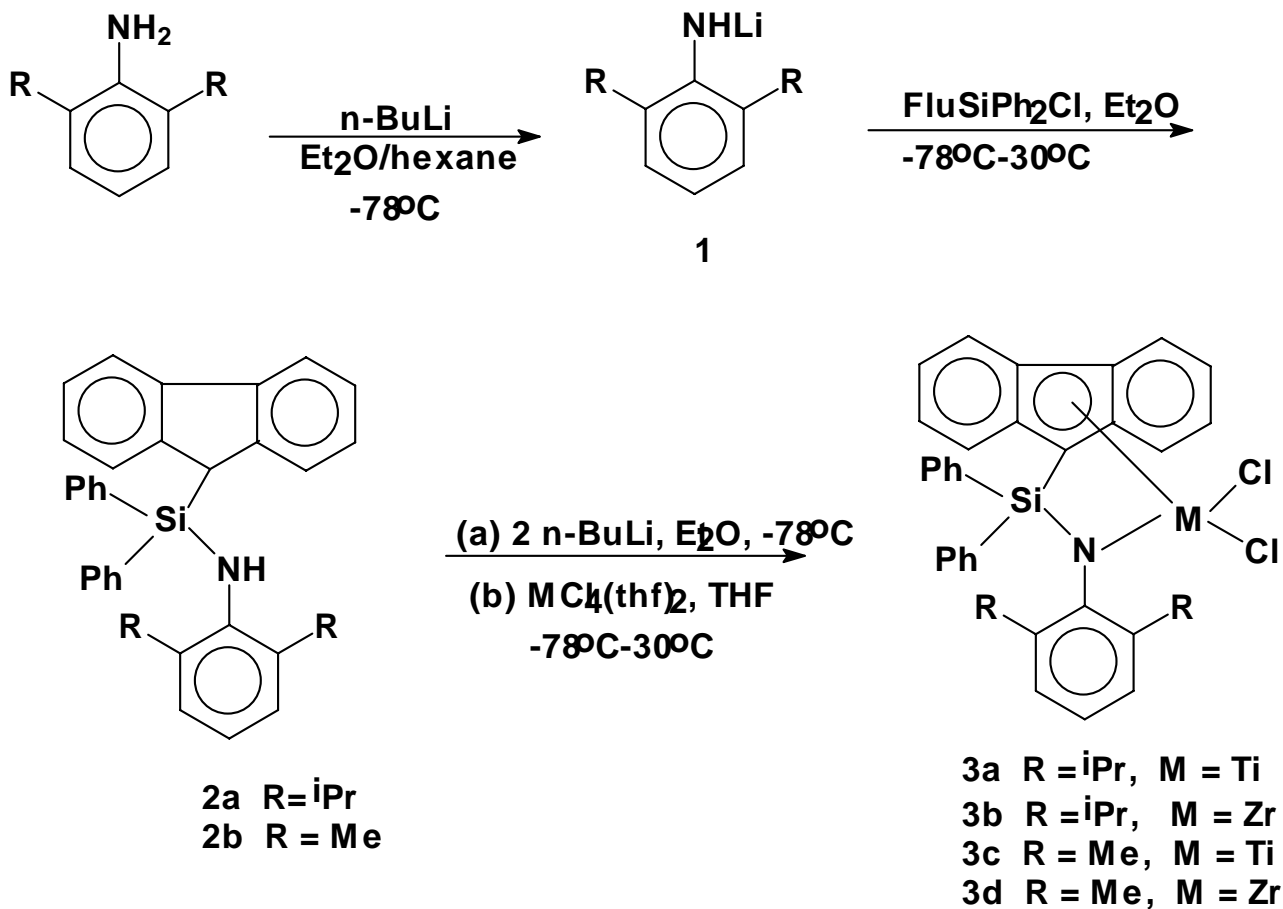
¹H NMR (C₆D₆, 500 MHz) δ ppm 1.8 (6 H), 6.7-7.8 (21H, Ar)

6.3. Results and Discussion

6.3.1. Synthesis and characterization of ligands and complexes

Synthetic methods for preparation of the ligands and complexes is shown in **Scheme 6.1**.

Compounds **2a** and **2b** were prepared by a two step procedure. In the first step, the dialkyl aniline was lithiated at -78°C to avoid abstraction of both the protons of the primary amine. The lithium salt was then reacted with 9-fluorenyl diphenyl chlorosilane, which in turn, was prepared by reaction of fluorenyl lithium with dichlorodiphenylsilane. **2a** and **2b** were obtained as pale yellow solids in fairly good yields. Single crystals of **2a** and **2b** suitable for X-ray diffraction studies were grown by slow evaporation of dichloromethane solution.



Scheme 6.1 Synthesis of ligands(2a-2b) and metal complexes 3a-3d

Compounds **2a** and **2b** were characterized by elemental analysis, ¹H and ¹³C NMR spectroscopy. NMR spectra, shown in **Figures 6.1-6.4**, are in agreement with the proposed structure.

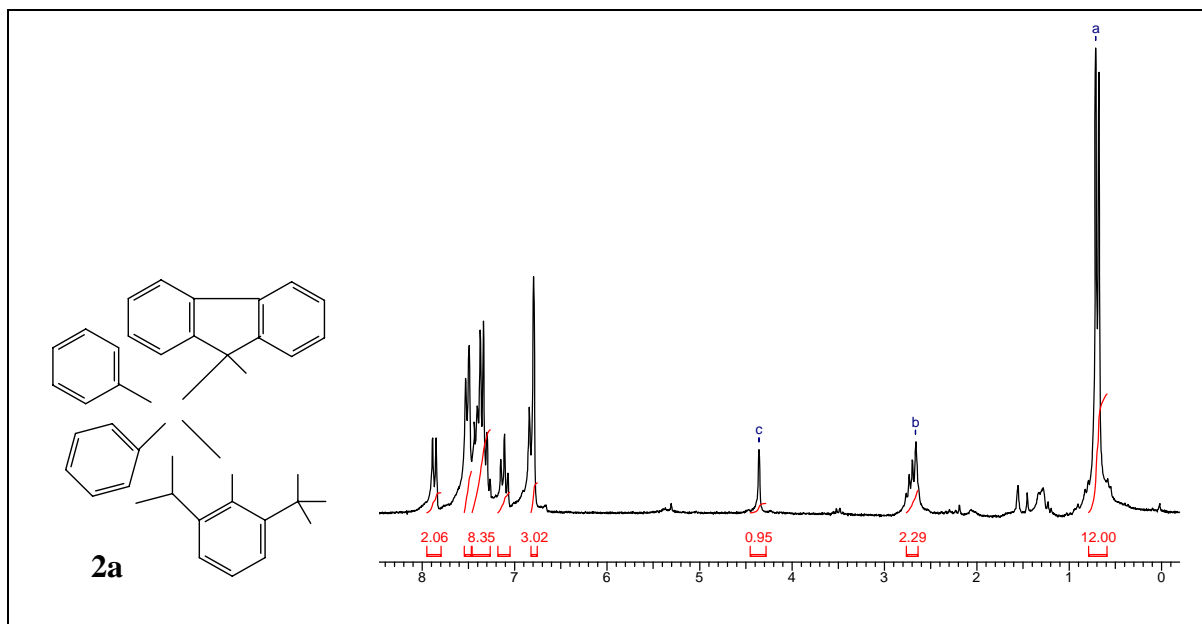


Figure 6.1 ^1H NMR spectrum (CDCl_3 , 200 MHz) of **2a**

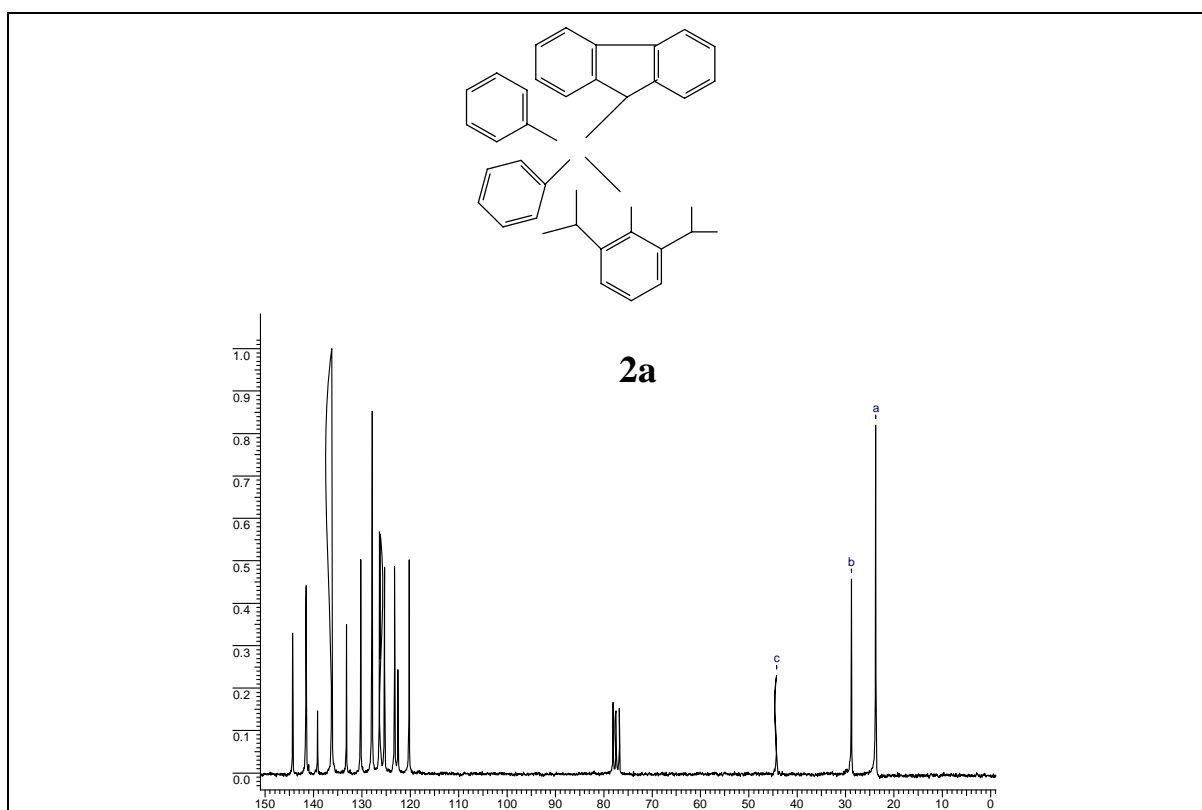


Figure 6.2 ^{13}C NMR spectrum (CDCl_3 , 50 MHz) of **2a**

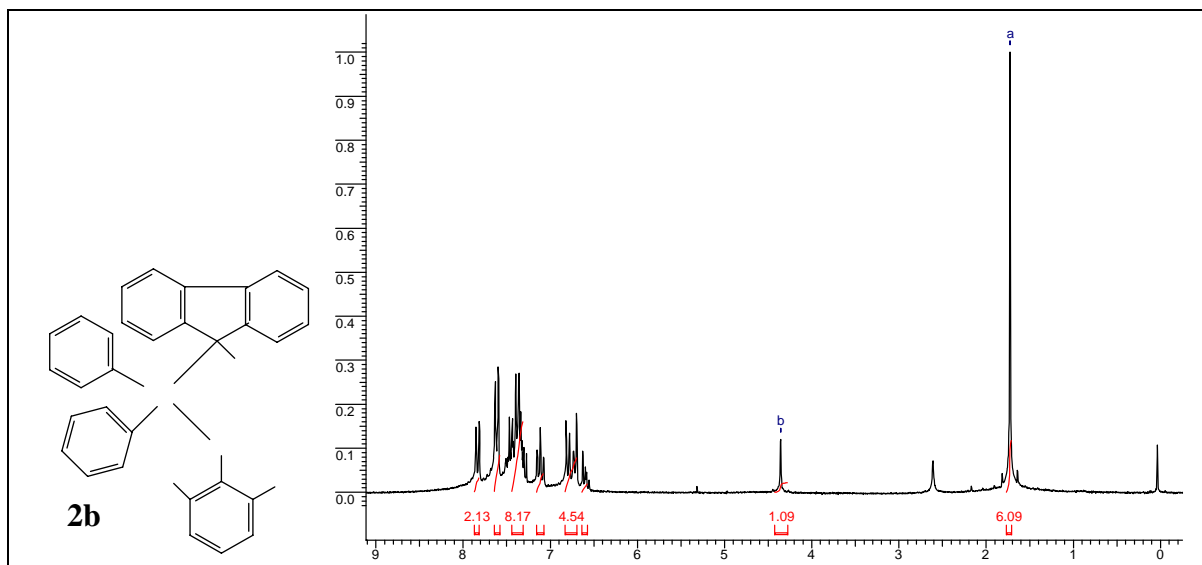


Figure 6.3 ^1H NMR spectrum (CDCl_3 , 200 MHz) of **2b**

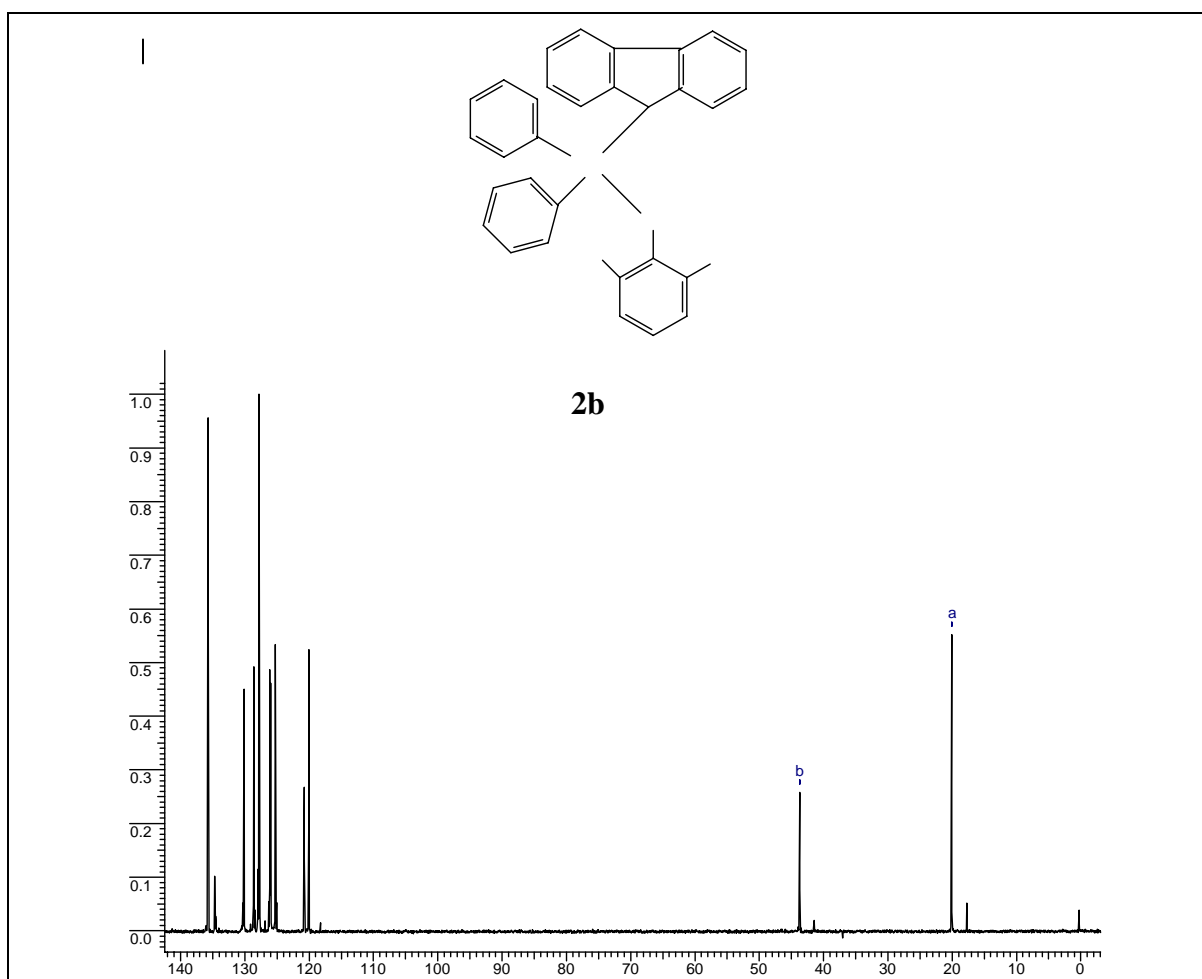


Figure 6.4 ^{13}C NMR spectrum (CDCl_3 , 50 MHz) of **2b**

Molecular structures of **2a** and **2b** are shown in **Figure 6.5** and **6.6** (X-ray crystal data and structure refinement are given in **Appendix B**). The diisopropyl substituted compound **2a** crystallized in the monoclinic space group $c2/c$, whereas, the dimethyl substituted compound **2b** crystallized in the orthorhombic space group $Pbca$. Selected bond lengths and bond angles are listed in **Table 6.1**.

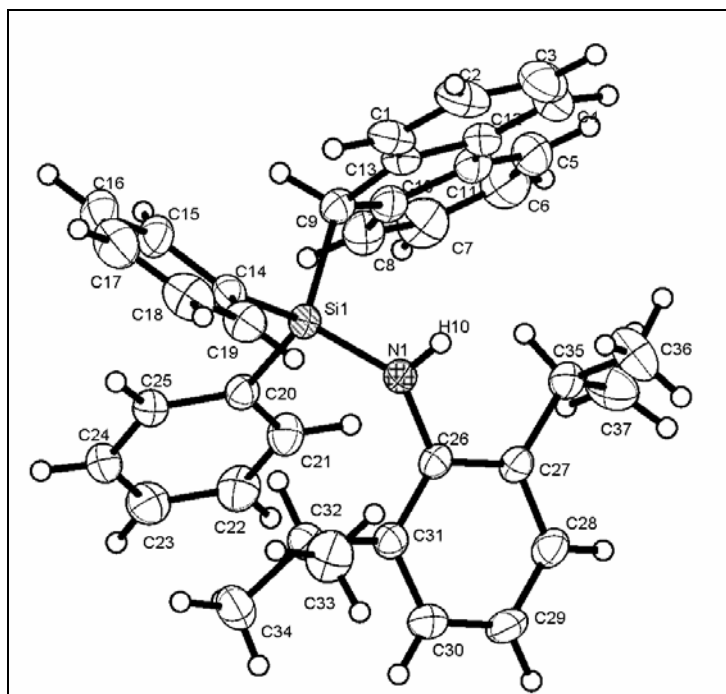


Figure 6.5 Molecular structure and numbering scheme for **2a**

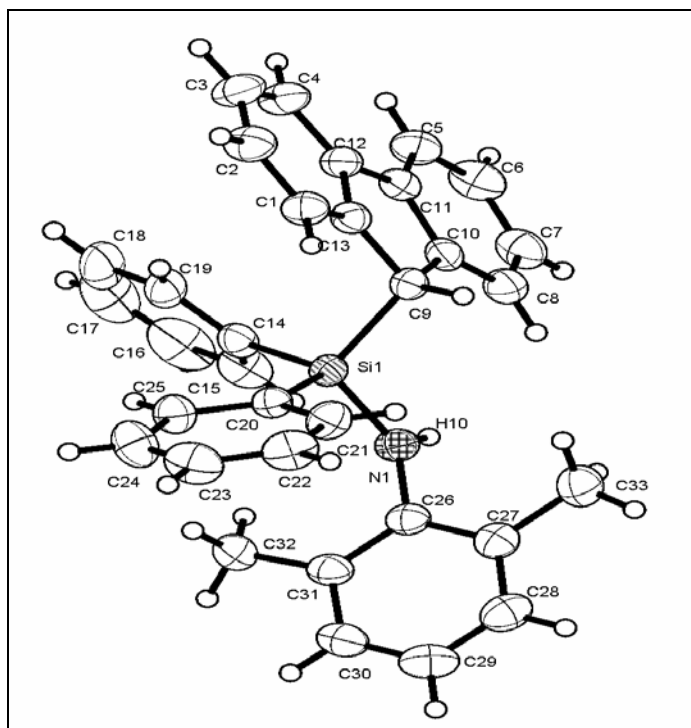


Figure 6.6 Molecular structure and numbering scheme for **2b**

Table 6.1 Selected bond lengths and bond angles for **2a** and **2b**

Bond lengths and bond angles	2a	2b
Si-N (Å)	1.714	1.718
Si-C(14) (Å)	1.887	1.861
Si-C(9) (Å)	1.908	1.906
N-H (Å)	0.81	0.86
C-N-Si (°)	130.66	128.10
C-N-H (°)	110.10	115.90
Si-N-H (°)	113.60	115.90
Σ N (°)	355.36	359.9

The sum of the bond angles around nitrogen (Σ N) is deviating from the expected value of 360°C in the case of **2a**. This may be due to the pyramidalization of nitrogen atom in **2a** whereas in **2b** the nitrogen atom is in the trigonal planar geometry.

Complexes **3a-3d** were synthesized by double lithiation of the respective ligands **2a** and **2b** with n-BuLi followed by reaction with $MCl_4(thf)_2$. Formation of complexes was confirmed by 1H NMR spectroscopy, wherein, peak **c** in the spectrum of **2a** disappears in the spectrum of **3a** and **3b** (Figure 6.1 and 6.7). Similarly peak **b** in the NMR spectrum of **2b** disappears after complexation in **3c** and **3d** (Figure 6.3 and 6.8).

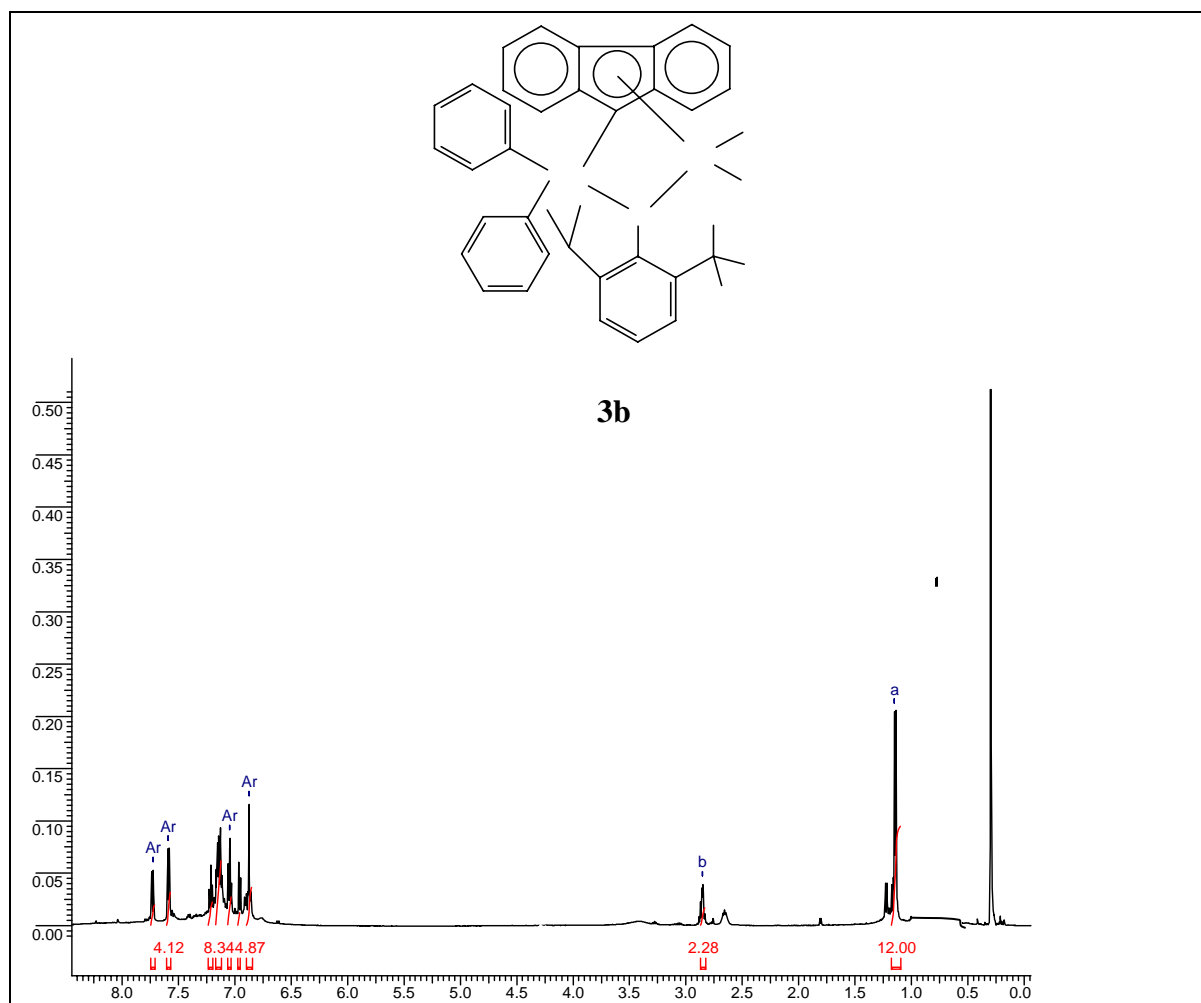


Figure 6.7 1H NMR spectrum (C_6D_6 , 500 MHz) of **3b**

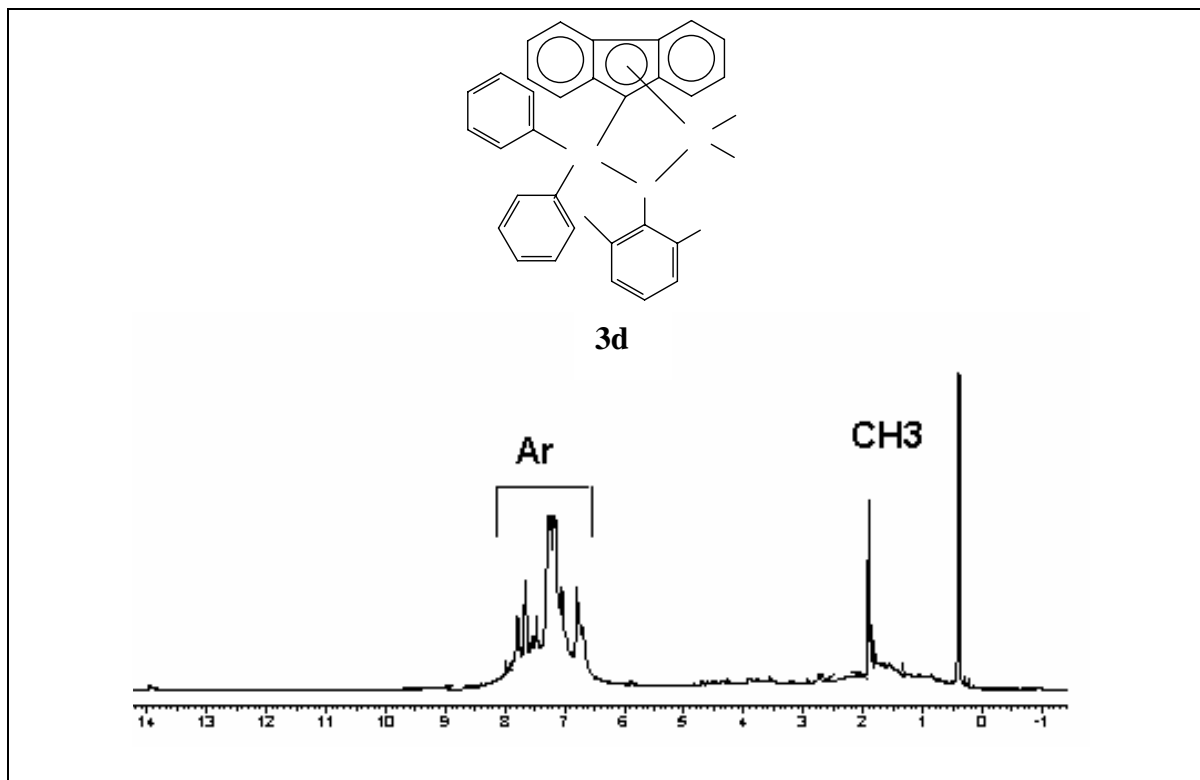


Figure 6.8 ^1H NMR spectrum (C_6D_6 , 500 MHz) of **3d**

6.3.2. Polymerization of ethylene using complexes **3a-3d**

Complexes **3a-3d** were investigated for polymerization of ethylene using MAO as the activator. The catalysts were not active at 1 bar ethylene pressure. Even at an ethylene pressure of 5 bar they exhibited only moderate activity. Polymers were characterized by DSC and intrinsic viscosity measurement. Attempts to analyze the polymers by GPC were not successful in view of the high viscosities of their solutions. Polymer solutions formed microgel and filtration of the solution was found to be difficult through a 0.45 micron size filter.

Zirconium complexes exhibited higher polymerization activity compared to the corresponding titanium complexes (**Table 6.2**). Zirconium complex **3d** with *ortho*-dimethyl substituents on the N-aryl ligand showed higher activity than **3b** with *ortho*-

diisopropyl substitution. Molecular weight of the obtained polymers was found to be fairly independent of the metal atom as well as the amido nitrogen substituent.

Table 6.2 Polymerization of ethylene using complexes 3a-3d: Effect of metal and amido nitrogen substituent ^a

Entry	Catalyst	Yield (g)	Activity g PE mmol ⁻¹ M.h ⁻¹	[η] dL/g	T _m (°C)
1	3a	0.20	13	5.68	132
2	3b	1.0	69	5.25	135
3	3c	0.15	8.7	5.34	135
4	3d	1.5	94	5.13	138

^a Toluene (30 mL), Cat: 15 μmol; Al/M:1000; T_p:30°C; P_{C₂H₄}: 5 bar; time: 1 h

Polymerization of ethylene was conducted using complex **3b**/MAO by varying the MAO concentration from 500-2000. Results are summarized in **Table 6.3**. Catalyst activity increased upon increasing the Al/Zr ratio from 500 to 1000. Intrinsic viscosity of the polymers decreased at higher MAO concentrations. Molecular weights (M_v) of the poly(ethylene)s obtained are estimated to exceed half a million.

Table 6.3 Polymerization of ethylene using complex 3b/MAO : Effect of Al/Zr ratio ^a

Entry	Al/Zr	Yield(g)	Activity g PE mmol ⁻¹ Zr.h ⁻¹	[η] dL/g	T _m (°C)
1	500	0.57	39	9.41	136
2	1000	1.0	69	6.35	138
3	2000	1.05	72	5.25	135

^a Toluene (30 mL), Cat: 15 μmol; T_p: 30°C; P_{C₂H₄}: 5 bar; time: 1 h

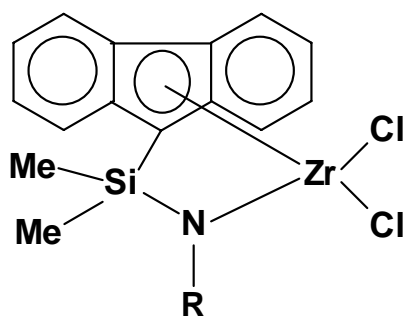
Polymerization of ethylene was performed using the complex **3b**/MAO in the temperature range 30-100°C. The catalyst exhibited maximum activity at 30°C and decreased thereafter (**Table 6.4**). Polymer molecular weights decreased with increase in temperature. Poly(ethylene)s obtained exhibited melting peaks in the range 130-138°C.

Table 6.4. Polymerization of ethylene using complex 3b/MAO : Effect of polymerization temperature ^a

Entry	Temp.	Yield (g)	Activity g PE mmol ⁻¹ Zr.h ⁻¹	[η] dL/g	Tm (°C)
1	30	1.00	69	9.41	138
2	60	0.66	45	2.37	136
3	80	0.68	47	2.12	134
4	100	0.75	51	1.78	130

^aToluene (30 mL), Cat: 15 μmol; Al/Zr:1000; P_{C₂H₄}: 5 bar; time: 1 h

It is interesting to compare the catalytic activity of **3b** with half-sandwich amido fluorenyl zirconium complexes bearing N-alkyl substituents (**4a-4c**) reported by Alt et al¹³ (**Table 6.5**). Catalyst activity of **3b** was lower than that of N-alkyl substituted complexes **4a-4c**. Molecular weight of poly(ethylene)s produced by **3b** was also lower than those of **4a-4c** at 60°C.



4a R = n-Bu

4b R = cyclopenty

4c R = t-Bu

Table 6.5 Comparison of 3b with N-alkyl substituted complexes

Entry	Complex	Temp (°C)	P _{C₂H₄} bar	Activity g PE mmol ⁻¹ Zr h ⁻¹	Mw	Tm (°C)
1	3b	60	5	45	131,000 ^a	136
2	4a	60	10	456	1,051,000	131
3	4b	60	10	182	1,023,000	137.3
4	4c	60	10	900	550,000	104.8, 123.4

^aviscosity average molecular weight

The following observations from this study are pertinent:

- Complexes **3a-3d** when activated with MAO were inactive for polymerization of ethylene at 1 bar pressure, but exhibited moderate activity at 5 bar pressure, resulting in linear poly(ethylene)s.
- Catalyst activity was found to increase in the order **3d>3b>3a>3c**. Zirconium complexes showed higher activities compared to the corresponding titanium complexes. Zirconium complex **3d** bearing *ortho*-methyl substituents exhibited marginally higher activity than **3b** with *ortho*-isopropyl substituents.
- Molecular weight of the polymers was found to be independent of metal and the nature of aromatic substituent present on the amido nitrogen.
- Catalyst activities of **3a-3d** were lower than similar half sandwich fluorenyl amido complexes (**4a-4c**) with N-alkyl substituents.

Lower activities of complexes **3a-3d** compared to N-alkyl substituted complexes (**4a-4c**) may be due to steric and electronic effects of the aromatic substituents. However, since free rotation is possible around the N-C bond, the aromatic group can assume a conformation that imparts less steric hindrance around the active center. Thus, steric factors are likely to be less important in determining catalyst activity. Resonance effect of the aromatic group can donate electrons towards the metal centre, thereby making it electron-rich. As the formation of a highly reactive species requires the presence of an electronically unsaturated metal centre, this may lead to a reduced catalyst activity.

Lower activities of titanium complexes than zirconium analogues may be attributed to the lower stability of the titanium species compared to zirconium.

6.4. Conclusions

Half sandwich titanium and zirconium complexes of fluorenyl amido ligands bearing aromatic substituents on the amido nitrogen were prepared. Polymerization of ethylene was carried out using the complexes along with MAO as activator. Complexes **3a-3d** exhibited moderate activity and resulted in high molecular weight linear poly (ethylene)s. Catalyst activities of these complexes were lower than the N-alkyl substituted complexes **4a-4c**, presumably due to resonance effect of the aromatic group present on the amido nitrogen.

6.5. References

- 1 Shapiro, P. J.; Bunel, E.; Schaefer, W. P.; Bercaw, J. E. *Organometallics* **1990**, *9*, 867
- 2 Pellecchia, C.; Proto, A.; Zambelli, A. *Macromolecules* **1992**, *25*, 4490
- 3 Aaltonen, P.; Seppala, J. *Eur. Polym. J.* **1991**, *10*, 310
- 4 Canich, J. A. M. (Exxon Chemical Patents Inc) *US patent 5026798*, **1991**
- 5 Stevens, J. C.; Timmers, F. J.; Wilson, D. R.; Schmidt, G. F.; Nickias, P. N.; Rosen, R. K.; Knight, G. W.; Lai, S. -Y. *EP 416815*, **1991**
- 6 Hughes, A. K.; Meetsma, A.; Teuben, J. H. *Organometallics* **1993**, *12*, 1996
- 7 Ready, T. E.; Day, R. O.; Chien, J. C. W.; Rausch, M. D. *Macromolecules* **1993**, *26*, 5822
- 8 van Leusen, D.; Beetstra, D. J.; Hessen, B.; Teuben, J. H. *Organometallics* **2000**, *19*, 2000
- 9 Galan – Fereres, M.; Koch, T.; Hey-Hawkins, E.; Eisen, M. S. *J. Organomet. Chem.* **1999**, 145
- 10 Alt, H. G.; Reb, A.; Milius, W.; Weis, A. *J. Organomet. Chem.* **2001**, 628, 2001
- 11 Musikabhumma, K.; Spaniol, T.P.; Okuda, J. *J. Mol. Catal. A. Chem.* **2003**, 192, 223
- 12 Okuda, J.; Schattenmann, F. J.; Wocadlo, S.; Massa, W. *Organometallics* **1995**, *14*, 789
- 13 (a) Alt, H. G.; Reb, A. *J. Mol. Catal. A. Chem.* **2001**, 175, 43 (b) Alt, H. G.; Föttinger, K.; Milius, W. *J. Organomet. Chem.* **1999**, 572, 21

CHAPTER 7
SUMMARY AND CONCLUSIONS

CHAPTER 7

SUMMARY AND CONCLUSIONS

There have been significant advances during the past decade in the area of non-metallocene olefin polymerization catalysts, based on both early and late transition metals. A variety of new ligands and complexes has been designed and studied that result in poly(olefin)s with diverse structures and properties. Late transition metal catalysts enable synthesis of polymers with varying molecular weights and microstructures depending on the nature of ligands and conditions of polymerization. Living or quasi-living polymerization has been achieved using some of these catalyst systems, thus opening up new opportunities to prepare block and graft copolymers. Development of single component catalyst systems has provided opportunities for aqueous emulsion polymerization of ethylene. Several bincuclear late transition metal catalysts have been more recently explored for olefin polymerization. There have also been considerable efforts to develop new families of catalysts based on non-metallocene early transition metals for the preparation of new polyolefinic materials.

This thesis describes the synthesis and characterization of selected non-metallocene early and late transition metal complexes and their usefulness as catalysts for polymerization of ethylene.

Several copper complexes based on α -diimine, bis(oxazoline)s and bis(benzimidazole)s were synthesized and characterized by elemental analysis, single crystal XRD, IR, UV, EPR and cyclic voltametry. Copper(II) complexes bearing α -diimine ligands were found have a distorted square planar geometry about the metal center. Polymerization of ethylene were conducted using the (α -diimine) copper(II) complexes along with MAO as the activator. Complexes bearing rigid acenaphthene moiety exhibited moderate catalytic activities at 5 bar ethylene pressure, whereas, the complex with an aliphatic ligand framework was inactive even at 5 bar. This indicates that the presence of an aromatic moiety plays a key role in the formation and stabilization of the active species. Linear, high molecular weight poly(ethylene)s with narrow molecular weight distributions were

produced using these catalysts. Copper(I) complexes were not active in polymerization ethylene which implying that the active species is not a Cu(I) center. Based on several evidences the active center was proposed to be a copper(II) species with μ -Cl or μ -Me bridges. Bis(oxazoline) and bis(benzimidazole) copper(II) complexes were inactive towards polymerization of ethylene at 5 bar pressure.

Trans-2-[9-(H)-fluorenyl cyclohexanol was synthesized and geometry confirmed by 1D and 2D NMR spectroscopy. Group 4 metal (Ti, Zr, Hf) complexes of this ligand were synthesized and studied for the polymerization of ethylene along with MAO as cocatalyst. Catalyst activity was found to increase in the order Zr>Ti>Hf. The catalysts were active at high temperatures (100°C). Poly(ethylene)s produced by the zirconium complex in the temperature range 25-60° consisted of only saturated chain ends and no branching. However, at temperatures above 80°C mixtures of insoluble solid polymer and soluble liquid oligomers were produced. The soluble oligomers consisted of a mixture of α -olefins and long chain alkanes, resulting from β -H transfer and chain transfer to aluminium, respectively. The solid polymer was found to be long chain branched poly(ethylene)s. It is proposed that the observed long chain branching is a result of the reincorporation of some of the α -olefins into the growing polymer chains.

Half-sandwich complexes of Group 4metals with ligands bearing aromatic substituents on the amido moiety were synthesized and studied for the polymerization of ethylene. The complexes exhibited moderate activities for polymerization of ethylene when activated with MAO and resulted in high molecular weight linear poly(ethylene)s. Catalyst activities were much lower than the analogous N-alkyl substituted catalysts.

APPENDIX A

Crystal data and structure refinement for [(N,N'-diisopropylbenzene)-2,3-naphthyl-(1,4-diaza butadiene)] dichlorocopper(II) (2a)

Identification code	2a
Empirical formula :	C ₃₆ H ₄₀ Cl ₂ CuN ₂
Formula weight :	635.14
Temperature :	193(2) K
Wavelength :	0.71073 Å
Crystal system, space group :	Orthorhombic, P2(1)2(1)2(1)
Unit cell dimensions:	a = 10.9750(14) Å alpha = 90 deg. b = 12.5036(16) Å beta = 90 deg. c = 23.938(3) Å gamma = 90 deg.
Volume :	3285.0(7) Å ³
Z, Calculated density :	4, 1.284 Mg/m ³
Absorption coefficient :	0.854 mm ⁻¹
F(000) :	1332
Crystal size :	0.05 x 0.15 x 0.25 mm
Theta range for data collection :	1.70 to 26.45 deg.
Limiting indices	-13<=h<=13, -15<=k<=15, -29<=l<=29
Reflections collected / unique	29094 / 6741 [R(int) = 0.1036]
Completeness to theta =	26.45 99.4 %
Absorption correction :	None
Refinement method :	Full-matrix least-squares on F ²
Data / restraints / parameters :	6741 / 0 / 370

Goodness-of-fit on F^2 :	0.989
Final R indices [$I > 2\sigma(I)$] :	$R_1 = 0.0547$, $wR_2 = 0.0912$
R indices (all data) :	$R_1 = 0.0947$, $wR_2 = 0.1017$
Absolute structure parameter :	-0.001(16)
Largest diff. peak and hole :	0.605 and -0.383 e. \AA^{-3}

Bond lengths [Å] and angles [deg] for 2a

Cu(1)-N(2)	2.021(3)
Cu(1)-N(1)	2.082(3)
Cu(1)-Cl(2)	2.1854(12)
Cu(1)-Cl(1)	2.1936(12)
N(1)-C(1)	1.289(5)
N(1)-C(13)	1.449(5)
N(2)-C(2)	1.293(5)
N(2)-C(25)	1.445(5)
C(1)-C(5)	1.452(5)
C(1)-C(2)	1.514(5)
C(2)-C(3)	1.461(6)
C(3)-C(12)	1.379(5)
C(3)-C(4)	1.417(5)
C(4)-C(9)	1.403(6)
C(4)-C(5)	1.426(5)
C(5)-C(6)	1.380(5)
C(6)-C(7)	1.423(6)
C(7)-C(8)	1.370(6)
C(8)-C(9)	1.425(5)
C(9)-C(10)	1.421(6)
C(10)-C(11)	1.365(6)
C(11)-C(12)	1.417(6)
C(13)-C(18)	1.398(5)
C(13)-C(14)	1.416(5)
C(14)-C(15)	1.390(6)
C(14)-C(22)	1.520(5)
C(15)-C(16)	1.385(6)
C(16)-C(17)	1.390(6)
C(17)-C(18)	1.395(5)
C(18)-C(19)	1.517(6)
C(19)-C(21)	1.522(7)
C(19)-C(20)	1.539(7)
C(22)-C(23)	1.526(6)
C(22)-C(24)	1.535(6)
C(25)-C(30)	1.400(6)
C(25)-C(26)	1.407(6)
C(26)-C(27)	1.389(6)
C(26)-C(34)	1.546(6)
C(27)-C(28)	1.388(6)
C(28)-C(29)	1.381(6)
C(29)-C(30)	1.400(6)
C(30)-C(31)	1.507(6)

C(31)-C(33)	1.525(7)
C(31)-C(32)	1.531(6)
C(34)-C(35)	1.511(6)
C(34)-C(36)	1.522(6)
N(2)-Cu(1)-N(1)	81.74(13)
N(2)-Cu(1)-Cl(2)	143.00(10)
N(1)-Cu(1)-Cl(2)	98.43(9)
N(2)-Cu(1)-Cl(1)	97.01(10)
N(1)-Cu(1)-Cl(1)	147.78(10)
Cl(2)-Cu(1)-Cl(1)	101.30(5)
C(1)-N(1)-C(13)	118.8(3)
C(1)-N(1)-Cu(1)	110.8(3)
C(13)-N(1)-Cu(1)	129.9(2)
C(2)-N(2)-C(25)	119.8(3)
C(2)-N(2)-Cu(1)	112.5(3)
C(25)-N(2)-Cu(1)	127.7(3)
N(1)-C(1)-C(5)	135.6(4)
N(1)-C(1)-C(2)	117.1(4)
C(5)-C(1)-C(2)	107.1(3)
N(2)-C(2)-C(3)	135.5(4)
N(2)-C(2)-C(1)	116.8(4)
C(3)-C(2)-C(1)	107.5(3)
C(12)-C(3)-C(4)	119.6(4)
C(12)-C(3)-C(2)	134.9(4)
C(4)-C(3)-C(2)	105.4(4)
C(9)-C(4)-C(3)	122.6(4)
C(9)-C(4)-C(5)	123.4(4)
C(3)-C(4)-C(5)	113.9(4)
C(6)-C(5)-C(4)	119.0(4)
C(6)-C(5)-C(1)	135.1(4)
C(4)-C(5)-C(1)	105.8(3)
C(5)-C(6)-C(7)	117.8(4)
C(8)-C(7)-C(6)	123.2(4)
C(7)-C(8)-C(9)	120.3(4)
C(4)-C(9)-C(10)	116.0(3)
C(4)-C(9)-C(8)	116.2(4)
C(10)-C(9)-C(8)	127.7(4)
C(11)-C(10)-C(9)	121.6(4)
C(10)-C(11)-C(12)	121.7(4)
C(3)-C(12)-C(11)	118.5(4)
C(18)-C(13)-C(14)	122.6(4)
C(18)-C(13)-N(1)	121.0(3)
C(14)-C(13)-N(1)	116.4(3)
C(15)-C(14)-C(13)	117.0(4)

C(15)-C(14)-C(22)	121.7(4)
C(13)-C(14)-C(22)	121.2(3)
C(16)-C(15)-C(14)	121.6(4)
C(15)-C(16)-C(17)	120.0(4)
C(16)-C(17)-C(18)	121.0(4)
C(17)-C(18)-C(13)	117.7(4)
C(17)-C(18)-C(19)	119.2(4)
C(13)-C(18)-C(19)	123.1(4)
C(18)-C(19)-C(21)	111.7(4)
C(18)-C(19)-C(20)	110.5(4)
C(21)-C(19)-C(20)	110.3(4)
C(14)-C(22)-C(23)	110.3(4)
C(14)-C(22)-C(24)	113.6(4)
C(23)-C(22)-C(24)	109.4(4)
C(30)-C(25)-C(26)	122.7(4)
C(30)-C(25)-N(2)	119.6(4)
C(26)-C(25)-N(2)	117.7(4)
C(27)-C(26)-C(25)	117.6(4)
C(27)-C(26)-C(34)	121.1(4)
C(25)-C(26)-C(34)	121.2(4)
C(28)-C(27)-C(26)	120.5(4)
C(29)-C(28)-C(27)	121.1(4)
C(28)-C(29)-C(30)	120.5(4)
C(25)-C(30)-C(29)	117.3(4)
C(25)-C(30)-C(31)	121.4(4)
C(29)-C(30)-C(31)	121.2(4)
C(30)-C(31)-C(33)	111.7(4)
C(30)-C(31)-C(32)	111.8(4)
C(33)-C(31)-C(32)	110.5(4)
C(35)-C(34)-C(36)	110.3(4)
C(35)-C(34)-C(26)	111.9(4)
C(36)-C(34)-C(26)	111.5(4)

Symmetry transformations used to generate equivalent atoms

Torsion angles [deg] for complex 2a.

N(2)-Cu(1)-N(1)-C(1)	-7.0(3)
Cl(2)-Cu(1)-N(1)-C(1)	135.6(3)
Cl(1)-Cu(1)-N(1)-C(1)	-97.1(3)
N(2)-Cu(1)-N(1)-C(13)	164.7(3)
Cl(2)-Cu(1)-N(1)-C(13)	-52.7(3)
Cl(1)-Cu(1)-N(1)-C(13)	74.7(4)
N(1)-Cu(1)-N(2)-C(2)	9.6(3)
Cl(2)-Cu(1)-N(2)-C(2)	-83.5(3)
Cl(1)-Cu(1)-N(2)-C(2)	157.1(3)
N(1)-Cu(1)-N(2)-C(25)	-169.8(4)
Cl(2)-Cu(1)-N(2)-C(25)	97.1(3)
Cl(1)-Cu(1)-N(2)-C(25)	-22.3(3)
C(13)-N(1)-C(1)-C(5)	4.8(7)
Cu(1)-N(1)-C(1)-C(5)	177.5(4)
C(13)-N(1)-C(1)-C(2)	-169.1(3)
Cu(1)-N(1)-C(1)-C(2)	3.7(4)
C(25)-N(2)-C(2)-C(3)	-4.1(7)
Cu(1)-N(2)-C(2)-C(3)	176.4(4)
C(25)-N(2)-C(2)-C(1)	169.0(3)
Cu(1)-N(2)-C(2)-C(1)	-10.4(4)
N(1)-C(1)-C(2)-N(2)	4.6(6)
C(5)-C(1)-C(2)-N(2)	-171.0(3)
N(1)-C(1)-C(2)-C(3)	179.5(4)
C(5)-C(1)-C(2)-C(3)	4.0(4)
N(2)-C(2)-C(3)-C(12)	-6.2(8)
C(1)-C(2)-C(3)-C(12)	-179.8(4)
N(2)-C(2)-C(3)-C(4)	170.9(4)
C(1)-C(2)-C(3)-C(4)	-2.7(4)
C(12)-C(3)-C(4)-C(9)	-0.9(6)
C(2)-C(3)-C(4)-C(9)	-178.5(4)
C(12)-C(3)-C(4)-C(5)	178.1(4)
C(2)-C(3)-C(4)-C(5)	0.4(5)
C(9)-C(4)-C(5)-C(6)	2.2(6)
C(3)-C(4)-C(5)-C(6)	-176.7(4)
C(9)-C(4)-C(5)-C(1)	-178.9(4)
C(3)-C(4)-C(5)-C(1)	2.1(5)
N(1)-C(1)-C(5)-C(6)	0.6(9)
C(2)-C(1)-C(5)-C(6)	174.9(4)
N(1)-C(1)-C(5)-C(4)	-177.9(5)
C(2)-C(1)-C(5)-C(4)	-3.6(4)
C(4)-C(5)-C(6)-C(7)	-1.3(6)
C(1)-C(5)-C(6)-C(7)	-179.7(4)

C(5)-C(6)-C(7)-C(8)	-0.1(6)
C(6)-C(7)-C(8)-C(9)	0.7(6)
C(3)-C(4)-C(9)-C(10)	-0.9(6)
C(5)-C(4)-C(9)-C(10)	-179.8(4)
C(3)-C(4)-C(9)-C(8)	177.3(4)
C(5)-C(4)-C(9)-C(8)	-1.6(6)
C(7)-C(8)-C(9)-C(4)	0.1(6)
C(7)-C(8)-C(9)-C(10)	178.0(4)
C(4)-C(9)-C(10)-C(11)	1.6(6)
C(8)-C(9)-C(10)-C(11)	-176.3(4)
C(9)-C(10)-C(11)-C(12)	-0.6(7)
C(4)-C(3)-C(12)-C(11)	1.9(6)
C(2)-C(3)-C(12)-C(11)	178.7(4)
C(10)-C(11)-C(12)-C(3)	-1.2(6)
C(1)-N(1)-C(13)-C(18)	-95.3(5)
Cu(1)-N(1)-C(13)-C(18)	93.5(4)
C(1)-N(1)-C(13)-C(14)	85.2(5)
Cu(1)-N(1)-C(13)-C(14)	-86.0(5)
C(18)-C(13)-C(14)-C(15)	1.5(7)
N(1)-C(13)-C(14)-C(15)	-178.9(4)
C(18)-C(13)-C(14)-C(22)	-175.7(4)
N(1)-C(13)-C(14)-C(22)	3.8(6)
C(13)-C(14)-C(15)-C(16)	0.1(7)
C(22)-C(14)-C(15)-C(16)	177.4(4)
C(14)-C(15)-C(16)-C(17)	-0.3(7)
C(15)-C(16)-C(17)-C(18)	-1.1(7)
C(16)-C(17)-C(18)-C(13)	2.6(7)
C(16)-C(17)-C(18)-C(19)	-178.7(5)
C(14)-C(13)-C(18)-C(17)	-2.9(7)
N(1)-C(13)-C(18)-C(17)	177.6(4)
C(14)-C(13)-C(18)-C(19)	178.5(4)
N(1)-C(13)-C(18)-C(19)	-1.0(7)
C(17)-C(18)-C(19)-C(21)	-69.9(6)
C(13)-C(18)-C(19)-C(21)	108.7(5)
C(17)-C(18)-C(19)-C(20)	53.3(6)
C(13)-C(18)-C(19)-C(20)	-128.1(5)
C(15)-C(14)-C(22)-C(23)	80.1(6)
C(15)-C(14)-C(22)-C(24)	26.2(7)
C(13)-C(14)-C(22)-C(24)	-156.6(5)
C(2)-N(2)-C(25)-C(30)	99.1(5)
Cu(1)-N(2)-C(25)-C(30)	-81.6(5)
C(2)-N(2)-C(25)-C(26)	-83.7(5)
Cu(1)-N(2)-C(25)-C(26)	95.7(4)
C(30)-C(25)-C(26)-C(27)	-5.6(6)
N(2)-C(25)-C(26)-C(27)	177.2(4)
C(30)-C(25)-C(26)-C(34)	172.5(4)
N(2)-C(25)-C(26)-C(34)	-4.7(5)

C(25)-C(26)-C(27)-C(28)	1.6(6)
C(34)-C(26)-C(27)-C(28)	-176.5(4)
C(26)-C(27)-C(28)-C(29)	2.2(7)
C(27)-C(28)-C(29)-C(30)	-2.2(7)
C(26)-C(25)-C(30)-C(29)	5.7(6)
N(2)-C(25)-C(30)-C(29)	-177.2(4)
C(26)-C(25)-C(30)-C(31)	-175.1(4)
N(2)-C(25)-C(30)-C(31)	2.0(6)
C(28)-C(29)-C(30)-C(25)	-1.7(7)
C(28)-C(29)-C(30)-C(31)	179.0(4)
C(25)-C(30)-C(31)-C(33)	-102.8(5)
C(29)-C(30)-C(31)-C(33)	76.4(5)
C(25)-C(30)-C(31)-C(32)	132.8(4)
C(29)-C(30)-C(31)-C(32)	-48.0(6)
C(27)-C(26)-C(34)-C(35)	-78.6(5)
C(25)-C(26)-C(34)-C(35)	103.3(5)
C(27)-C(26)-C(34)-C(36)	45.4(6)
C(25)-C(26)-C(34)-C(36)	-132.6(4)

Symmetry transformations used to generate equivalent atoms

Crystal data and structure refinement for [(N,N'-diisopropylbenzene)-2,3-naphthyl-(1,4-diazabutadiene)] dibromocopper(II) (**2b**)

Identification code	2b
Empirical formula	C ₃₆ H ₄₀ Br ₂ Cu N ₂
Formula weight	724.06
Temperature	293(2) K
Wavelength	0.71073 Å
Crystal system, space group	Orthorhombic, P2 ₁ 2 ₁ 2 ₁
Unit cell dimensions	a = 11.3108(13) Å alpha = 90 deg b = 12.7331(15) Å beta = 90 deg. c = 23.847(3) Å gamma = 90 deg.
Volume	3434.4(7) Å ³
Z, Calculated density	4, 1.400 Mg/m ³
Absorption coefficient	2.988 mm ⁻¹
F(000)	1476
Crystal size	0.67 x 0.20 x 0.05
Theta range for data collection	1.81 to 25.00 deg.
Limiting indices	-13<=h<=13, -15<=k<=15 -28<=l<=28
Reflections collected / unique	32634 / 6050 [R(int)= 0.0997]
Completeness to theta = 25.00	99.9 %
Max. and min. transmission	0.8553 and 0.2387
Refinement method	Full-matrix least squares on F ²

Data / restraints / parameters 6050 / 0 / 378

Goodness-of-fit on F^2 1.006

Final R indices [$I > 2\sigma(I)$] R1 = 0.0603, wR2 = 0.1206

R indices (all data) R1 = 0.1072, wR2 = 0.1371

Absolute structure parameter 0.012(16)

Largest diff. peak and hole 0.750 and -0.466 e. \AA^{-3}

Bond lengths [Å] and angles [deg] for complex 2b

Cu(1)-N(2)	2.042(5)
Cu(1)-N(1)	2.072(5)
Cu(1)-Br(2)	2.3169(12)
Cu(1)-Br(1)	2.3178(12)
C(1)-N(2)	1.269(8)
C(1)-C(2)	1.493(9)
C(1)-C(5)	1.502(9)
N(1)-C(2)	1.294(8)
N(1)-C(13)	1.444(8)
C(8)-C(7)	1.364(11)
C(8)-C(9)	1.431(10)
N(2)-C(25)	1.433(9)
C(5)-C(6)	1.355(9)
C(5)-C(4)	1.402(9)
C(14)-C(13)	1.393(10)
C(14)-C(15)	1.399(10)
C(14)-C(22)	1.486(12)
C(29)-C(28)	1.375(13)
C(29)-C(30)	1.393(11)
C(18)-C(13)	1.390(10)
C(18)-C(17)	1.395(10)
C(18)-C(19)	1.505(10)
C(2)-C(3)	1.451(9)
C(10)-C(11)	1.354(11)
C(10)-C(9)	1.397(10)
C(7)-C(6)	1.425(10)
C(4)-C(9)	1.389(9)
C(4)-C(3)	1.430(9)
C(31)-C(32)	1.506(13)
C(31)-C(30)	1.514(12)
C(31)-C(33)	1.539(13)
C(26)-C(25)	1.383(10)
C(26)-C(27)	1.412(11)
C(26)-C(34)	1.488(11)
C(28)-C(27)	1.373(13)
C(12)-C(3)	1.362(10)
C(12)-C(11)	1.444(10)
C(30)-C(25)	1.381(11)
C(22)-C(24)	1.497(14)
C(22)-C(23)	1.521(14)
C(15)-C(16)	1.349(12)
C(19)-C(21)	1.473(14)
C(19)-C(20)	1.490(14)
C(35)-C(34)	1.520(11)

C(16)-C(17)	1.388(12)
C(36)-C(34)	1.533(13)
N(2)-Cu(1)-N(1)	81.9(2)
N(2)-Cu(1)-Br(2)	142.08(19)
N(1)-Cu(1)-Br(2)	98.90(15)
N(2)-Cu(1)-Br(1)	98.10(16)
N(1)-Cu(1)-Br(1)	147.40(17)
Br(2)-Cu(1)-Br(1)	100.52(5)
N(2)-C(1)-C(2)	120.0(6)
N(2)-C(1)-C(5)	133.4(6)
C(2)-C(1)-C(5)	106.5(5)
C(2)-N(1)-C(13)	118.9(5)
C(2)-N(1)-Cu(1)	110.9(4)
C(13)-N(1)-Cu(1)	129.6(4)
C(7)-C(8)-C(9)	120.3(7)
C(1)-N(2)-C(25)	121.1(5)
C(1)-N(2)-Cu(1)	110.4(4)
C(25)-N(2)-Cu(1)	128.4(4)
C(6)-C(5)-C(4)	120.6(6)
C(6)-C(5)-C(1)	134.1(6)
C(4)-C(5)-C(1)	105.1(6)
C(13)-C(14)-C(15)	116.7(7)
C(13)-C(14)-C(22)	124.9(7)
C(15)-C(14)-C(22)	118.4(7)
C(28)-C(29)-C(30)	121.6(9)
C(13)-C(18)-C(17)	117.2(8)
C(13)-C(18)-C(19)	122.6(7)
C(17)-C(18)-C(19)	120.1(8)
N(1)-C(2)-C(3)	135.5(6)
N(1)-C(2)-C(1)	116.0(6)
C(3)-C(2)-C(1)	108.2(5)
C(11)-C(10)-C(9)	121.2(7)
C(8)-C(7)-C(6)	122.5(7)
C(9)-C(4)-C(5)	123.2(6)
C(9)-C(4)-C(3)	122.7(6)
C(5)-C(4)-C(3)	114.2(6)
C(32)-C(31)-C(30)	113.6(8)
C(32)-C(31)-C(33)	108.9(8)
C(30)-C(31)-C(33)	111.5(9)
C(25)-C(26)-C(27)	117.3(8)
C(25)-C(26)-C(34)	123.0(6)
C(27)-C(26)-C(34)	119.6(8)
C(5)-C(6)-C(7)	117.4(7)
C(18)-C(13)-C(14)	123.0(7)
C(18)-C(13)-N(1)	116.6(6)
C(14)-C(13)-N(1)	120.4(7)

C(27)-C(28)-C(29)	120.3(8)
C(3)-C(12)-C(11)	117.6(7)
C(25)-C(30)-C(29)	116.9(8)
C(25)-C(30)-C(31)	123.3(7)
C(29)-C(30)-C(31)	119.8(8)
C(4)-C(9)-C(10)	117.0(7)
C(4)-C(9)-C(8)	115.8(6)
C(10)-C(9)-C(8)	127.1(7)
C(12)-C(3)-C(4)	119.3(7)
C(12)-C(3)-C(2)	135.0(7)
C(4)-C(3)-C(2)	105.7(6)
C(30)-C(25)-C(26)	123.5(7)
C(30)-C(25)-N(2)	118.4(7)
C(26)-C(25)-N(2)	118.1(7)
C(14)-C(22)-C(24)	114.0(9)
C(14)-C(22)-C(23)	113.0(9)
C(24)-C(22)-C(23)	109.1(9)
C(16)-C(15)-C(14)	122.0(9)
C(10)-C(11)-C(12)	122.1(7)
C(21)-C(19)-C(20)	110.2(11)
C(21)-C(19)-C(18)	111.5(9)
C(20)-C(19)-C(18)	113.9(8)
C(15)-C(16)-C(17)	120.2(8)
C(26)-C(34)-C(35)	114.1(7)
C(26)-C(34)-C(36)	112.0(7)
C(35)-C(34)-C(36)	109.5(8)
C(28)-C(27)-C(26)	120.2(9)
C(16)-C(17)-C(18)	120.7(9)

Symmetry transformations used to generate equivalent atoms

Torsion angles [deg] for complex 2b

N(2)-Cu(1)-N(1)-C(2)	-6.2(5)	Br(2)-
Cu(1)-N(1)-C(2)	135.5(5)	
Br(1)-Cu(1)-N(1)-C(2)	98.5(5)	
N(2)-Cu(1)-N(1)-C(13)	165.2(6)	
Br(2)-Cu(1)-N(1)-C(13)	53.1(6)	
Br(1)-Cu(1)-N(1)-C(13)	72.9(7)	
C(2)-C(1)-N(2)-C(25)	168.9(7)	
C(5)-C(1)-N(2)-C(25)	7.3(13)	
C(2)-C(1)-N(2)-Cu(1)	8.8(8)	
C(5)-C(1)-N(2)-Cu(1)	175.0(7)	
N(1)-Cu(1)-N(2)-C(1)	8.0(5)	
Br(2)-Cu(1)-N(2)-C(1)	86.0(6)	
Br(1)-Cu(1)-N(2)-C(1)	155.1(5)	
N(1)-Cu(1)-N(2)-C(25)	169.5(7)	
Br(2)-Cu(1)-N(2)-C(25)	96.4(7)	
Br(1)-Cu(1)-N(2)-C(25)	22.5(7)	
N(2)-C(1)-C(5)-C(6)	4.7(16)	
C(2)-C(1)-C(5)-C(6)	178.7(9)	
N(2)-C(1)-C(5)-C(4)	171.1(8)	
C(2)-C(1)-C(5)-C(4)	5.4(8)	C(13)-
N(1)-C(2)-C(3)	3.2(13)	
Cu(1)-N(1)-C(2)-C(3)	175.6(7)	
C(13)-N(1)-C(2)-C(1)	-169.0(6)	
Cu(1)-N(1)-C(2)-C(1)	3.4(8)	
N(2)-C(1)-C(2)-N(1)	3.8(10)	
C(5)-C(1)-C(2)-N(1)	-179.1(7)	
N(2)-C(1)-C(2)-C(3)	-170.4(7)	
C(5)-C(1)-C(2)-C(3)	6.7(8)	
C(9)-C(8)-C(7)-C(6)	-2.0(14)	
C(6)-C(5)-C(4)-C(9)	0.0(12)	
C(1)-C(5)-C(4)-C(9)	176.5(7)	
C(6)-C(5)-C(4)-C(3)	178.9(8)	
C(1)-C(5)-C(4)-C(3)	2.3(9)	
C(4)-C(5)-C(6)-C(7)	1.5(12)	
C(1)-C(5)-C(6)-C(7)	176.8(8)	
C(8)-C(7)-C(6)-C(5)	-0.5(14)	
C(17)-C(18)-C(13)-C(14)	2.8(11)	
C(19)-C(18)-C(13)-C(14)	-175.6(8)	
C(17)-C(18)-C(13)-N(1)	-177.7(6)	
C(19)-C(18)-C(13)-N(1)	3.8(11)	
C(15)-C(14)-C(13)-C(18)	-3.6(12)	

C(22)-C(14)-C(13)-C(18)	176.3(8)
C(15)-C(14)-C(13)-N(1)	176.9(7) C(22)-
C(14)-C(13)-N(1)	-3.1(12)
C(2)-N(1)-C(13)-C(18)	91.8(8)
Cu(1)-N(1)-C(13)-C(18)	79.0(8)
C(2)-N(1)-C(13)-C(14)	-88.7(9)
Cu(1)-N(1)-C(13)-C(14)	100.5(7)
C(30)-C(29)-C(28)-C(27)	0.6(14)
C(28)-C(29)-C(30)-C(25)	0.8(12)
C(28)-C(29)-C(30)-C(31)	-177.1(8)
C(32)-C(31)-C(30)-C(25)	-125.9(8)
C(33)-C(31)-C(30)-C(25)	110.6(9)
C(32)-C(31)-C(30)-C(29)	51.9(11)
C(33)-C(31)-C(30)-C(29)	-71.7(10)
C(5)-C(4)-C(9)-C(10)	178.1(7)
C(3)-C(4)-C(9)-C(10)	-0.7(11)
C(5)-C(4)-C(9)-C(8)	-2.3(11)
C(3)-C(4)-C(9)-C(8)	178.9(8)
C(11)-C(10)-C(9)-C(4)	-2.4(12)
C(11)-C(10)-C(9)-C(8)	178.2(8)
C(7)-C(8)-C(9)-C(4)	3.3(12)
C(7)-C(8)-C(9)-C(10)	-177.2(8)
C(11)-C(12)-C(3)-C(4)	-2.3(11)
C(11)-C(12)-C(3)-C(2)	-179.2(9)
C(9)-C(4)-C(3)-C(12)	3.0(11)
C(5)-C(4)-C(3)-C(12)	-175.8(7)
C(9)-C(4)-C(3)-C(2)	-179.3(7)
C(5)-C(4)-C(3)-C(2)	1.8(9)
N(1)-C(2)-C(3)-C(12)	-0.7(16)
C(1)-C(2)-C(3)-C(12)	171.9(9)
N(1)-C(2)-C(3)-C(4)	-177.9(9)
C(1)-C(2)-C(3)-C(4)	-5.3(8)
C(29)-C(30)-C(25)-C(26)	-4.2(10)
C(31)-C(30)-C(25)-C(26)	173.6(7)
C(29)-C(30)-C(25)-N(2)	177.9(6)
C(31)-C(30)-C(25)-N(2)	-4.3(10)
C(27)-C(26)-C(25)-C(30)	6.0(10)
C(34)-C(26)-C(25)-C(30)	-176.4(7)
C(27)-C(26)-C(25)-N(2)	-176.2(6)
C(34)-C(26)-C(25)-N(2)	1.5(10)
C(1)-N(2)-C(25)-C(30)	-79.0(9)
Cu(1)-N(2)-C(25)-C(30)	98.4(7)
C(1)-N(2)-C(25)-C(26)	103.1(8)
Cu(1)-N(2)-C(25)-C(26)	-79.6(8)
C(13)-C(14)-C(22)-C(24)	-124.8(10)
C(15)-C(14)-C(22)-C(24)	55.2(12)
C(13)-C(14)-C(22)-C(23)	109.9(10)

C(15)-C(14)-C(22)-C(23)	-70.2(11)
C(13)-C(14)-C(15)-C(16)	2.2(13)
C(22)-C(14)-C(15)-C(16)	-177.7(9)
C(9)-C(10)-C(11)-C(12)	3.1(14)
C(3)-C(12)-C(11)-C(10)	-0.6(13)
C(13)-C(18)-C(19)-C(21)	92.5(12)
C(17)-C(18)-C(19)-C(21)	-85.9(11)
C(13)-C(18)-C(19)-C(20)	-142.0(11)
C(17)-C(18)-C(19)-C(20)	39.6(15)
C(14)-C(15)-C(16)-C(17)	-0.1(15)
C(25)-C(26)-C(34)-C(35)	134.8(8)
C(27)-C(26)-C(34)-C(35)	-47.6(10)
C(25)-C(26)-C(34)-C(36)	-100.1(9)
C(27)-C(26)-C(34)-C(36)	77.5(9)
C(29)-C(28)-C(27)-C(26)	1.2(13)
C(25)-C(26)-C(27)-C(28)	-4.3(11)
C(34)-C(26)-C(27)-C(28)	177.9(8)
C(15)-C(16)-C(17)-C(18)	-0.8(15)
C(13)-C(18)-C(17)-C(16)	-0.5(13)
C(19)-C(18)-C(17)-C(16)	178.0(9)

Symmetry transformations used to generate equivalent atoms

Crystal data and structure refinement for [(N,N'-2-tert-butylbenzene)-2,3-naphthyl-(1,4-diazabutadiene)] dichloro copper(II) (2c)

Identification code	2c
Empirical formula	C ₃₃ H ₃₄ Cl ₄ CuN ₂
Formula weight	663.96
Temperature	293(2) K
Wavelength	0.71073 Å
Crystal system, space group	Monoclinic, P21/n
Unit cell dimensions	a = 12.033(4) Å α = 90 deg. b = 22.361(8) Å β = 103.664(6) deg. c = 12.481(4) Å γ = 90 deg.
Volume	3263.3(19) Å ³
Z, Calculated density	4, 1.351 Mg/m ³
Absorption coefficient	1.021 mm ⁻¹
F(000)	1372
Crystal size	0.68 x 0.44 x 0.28 mm
Theta range for data collection	1.82 to 28.58 deg.
Limiting indices	-15 ≤ h ≤ 15 -29 ≤ k ≤ 17 -16 ≤ l ≤ 13
Reflections collected / unique	17573 / 7153 [R(int) = 0.0290]
Completeness to theta = 28.58	85.8 %
Absorption correction	Multiscan
Max. and min. transmission	0.7630 and 0.5448
Refinement method	Full-matrix least-squares on F ²

Data / restraints / parameters	7153 / 0 / 367
Goodness-of-fit on F^2	1.071
Final R indices [$I > 2\sigma(I)$]	R1 = 0.0551, wR2 = 0.1662
R indices (all data)	R1 = 0.0695, wR2 = 0.1790
Largest diff. peak and hole	0.944 and -0.926 e.A ⁻³

Bond lengths [Å] and angles [deg] for complex **2c**

Cu(1)-N(1)	2.059(2)
Cu(1)-N(2)	2.088(2)
Cu(1)-Cl(1)	2.2202(10)
Cu(1)-Cl(2)	2.2463(10)
Cl(3)-C(33)	1.703(6)
Cl(4)-C(33)	1.716(6)
N(1)-C(2)	1.285(3)
N(1)-C(13)	1.448(3)
N(2)-C(1)	1.291(4)
N(2)-C(23)	1.448(3)
C(1)-C(5)	1.475(4)
C(1)-C(2)	1.506(4)
C(2)-C(3)	1.485(4)
C(3)-C(12)	1.371(5)
C(3)-C(4)	1.413(5)
C(4)-C(9)	1.421(4)
C(4)-C(5)	1.429(5)
C(5)-C(6)	1.379(4)
C(6)-C(7)	1.431(5)
C(7)-C(8)	1.377(7)
C(8)-C(9)	1.422(7)
C(9)-C(10)	1.405(7)
C(10)-C(11)	1.369(7)
C(11)-C(12)	1.430(5)
C(13)-C(14)	1.402(5)
C(13)-C(18)	1.413(4)
C(14)-C(15)	1.380(4)
C(15)-C(16)	1.378(5)
C(16)-C(17)	1.374(5)
C(17)-C(18)	1.416(4)
C(18)-C(19)	1.540(4)
C(19)-C(22)	1.533(5)
C(19)-C(21)	1.554(5)
C(19)-C(20)	1.558(5)
C(23)-C(24)	1.396(4)
C(23)-C(28)	1.409(4)
C(24)-C(25)	1.385(4)
C(25)-C(26)	1.383(5)
C(26)-C(27)	1.390(5)
C(27)-C(28)	1.408(4)
C(28)-C(29)	1.541(5)
C(29)-C(30)	1.510(7)
C(29)-C(31)	1.514(8)
C(29)-C(32)	1.514(6)

N(1)-Cu(1)-N(2)	80.98(9)
N(1)-Cu(1)-Cl(1)	94.06(6)
N(2)-Cu(1)-Cl(1)	151.28(7)
N(1)-Cu(1)-Cl(2)	161.66(8)
N(2)-Cu(1)-Cl(2)	95.27(7)
Cl(1)-Cu(1)-Cl(2)	97.50(3)
C(2)-N(1)-C(13)	119.9(2)
C(2)-N(1)-Cu(1)	111.85(18)
C(13)-N(1)-Cu(1)	126.66(17)
C(1)-N(2)-C(23)	120.6(2)
C(1)-N(2)-Cu(1)	110.76(17)
C(23)-N(2)-Cu(1)	127.10(17)
N(2)-C(1)-C(5)	135.5(3)
N(2)-C(1)-C(2)	117.5(2)
C(5)-C(1)-C(2)	106.9(2)
N(1)-C(2)-C(3)	134.7(3)
N(1)-C(2)-C(1)	117.3(2)
C(3)-C(2)-C(1)	107.9(2)
C(12)-C(3)-C(4)	120.1(3)
C(12)-C(3)-C(2)	135.0(3)
C(4)-C(3)-C(2)	104.9(3)
C(3)-C(4)-C(9)	122.3(3)
C(3)-C(4)-C(5)	114.7(3)
C(9)-C(4)-C(5)	122.9(3)
C(6)-C(5)-C(4)	119.9(3)
C(6)-C(5)-C(1)	134.6(3)
C(4)-C(5)-C(1)	105.5(3)
C(5)-C(6)-C(7)	117.7(4)
C(8)-C(7)-C(6)	122.5(4)
C(7)-C(8)-C(9)	121.5(3)
C(10)-C(9)-C(4)	116.0(4)
C(10)-C(9)-C(8)	128.5(4)
C(4)-C(9)-C(8)	115.5(4)
C(11)-C(10)-C(9)	121.9(3)
C(10)-C(11)-C(12)	121.6(4)
C(3)-C(12)-C(11)	118.1(4)
C(14)-C(13)-C(18)	121.9(3)
C(14)-C(13)-N(1)	113.9(2)
C(18)-C(13)-N(1)	124.2(3)
C(15)-C(14)-C(13)	121.0(3)
C(16)-C(15)-C(14)	118.8(3)
C(17)-C(16)-C(15)	120.2(3)
C(16)-C(17)-C(18)	124.0(3)
C(13)-C(18)-C(17)	114.1(3)
C(13)-C(18)-C(19)	129.0(3)
C(17)-C(18)-C(19)	116.9(3)

C(22)-C(19)-C(18)	115.8(3)
C(22)-C(19)-C(21)	107.3(3)
C(18)-C(19)-C(21)	108.5(3)
C(22)-C(19)-C(20)	107.3(3)
C(18)-C(19)-C(20)	109.1(3)
C(21)-C(19)-C(20)	108.6(3)
C(24)-C(23)-C(28)	122.1(3)
C(24)-C(23)-N(2)	114.5(2)
C(28)-C(23)-N(2)	123.3(3)
C(25)-C(24)-C(23)	120.7(3)
C(26)-C(25)-C(24)	118.9(3)
C(25)-C(26)-C(27)	120.0(3)
C(26)-C(27)-C(28)	123.2(3)
C(27)-C(28)-C(23)	115.0(3)
C(27)-C(28)-C(29)	120.3(3)
C(23)-C(28)-C(29)	124.8(3)
C(30)-C(29)-C(31)	110.1(6)
C(30)-C(29)-C(32)	106.0(5)
C(31)-C(29)-C(32)	108.4(6)
C(30)-C(29)-C(28)	111.1(4)
C(31)-C(29)-C(28)	108.7(4)
C(32)-C(29)-C(28)	112.5(4)
Cl(3)-C(33)-Cl(4)	115.2(3)

Symmetry transformations used to generate equivalent atoms

Hydrogen bonds for complex 2c [A and deg.].

Donor --- H....Acceptor	D - H	H...A	D...A	D - H...A
C(14) -- H(14) .. Cl(2)	0.9300	2.7575	3.6081	152.51
C(33) -- H(33A).. Cl(1)	0.9700	2.8151	3.6414	143.56
C(33) -- H(33A).. Cl(2)	0.9700	2.8135	3.6094	139.83'

:: No Classic Hydrogen Bonds Found

Torsion angles [deg] for complex 2c

N(2)-Cu(1)-N(1)-C(2)	11.1(2)
Cl(1)-Cu(1)-N(1)-C(2)	162.7(2)
Cl(2)-Cu(1)-N(1)-C(2)	-68.3(3)
N(2)-Cu(1)-N(1)-C(13)	176.8(2)
Cl(1)-Cu(1)-N(1)-C(13)	-31.7(2)
Cl(2)-Cu(1)-N(1)-C(13)	97.4(3)
N(1)-Cu(1)-N(2)-C(1)	9.82(19)
Cl(1)-Cu(1)-N(2)-C(1)	-91.7(2)
Cl(2)-Cu(1)-N(2)-C(1)	152.09(19)
N(1)-Cu(1)-N(2)-C(23)	-175.5(2)
Cl(1)-Cu(1)-N(2)-C(23)	102.6(2)
Cl(2)-Cu(1)-N(2)-C(23)	-13.6(2)
C(23)-N(2)-C(1)-C(5)	-9.0(5)
Cu(1)-N(2)-C(1)-C(5)	-175.8(3)
C(23)-N(2)-C(1)-C(2)	174.0(2)
Cu(1)-N(2)-C(1)-C(2)	7.3(3)
C(13)-N(1)-C(2)-C(3)	4.8(5)
Cu(1)-N(1)-C(2)-C(3)	171.5(3)
C(13)-N(1)-C(2)-C(1)	-177.4(2)
Cu(1)-N(1)-C(2)-C(1)	-10.7(3)
N(2)-C(1)-C(2)-N(1)	2.3(4)
C(5)-C(1)-C(2)-N(1)	-175.5(3)
N(2)-C(1)-C(2)-C(3)	-179.4(3)
C(5)-C(1)-C(2)-C(3)	2.8(3)
N(1)-C(2)-C(3)-C(12)	-3.9(6)
C(1)-C(2)-C(3)-C(12)	178.2(4)
N(1)-C(2)-C(3)-C(4)	175.9(3)
C(1)-C(2)-C(3)-C(4)	-2.0(3)
C(12)-C(3)-C(4)-C(9)	2.1(5)
C(2)-C(3)-C(4)-C(9)	-177.8(3)
C(12)-C(3)-C(4)-C(5)	-179.7(3)
C(2)-C(3)-C(4)-C(5)	0.5(4)
C(3)-C(4)-C(5)-C(6)	-176.9(3)
C(9)-C(4)-C(5)-C(6)	1.3(5)
C(3)-C(4)-C(5)-C(1)	1.3(4)
C(9)-C(4)-C(5)-C(1)	179.5(3)
N(2)-C(1)-C(5)-C(6)	-1.9(6)
C(2)-C(1)-C(5)-C(6)	175.3(4)
N(2)-C(1)-C(5)-C(4)	-179.7(3)
C(2)-C(1)-C(5)-C(4)	-2.5(3)
C(4)-C(5)-C(6)-C(7)	-0.6(5)
C(1)-C(5)-C(6)-C(7)	-178.2(3)
C(5)-C(6)-C(7)-C(8)	-0.2(6)

C(6)-C(7)-C(8)-C(9)	0.3(7)
C(3)-C(4)-C(9)-C(10)	-1.8(5)
C(5)-C(4)-C(9)-C(10)	-179.9(3)
C(3)-C(4)-C(9)-C(8)	177.0(3)
C(5)-C(4)-C(9)-C(8)	-1.1(5)
C(7)-C(8)-C(9)-C(10)	178.9(4)
C(7)-C(8)-C(9)-C(4)	0.3(6)
C(4)-C(9)-C(10)-C(11)	0.0(6)
C(8)-C(9)-C(10)-C(11)	-178.6(4)
C(9)-C(10)-C(11)-C(12)	1.5(7)
C(4)-C(3)-C(12)-C(11)	-0.5(5)
C(2)-C(3)-C(12)-C(11)	179.3(4)
C(10)-C(11)-C(12)-C(3)	-1.3(6)
C(2)-N(1)-C(13)-C(14)	87.3(3)
Cu(1)-N(1)-C(13)-C(14)	-77.4(3)
C(2)-N(1)-C(13)-C(18)	-94.4(3)
Cu(1)-N(1)-C(13)-C(18)	101.0(3)
C(18)-C(13)-C(14)-C(15)	2.2(5)
N(1)-C(13)-C(14)-C(15)	-179.4(3)
C(13)-C(14)-C(15)-C(16)	-2.4(6)
C(14)-C(15)-C(16)-C(17)	1.2(6)
C(15)-C(16)-C(17)-C(18)	0.3(6)
C(14)-C(13)-C(18)-C(17)	-0.7(4)
N(1)-C(13)-C(18)-C(17)	-178.9(3)
C(14)-C(13)-C(18)-C(19)	-179.6(3)
N(1)-C(13)-C(18)-C(19)	2.2(5)
C(16)-C(17)-C(18)-C(13)	-0.5(5)
C(16)-C(17)-C(18)-C(19)	178.5(3)
C(13)-C(18)-C(19)-C(22)	-3.2(5)
C(17)-C(18)-C(19)-C(22)	177.9(3)
C(13)-C(18)-C(19)-C(21)	-124.0(3)
C(17)-C(18)-C(19)-C(21)	57.2(4)
C(13)-C(18)-C(19)-C(20)	117.9(4)
C(17)-C(18)-C(19)-C(20)	-60.9(4)
C(1)-N(2)-C(23)-C(24)	-75.0(3)
Cu(1)-N(2)-C(23)-C(24)	89.4(3)
C(1)-N(2)-C(23)-C(28)	108.7(3)
Cu(1)-N(2)-C(23)-C(28)	-86.9(3)
C(28)-C(23)-C(24)-C(25)	-0.4(4)
N(2)-C(23)-C(24)-C(25)	-176.6(3)
C(23)-C(24)-C(25)-C(26)	1.4(5)
C(24)-C(25)-C(26)-C(27)	-1.6(5)
C(25)-C(26)-C(27)-C(28)	0.6(5)
C(26)-C(27)-C(28)-C(23)	0.4(4)
C(26)-C(27)-C(28)-C(29)	-179.7(3)
C(24)-C(23)-C(28)-C(27)	-0.6(4)

N(2)-C(23)-C(28)-C(27)	175.4(2)
C(24)-C(23)-C(28)-C(29)	179.6(3)
N(2)-C(23)-C(28)-C(29)	-4.5(4)
C(27)-C(28)-C(29)-C(30)	127.2(5)
C(23)-C(28)-C(29)-C(30)	-53.0(6)
C(27)-C(28)-C(29)-C(31)	-111.6(6)
C(23)-C(28)-C(29)-C(31)	68.3(6)
C(27)-C(28)-C(29)-C(32)	8.5(6)
C(23)-C(28)-C(29)-C(32)	-171.7(5)

Symmetry transformations used to generate equivalent atoms

APPENDIX B

Crystal data and structure refinement for [(2,6-diisopropylphenylamido) (fluorenyl) diphenylsilane] (2a)

Identification code	2a
Empirical formula	C ₃₇ H ₃₇ N Si
Formula weight	523.77
Temperature	293(2) K
Wavelength	0.71073 Å
Crystal system, space group	Monoclinic, <i>c2/c</i>
Unit cell dimensions	a = 27.053(11) Å alpha = 90 deg. b = 11.099(5) Å beta = 98.150(7) deg. c = 20.194(8) Å gamma = 90 deg.
Volume	6002(4) Å ³
Z, Calculated density	8, 1.159 Mg/m ³
Absorption coefficient	0.104 mm ⁻¹
F(000)	2240
Crystal size	0.48 x 0.38 x 0.10 mm
Theta range for data collection	1.52 to 25.00 deg.
Limiting indices	-30 ≤ h ≤ 32, -9 ≤ k ≤ 13, -24 ≤ l ≤ 23
Reflections collected / unique	14597 / 5300 [R(int) = 0.0250]
Completeness to theta =	25.00 99.9 %
Max. and min. transmission	0.9897 and 0.9523
Refinement method	Full-matrix least-squares on F ²

Data / restraints / parameters	5300 / 0 / 500
Goodness-of-fit on F^2	1.026
Final R indices [$I > 2\sigma(I)$]	R1 = 0.0411, wR2 = 0.1044
R indices (all data)	R1 = 0.0587, wR2 = 0.1131
Largest diff. peak and hole	0.280 and -0.195 e. \AA^{-3}

Bond lengths [Å] and angles [deg] for 2a

Si(1)-N(1)	1.7144(15)
Si(1)-C(20)	1.8639(18)
Si(1)-C(14)	1.8877(18)
Si(1)-C(9)	1.9085(19)
N(1)-C(26)	1.429(2)
C(1)-C(2)	1.385(3)
C(1)-C(13)	1.387(3)
C(2)-C(3)	1.379(4)
C(3)-C(4)	1.368(4)
C(4)-C(12)	1.391(3)
C(5)-C(6)	1.366(4)
C(5)-C(11)	1.399(3)
C(6)-C(7)	1.375(4)
C(7)-C(8)	1.390(3)
C(8)-C(10)	1.380(3)
C(9)-C(10)	1.512(3)
C(9)-C(13)	1.512(3)
C(10)-C(11)	1.400(3)
C(11)-C(12)	1.460(3)
C(12)-C(13)	1.408(3)
C(14)-C(19)	1.387(3)
C(14)-C(15)	1.392(3)
C(15)-C(16)	1.387(3)
C(16)-C(17)	1.366(4)
C(17)-C(18)	1.362(4)
C(18)-C(19)	1.394(3)
C(20)-C(25)	1.395(2)
C(20)-C(21)	1.402(2)
C(21)-C(22)	1.377(3)
C(22)-C(23)	1.377(3)
C(23)-C(24)	1.367(3)
C(24)-C(25)	1.384(3)
C(26)-C(31)	1.402(2)
C(26)-C(27)	1.416(2)
C(27)-C(28)	1.387(3)
C(27)-C(35)	1.515(3)
C(28)-C(29)	1.369(3)
C(29)-C(30)	1.378(3)
C(30)-C(31)	1.385(3)
C(31)-C(32)	1.524(2)
C(32)-C(34)	1.520(3)
C(32)-C(33)	1.522(3)

C(35)-C(36)	1.507(3)
C(35)-C(37)	1.522(3)
N(1)-Si(1)-C(20)	109.45(8)
N(1)-Si(1)-C(14)	112.57(8)
C(20)-Si(1)-C(14)	109.48(7)
N(1)-Si(1)-C(9)	108.51(8)
C(20)-Si(1)-C(9)	113.64(8)
C(14)-Si(1)-C(9)	103.13(8)
C(26)-N(1)-Si(1)	130.64(12)
C(2)-C(1)-C(13)	118.7(2)
C(3)-C(2)-C(1)	121.0(3)
C(4)-C(3)-C(2)	121.0(2)
C(3)-C(4)-C(12)	119.1(2)
C(6)-C(5)-C(11)	118.9(2)
C(5)-C(6)-C(7)	120.9(2)
C(6)-C(7)-C(8)	120.9(3)
C(10)-C(8)-C(7)	119.3(2)
C(10)-C(9)-C(13)	102.25(15)
C(10)-C(9)-Si(1)	117.43(13)
C(13)-C(9)-Si(1)	110.57(12)
C(8)-C(10)-C(11)	119.46(18)
C(8)-C(10)-C(9)	129.91(18)
C(11)-C(10)-C(9)	110.63(17)
C(5)-C(11)-C(10)	120.5(2)
C(5)-C(11)-C(12)	131.2(2)
C(10)-C(11)-C(12)	108.25(17)
C(4)-C(12)-C(13)	120.0(2)
C(4)-C(12)-C(11)	131.1(2)
C(13)-C(12)-C(11)	108.87(17)
C(1)-C(13)-C(12)	120.06(19)
C(1)-C(13)-C(9)	130.12(18)
C(12)-C(13)-C(9)	109.80(17)
C(19)-C(14)-C(15)	116.67(18)
C(19)-C(14)-Si(1)	123.12(15)
C(15)-C(14)-Si(1)	120.16(14)
C(16)-C(15)-C(14)	121.6(2)
C(17)-C(16)-C(15)	120.2(2)
C(18)-C(17)-C(16)	119.8(2)
C(17)-C(18)-C(19)	120.1(2)
C(14)-C(19)-C(18)	121.5(2)
C(25)-C(20)-C(21)	117.00(16)
C(25)-C(20)-Si(1)	121.32(13)
C(21)-C(20)-Si(1)	121.63(13)
C(22)-C(21)-C(20)	120.80(18)
C(23)-C(22)-C(21)	120.6(2)

C(24)-C(23)-C(22)	120.0(2)
C(23)-C(24)-C(25)	119.69(19)
C(24)-C(25)-C(20)	121.87(18)
C(31)-C(26)-C(27)	120.63(15)
C(31)-C(26)-N(1)	120.13(15)
C(27)-C(26)-N(1)	119.24(15)
C(28)-C(27)-C(26)	118.23(16)
C(28)-C(27)-C(35)	119.45(16)
C(26)-C(27)-C(35)	122.32(16)
C(29)-C(28)-C(27)	121.58(18)
C(28)-C(29)-C(30)	119.54(19)
C(29)-C(30)-C(31)	121.95(19)
C(30)-C(31)-C(26)	118.06(16)
C(30)-C(31)-C(32)	119.10(16)
C(26)-C(31)-C(32)	122.76(16)
C(34)-C(32)-C(33)	111.6(2)
C(34)-C(32)-C(31)	113.33(17)
C(33)-C(32)-C(31)	110.57(17)
C(36)-C(35)-C(27)	111.11(19)
C(36)-C(35)-C(37)	109.9(2)
C(27)-C(35)-C(37)	113.76(18)

Symmetry transformations used to generate equivalent atoms:

Torsion angles [deg] for 2a

C(20)-Si(1)-N(1)-C(26)	1.26(17)
C(14)-Si(1)-N(1)-C(26)	123.25(15)
C(9)-Si(1)-N(1)-C(26)	-123.26(16)
C(13)-C(1)-C(2)-C(3)	-0.7(3)
C(1)-C(2)-C(3)-C(4)	1.8(4)
C(2)-C(3)-C(4)-C(12)	-0.7(4)
C(11)-C(5)-C(6)-C(7)	-0.2(4)
C(5)-C(6)-C(7)-C(8)	0.9(4)
C(6)-C(7)-C(8)-C(10)	-0.9(4)
N(1)-Si(1)-C(9)-C(10)	68.62(15)
C(20)-Si(1)-C(9)-C(10)	-53.38(16)
C(14)-Si(1)-C(9)-C(10)	-171.80(13)
N(1)-Si(1)-C(9)-C(13)	-48.13(14)
C(20)-Si(1)-C(9)-C(13)	-170.13(12)
C(14)-Si(1)-C(9)-C(13)	71.45(14)
C(7)-C(8)-C(10)-C(11)	0.3(3)
C(7)-C(8)-C(10)-C(9)	179.48(19)

C(13)-C(9)-C(10)-C(8)	-176.66(19)
Si(1)-C(9)-C(10)-C(8)	62.2(2)
C(13)-C(9)-C(10)-C(11)	2.57(19)
Si(1)-C(9)-C(10)-C(11)	-118.61(15)
C(6)-C(5)-C(11)-C(10)	-0.4(3)
C(6)-C(5)-C(11)-C(12)	-179.1(2)
C(8)-C(10)-C(11)-C(5)	0.4(3)
C(9)-C(10)-C(11)-C(5)	-178.95(18)
C(8)-C(10)-C(11)-C(12)	179.29(17)
C(9)-C(10)-C(11)-C(12)	0.0(2)
C(3)-C(4)-C(12)-C(13)	-1.5(3)
C(3)-C(4)-C(12)-C(11)	177.9(2)
C(5)-C(11)-C(12)-C(4)	-3.5(4)
C(10)-C(11)-C(12)-C(4)	177.8(2)
C(5)-C(11)-C(12)-C(13)	176.0(2)
C(10)-C(11)-C(12)-C(13)	-2.8(2)
C(2)-C(1)-C(13)-C(12)	-1.4(3)
C(2)-C(1)-C(13)-C(9)	176.77(19)
C(4)-C(12)-C(13)-C(1)	2.6(3)
C(11)-C(12)-C(13)-C(1)	-176.94(17)
C(4)-C(12)-C(13)-C(9)	-175.97(17)
C(11)-C(12)-C(13)-C(9)	4.5(2)
C(10)-C(9)-C(13)-C(1)	177.36(19)
Si(1)-C(9)-C(13)-C(1)	-56.8(2)
C(10)-C(9)-C(13)-C(12)	-4.29(18)
Si(1)-C(9)-C(13)-C(12)	121.52(14)
N(1)-Si(1)-C(14)-C(19)	-6.60(18)
C(20)-Si(1)-C(14)-C(19)	115.38(16)
C(9)-Si(1)-C(14)-C(19)	-123.34(16)
N(1)-Si(1)-C(14)-C(15)	170.51(14)
C(20)-Si(1)-C(14)-C(15)	-67.51(16)
C(9)-Si(1)-C(14)-C(15)	53.77(16)
C(19)-C(14)-C(15)-C(16)	-1.8(3)
Si(1)-C(14)-C(15)-C(16)	-179.07(16)
C(14)-C(15)-C(16)-C(17)	1.2(3)
C(15)-C(16)-C(17)-C(18)	0.3(4)
C(16)-C(17)-C(18)-C(19)	-1.0(4)
C(15)-C(14)-C(19)-C(18)	1.0(3)
Si(1)-C(14)-C(19)-C(18)	178.23(16)
C(17)-C(18)-C(19)-C(14)	0.4(3)
N(1)-Si(1)-C(20)-C(25)	131.13(14)
C(14)-Si(1)-C(20)-C(25)	7.30(16)
C(9)-Si(1)-C(20)-C(25)	-107.40(15)
N(1)-Si(1)-C(20)-C(21)	-46.40(16)
C(14)-Si(1)-C(20)-C(21)	-170.22(14)
C(9)-Si(1)-C(20)-C(21)	75.08(16)

C(25)-C(20)-C(21)-C(22)	0.5(3)
Si(1)-C(20)-C(21)-C(22)	178.12(15)
C(20)-C(21)-C(22)-C(23)	-0.9(3)
C(21)-C(22)-C(23)-C(24)	0.8(3)
C(22)-C(23)-C(24)-C(25)	-0.4(3)
C(23)-C(24)-C(25)-C(20)	0.0(3)
C(21)-C(20)-C(25)-C(24)	-0.1(3)
Si(1)-C(20)-C(25)-C(24)	-177.71(14)
Si(1)-N(1)-C(26)-C(31)	-67.7(2)
Si(1)-N(1)-C(26)-C(27)	112.57(16)
C(31)-C(26)-C(27)-C(28)	-0.9(2)
N(1)-C(26)-C(27)-C(28)	178.84(15)
C(31)-C(26)-C(27)-C(35)	179.61(15)
N(1)-C(26)-C(27)-C(35)	-0.7(2)
C(26)-C(27)-C(28)-C(29)	1.1(3)
C(35)-C(27)-C(28)-C(29)	-179.38(18)
C(27)-C(28)-C(29)-C(30)	-0.7(3)
C(28)-C(29)-C(30)-C(31)	0.1(3)
C(29)-C(30)-C(31)-C(26)	0.1(3)
C(29)-C(30)-C(31)-C(32)	-176.70(17)
C(27)-C(26)-C(31)-C(30)	0.3(2)
N(1)-C(26)-C(31)-C(30)	-179.39(15)
C(27)-C(26)-C(31)-C(32)	176.95(14)
N(1)-C(26)-C(31)-C(32)	-2.8(2)
C(30)-C(31)-C(32)-C(34)	-44.4(3)
C(26)-C(31)-C(32)-C(34)	139.0(2)
C(30)-C(31)-C(32)-C(33)	81.7(2)
C(26)-C(31)-C(32)-C(33)	-94.9(2)
C(28)-C(27)-C(35)-C(36)	-89.2(3)
C(26)-C(27)-C(35)-C(36)	90.4(2)
C(28)-C(27)-C(35)-C(37)	35.6(3)
C(26)-C(27)-C(35)-C(37)	-144.9(2)

Symmetry transformations used to generate equivalent atoms:

Crystal data and structure refinement for [(2,6-dimethylamido) (fluorenyl) diphenylsilane]

(2b)

Identification code	2b
Empirical formula	C ₃₃ H ₂₉ N Si
Formula weight	467.66
Temperature	293(2) K
Wavelength	0.71073 Å
Crystal system, space group	Orthorhombic, Pbca
Unit cell dimensions	a = 18.275(4) Å alpha = 90°. b = 13.255(3) Å beta = 90°. c = 21.355(5) Å gamma = 90°.
Volume	5173.3(19) Å ³
Z, Calculated density	8, 1.201 Mg/m ³
Absorption coefficient	0.112 mm ⁻¹
F(000)	1984
Crystal size	0.59 x 0.26 x 0.13 mm
Theta range for data collection	1.91 to 25.00 deg.
Limiting indices	-19 ≤ h ≤ 21 -11 ≤ k ≤ 15 -25 ≤ l ≤ 24
Reflections collected / unique	24447 / 4550 [R(int) = 0.0516]
Completeness to theta = 25.00	100.0 %
Absorption correction	Semi-empirical from equivalents
Max. and min. transmission	0.9850 and 0.9368
Refinement method	Full-matrix least-squares on F ²
Data / restraints / parameters	4550 / 0 / 318
Goodness-of-fit on F ²	1.031
Final R indices [I > 2sigma(I)]	R1 = 0.0489, wR2 = 0.1169

R indices (all data)

$R_1 = 0.0848$, $wR_2 = 0.1331$

Largest diff. peak and hole

0.243 and -0.200 e. Å⁻³

Bond lengths [Å] and angles [deg] for 2b.

Si(1)-N(1)	1.718(2)
Si(1)-C(14)	1.861(3)
Si(1)-C(20)	1.865(2)
Si(1)-C(9)	1.906(2)
N(1)-C(26)	1.423(3)
C(1)-C(13)	1.380(3)
C(1)-C(2)	1.381(4)
C(2)-C(3)	1.377(4)
C(3)-C(4)	1.371(4)
C(4)-C(12)	1.380(3)
C(5)-C(6)	1.373(4)
C(5)-C(11)	1.385(3)
C(6)-C(7)	1.374(4)
C(7)-C(8)	1.383(4)
C(8)-C(10)	1.381(3)
C(9)-C(13)	1.505(3)
C(9)-C(10)	1.509(3)
C(10)-C(11)	1.402(3)
C(11)-C(12)	1.457(3)
C(12)-C(13)	1.402(3)
C(14)-C(19)	1.389(4)
C(14)-C(15)	1.396(4)
C(15)-C(16)	1.370(5)
C(16)-C(17)	1.346(6)
C(17)-C(18)	1.378(6)
C(18)-C(19)	1.381(4)
C(20)-C(25)	1.377(3)
C(20)-C(21)	1.388(3)
C(21)-C(22)	1.378(4)
C(22)-C(23)	1.362(4)
C(23)-C(24)	1.372(4)
C(24)-C(25)	1.376(4)
C(26)-C(27)	1.397(3)
C(26)-C(31)	1.399(3)
C(27)-C(28)	1.388(4)
C(27)-C(33)	1.503(4)
C(28)-C(29)	1.375(4)
C(29)-C(30)	1.361(4)
C(30)-C(31)	1.389(4)
C(31)-C(32)	1.497(4)
N(1)-Si(1)-C(14)	110.99(12)
N(1)-Si(1)-C(20)	107.10(10)

C(14)-Si(1)-C(20)	112.78(11)
N(1)-Si(1)-C(9)	109.01(10)
C(14)-Si(1)-C(9)	105.98(11)
C(20)-Si(1)-C(9)	110.98(11)
C(26)-N(1)-Si(1)	128.11(16)
C(13)-C(1)-C(2)	118.6(3)
C(3)-C(2)-C(1)	121.1(3)
C(4)-C(3)-C(2)	120.6(3)
C(3)-C(4)-C(12)	119.2(3)
C(6)-C(5)-C(11)	119.0(3)
C(5)-C(6)-C(7)	120.4(3)
C(6)-C(7)-C(8)	121.1(3)
C(10)-C(8)-C(7)	119.5(3)
C(13)-C(9)-C(10)	102.53(19)
C(13)-C(9)-Si(1)	110.08(15)
C(10)-C(9)-Si(1)	109.38(16)
C(8)-C(10)-C(11)	118.9(2)
C(8)-C(10)-C(9)	131.1(2)
C(11)-C(10)-C(9)	109.9(2)
C(5)-C(11)-C(10)	121.1(2)
C(5)-C(11)-C(12)	130.5(2)
C(10)-C(11)-C(12)	108.4(2)
C(4)-C(12)-C(13)	120.2(2)
C(4)-C(12)-C(11)	131.1(2)
C(13)-C(12)-C(11)	108.7(2)
C(1)-C(13)-C(12)	120.2(2)
C(1)-C(13)-C(9)	130.0(2)
C(12)-C(13)-C(9)	109.8(2)
C(19)-C(14)-C(15)	117.2(3)
C(19)-C(14)-Si(1)	122.6(2)
C(15)-C(14)-Si(1)	120.2(2)
C(16)-C(15)-C(14)	120.9(4)
C(17)-C(16)-C(15)	121.4(4)
C(16)-C(17)-C(18)	119.3(4)
C(17)-C(18)-C(19)	120.3(4)
C(18)-C(19)-C(14)	120.8(3)
C(25)-C(20)-C(21)	116.7(2)
C(25)-C(20)-Si(1)	122.80(19)
C(21)-C(20)-Si(1)	120.37(18)
C(22)-C(21)-C(20)	121.7(3)
C(23)-C(22)-C(21)	120.0(3)
C(22)-C(23)-C(24)	119.9(3)
C(23)-C(24)-C(25)	119.6(3)
C(24)-C(25)-C(20)	122.2(3)
C(27)-C(26)-C(31)	120.4(2)
C(27)-C(26)-N(1)	119.6(2)

C(31)-C(26)-N(1)	120.0(2)
C(28)-C(27)-C(26)	119.0(3)
C(28)-C(27)-C(33)	120.0(3)
C(26)-C(27)-C(33)	120.9(2)
C(29)-C(28)-C(27)	120.7(3)
C(30)-C(29)-C(28)	119.9(3)
C(29)-C(30)-C(31)	121.8(3)
C(30)-C(31)-C(26)	118.1(3)
C(30)-C(31)-C(32)	118.8(3)
C(26)-C(31)-C(32)	123.1(2)

Symmetry transformations used to generate equivalent atoms:

Torsion angles [deg] for 2b

C(14)-Si(1)-N(1)-C(26)	-121.2(2)
C(20)-Si(1)-N(1)-C(26)	2.3(2)
C(9)-Si(1)-N(1)-C(26)	122.5(2)
C(13)-C(1)-C(2)-C(3)	1.5(4)
C(1)-C(2)-C(3)-C(4)	-2.0(5)
C(2)-C(3)-C(4)-C(12)	0.4(5)
C(11)-C(5)-C(6)-C(7)	0.3(4)
C(5)-C(6)-C(7)-C(8)	-0.2(5)
C(6)-C(7)-C(8)-C(10)	0.2(4)
N(1)-Si(1)-C(9)-C(13)	-179.38(15)
C(14)-Si(1)-C(9)-C(13)	61.10(19)
C(20)-Si(1)-C(9)-C(13)	-61.66(18)
N(1)-Si(1)-C(9)-C(10)	68.70(18)
C(14)-Si(1)-C(9)-C(10)	-50.83(18)
C(20)-Si(1)-C(9)-C(10)	-173.58(15)
C(7)-C(8)-C(10)-C(11)	-0.3(4)
C(7)-C(8)-C(10)-C(9)	175.7(3)
C(13)-C(9)-C(10)-C(8)	176.0(3)
Si(1)-C(9)-C(10)-C(8)	-67.2(3)
C(13)-C(9)-C(10)-C(11)	-7.7(2)
Si(1)-C(9)-C(10)-C(11)	109.08(19)
C(6)-C(5)-C(11)-C(10)	-0.4(4)
C(6)-C(5)-C(11)-C(12)	178.2(3)
C(8)-C(10)-C(11)-C(5)	0.4(4)
C(9)-C(10)-C(11)-C(5)	-176.4(2)
C(8)-C(10)-C(11)-C(12)	-178.4(2)
C(9)-C(10)-C(11)-C(12)	4.7(3)
C(3)-C(4)-C(12)-C(13)	1.5(4)
C(3)-C(4)-C(12)-C(11)	-177.9(3)
C(5)-C(11)-C(12)-C(4)	1.3(5)
C(10)-C(11)-C(12)-C(4)	180.0(3)
C(5)-C(11)-C(12)-C(13)	-178.1(3)
C(10)-C(11)-C(12)-C(13)	0.6(3)
C(2)-C(1)-C(13)-C(12)	0.4(4)
C(2)-C(1)-C(13)-C(9)	-175.6(2)
C(4)-C(12)-C(13)-C(1)	-1.9(4)
C(11)-C(12)-C(13)-C(1)	177.6(2)
C(4)-C(12)-C(13)-C(9)	174.8(2)
C(11)-C(12)-C(13)-C(9)	-5.7(3)
C(10)-C(9)-C(13)-C(1)	-175.6(2)
Si(1)-C(9)-C(13)-C(1)	68.1(3)
C(10)-C(9)-C(13)-C(12)	8.1(2)
Si(1)-C(9)-C(13)-C(12)	-108.23(19)

N(1)-Si(1)-C(14)-C(19)	171.4(2)
C(20)-Si(1)-C(14)-C(19)	51.2(2)
C(9)-Si(1)-C(14)-C(19)	-70.4(2)
N(1)-Si(1)-C(14)-C(15)	-12.3(2)
C(20)-Si(1)-C(14)-C(15)	-132.4(2)
C(9)-Si(1)-C(14)-C(15)	106.0(2)
C(19)-C(14)-C(15)-C(16)	-1.1(4)
Si(1)-C(14)-C(15)-C(16)	-177.7(2)
C(14)-C(15)-C(16)-C(17)	-0.3(6)
C(15)-C(16)-C(17)-C(18)	1.6(7)
C(16)-C(17)-C(18)-C(19)	-1.5(6)
C(17)-C(18)-C(19)-C(14)	0.0(5)
C(15)-C(14)-C(19)-C(18)	1.2(4)
Si(1)-C(14)-C(19)-C(18)	177.7(2)
N(1)-Si(1)-C(20)-C(25)	-112.3(2)
C(14)-Si(1)-C(20)-C(25)	10.1(3)
C(9)-Si(1)-C(20)-C(25)	128.8(2)
N(1)-Si(1)-C(20)-C(21)	63.0(2)
C(14)-Si(1)-C(20)-C(21)	-174.6(2)
C(9)-Si(1)-C(20)-C(21)	-55.8(2)
C(25)-C(20)-C(21)-C(22)	1.3(4)
Si(1)-C(20)-C(21)-C(22)	-174.3(2)
C(20)-C(21)-C(22)-C(23)	0.5(5)
C(21)-C(22)-C(23)-C(24)	-2.0(5)
C(22)-C(23)-C(24)-C(25)	1.7(5)
C(23)-C(24)-C(25)-C(20)	0.2(5)
C(21)-C(20)-C(25)-C(24)	-1.6(4)
Si(1)-C(20)-C(25)-C(24)	173.9(2)
Si(1)-N(1)-C(26)-C(27)	-112.5(2)
Si(1)-N(1)-C(26)-C(31)	67.4(3)
C(31)-C(26)-C(27)-C(28)	-0.7(4)
N(1)-C(26)-C(27)-C(28)	179.1(2)
C(31)-C(26)-C(27)-C(33)	-178.2(2)
N(1)-C(26)-C(27)-C(33)	1.6(4)
C(26)-C(27)-C(28)-C(29)	-1.5(4)
C(33)-C(27)-C(28)-C(29)	176.0(3)
C(27)-C(28)-C(29)-C(30)	1.1(5)
C(28)-C(29)-C(30)-C(31)	1.6(5)
C(29)-C(30)-C(31)-C(26)	-3.7(4)
C(29)-C(30)-C(31)-C(32)	175.8(3)
C(27)-C(26)-C(31)-C(30)	3.3(4)
N(1)-C(26)-C(31)-C(30)	-176.6(2)
C(27)-C(26)-C(31)-C(32)	-176.2(2)
N(1)-C(26)-C(31)-C(32)	3.9(4)

Symmetry transformations used to generate equivalent atoms